The Interaction of Cytokinin and Strigolactone in controlling Shoot Branching in Arabidopsis thaliana

By

Neelam Chaudhary

Imperial College London
Department of Life Sciences
November 2013

A thesis submitted for the degree of Doctor of Philosophy and the Diploma of Imperial College London

For my Father (Late) and Mother

They struggled hard to strengthen my faith in Almighty Allah and supported me to fulfil my dreams and to achieve my goals through their constant unconditional love, encouragement and prayers.

For Scientists especially Life Scientists

They spare time learning new ways to understand and solve problems in hopes of paving a better future for newer generations. They are more dedicated to making solid achievements than in running after swift but synthetic happiness.

ABSTRACT

Shoot branching is regulated by auxin, cytokinin (CK) and strigolactone (SL). Cytokinin, being the only promoter of shoot branching, is antagonistic in function to auxin and strigolactone, which inhibit shoot branching. There is a close relationship between auxin and strigolactone, mediating each other to suppress shoot branching. Strigolactone reduces auxin transport from the buds, thus arresting bud outgrowth. On the other hand, auxin increases strigolactone production to control apical dominance. Antagonistic interaction between auxin and cytokinin has been reported as auxin inhibits lateral bud outgrowth by limiting CK supply to axillary buds. Previously, it has been found that levels of tZ-type CKs are extremely low in xylem sap of strigolactone mutants of *Arabidopsis* and pea.The current research aimed to explore the interaction between cytokinin and strigolactone, especially the regulatory mechanisms behind these low cytokinin levels. It was hypothesized that xylem-CKs may be controlled by strigolactone-mediated regulation of *AtIPT* genes in *Arabidopsis thaliana*. For this investigation, *atipt* double (*atipt5,7, atipt3,5* and *atipt3,7*) and triple (*atipt3,5,7*) knockout mutants in wild-type and *max* backgrounds were screened and characterized. The GUS promoter-reporter system was used to study regulation of *AtIPT* expression by strigolactone. For this purpose, *AtIPTs::GUS* lines were generated in *max* SL mutant backgrounds. Further, cytokinin levels were quantified in root and shoot tissues as well as in phloem and xylem sap of *atipt* mutants in wild-type and *max* background.

Cytokinin biosynthetic genes (*AtIPTs*) were shown to be regulated by strigolactone and cytokinin synthesis played an important role in the phenotype of *max* mutants. Loss of *AtIPT3* from the SL-deficient mutant, *max4,* resulted in reduced growth and suppression of shoot branching. However, it was not possible to knockout *AtIPT3* from the SL-insensitive mutant, *max2*, because double mutation of *AtIPT3* and *MAX2* genes was unexpectedly found to be lethal. Both *max2* and *max4* showed upregulation of *AtIPT3* in phloem and downregulation of *AtIPT5* in root and shoot. Application of GR24 (SL synthetic analogue) and NAA (auxin) reversed the regulation in *max4*. Auxin- and strigolactone-mediated regulation of *AtIPT3* and *AtIPT5* in root and shoot were strictly MAX2-dependent, apart from auxin upregulation of *ATIPT5* in roots, independent of strigolactone. The phloem sap showed elevated levels of the CK metabolite, iPRP, and this was correlated with high expression of *AtIPT3* in phloem of *max* mutants. The increased transport of iPRP to roots did not increase the production of tZ-type CKs in roots of *max* mutants. Rather the levels of tZ-type CKs in xylem sap of *max* mutants were highly reduced. The results lead to the conclusionthat SL controls shoot branching partly by mediating CK biosynthesis and iPRP in phloem may function as a feedback signal to modulate translocation of tZ-type CKs through xylem.

ACKNOWLEDGMENT

According to Goethe, “All the knowledge I possess everyone else can acquire, but my heart is all my own”. That’s why, from the core of my heart I acknowledge everyone mentioned here.

I would like to express my sincere gratitude to my supervisor, **Dr. Colin Turnbull**, for his great assistance and ever-presencethroughout this project. His immense encouragement and help in every possible way is appreciated beyond words. I feel lucky to be supervised by such a nice and humble person, who provided not only for learning the science but also for the development of my personality. The last degree under the guidance of such a great mentor fulfils the purpose of being highly educated. I am also grateful for his constant patience with this manuscript.

I would also appreciateall the support from my advisors, **Dr. John Rossiter** and **Dr. Alexander Grabov**. I extend my heartiest gratitude to the members of my lab, especially **Dr.Rosa Lopez-Cobollo**, for their full support and company. I am also thankful to**Mark Bennett** for his assistance with LC-MS/MS, **Ian Morris** for all his help in the lab and department, **Dr.Martin Selby** for taking care of plants in growth rooms and **Fiona May** for her patience with the ordering of materials required in the project.

I wish to thank **Higher Education Commission, Pakistan**and **International Student House**for the scholarship which made this study possible.

I am really indebted to my brothers and sisters, especially **Saima Farnaz** for her great help in learning English grammar during my school days as well as for her invaluable advices and encouragement throughout my studies, **Rubina Ghazal** for her assistance in resolving computer-related problems, **Farah Zaib** for her humorous attitude to make me relaxed, and **Amjad Javaid** for his special aid to accomplish all the requirements of scholarship and travel to UK.

Special thanks are due to my friends who always stand with me in the time of trial.I am really obliged to **Dr. Nazia Nisar**. She is truly an example of “A friend in need is a friend indeed”. I am really thankful to **Durr e Shahwar** for her very good company when I was feeling lonely away from my family and husband.

I have no words to thank my husband, **Dr. Muhammad Umer**. This PhD would not have been possible without his constant support, encouragement and patience. I can never forget his efforts to facilitate me in completing my PhD, especially during thesis writing. His calm acceptance and compassionate understanding kept me going at tough times and his PhD experience gave me an inspiration to finish this most difficult task of my life.

I conclude my acknowledgement by saying that all was done only by the grace and mercy of **Almighty Allah**.

DECLARATION OF ORIGINALITY

I hereby declare that this thesis is my own work. To the best of my knowledge, none of the work presented in this thesis has been previously submitted for a qualification either at Imperial College London or at any other institution. It contains no materials previously published, however, some parts of this work have been presented in a poster at the 2nd Cytokinin meeting (July 2012) held at Dahlem Centre of Plant Sciences, Free University of Berlin, Germany. I also declare that the intellectual content of this thesis is the product of my own work.

Signature: **Date: 19-11-2013**

COPYRIGHT DECLARATION

ABBREVIATIONS

AHK	Arabidopsis histidine kinase
AHP	Arabidopsis histidine phosphotranspher
AM	Axillary meristem
ARR	Arabidopsis response regulator
BAP	Benzyl amino purine
CaMV	Cauliflower mosaic virus
CCD	Carotenoid cleavage dioxygenase
CK	Cytokinin
CRF	Cytokinin response factors
cZ	*cis*-Zeatin
cZR	*cis*-Zeatin riboside
cZRP	*cis*-Zeatin ribotide phosphate
DMAPP	Dimethylallyl diphosphate
DZ	Dihydrozeatin
EMS	Ethyl methanesulfonate
GFP	Green fluorescent protein
GUS	Beta Glucuronidase
HMBDP	Hydroxymethylbutenyl diphosphate
iP	Isopentenyladenine
iPR	Isopentenyladenine riboside
iPRP	Isopentenyladenine ribotide phosphate
IPT	Isopentenyltransferase
MAX	More axillary shoots
NAA	1-Naphthaleneacetic acid
NADPH	Nicotinamide adenine dinucleotide phosphate
NOA	Naphthoxyacetic acid
NPA	1-N-Naphthylphthalamic acid
OE	Overexpressor
PAT	Polar auxin transport
SAM	Shoot apical meristem
SL	Strigolactone
TIBA	2,3,5-triiodobenzoic acid
tZ	*trans*-Zeatin
tZR	*trans*-Zeatin riboside
tZRP	*trans*-Zeatin ribotide phosphate
WT	Wild-type
w.r.t	with respect to

TABLE OF CONTENTS

LIST OF FIGURES

LIST OF TABLES

Chapter 1

Introduction

1.1 Importance of studies on Shoot Branching

The world population is expected to reach about 8.9 billion in the year 2050 (Cohen, 2003) and on the other hand, the cultivated area is being reduced due to increasing population, deforestation, urbanization, industrialization and acreage under cultivation of forage, fiber and bio-fuel crops (Siedow, 2001). Therefore, it will be crucial to increase food production to fulfill the rising human demand for quality and quantity of food (Altman, 1999). This issue can be resolved by using improved plant varieties on the available arable land (Wang and Li, 2008). As a consequence, the output of agriculture has become a major concern and focus of research for eradication of hunger (Rosegrant and Cline, 2003). In this context, modification of crop plant architecture with its desirable characters can augment yield.

Plant architecture can be differentiated into two zones: underground and aboveground zone representing root and shoot architecture, respectively. The former contributes to water acquisition, extraction of micro and macronutrients from the soil, anchorage and adaptability to changing soil environment (Casimiro *et al*., 2003) and the latter, determined by factors including shoot branching, plant height as well as inflorescence morphology and branching, contributes to lodging resistance, photosynthesis, reproductive phase and yield (Wang and Li, 2006).

A substantial increase in production was observed in new varieties of wheat and rice as a part of the so-called Green Revolution (Wang and Li, 2006; Gilland, 2002; Siedow, 2001). Two semi-dwarf rice varieties of IRRI (International Rice Research Institute), IR8 and IR36, became well known for their surprising yield potential. Dwarfing *Rht* (*Reduced height*) genes (*Rht1* and *Rht2*) were incorporated into wheat from a Japanese variety Norin 10 and hence harvest index was increased by 60%. *Rht* genes encode proteins that are involved in signal transduction of gibberellic acid (GA) (Hedden, 2003). Mutations in *Rht1* and *Rht2* genes resulted in formation of truncated Rht proteins, which function as GA-insensitive repressors of plant height (Peng *et al*., 1999).

The dwarf varieties of wheat and rice also had other desirable characters like high tillering, dark and erect leaves and sturdy stems. With application of fertilizers, their yield was doubled to about 9 tons per hectare. Thus these varieties constituted a breakthrough in crop improvement (Khush and Virk, 2005; Sakamoto and Matsuoka, 2004; Hedden, 2003; Khush, 2001; Khush, 1995; Khush, 1987). Over the past four decades, an increase in agricultural food production has happened worldwide due to the extensive use of fertilizers. However, these fertilizers caused many environmental problems such as the eutrophication of freshwater and marine ecosystems (Kudo *et al*., 2010).

Branching has great significance in agriculture as it is evident from crop domestication during which plant architecture has been altered by selecting shoot branching patterns of interest. Therefore, specific architectural traits are existent due to artificial selection for desirable characters (Hufford *et al*., 2007). Maize and sunflower are the excellent examples of modified shoot architecture with reduced branching as compared to its wild ancestors (Doebley *et al*., 2006). Other examples of the domesticated crops are wheat, oat and barley, having few vegetative branches and a higher order of inflorescence branching (Doust, 2007). Such selection over a relatively restricted period of time has contributed to seed production, with improved plant characters such as more determinate growth, early maturation, and increased apical dominance as well as reduced seed dispersal that helps to avoid yield loss during harvesting (Doebley *et al*., 2006). For example, a wild ancestor of maize, teosinte, is very sensitive to planting density due to having higher levels of branching. Therefore, the relatively high density planting of unbranched plants yields more than lower density branching plants (Doust, 2007). The examples of domesticated crops demonstrate the importance of shoot branching from an agricultural point of view. However, traditional methods alone can no longer be used to modify crop plants. Instead, biotechnological breeding to alter plant architecture is now a necessity to increase food production with the limited use of fertilizers, thus protecting the global environment.

Before developing biotechnological techniques for the application in agriculture, it is crucial to understand the genetics and physiological mechanisms behind plant architecture, which is also controlled by phytohormones. For example, the genetics of plant architecture can be manipulated to generate high yielding varieties. Two tillering genes *OsTB1* (ortholog of maize *TEOSINTE BRANCHED1*, *TB1*) and *MONOCULM1* (*MOC1*) were identified in rice. The mutants of these genes showed antagonistic impact on the number of tillers because

OsTB1 is negative regulator and *MOC1* is a positive regulator of lateral branching. The mutation in *OsTB1* increases the tillers number whereas *moc1* reduces tillering ability. Both tiller-related genes *OsTB1* and *MOC1* could play a significant role in future to improve rice through the regulation of tillers resulting in the increase in yield (Khush, 1999: Sakamoto and Matsuoka, 2004; Yang and Hwa, 2008). Recently, a transcription factor *BRC1* (*BRANCHED1*), which is closely related to *TEOSINTE BRANCHED1* (*TB1*) from maize (Hubbard *et al*., 2002), has been identified in *Arabidopsis* (Aguilar-Martínez *et al*., 2007) and in pea (Braun *et al*., 2012). *BRC1* acting downstream of strigolactone controls axillary bud outgrowth. It is upregulated by strigolactone treatment and downregulated by cytokinin application. Therefore, antagonistic relationship between strigolactone and cytokinin establishes through their common target, *BRC1* (Braun *et al*., 2012; Dun *et al*., 2012).

There are two types of attributes including morphological (such as seed size, weight, number) and metabolic (like nutrients uptake and their efficient use), on which plant productivity may depend (Kudo *et al*., 2010). Phytohormones controlling shoot branching are closely relevant to both of these aspects. In my study, the aim is to understand the functions and interactions of plant hormones in controlling shoot branching in a model plant *Arabidopsis thaliana*.

1.2 Shoot Branching

Conventional concepts of architecture relate to structural designs and forms of buildings. Accordingly, a great diversity of aesthetically pleasing structures of plants is also described as shoot architecture, implicating both art and science for determination of plant shape and functionality (Wang and Li, 2008). Shoot architecture is determined by factors including shoot branching, plant height and inflorescence morphology and branching (Wang and Li, 2006). Shoot branching, a key contributor to the aboveground plant structure, is a collective term for all processes involved in formation and development of side shoots or branches from axillary buds on the main shoot of a plant (Evers *et al*., 2011).

During seed development, embryogenesis results in the establishment of basic body plan laid on an apical-basal axis in the form of primary meristems (a root apical meristem and a shoot apical meristem in opposite directions). During postembryonic development after seed germination, the primary meristems give rise to the complex body plan of plants. The establishment of secondary axes of growth diversifies the whole aboveground plant shoot system with the development of axillary meristems. The entire shoot system is based on a series of modules or phytomers derived from shoot apical meristem. A phytomer or module is comprised of a stem segment associated with a leaf, a node (where a leaf adjoins the stem) and one or more axillary meristems (AM) at the leaf axils (McSteen and Leyser, 2005).

The growth potential of axillary meristems is considered the same as of primary shoot apical meristem, but initially axillary meristems are developed into axillary buds containing small unexpanded leaves (Aguilar-Martínez *et al*., 2007; Schmitz and Theres, 2005; Müller and Leyser, 2011). After formation of a few immature leaves, axillary buds located on the axils of

leaf primordia cease to grow, depending on genetics of a plant and/or a type of species. Therefore, axillary buds become dormant due to suppression of outgrowth (Mouchel and Leyser, 2007; Schmitz and Theres, 2005; Shimizu-Sato *et al*., 2009). Such buds have a set of specific transcripts and proteins, which function either to switch on the bud activity or to reverse the activation into dormancy. Therefore, the axillary buds can be considered as a cycle between the dormant and active states (Shimizu-Satoand Mori, 2001; Horvath *et al*., 2003; Leyser, 2003).

Unlike animals, plants are sessile organisms and cannot escape from unfavourable environmental conditions (Domagalska and Leyser, 2011). Therefore, plant development is dependent on their degree of phenotypic plasticity, which is an ability of plants to cope with the changing environmental conditions for their survival throughout the life cycle. Consequently, a plant with one genotype can give rise to a diverse range of phenotypes in response to growth conditions to which it is exposed (Pigliucci, 2001). An excellent example of such a plant plastic response is shoot branching (Domagalska and Leyser, 2011), which depends on two developmental processes; release of bud dormancy and its subsequent outgrowth. The fate of axillary buds, whether to remain dormant or to grow out to produce branches, is controlled by the coordination between internal developmental programmes of plants and external cues from the environment (Wang and Li, 2008; Horvath *et al*., 2003). This coordinated regulatory mechanism determines the plant potential to adjust and survive in the changing conditions (Ongaro and Leyser, 2008). For instance, removal of primary shoot apex by herbivores or pruning triggers the activation of axillary buds resulting in increased shoot branching (Cline, 1997).

Shoot branching is an important developmental process to study for many reasons (Ward and Leyser, 2004). The total number, size and alignment of branches, which determine total plant area and spatial distribution of leaf area, contributes to light harvesting potential affecting the photosynthetic performance of a plant (Evers *et al*., 2011). Synchronization of flowering and seed setting is also influenced by the shoot system (Ward and Leyser, 2004). Consequently, the harvest index of plants depends on shoot biomass accumulation and seed yield, thus establishing the significance of shoot branching from an agricultural point of view (Huang *et al*., 2012; Wang and Li, 2006). Shoot branching is modulated by a myriad of external and internal factors, which include environmental stimuli, genetic constitution and hormonal signals (Dun *et al*., 2013). A complex interplay among three main phytohormones to control bud outgrowth is associated with auxin and strigolactone as repressors (Thimann and Skoog, 1933, 1934; Gomez-Roldan *et al*., 2008; Umehara *et al*., 2008) and cytokinin as a promoter (Sachs and Thimann, 1967).

The next part of this introduction gives an overview of the nature, occurrence and biochemical characteristics of three plant hormones, namely cytokinin, strigolactone and auxin. The following part is an outline of the role of hormones in controlling shoot branching, with particular focus on the interaction between three hormones. The final section covers aims and objectives of the research presented in this thesis.

1.3 Cytokinin

1.3.1 Functions of Cytokinins

Cytokinins (CKs) are plant hormones involved in various developmental processes including cell division, cell enlargement and cell differentiation, bud formation, shoot branching, leaf expansion, delay of senescence, seed dormancy and seed germination and chloroplast formation, de-etiolation, chloroplast differentiation, plant-pathogen interactions, flower and fruit development (Mok, 1994; Chen, 1997; Mok *et al*., 2000; Haberer and Kieber, 2002).

1.3.2 Types of Cytokinins

Since the discovery of the first cytokinin, kinetin, many chemicals fitting the definition of cytokinin, "a generic name for substances which promote cell division and exert other growth regulatory functions in the same manner as kinetin" (Skoog and Armstrong 1970), have been identified. These are adenine derived compounds with a side chain at the position N^6. Depending on the side chain, cytokinins can be classified into two types: naturally occurring compounds including isoprenoid and aromatic cytokinins, and synthetic compounds including structurally unrelated phenyl urea type cytokinins along with Kinetin, an adenine derivative. Isoprenoid CKs (Fig.1.1), the most abundant in occurrence, consist of isopentenyladenine (iP), *trans*-Zeatin (tZ), dihydrozeatin (DZ) and *cis*-zeatin (cZ) (Mok, 1994; Mok *et al*., 2000; Haberer and Kieber, 2002; Kakimoto, 2003; Sakakibara, 2005). On the other hand, aromatic CKs are rare and their biosynthetic pathways remain to be explicated (Sakakibara, 2006).

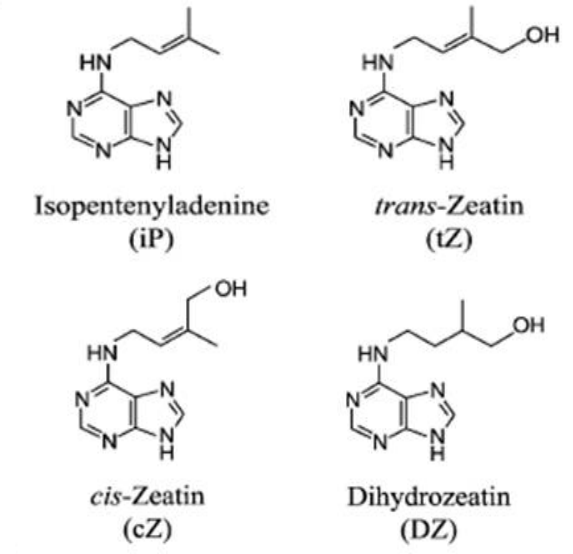

***Figure - 1.1**: **Chemical Structures of Isoprenoid Cytokinins** (Taken from Sakakibara, 2005)*

1.3.3 Biosynthesis of Cytokinins

Until now, isoprenoid cytokinins have been found to be synthesized in three possible pathways: (A) tRNA derived Pathway; (B) Adenine derived Pathway and (C) Alternate Biosynthetic Pathway of *trans*-zeatin

(A) tRNA Derived Pathway:

Primarily, breakdown of tRNA was assumed a possible source for cytokinin biosynthesis because isoprenoid cytokinin nucleotides were found in tRNAs (Skoog *et al*., 1966; Vreman and Skoog, 1972; Vreman *et al*., 1978; Edwards *et al*., 1981). Some tRNA species with anticodons complementary to codons starting with Uridine, contain a prenylated adenosine adjacent to the 3'end of the anticodon (Skoog and Armstrong, 1970). Thus, the prenylated tRNA could be the contributor to *cis*-zeatin (cZ) production because a *cis*-hydroxyl group was found to be attached to it (Vreman *et al*., 1978). Two *tRNA*- isopentenyltransferases (tRNA-IPTs) genes identified in *Arabidopsis* (Kakimoto, 2001; Takei *et al*., 2001; Golovko *et al*., 2002) are *AtIPT2* and *AtIPT9* which catalyze prenylation of tRNAs. The cZ-type cytokinins were undetectable in an *Arabidopsis* mutant generated by knocking out both *tRNA-IPT* genes. In the same mutant, the levels of iP- and tZ-type cytokinins were not changed from wild-type levels (Miyawaki *et al*., 2006). This finding showed the degradation of prenylated tRNA as a main pathway to produce cZ (Fig. 1.2) in *Arabidopsis*.

(B) Adenine Derived Pathway:

In the first step of this pathway (Fig. 1.2), *N*-prenylation at N^6-terminus of adenosine 5′ phosphates (ATP, ADP or AMP) with hydroxymethylbutenyl diphosphate (HMBDP) or dimethylallyl diphosphate (DMAPP), is catalyzed by adenosine phosphate-isopentenyl transferases (IPTs). The IPT enzymes, encoded by seven *AtIPT* genes (*AtIPT1* and *AtIPT3* to *AtIPT8*) identified in *Arabidopsis* (Kakimoto, 2001; Takei *et al.*, 2001), are responsible for the synthesis of iP, tZ, and DZ- type cytokinins (Miyawaki *et al*., 2006). Specificities of IPTs substrates vary depending on species. In higher plants, IPTs prefer ADP and ATP to AMP as prenyl acceptors and generally DMAPP as a prenyl donor (Kakimoto, 2001). HMBDP is an intermediate of MEP (Methylerythritol phosphate) pathway while DMAPP is produced by MEP pathway in plastids and by MVA (Mevalonate) pathway in cytosol (Sakakibara, 2005). Isotope-labeling in *Arabidopsis* seedlings showed that prenyl donors are mainly produced by the MEP pathway. Accordingly, the localization of four AtIPT proteins (AtIPT1, AtIPT3, AtIPT5, AtIPT8) were shown to be in plastids while AtIPT4 and AtIPT7 were found to be localized in the cytosol and mitochondria, respectively (Kasahara *et al*., 2004). Quantification of transcript levels showed that two genes *AtIPT3* and *AtIPT5* are expressed relatively at higher levels than the other *AtIPTs* (Takei *et al*., 2004a). The consensus view is that initiation of cytokinin biosynthesis is by catalytic transfer of DMAPP to adenosine 5′ phosphates by an IPT enzyme (Fig. 1.3), producing iPRP (Collective term for iPRMP, iPRDP and iPRTP) as the first cytokinin metabolite.

Hydroxylation of iP-nucleotides (iPRP) at the prenyl side chain to synthesize tZ-nucleotides is catalyzed by Cytochrome P450 monooxygenase enzyme (CYP735A1 or CYP735A2), which only consumes iPRP as a substrate rather than iP-nucleoside (iPR) or free base iP. The conversion reaction of iPRP to tZRP is stereo-specific, therefore, cZ-nucleotides are not produced by CYP735As (Takei *et al.*, 2004b).

All types of CK-nucleotides are converted into biological active cytokinin free bases in two ways. One is direct generation by LOG (Lonely Guy) enzymes (Kurakawa *et al.*, 2007) whereas the second is a two-step conversion reaction suggested about 30 years ago (Chen and Kristopeit, 1981a, b). CK-ribotides are dephosphorylated to CK-ribosides, which on their deribosylation produce free CK-nucleobases. Enzymatic activities involved in this conversion were found in wheat germ but corresponding genes related to the enzymes (nucleotidase and nucleosidase) are yet to be identified.

(C) Alternate Biosynthetic Pathway of *trans*-zeatin:

It was thought that *trans*-zeatin is synthesized indirectly by hydroxylation of iPRP, the first product formed in an adenine derived CK biosynthetic pathway, but the direct *de novo* biosynthesis of *trans*-zeatin riboside phosphate (tZRP is collective term for tZRMP, tZRDP and tZRTP) was also found in *Agrobacterium* and *Arabidopsis* (Åstot *et al.*, 2000). The tobacco plant over-expressing *Agrobacterium ipt* gene (Redig *et al.*, 1996a; Faiss *et al.*, 1997) showed a significant increase in zeatin-type cytokinins, and this was attributed to immediate conversion of iPRP into tZRP (Palni & Horgan, 1983).

The bacteria expressing the genes of *tzs* (*trans*-zeatin secretion) and *ptz* (*Pseudomonas trans*-zeatin producing) release *trans*-zeatin (Beaty *et al.*, 1986; Powell and Morris, 1986; Akiyoshi *et al.*, 1987). The production and secretion of trans-zeatin was thought to be due to two possibilities, either the presence of an isopentenyladenine hydroxylase enzyme or the existence of an iPRP-independent pathway. About a decade ago, tzs protein was purified and shown to be responsible for tZRP production by the transfer of a hydroxylated side chain from HMBDP to AMP, (Krall *et al.*, 2002), but it is yet to be proved whether plant IPTs also utilize HMBDP as a substrate for the direct synthesis of tZRP (Kakimoto, 2003).

An *Arabidopsis* transgenic plant overexpressing *Agrobacterium ipt* gene was studied to compare the biosynthetic rates of tZRP and iPRP. Direct product synthesized by transfer of DMAPP to AMP is iPRP that is converted to tZRP by CYP735s. The *in vivo* deuterium incorporation to *ipt*-induced transgenic plants showed a 66-fold higher tZRP than iPRP. The iPRP-dependent synthesis of tZRP was completely blocked by the application of Metapyrone (Generic name is Metyrapone), a known inhibitor of cytochrome P450 enzymes. With the inhibition of CYP735s, the plants were able to produce tZRP, suggesting the presence of an iPRP-independent pathway (Fig. 1.2), which synthesizes tZRP directly by IPTs (Åstot *et al.*, 2000).tZ- and iP-type cytokinins were generated by expressing *AtIPT7* in *E. coli* and then *in vitro* reactions were used for the actual synthesis. It was found that the enzyme can catalyze

the synthesis of tZ-type cytokinins with HMBDP and ADP in vitro, although the reaction efficiency was lower using HMBPP as a substrate than DMAPP (Takei *et al*., 2003a).

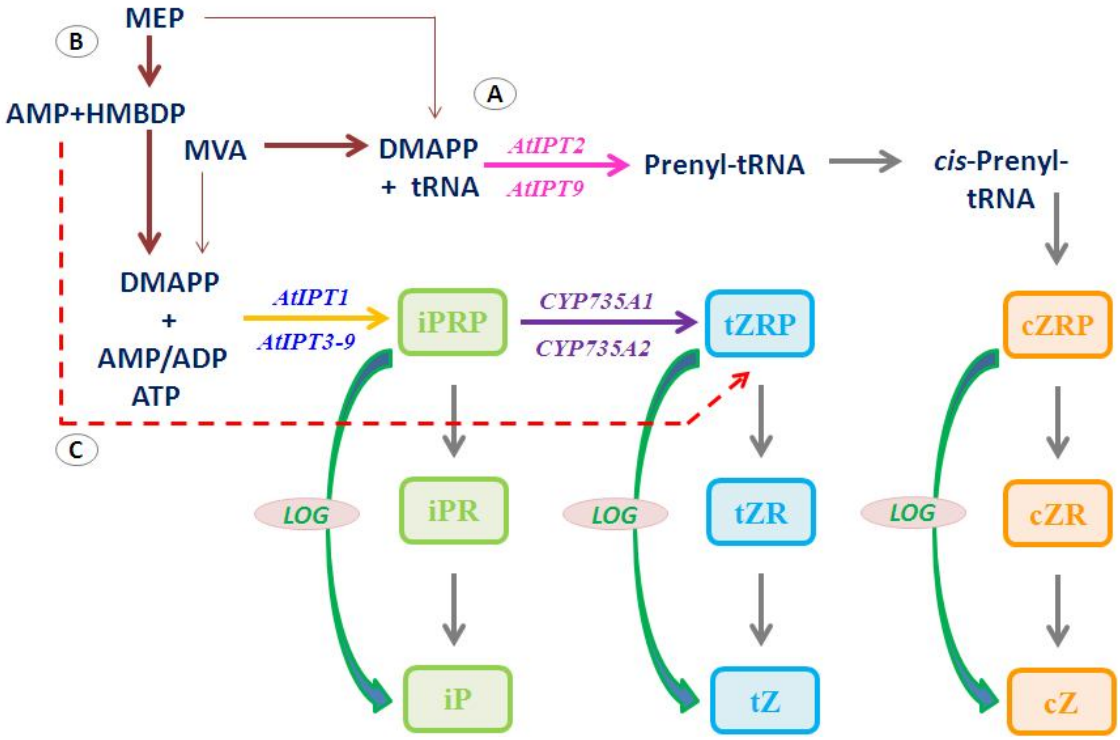

***Figure - 1.2**: **Current Pathway of Cytokinin Biosynthesis** (adapted and modified from Kamada-Nobusada and Sakakibara, 2009). **(A)** The prenyl donor substrates from MVA (Mevalonate) pathway are mostly used to form cZ (cis-zeatin). The tRNA-IPTs (tRNA-isopentenyl transferases) catalyze prenylation of tRNA resulting in the production of cZRP (cZ-riboside phosphate). **(B)**The prenyl donor substrates from MEP (Methylerythritol phosphate) pathway are utilized predominantly to produce iP (isopentenyladenine) and tZ (trans-zeatin). The ATP/ADP-IPTs (adenosine phosphate-isopentenyltransferases) prefer ATP and ADP (Adenosine 5' tri- and di-phosphate) as prenyl acceptor and DMAPP (dimethylallyl diphosphate) as a prenyl donor to produce iPRP (iP-ribotide phosphates). The conversion of iP-nucleotides into the corresponding tZ-nucleotides is catalyzed by CYP735A1/A2. **(A-B)** Dephosphorylation of iP-, tZ- and cZ-nucleotides may occur by phosphatase enzymes. The CK-nucleotide phosphates are directly converted to active forms of CKs by LOG enzymes. **(C)** The N-prenylation of AMP (Adenosine 5' mono-phosphate) with HMBDP (hydroxymethylbutenyl diphosphate) to form directly tZRP (trans-zeatin phosphates), also catalyzed by IPTs. This alternate direct biosynthesis of tZ-CKs occurs in bacteria and Arabidopsis. Abbreviations: LOG is Lonely Guy; iPR, tZR and cZR are corresponding ribosides. [CK biosynthetic pathway (taken from Kamada-Nobusada and Sakakibara, 2009) with structural formulas is given in Appendix I-A]*

1.3.4 Sites of Cytokinin Biosynthesis

A large number of earlier experiments demonstrated that the main sites of cytokinin biosynthesis are roots, especially root tips (Van Staden and Smith, 1978; Koda and Okazawa, 1978; Chen *et al*., 1985; Sossountzov *et al*., 1988; Feldman, 1979). Afterwards, it was also reported that cytokinin is not synthesized only in roots but in aerial plant parts as well (Chen & Petschow, 1978; Nordstrom *et al*., 2004).

After identification of nine *AtIPT* genes (*AtIPT1* to *AtIPT9)* involved in catalyzing the first step of cytokinin biosynthesis (Kakimoto, 2001; Takei *et al*., 2001a), their spatial expression patterns were analyzed using transgenic *Arabidopsis* plants expressing a gene for beta-Glucuronidase protein (GUS) and green fluorescent protein (GFP) fused to the regulatory sequence of each *AtIPT* gene. These analyses suggest that CK synthesis is restricted to specific tissues and organs. The genes expressed in the vegetative phase are *AtIPT1*, *AtIPT3*, *AtIPT5* and *AtIPT7*. The GPF fluorescence of these genes has been shown in roots whereas their GUS activity has been found in roots as well as in other plant parts. These genes are also expressed in the reproductive phase (Miyawaki *et al*., 2004; Takei *et al*., 2004a).

AtIPT1::GUS is expressed in primary and lateral root procambium linked to xylem, at leaf axils and base of axillary buds, in ovule and mature embryo. *AtIPT1::GFP* is expressed in root elongation area and vascular stele of primary root. Activity for both *AtIPT3::GUS* and *AtIPT3::GFP* is localized to phloem throughout the whole seedling. Expression patterns of *AtIPT5::GUS* are found to be in root caps and root primordia of primary and lateral roots, stem of lateral buds, base of young inflorescence and fruit abscission zone. In case of *AtIPT5::GFP*, expression is in lateral root primordium, pericycle and emerging lateral roots. *AtIPT7::GUS* is expressed in trichomes (outgrowths on young leaves), root elongation area and pollen tube. The fluorescence of *AtIPT7::GFP* appears in the elongation area but that does not overlap with that of *AtIPT1::GFP* (Miyawaki *et al*., 2004; Takei *et al*., 2004a). The activity of *AtIPT4::GUS* and *AtIPT8::GUS* is found in immature seeds with highest expression in the chalazal endosperm (CZE; a structure in the nutritious tissue that surrounds embryo). *AtIPT2::GUS* and *AtIPT9::GUS* are found to be expressed ubiquitously (Miyawaki *et al*., 2004).

Expression levels of hydroxylase genes *CYP735A1* and *CYP735A2* were quantified in different tissues of *Arabidopsis,* such as rosette leaves, flowers, roots and stems. Both genes were abundantly expressed in roots while very low levels of their transcripts were detected in the aerial plant parts (Takei *et al*., 2004b). These results suggest that tZ-type cytokinins are predominantly produced in roots.

Seven *LOG* genes (*LOG1-LOG5, LOG7* and *LOG8*) have been identified in *Arabidopsis*. Expression patterns of *LOGs* in different tissues of *Arabidopsis* have been analyzed by quantitative RT-PCR and GUS reporter::promoter system.

RT-PCR has shown that both roots and shoots have transcripts of all seven *LOG* genes. Transcript levels of *LOG8* were found to be the most abundant whereas *LOG2*expressed at extremely low level. *LOG1* was also shown to be express moderately in all aerial parts (rosette leaves, cauline leaves, stem and flower) of plant. *LOG4* was found to be expressed abundantly in stem and flower, *LOG5* in flower and *LOG7* in rosette leaves.

Expression of *LOG::GUS* genes were detected in root and shoot tissues as well as in reproductive organs (Kuroha *et al*., 2009). Details of GUS expression in root, shoot and flower are given below:

Roots: *GUS* expression of *LOG1, LOG5* and *LOG8* are found in vascular tissues of roots. But *LOG8::GUS* activity is also detected in quiescent centres of mature roots. The activity of *LOG2::GUS* is shown in root hairs and in the root regions where root hairs are formed. *LOG3::GUS* and *LOG4::GUS* are found to be expressed in root procambium, root primordia, immature vascular tissues of lateral roots soon after emergence. *GUS* activity of *LOG7* is shown in epidermis of root elongation zone (Kuroha *et al*., 2009).

Shoot: All seven *LOG* genes are shown to have *GUS* expression in cotyledons and immature leaves, especially in vascular tissues. *LOG1::GUS*, *LOG3::GUS* and *LOG5::GUS* are also found to be expressed at the base of axillary buds. Expression of *LOG1::GUS* and *LOG4::GUS* are shown in shoot apical region including meristem. *LOG4::GUS* is also expressed in vascular tissues of stem and expression of *LOG8::GUS* is also found in hypocotyls and stomata (Kuroha *et al*., 2009).

Flower: *LOG1::GUS* expression is found in immature flowers and vascular tissues of pistil. Activity of *LOG3::GUS* is detected in styles and ovular foniculus. *LOG4::GUS* is expressed in young inflorescence, base of ovules and fruit abscission zone. Immature and mature flowers as well as ovules show expression of *LOG5::GUS*. *LOG7::GUS* is found to be expressed in pollens. Staining of *LOG8::GUS* is found in stems of inflorescence, flowers and fruit abscission zone (Kuroha *et al*., 2009).

The findings from expression systems of cytokinin biosynthetic genes indicate that cytokinin biosynthesis occurs in different tissues throughout the plant.

1.3.5 Cytokinin Metabolism

Interconversion of CK bases, ribosides and ribotides, a characteristic feature of cytokinin metabolism, is presumably a regulatory mechanism to control concentration of active CK compounds and may have evolved as a part of general purine metabolism. CK nucleosides converted into CK nucleotides by adenosine kinase enzymes (ADK) (Chen and Eckert, 1977; Schoor *et al.*, 2011). On the other hand, CK free bases are substrates of adenine phosphoribosyltransferase (APRT) enzyme to be transformed into corresponding CK nucleotides (Allen *et al.*, 2002; Moffatt *et al.*, 1991; Schnorr *et al.*, 1996), which are utilized to produce CK free bases by activity of LOG enzymes (Kurakawa *et al.*, 2007). Interconversion between *cis*- and *trans*-zeatin occurs by *cis-trans* zeatin isomerase enzyme (Bassil *et al.*, 1993).

It is not yet clear how dihydrozeatin (DZ) form of cytokinin is synthesized. Until now, the only known origin is a NADPH-dependent zeatin reductase that catalyzes conversion of *trans*-zeatin into dihydrozeatin (Martin *et al.*, 1989). This reaction was first detected in *P. vulgaris* and later, in the leaves of *P. sativum* (Frébort *et al.*, 2011). The only and highly specific substrate of this enzyme is *trans*-zeatin (Mok and Mok, 2001).

Glycosylation or conjugation is a key process in cytokinin metabolism. Biologically active CK levels are regulated and maintained through their permanent or temporary inactivation by glycosylation of the adenine ring or of the side chain. Modification at the N^3, N^7, and N^9positions of the adenine moiety produce *N*-glucosides, and that of the hydroxyl group of side chains (tZ, DZ, and cZ) form *O*-glucosides or *O*-xylosides (Sakakibara, 2006).

A glucosyltransferase responsible for the formation of cytokinin N^7- and N^9-glucosides was isolated from cotyledons of radish (*Raphanus sativus*). Adenine derivatives are substrates of this enzyme but isoprenoid CKs show the highest specificity for this enzyme (Entsch and Letham, 1979; Entsch *et al.*, 1979). Two genes encoding for glucosyltransferase enzymes (UGT76C1 and UGT76C2) were identified in *Arabidopsis*. Both enzymes catalyze glycosylation of cytokinins at the N^7- or N^9-positions (Hou *et al.*, 2004).

O-Glucosylation of zeatin at the N^6-side chain bearing a hydroxyl group is thought to be a universal CK metabolism found in the plants. Mostly, the conjugated sugar molecule is glucose, but rarely xylose is also conjugated, as *O*-xylosylation of zeatin has been discovered only in *Phaseolus* (Mok and Mok, 2001; Schmulling, 2004). The *O*-glycosylation is catalyzed by Zeatin-*O*-glycosyltransferase, which were purified from *Phaseolus* and found to have a high specificity to the substrates of both zeatin and dihydrozeatin (Dixon *et al.*, 1989). Two genes (*ZOG1* and *ZOX1*) encoding zeatin-*O*-glucosyltransferase (ZOG1) and zeatin-*O*-xylosyltransferase (ZOX1), respectively, were isolated from *Phaseolus.* The ZOG1 enzyme prefers glucose while ZOX1 utilizes UDP-xylose (Martin *et al.*, 1999a,b).

About a decade ago, a novel gene (*cisZOG1*) encoding an enzyme, responsible for *O*-glucosylation of *cis*-zeatin, was identified in maize. The enzyme utilizes *cis*-zeatin as a substrate, but does not show specificity to *trans*-zeatin, dihydrozeatin, *cis*-zeatin riboside (Martin *et al*., 2001).

Deglycosylation is essential in order to restore and maintain cytokinin activity by conversion of glucosides to corresponding aglycones. All cytokinin conjugates are biologically inactive, but only N^7- and N^9-glucosides cannot be hydrolysed and thus are permanently inactivated forms, whereasN^3- and O-glucosides are temporary storage forms of cytokinins and readily converted back to their active forms by β-glucosidases (Brzobohaty *et al*., 1993; Mok & Mok, 2001; Schmulling, 2004)

Cytokinin Catabolism is an irreversible degradation by cleavage of an unsaturated side chain. This was first identified in a crude tobacco culture (Pačes *et al.*, 1971) and later on was described in *Zea mays* kernels. The enzyme catalyzing the cleavage reaction was named as cytokinin oxidase (CKX) (Whitty and Hall, 1974). Oxidative cleavage of N^6 side chain results in the formation of adenine and a side chain-derived aldehyde fragment as 3-methyl-2-butenal (Brownlee *et al.*, 1975). For years, it was thought that enzyme activity needs molecular oxygen. However, it has been shown that the enzyme uses flavin co-factor as an electron acceptor rather than molecular oxygen (Galuszka *et al.*, 2001) and thus reclassified and renamed as a dehydrogenase (Frébort *et al*., 2011).

CKX activity has been reported in a variety of tissues and species, including *Arabidopsis,* maize, wheat, barley, rice, orchids, poplar, beans and *Vinca rosea* crown gall tissues (Haberer and Kieber, 2002; Schmulling *et al*., 2003). Analysis of the entire genome of *A. thaliana* has revealed seven homologous genes (*AtCKX1–AtCKX7*) encoding CKX enzymes (Bilyeu *et al.*, 2001; Werner *et al.*, 2001; Schmulling *et al*., 2003). Expression studies of *AtCKX* genes using GUS promoter::reporter system reveal functional diversification during plant development, with the highest activity preferentially in the regions or zones of active cell division and growth (shoots, root meristems and emerging leaves). This also confirms cytokinin functions in different organs and at different stages of plant development (Werner *et al*., 2003).

Post-translational modification of AtCKX proteins occurs by glycosylation, as these proteins have several *N*-glycosylation sites. However, not all CKX proteins are glycosylated, as the occurrence of both glycosylated and non-glycosylated forms of CKX enzymes have been confirmed in various plant sources like tobacco and *Phaseolus* (Kamínek and Armstrong, 1990; Motyka and Kamínek, 1994; Motyka *et al*., 2003). The enzyme localization is also dependent on the differences in glycosylation (Kamínek and Armstrong, 1990). CKX enzyme activity is up-regulated upon cytokinin treatment, and this higher activity is associated with the glycosylated form of enzyme (Dietrich *et al*., 1995; Motyka *et al*., 1996; Motyka *et al*., 2003). Therefore, regulation of enzymatic activity, translocation and protein stability may occur due to such modifications (Schmülling *et al.*, 2003).

Cytokinin oxidase/dehydrogenase enzymes catalyse degradation of CK free bases as well as their corresponding ribosides and ribotides (Schmülling *et al*., 2003). Adenine ring of cytokinin is attached to a binding site (a funnel-shaped region) of CKX protein (Malito *et al.*, 2004). Presence of specific amino acid residues in the binding site of CKX proteins helps to recognize specific substrates and to regulate their turnover rates (Frébort *et al*., 2011). The most active enzymes AtCKX2 and AtCKX4 bind with free cytokinin bases in neutral or slightly basic pH (Galuszka *et al.*, 2007), whereas AtCKX7 prefers cytokinin N^9-glucosides and AtCKX1 utilizes cytokinin nucleotides over free bases (Kowalska *et al.*, 2010). Recently, maize CKX enzyme, ZmCKX10, showed a higher specificity to *cis*-zeatin and cytokinin N^9-glucosides, but low preference for *cis*-zeatin ribosides (Šmehilová *et al.*, 2009).

Dihydrozeatin is not degraded by CKX activity. Therefore, reduction of *trans*- zeatin side chain may contribute to maintaining cytokinin activity, particularly in tissues with higher levels of oxidase activity. Cytokinin O-glucosides (O-glucoside or O-xyloside) are also resistant to cytokinin-degrading enzymes (Laloue and Pethe, 1982; McGaw and Horgan 1983; Laloue and Fox 1989), but can be cleaved by β-glucosidase (Brzobohatý *et al*., 1993) to form active aglycones. Both enzymes (zeatin O-glucosyltransferase and β-glucosidase) involved in glycosylation and deglycosylation are considered to play significant roles in regulating the levels of biologically active cytokinins (Frébort *et al*., 2011).

1.3.6 Cytokinin Transport and Translocation

Expression patterns of genes related to cytokinin biosynthesis, degradation and signalling suggest local synthesis and metabolism of cytokinin. However, this does not imply that every cell possesses all these CK mechanisms. As intercellular communication via signalling molecules is essential for coordinated development, cytokinin may act as a paracrine mobile signal (Hirose *et al*., 2008). Therefore, plants must have some import and export system to transport cytokinins across the plasma membrane. Till now, the members of a purine permease (PUP) family and an equilibrative nucleoside transporter (ENT) family have been reported as candidates for cytokinin transporters (Kudo *et al*., 2010).

Two members of the *Arabidopsis* purine permease (PUP) family, AtPUP1 and AtPUP2, were found to facilitate transport of cytokinin nucleobases tZ and iP, using a yeast system (Gillissen *et al*., 2000; Bürkle *et al*., 2003). AtPUP1 transporter was identified in *Arabidopsis* by functional complementation of a yeast mutant deficient in adenine uptake, which was repressed by free cytokinin bases. This competitive inhibition led to a proposed role of AtPUP1 as a possible cytokinin transporter (Gillissen *et al*., 2000). Within the PUP family, AtPUP2 is the closest relative of AtPUP1 showing 64% identity, and a full-length cDNA of *AtPUP2* was isolated by RT-PCR to study its function (Bürkle *et al*., 2003).

Eight genes (*AtENT1–AtENT8*) in *Arabidopsis* (Li *et al*., 2003) and four genes (*OsENT1–OsENT4*) in rice (Hirose *et al*., 2005) were identified showing homology with equilibrative nucleoside transporter (ENT) family. Competitive uptake studies in yeast cells revealed the

ability of AtENT3, AtENT6 and AtENT7 proteins to transport nucleosides such as iP-riboside (iPR) and tZ-riboside (tZR), but the yeast cells expressing AtENT3 and AtENT7 showed weak inhibitory effects of cytokinin nucleosides on adenosine transport. This finding suggests participation of AtENT6 in the transport of ribosides, with stronger affinity for iPR than for tZR (Wormit *et al*., 2004). OsENT2 transporter has also been shown to mediate uptake of CK nucleosides, again with a preference for iPR over tZR (Hirose *et al*., 2005).

In plants, cytokinin translocation is mediated by the transpiration flow in xylem that transports water and nutrients from soil to aerial plant parts, and by phloem that delivers photosynthates throughout the plant. A number of experiments have been performed to gain insight into the physiological roles of cytokinin translocation, but have not yet led to definitive conclusions (Hisrose *et al*., 2008; Kudo *et al*., 2010).

tZ-type cytokinins, mainly tZR, were found in xylem sap (Beveridge *et al*., 1997; Takei *et al*., 2001a). Consistent with this report, *CYP735A1* and *CYP735A2*genes were found to be expressed predominantly in roots (Takei *et al*., 2004b), suggesting roots as a main production site of tZ-type CKs. In contrast to xylem sap cytokinin, mainly iP-type cytokinins, such as iPR and iP-ribotides, were found in phloem sap (Corbesier *et al*., 2003). From these findings, a view has emerged that plants might translocate tZ-type CKs as an acropetal signal and iP-type cytokinins as a systemic or basipetal signal. This idea was supported by a recent grafting experiment performed using a quadruple *atipt1,3,5,7* mutant, which showed decreased levels of both iP-type and tZ-type cytokinins in comparison with wild-type plants (Miyawaki *et al*., 2006). Partial recovery of tZ-type cytokinins in the mutant shoot-scions were observed when grafted to wild-type root-stocks. On the other hand, the mutant root-stocks showed recovery of iP-type cytokinins from wild-type shoot-scions up to normal levels. In these reciprocal grafting experiments, the mutant phenotype (reduced cambium development and secondary growth) was also restored to wild type-phenotype, irrespective of the grafting direction (Matsumoto-Kitano *et al*., 2008).

Environmental and endogenous signals also control cytokinin translocation via xylem and phloem. Nitrate supplementation caused significant increase in tZR content and flow rate of xylem sap in barley (Samuelson *et al*., 1992) and maize (Takei *et al*., 2001b), indicating tZR function in nitrate signalling. Accumulation of *AtIPT3* transcripts in *Arabidopsis* shoot and roots was induced by nitrate (Takei *et al*., 2002, 2004a). In addition, nitrate-dependent accumulation of cytokinins was clearly reduced in an *atipt3* mutant, demonstrating that *AtIPT3* is responsible for nitrate-dependent CK synthesis. Expression analysis of *AtIPT3* in *Arabidopsis* plants showed activity in phloem companion cells rather than in xylem tissues (Takei *et al*., 2004a). Thus, a cytokinin translocation system may be operating via phloem and xylem (Kudo *et al*., 2010). Hence, a model was proposed explaining cytokinin translocation, as shown in Fig. 1.3.In summary, CK translocation is achieved by CK transport that is also mediated by the transporters of nucleobases and nucleosides.

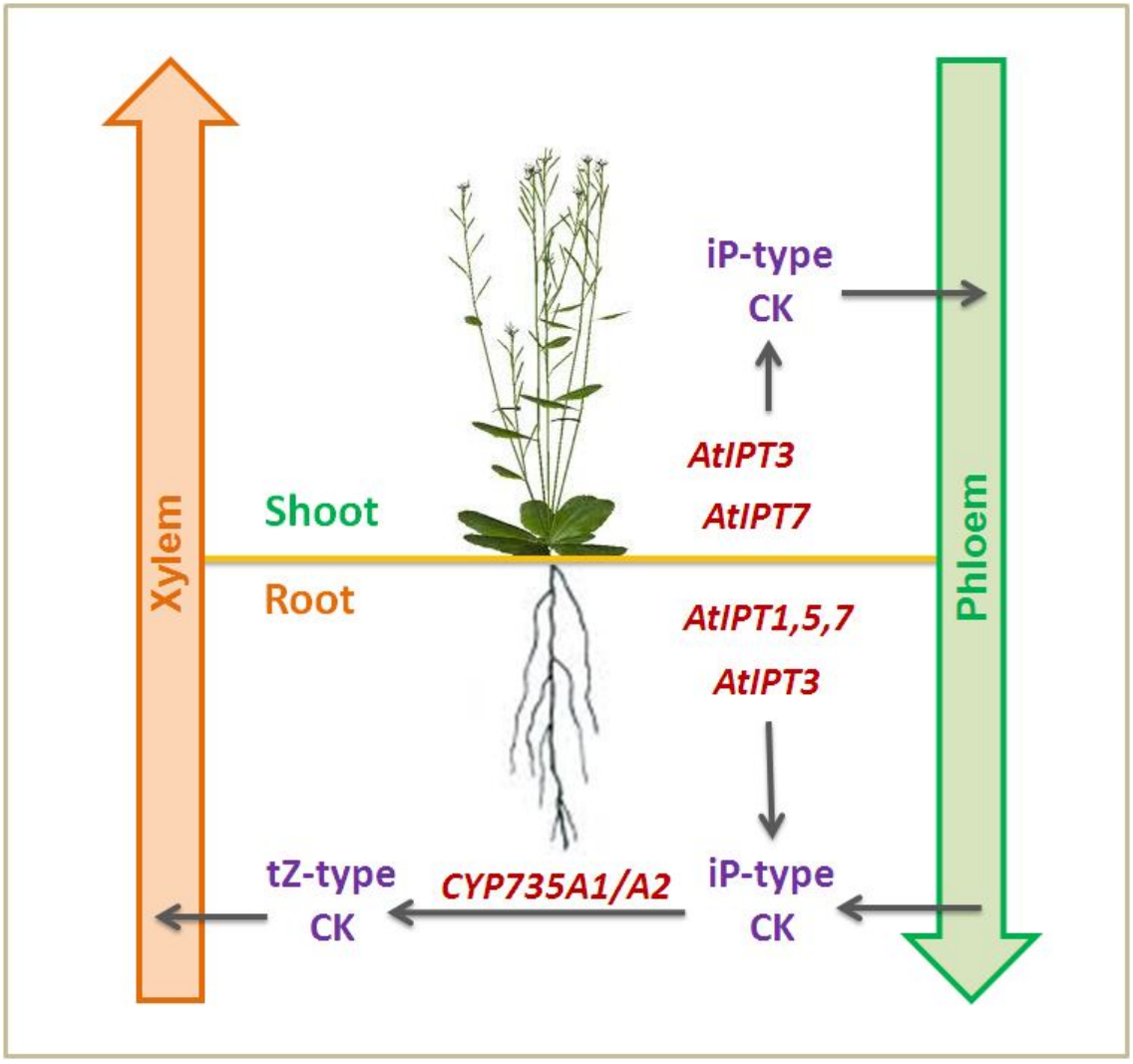

Figure – 1.3: Cytokinin Translocation Model in Arabidopsis thaliana *(Adapted and modified from Sakakibara, 2006 and Kudo et al., 2010). Expression of CK biosynthetic genes AtIPTs are tissue specific. In the vegetative phase, AtIPT3 is expressed in phloem throughout plant, AtIPT7 in trichomes and root elongation zone, AtIPT1 in root procambium and AtIPT5 in root cap and primordia. iP-type CKs synthesized in shoot are translocated through phloem (green arrow) to roots where both phloem-derived and root-derived iP-type CKs are converted to tZ-type CKs by the activity of CYP735A1 and CYP735A2 enzymes. tZ-type CKs are then transported to aerial plant part through the xylem (orange arrow).Phloem cytokinins are translocated as systemic or basipetal signal, whereas xylem cytokinins are translocated as acropetal signal.*

1.3.7 Cytokinin Signalling

Since the discovery of cytokinin as a promoter of cell division (Miller *et al*., 1955), a cytokinin signalling pathway in the model plant *Arabidopsis thaliana* emerged around the turn of the century as a two-component signalling system mediated by phosphorelay events. This CK signalling model is similar to the bacterial two-component signalling system (TCS), which simply works with two proteins using a His-to-Asp phosphorelay system. The complex version of this two-component signalling system evolved through the development of multistep phosphotransfer events involving more than two proteins. In summary, the cytokinin signalling circuit in *Arabidopsis* (Fig. 1.4) initiates with autophosphorylation of a histidine kinase (AHK) proteins, transferring a phosphoryl group through histidine phosphotransferase (AHP) proteins to aspartate-containing response regulator (ARR) proteins (Hwang *et al*., 2012; El-Showk *et al*., 2013).

***Arabidopsis* Histidine Kinase Proteins (AHKs):** The first evidence supporting a connection between cytokinin and bacterial TCS came from identification of CYTOKININ INDEPENDENT 1 (CKI1) as a transmembrane hybrid histidine kinase (HK), which was homologous to the HKs in the bacterial TCS. Overexpression of CKI resulted in cytokinin responses but independent of cytokinin in culture (Kakimoto, 1996), protoplasts and whole plants (Hwang and Sheen, 2001). A few years later, independent research of several groups succeeded in identification of the first cytokinin receptor, known as WOL1/CRE1/AHK4 (Mähönen *et al*., 2000; Inoue *et al*., 2001; Yamada *et al*., 2001). It has been shown that AHK4 functions as a cytokinin sensor in bacteria (Suzuki *et al*., 2001) and its kinase activity depends on cytokinin (Ueguchi *et al*., 2001). A search from the *Arabidopsis* genome database helped to find two AHK4 homologs, named as AHK2 and AHK3 (Yamada *et al*., 2001; Hwang and Sheen, 2001). All three cytokinin receptors are transmembrane hybrid kinase proteins with an extracellular CHASE domain sensing cytokinin, together with cytoplasmic His transmitter and receiver domains (To and Kieber, 2008).

***Arabidopsis* Histidine Phosphotransferase Proteins (AHPs):** Downstream to AHKs, phosphorelay events are passed through a multigene phosphotransfer protein family, including five authentic HP proteins (AHP1-AHP5) and one pseudo HP protein, because it lacks the conserved histidine residue. On phosphorylation, these proteins are translocated from cytosol to nucleus (El-Showk *et al*., 2013), as the translocation of AHP1 and AHP2 to nucleus has evidently happened in response to CK treatment (Hwang and Sheen, 2001).

***Arabidopsis* Response Regulator Proteins (ARRs):** Phosphorylation of ARR proteins results in cytokinin response. In *Arabidopsis*, 23 functional response regulator proteins are divided into three groups. Two groups (type-A and type-B) are known to be involved in cytokinin signalling pathway. Ten members (ARR3–ARR9; ARR15–ARR17) are included in type-A ARRs, while 11 members in type-B ARRs (ARR1–ARR2; ARR10–ARR14; ARR18–ARR21). Phosphorylation of type-B ARRs containing the DNA-binding and transactivating domains at the C-terminal initiates transcription of their targets, including type-A ARRs,

whose phosphorylation acts to stabilize them. Type-A ARRs consist of short C-terminal domains and have been shown to be upregulated transcriptionally by cytokinin treatment. However, type-B ARRs containing extra domains can activate transcription of cytokinin response genes (To and Kieber, 2008; El-Showk *et al*., 2013). Type-A ARRs are generally thought to be involved in feedback regulation of cytokinin response by inhibiting cytokinin signalling (To *et al*., 2004).

Rashotte *et al*. (2006) reported a novel class of response regulators, CYTOKININ RESPONSE FACTORS (CRFs), consisting of six closely related transcription factors. On cytokinin treatment, all CRFs have been shown to rapidly accumulate in the nucleus. This translocation is independent of ARRs downstream of HK and HP proteins, thus suggesting a branching of the two-component signalling pathway.

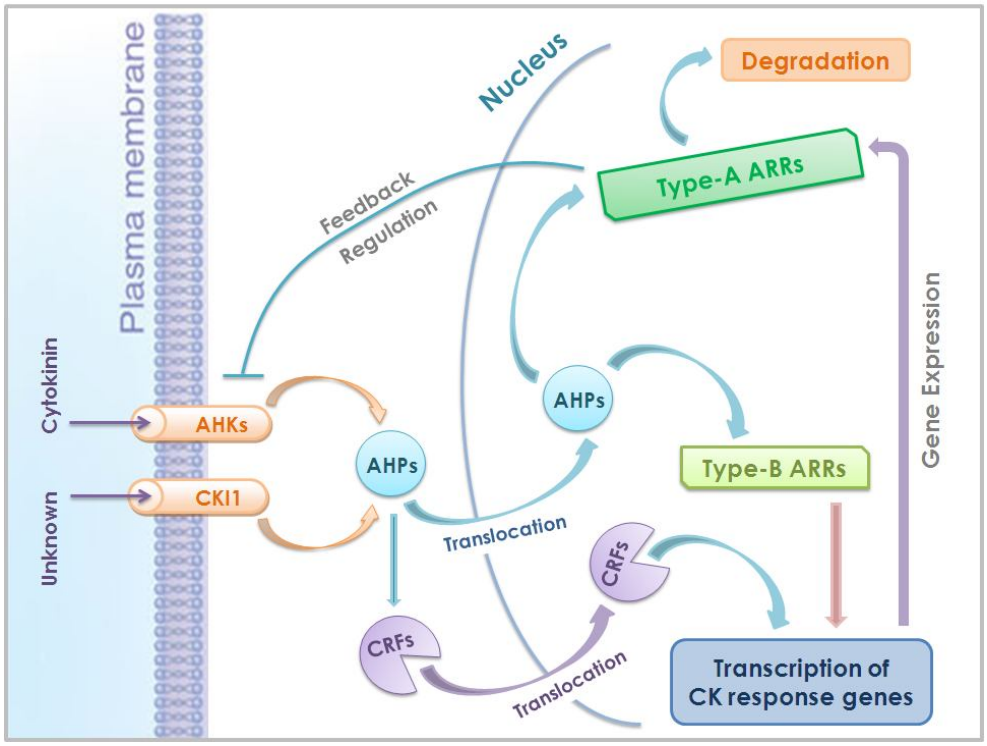

Figure - 1.4: Cytokinin Two-Component Signalling Pathway *(Adapted and modified from Santner et al., 2009). AHK and CKI1 receptors, localized in plasma membrane, perceive their respective cytokinin and unknown signals that induces phosphorylation in AHKs, which activates AHP proteins to be translocated to nucleus. Furthermore, phosphoryl group is transferred from AHP proteins to type-A or type-B ARR proteins. The former controls feedback regulation of cytokinin signalling, whereas the latter induces transcription of cytokinin-response genes, including type-A ARR genes. CRF proteins are also activated by cytokinin downstream of AHK-AHP and translocated to the nucleus to act as transcription regulators of cytokinin-response genes. Abbreviations: CKI, Cytokinin Independent; AHK, Arabidopsis Histidine Kinase; AHP, Arabidopsis Histidine Phosphotransfer Proteins; ARR, Arabidopsis Response Regulators; CRF, Cytokinin Response Factors.*

1.4 Strigolactone

1.4.1 A Plant Hormone with Past and New Functions

Strigolactone (SL) has long been of interest for scientists investigating its role as a germination stimulant for seeds of parasitic weeds, belonging to the genera *Striga* and *Orobanche*. This parasitism is one of the most serious threats and constraints to agriculture in the developing world (Tsuchiya and McCourt, 2009). Strigolactone extraction from non-host plants of parasitic weeds, following its potential to induce germination of parasitic plant seeds led to the proposal that strigolactones are ubiquitously found in higher plants, having other functions as well. This idea was supported by the isolation of strigolactone from the root exudates of *Lotus japonicus*, a host plant for mycorrihzal symbiosis. Strigolactone was shown to be required for branching of arbuscular mycorrhizal fungi to facilitate their interaction with plant roots, from which fungi get food for their survival (Akiyama *et al*., 2005).

In the absence of a natural plant parasite or a mycorrhizal interaction for some plants like *Arabidopsis* and white lupin, purification of strigolactones from such non-host plants (Goldwasser *et al*., 2008; Yoneyama *et al*., 2008) indicates that strigolactones play significant roles not only in rhizosphere communication but also they may have other important roles inside plants. Recent reports divulged a hidden function of strigolactones as a shoot branching inhibitor (Gomez-Roldan *et al*., 2008; Umehara *et al*., 2008) and led to strigolactone being considered a plant hormone. The pleiotropic phenotypes of mutants deficient in strigolactone synthesis and perception indicate that SL function is not limited to shoot branching. Indeed, strigolactone has been found to be involved in multiple additional new physiological functions such as photo-morphogenesis, root development, leaf senescence, secondary growth of root and shoot, karrikin signalling and adaptation to environment (Seto *et al*., 2012).

1.4.2 Chemical Nature and Types of Strigolactone

The chemical nature of a germination stimulant was revealed first time when strigol was isolated from root exudates of Cotton. Strigol was observed to stimulate germination at a very low concentration. Subsequently strigol was extracted from the roots of host plants including sorghum, maize and millets. Subsequently, sorgolactone and alectrol were isolated from sorghum and cowpea, and orobanchol from red clover and solanacol from tobacco. This wide range of chemicals suggests that strigolactones are utilized by parasitic weeds as germination stimulant (Humphrey *et al*., 2006; Yoneyama *et al*., 2009; Yokota *et al*., 1998).

Until now, fifteen chemical substances related to strigol have been purified and structurally characterized (Ruyter-Spira *et al*., 2013). Collectively, all members are classified as strigolactones (Yoneyama *et al*., 2009). The core structure of strigolactone (Fig. 1.5) is comprised of four rings (A-D). Bioactivity of strigolactones depends on the presence of the

C-D ring, which is highly conserved. Considerable variations are found in the A and B rings due to different side groups attached to them (Ruyter-Spira, *et al*., 2013). Synthetic analogues of strigolactones include GR24, GR5 and GR7 (Xie *et al*., 2010).

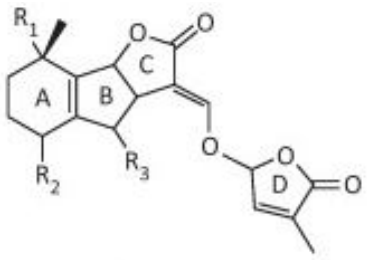

Figure - 1.5: Structure of Strigolactone *(taken from Ruyter-Spira et al., 2013).*

1.4.3 Biosynthesis of Strigolactone

Although SLs were identified a long time ago, very limited information is available about their biosynthetic pathway. Strigolactone in higher plants was proposed to be synthesized in plastids from carotenoid pigment molecules (Booker *et al*., 2004; Matusova *et al*., 2005). The root exudates of maize and cowpea treated with fluridone, a carotenoid synthesis inhibitor, showed a lower stimulating activity for germination of *Striga* seeds. In addition to this, significantly reduced activity in inducing seed germination of striga weed was observed from root exudates of some mutants involved in carotenoid metabolism. These findings suggested a carotenoid-derived biosynthesis of strigolactone (Matusova *et al*. 2005).

Two studies, reported in 2008, showed that strigolactone is a novel plant hormone involved in shoot branching inhibition, using shoot branching mutants defective in carotenoid cleavage dioxygenases (CCD7 and CCD8) and Cytochrome P450 enzymes. These studies demonstrated that branching phenotypes of mutants could be suppressed by the application of GR24, a synthetic analog of strigolactone (Gomez-Roldan *et al*., 2008; Umehara *et al*., 2008). Although shoot branching mutants had been reported for a long time, it was not until 2008 that shoot branching mutants were correlated with SL biosynthesis catalyzed by CCD7, CCD8 and Cytochrome P450 enzymes. The orthologs of CCD and Cytochrome P450 enzymes have been identified in different higher plants (Dun *et al*., 2009 and Beveridge and Kyozuka, 2010). Recently, another SL-deficient mutant, d27, has been characterized in rice and *Arabidopsis* (Lin *et al*., 2009; Waters *et al*., 2012). D27 gene encodes an iron-containing protein, which is found to be localized to chloroplasts (Lin *et al*. 2009).

Primary steps in SL biosynthetic have been shown to be catalyzed by three biosynthetic enzymes, D27, CCD7 and CCD8, which are localized in plastids (Alder *et al*. 2012). Previously, all-trans-β-carotene was found to be a substrate of an *Arabidopsis* CCD7/MAX3 enzyme (Schwartz *et al*., 2004; Booker *et al*., 2005; Auldridge *et al*., 2006a; Auldridge *et al*., 2006b). However, it has now been demonstrated using CCD7 proteins from *Arabidopsis*, pea

and rice that 9-cis-β-carotene is a better substrate for CCDs than all-trans-β-carotene to produce an apocarotenoid. Further to this, D27 protein was characterized to be involved in isomerization of all-trans-β-carotene into 9-cis-β-carotene, which provides an efficient substrate for CCD7. In the next step, the reaction product of CCD7, apocarotenoid, was oxidized by CCD8, resulting in production of a SL intermediate compound named carlactone. Rescue of branching phenotypes of rice *d27* and *d10*mutants with the exogenous application of carlactone supported the idea that carlactone is an intermediate in the SL biosynthetic pathway (Alder *et al*., 2012). Regardless of many unclear questions related to activity of carlactone, its detection is a major step towards understanding of SL biosynthetic pathway (Seto *et al*., 2012).

As further oxidation of carlactone is required to be converted finally to SLs, SL biosynthetic pathway was explained by grafting experiments, in which a shoot branching phenotype was restored using an *Arabidopsis* Cytochrome P450 mutant, *max1*, as a rootstock and *max3* or *max4* as a scion. This result indicates that MAX1 acts downstream of MAX3 and MAX4, and the substrate of MAX1 can move from roots to shoots (Booker *et al*. 2005). The current evidence suggests that MAX1 may be responsible for oxidation of carlactone. The reasoning is that there would be no response of *max1* mutant plants to exogenously applied carlactone, if carlactone exists downstream of MAX1. Taking the structures of carlactone and SLs into consideration, it is expected that there may be more uncharacterized enzymes (one or two) to complete SL biosynthesis (Seto *et al*., 2012). Figure 1.6 illustrates a newly proposed SL biosynthetic pathway in *Arabidopsis* with the orthologous genes in other species.

1.4.4 Biosynthetic Inhibitors

Strigolactone was proposed to be derived from carotenoids, using fluridone, a chemical inhibiting carotenoid biosynthesis. Therefore, the compounds like fluridone and norflurazon, could be used to decrease SL production (Matusova *et al*., 2005). As these chemicals have herbicidal effects, it is better to find compounds that could inhibit the intermediate steps of SL biosynthetic pathway. Recently developed SL biosynthetic inhibitors are categorized into two groups, CCD inhibitors and Cytochrome P450 inhibitors. Related to first group, Hydroxamic acid was synthesized and tested for effects on *Arabidopsis* CCDs (Sergeant *et al*., 2009). Treatment of *Arabidopsis* with these inhibitors resulted in an increased shoot branching, similar to phenotype of *ccd7/8* mutants, suggesting these chemicals as SL biosynthetic inhibitors. Related to second group, a triazole-type lead chemical, TIS13, was discovered to inhibit SL biosynthesis in rice (Ito *et al*., 2010). Application of this chemical on rice seedlings decreased SL levels effectively in roots tissues and in root exudates. It was also able to trigger tiller bud outgrowth in a dose-dependent manner. However, treatment with TIS13 also resulted in growth retardation. To make more specific inhibitors from TIS13, its structure was modified and renamed as TIS108, which was shown to be more potent and specific to SL biosynthesis (Ito *et al*. 2011). Although TIS108 was able to reduce SL levels in root tissues and root exudates, it did not decrease plant height (Seto *et al*., 2012).

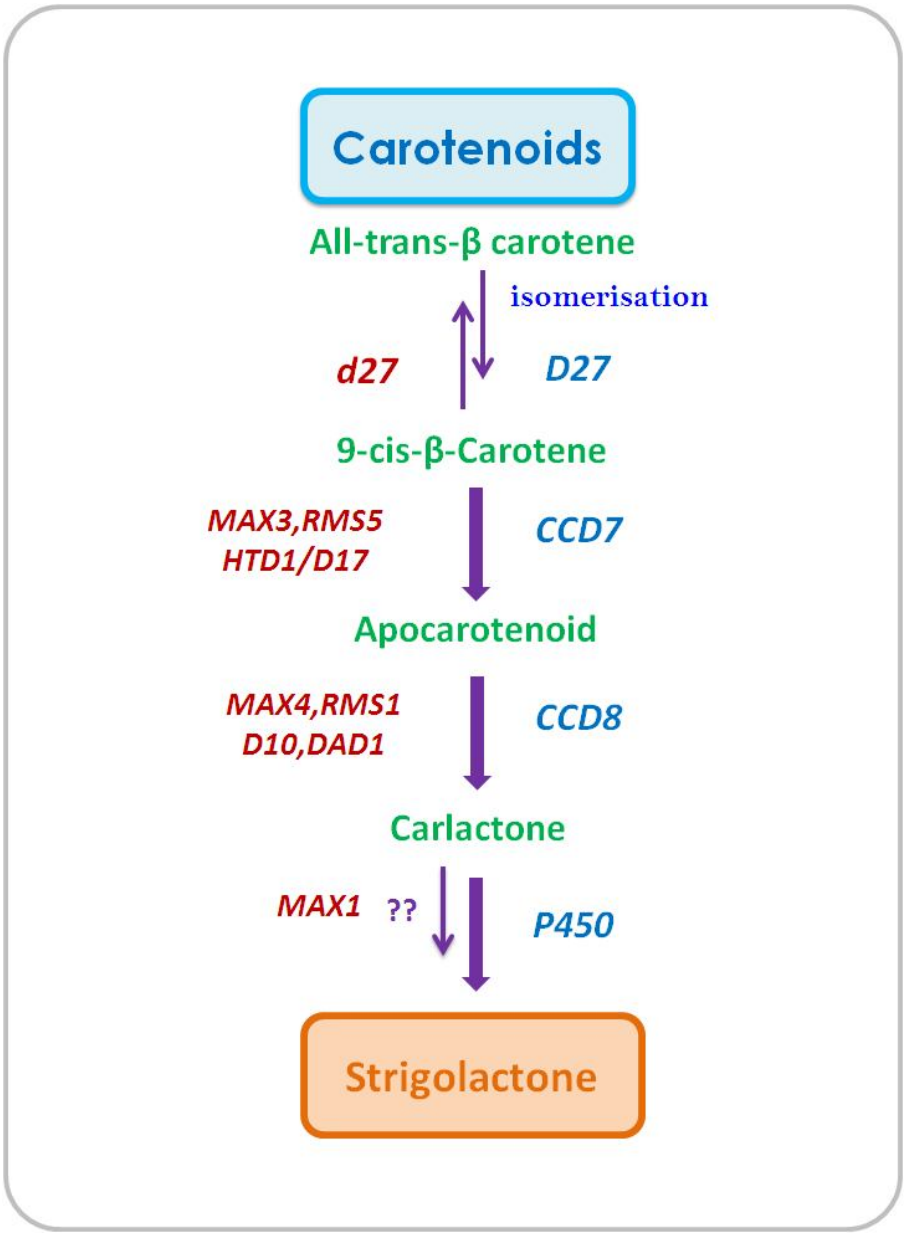

Figure - 1.6: Current Pathway of Strigolactone Biosynthesis *(Adapted and modified from Brewer et al., 2013 and Seto et al., 2013). MAX (More Axillary Shoots) genes in Arabidopsis and RMS (Ramosus) genes in pea, D (Dwarf) genes in rice and DAD (Decreased Apical Dominance) genes in petunia. The stepwise conversion of all-trans-β-carotene into carlocatone is catalyzed by D27, CCD7 and CCD8 enzymes. Strigolactone is produced by the unknown enzymes, which may include Cytochrome P450.*

1.4.5 Strigolactone Perception

The signal transduction pathway of strigolactone is still very poorly known. Only two proteins have been identified in both monocots and dicots. One protein belongs to F-box protein family and known as MAX2 in *Arabidopsis* (Stirnberg *et al*., 2002; Stirnberg *et al*., 2007), D3 in rice (Ishikawa *et al*., 2005) and RMS4 in pea (Johnson *et al*., 2006). The other protein related to α/β-fold hydrolase family is identified as D14 in rice (Arite *et al*., 2009) and DAD2 in petunia (Hamiaux *et al*., 2012). Both proteins are thought to be candidates for the strigolactone receptors (Ruyter-Spira, *et al*., 2013). Recently, a TCP transcription factor *BRC1* (*BRANCHED1*) identified in *Arabidopsis* (Aguilar-Martínez *et al*. 2007) and in pea (Braun *et al*., 2012) that is closely related to *TEOSINTE BRANCHED1* (*TB1)* from maize (Hubbard *et al*., 2002). It has been shown to act downstream of SL to control axillary bud outgrowth.

1.5Auxin

1.5.1 Functions of Auxin

The signalling molecule auxin is involved in controlling numerous aspects of plant growth and development as well as defense mechanism (Santner *et al*, 2009; Mockaitis and Estelle, 2008). The multiple functions of this plant hormone include flower initiation, embryo and fruit development, phyllotaxis, apical dominance, phototropism and gravitropism, pathogen interaction, root growth and lateral root development (Vogler and Kuhlemeier, 2003).

1.5.2 Auxin Transport

The most abundant and physiologically most active endogenous auxin is indole -3- acetic acid (IAA) (Mockaitis and Estelle, 2008; Kende and Zeevaart, 1997). It is synthesized in young developing plant parts like shoot apex, young leaves and developing seeds (Ljung 2001; Ljung 2002), and functions as a mobile signal in spatial and temporal coordination of plant development (Zažímalová *et al*., 2007). The meristems of primary root tip and developing lateral roots have also been shown to be sites of auxin production (Ljung *et al*., 2005). From the sites of synthesis, auxin is distributed to all plant parts, thus it needs a transport system (Michniewicz *et al*., 2007). Due to mobility along with local asymmetric distribution of auxin (Tanaka *et al*., 2006), it controls a broad spectrum of physiological effects and developmental process (see section 1.2.1) from root to shoot in vegetative and reproductive phases (Zažímalová *et al*., 2007), hence involved in shaping the plant (Friml, 2003a). Auxin can be distributed through two distinct transport pathways; one is a fast, passive and non-polar system in phloem (Cambridge and Morris, 1996) and the other is a slower, active and cell-to-cell polar system in cambium and xylem parenchyma cells (Blakeslee *et al*., 2005).

1.5.2.1 Non-polar transport

Radioactively labeled auxin is loaded into phloem when applied directly to leaves. Auxin is transported passively and moves relatively fast at 5-20cm/h. IAA was detected in xylem but only in traces, thus auxin translocation through xylem seems to be minimal (Baker, 2000). Auxin moving in phloem sap is unloaded to different tissues and organs and enters another transport system i.e. polar auxin transport to redistribute to the site of action (Cambridge and Morris, 1996). Non-polar passive transport of auxin through phloem is important and significant for long-distance auxin translocation especially in larger plant species (Michniewicz *et al.*, 2007).

1.5.3.2 Polar transport

In bryophytes and all higher plant species, a polar auxin transport (PAT) system has been found, and characterized by its strict directionality and polarity. PAT requires energy to move auxin actively from cell to cell in a polar manner. This form of auxin transport is slower than phloem with a velocity of 5-20 mm/h. PAT can be categorized into two types; long distance and short distance. The former is along the whole body of plant and the latter is within specific tissues. Both types of PAT use the same mechanism of polar transport (Michniewicz *et al*., 2007).

Chemiosmotic Model of polar transport

The mechanism of polar auxin transport was explained from the chemical nature of auxin and from early physiological studies, from which a chemiosmotic model (Fig.1.7) was formulated in the 1970s (Rubery and Sheldrake, 1974; Raven, 1975; Friml and Palme, 2002). According to the model, a proton gradient is generated across plasma membrane through proton pumps localized in the membrane. Due to the proton gradient, a pH difference between apoplast of extracellular space and cytoplasm in cell is created by membrane H+-ATPases. Auxin (IAA) being a weak acid undergoes a reversible dissociation, with an equilibrium which is dependent on pH. In the acidic pH (5.5) of apoplast, some of IAA (approximately 16%) is protonated and this hydrophobic IAA can pass through plasma membrane passively into a cell. The passive transport is facilitated by auxin influx carriers. In basic environment of cytoplasm, most IAA (> 99%) is dissociated into anionic form and becomes unable to pass though plasma membrane, hence it is trapped inside the cell and can only be transported actively out of the cell through auxin efflux carriers, asymmetric localization of which were explained as polar diffusion model (Robert and Friml, 2009; Tanaka *et al*., 2006; Zažímalová *et al*., 2007; Vieten *et al*., 2007; Michniewicz *et al*., 2007).

1.5.3.3 Auxin Transport Proteins

Different classes of auxin transporters have been identified which comprise AUX1 protein, PGP proteins and PIN proteins.

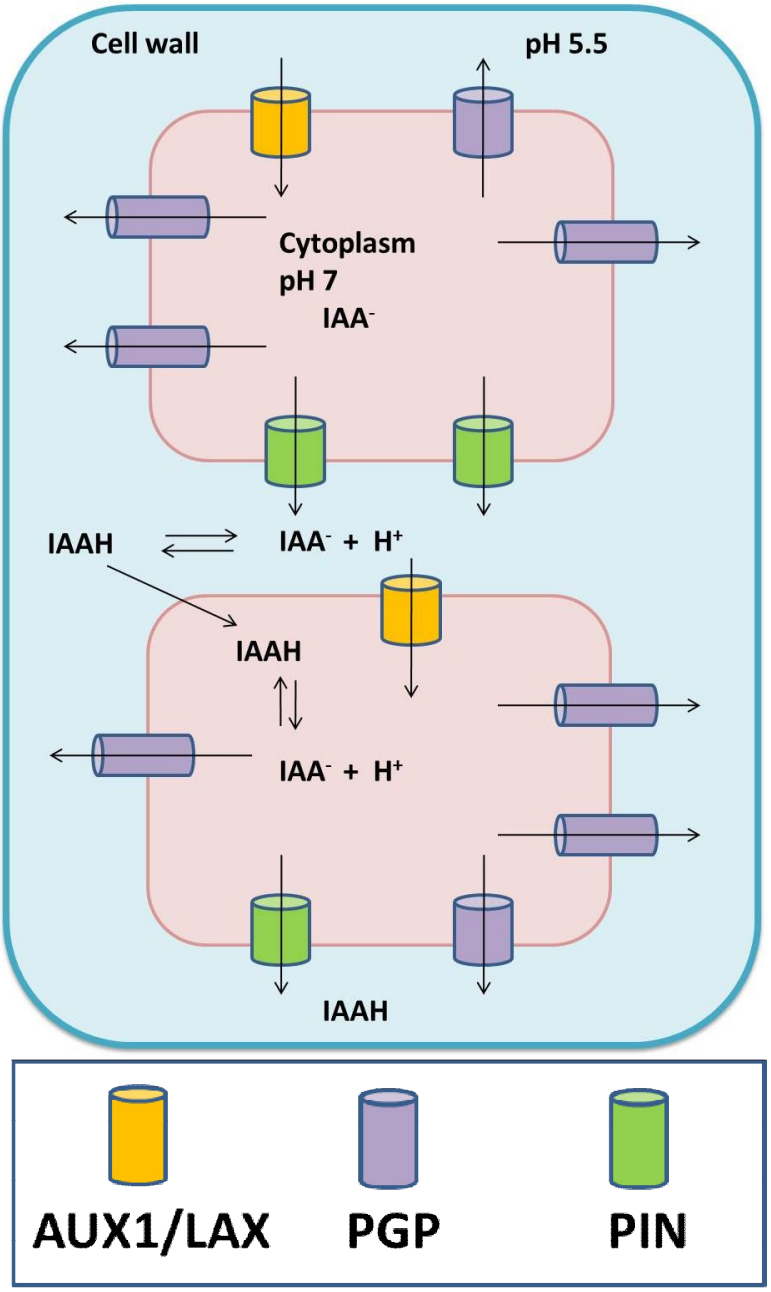

Figure – 1.7: Chemiosmotic Model of Polar Auxin Transport *(Adapted from Robert and Friml, 2009). According to the model, in the acidic pH (5.5) of apoplast, IAA is protonated and diffuses passively into the cell through auxin influx carrier protein AUX1/LAX. At the basic pH of cytoplasm, IAA is dissociated and ionic form of auxin (IAA^-) is generated which get trapped inside the cell and requires energy to leave the cell via auxin efflux proteins PGPs or PINs. The polar localization of PIN proteins in cell membrane determines the direction of intercellular auxin transport.*

AUX1/LAX proteins: *AUXIN1* (*AUX1*) gene, identified in a screen for auxin resistant and agravitropic mutants (Maher and Martindale, 1980), encodes a protein that is localized across plasma membrane and significantly similar to plant amino acid permeases. This similarity supported and suggested its function as an influx carrier of tryptophan like IAA (Bennett *et al*., 1996; Swarup *et al*., 2004). Evidence for the role of AUX1as an auxin uptake carrier came from experiments using *Xenopus* oocyte expression system in which *AUX1*-expressing oocytes exhibited increased uptake of radio-labeled IAA that was decreased by application of auxin influx specific inhibitors 1-NOA and 2-NOA but not by auxin-efflux inhibitors NPA or TIBA. Moreover substrate affinity experiments have proved AUX1 as a specific auxin influx carrier (Yang *et al*., 2006).

AUX1 protein plays a role in root basipetal auxin transport as well as in acropetal transport toward the organ apex in the phloem transport stream. AUX1 is highly localized within cell membrane of protophloem, columella, lateral root cap and epidermal cells in *Arabidopsis* root tips. A uniform distribution of AUX1 around all sides of the cells has been found in most of these tissues, but was shown to be enriched only on upper sides of the cells in protophloem. This is hypothesized, on the basis of its expression in protophloem, to be involved in unloading auxin from the mature phloem through protophloem into PAT system of root meristem (Swarup *et al*., 2001). Therefore, influx carrier protein AUX1 would develop a link between non-polar and polar auxin transport routes.

Three other *LIKE-AUX1* (*LAX*) genes have been characterized in *Arabidopsis*. The AUX1/LAX proteins act as influx carriers and play roles in root growth, tropisms and organogenesis (Robert and Friml, 2009; Swarup *et al*., 2008; Parry *et al*., 2001).

PGP proteins: Phosphoglycoproteins (PGPs), involved in auxin transport, are plant orthologs of the mammalian B-type ATP binding cassette (ABCB) transporters of the multidrug resistance/phosphoglycoprotein (ABCB/MDR/PGP) protein family (Noh *et al*., 2001; Verrier *et al*., 2008). Members of MDR/PGP protein subfamily (AtPGP1, AtPGP2, AtPGP4, AtPGP10 and AtPGP19) were identified and isolated as proteins binding to auxin transport inhibitor NPA. PGP protein function to mediate auxin cellular efflux (Geisler *et al*., 2005; Cho *et al*., 2007; Murphy *et al*., 2002; Terasaka *et al*., 2005; Santelia *et al*., 2005; Geisler and Murphy, 2006).

PIN proteins: In the early nineties, an *Arabidopsis* mutant with its unique characteristic needle-like inflorescence lacking flowers was identified and named as *pinformed1* (*pin1*) mutant. This phenotype resembles that of wild type plants treated with auxin transport inhibitor. A significant decrease in basipetal auxin transport was observed in *pin1* mutant that suggests its function in auxin efflux (Okada *et al*., 1991). Therefore, PIN1 appeared to play an important role in polar auxin transport. In support of this role, polar localization of PIN1 protein has been found in plasma membrane at the base of xylem parenchyma cells in primary stem, which explains an efficient basipetal transport of auxin from shoot to root (Gälweiler *et al*., 1998; Petrasek *et al*., 2006; Wisniewska *et al*., 2006).

Since PIN1 protein has been identified, seven (PIN2-PIN8) other members of PIN protein family have been characterized in *Arabidopsis* (Vieten *et al*., 2007; Zažímalová *et al*., 2007). Out of eight PIN proteins, five (PIN1, PIN2, PIN3, PIN4 and PIN7 proteins) are localized at cell membrane and function as auxin efflux carriers (Mravec *et al*., 2008; Petrášek *et al*., 2006). PIN homologs have also been identified in other monocot and dicot plant species (Paponov *et al*., 2005; Zažímalová *et al*., 2007)

The most interesting feature of PIN proteins, which fits well with the chemiosmotic model of polar auxin transport (Fig.1.1), is their asymmetric transmembrane localization at the lower sides of cells (Friml *et al*., 2003b; Vieten *et al*., 2007). Experiments investigating PIN polarity and monitoring auxin transport correlated the direction of intercellular auxin flow with the polar localization of PINs (Wiśniewska *et al*., 2006).

1.6 Roles of Hormones in Controlling Shoot Branching

1.6.1 Role of Auxin

The earliest studies on apical dominance from a system developed with two-branched pea and bean plants showed that removal of the primary shoot just above the cotyledons initiated lateral bud outgrowth. Therefore, it was suggested that an unknown signal coming from the dominant primary shoot inhibited outgrowth of axillary buds (Snow, 1931). Later on, an experiment, in which application of indole-3-acetic acid (IAA) to the decapitated stump of *Vicia* spp. plants inhibited axillary bud outgrowth, led to the proposal of auxin as a signal coming from shoot apex (Thimann and Skoog, 1934). Decapitation of shoot apex (a biosynthetic site of auxin) implies removal of a main source of auxin supply. Further investigations revealed the mechanisms of auxin controlling shoot branching. Application of auxin-transport inhibitor TIBA (2, 3, 5-triiodobenzoic acid) in lanolin to the stem of an intact plant minimized the effect of apical dominance (Snyder, 1949). Suppression of axillary buds outgrowth was not observed when 2,4-dichlorophenoxyacetic acid, which cannot be transported basipetally in plants, was applied to decapitated stump (Brown *et al*., 1979). These findings suggested that the inhibition of axillary bud outgrowth was due to basipetal flow of auxin derived from the shoot apex.

Although the mechanism of auxin polar transport is well understood, it is still to be explained how shoot derived auxin flow causes axillary buds to be dormant. In pea, expression of *PsPIN1* gene was found specifically in the nodal stem and after decapitation, decreased IAA levels in the stem was observed as a result of reduced *PsPIN1* expression. With the recovery of auxin transport due to its synthesis in growing axillary buds, *PsPIN1*expression in the stem is also recovered. Both the levels of IAA and *PsPIN1* expression showed similar trend by being low in axillary buds during dormancy and high in growing axillary buds. These findings suggest that auxin transport in the stem is correlated with the *PsPIN1* expression pattern, both before and after decapitation (Tanaka *et al*., unpublished reviewed by Shimizu-Sato *et al*., 2009).

The evidence in support of a key role of auxin transport in bud dormancy have been reported to show a strong link between auxin export from axillary buds and the phenomenon of shoot branching (Morris, 1977; Li and Bangerth, 1999; Balla *et al*., 2011). The mechanism of auxin export required for bud activation can be explained by the canalization-based model of auxin transport, which was proposed by Sachs (1981).Initially this canalization hypothesis was suggested to explain a wide range of processes involving auxin transport streams between auxin sources and auxin sinks. The process of canalization has been described as the initial flow of auxin from a source to a sink into files of cells with high level of auxin transport polarized towards the auxin sink. Such cell files result in the formation of auxin transport canals, connecting the source to the sink. Later on, these canals may differentiate into vascular strands. A positive feedback regulation of auxin flow is a core mechanism of canalization, in which auxin flux controls polarization and upregulation of its own active transport in the direction of the flux. Auxin moving down in main stem would lower sink strength of the stem resulting in reduced basipetal auxin flow between bud and the main stem. A bud will remain dormant, if auxin flow is too low to trigger the positive feedback mechanism. Recently, non-polar localization of PIN1 protein has been observed in dormant buds, but upon breaking of bud dormancy PIN1 protein is polarized into cell files connecting auxin flow from the axillary bud to PAT in the main stem (Prusinkiewicz *et al*., 2009; Kalousek *et al*., 2010; Balla *et al*., 2011).

Direct application of auxin to axillary buds cannot suppress bud outgrowth after decapitation. Additionally, radiolabeled auxin does not enter the axillary buds when applied to decapitated stump (Hall and Hillman 1975). These findings indicate basipetal auxin transport in the stem and indirect mode of auxin action to control the bud dormancy (Morris 1977). However, a mechanism of auxin action in this process is still unclear.

The indirect mode of auxin action to inhibit bud outgrowth suggests that site of auxin action is located outside the bud. Recent studies have proposed the sites for auxin action. Mutation in a signalling gene *AXR1* (auxin resistant1) caused increased shoot branching (Stirnberg *et al*., 1999). Experiments performed with isolated nodes indicate that the inhibition of bud outgrowth can be mediated by auxin acting in the stem. In this system, apical application of auxin induces bud outgrowth inhibition, which is dependent on polar auxin transport (Chatfield *et al*., 2000). But apically applied auxin does not have such inhibitory effects on the individual buds carried on isolated nodes of *axr1-12* plants. This finding supports the assumption that branching phenotype of *axr1-12* mutant is not the outcome of secondary effects from increased node number, reduced fertility and/or differences in the root development (Stirnberg *et al*., 1999).

In *Arabidopsis*, reciprocal grafting between wild-type and *axr1-12* mutant reported the shoot to be the site for auxin action to suppress shoots branching. Several tissue-specific promoters were used to determine specific site for auxin action. One of them is 4-coumarate-CoA ligase1 (4CL1), which is expressed in xylem cells. Expression of 4CL1 promoter was observed in *Arabidopsis* plants carrying 4CL1::GUS construct. GUS staining was found in the parenchymatous cells surrounding xylem vessel and the interfascicular region between

vascular bundles. When a 4CL1::AXR1 construct was introduced in *axr1-12* background, the branching pattern in *axr1-12* plants was restored to the wild-type pattern. This finding demonstrates xylem and/or interfascicular tissue is the site of auxin perception for the inhibition of bud outgrowth (Booker *et al*., 2003).

1.6.2 Role of Cytokinin

Cytokinin is well known to release axillary buds from dormancy. Contrary to the indirect mode of auxin action to arrest bud growth, cytokinin acts directly in buds to break dormancy, as it has been shown that direct application of exogenous cytokinin to axillary buds induces axillary bud outgrowth (Sachs and Thimann, 1967). Transformation of the *ipt* gene from *Agrobacterium tumefaciens* under the control of a heat-inducible promoter (maize hsp 70) into tobacco and *Arabidopsis* resulted in elevated CK levels, with plants exhibiting reduced apical dominance (Medford *et al*., 1989). After decapitation in chickpea, axillary bud outgrowth was correlated with increasing CK levels (7-fold within 6 h and 25-fold within 24 h) in the axillary buds (Turnbull *et al*., 1997). In another study, a marginal increase in CK levels was observed in the actively growing buds of *Lupinus angustifolius* (Emery *et al*., 1998). In an activation tagging experiment, a petunia *sho* (shooting) mutant was isolated with the phenotype of enhanced shoot branching and reduced apical dominance. This specific phenotype was associated with increased CK levels as a result of enhanced expression of *SHO*, encoding a protein with homology to isopentenyl transferases (IPTs). The same phenotypic effects were observed when *SHO* was expressed in tobacco plants (Zubko *et al*., 2002). Despite a number of results indicating cytokinin as a promoter of shoot branching, it was unclear whether cytokinin acts as a long distance signal or as a local signal in controlling axillary bud outgrowth.

Role of root-derived cytokinin as a long distance signal to regulate shoot branching remains a matter of debate. Cytokinins synthesized in roots (Chen *et al*., 1985) are transported through the xylem transpiration stream to the shoot (Ongaro and Leyser, 2008; Shimizu-Sato *et al*., 2009). It has been reported that CK levels in xylem sap were increased after decapitation in bean (Bangerth, 1994; Li *et al*., 1995), which leads to the suggestion that root-derived CK triggers axillary bud outgrowth after decapitation. The idea of CK action as a local signal was supported by two reports. Faiss *et al*. (1997) showed that the growth of single buds in tobacco was caused by *Agrobacterium ipt* gene expression, induced locally in the lateral buds. They also performed grafting experiments using wild-type shoot with CK overproducing rootstocks and found no increase in cytokinin levels in the shoot; rather the effects of elevated cytokinin were restricted onto the root phenotype only. To avoid possible problems related to transport in the grafts, a dexamethasone-inducible/tetracycline-repressible expression system of bacterial *ipt* gene was used in tobacco. The *ipt* gene induced in tobacco plants released the axillary buds from dormancy and following application of tetracycline to leaf axils immediately arrested the axillary bud outgrowth, which was due to downregulation of *ipt* gene expression. These results demonstrated that locally produced cytokinin is sufficient for

bud outgrowth (Böhner & Gatz, 2001). Consequently, it was concluded that cytokinin acts as a paracrine signal in reducing apical dominance.

Experiments performed by Tamas and co-workers showed locally controlled axillary bud outgrowth, as it was observed in excised stem segments inserted into a control medium without hormones that bud growth was activated and in about ten days, the axillary buds were mostly between 200-400% of their initial length (Tamas *et al.*, 1989). Cytokinin is synthesized locally in nodal stem to act as a paracrine signal involving in the regulation of axillary bud outgrowth. The first supporting evidence came from experiments on pea (Tanaka *et al.*, 2006), in which it has been shown that two CK biosynthetic *IPT* genes of pea (*PsIPT1* and *PsIPT2*) are differentially expressed in the nodal stem, before and after decapitation. Expression of both genes was induced rapidly in the stem but not in the axillary buds after decapitation. Measurement of CK levels in the nodal stems and axillary buds revealed that CK levels were increased firstly in the nodal tissue and later in the axillary buds as well. These findings lead to the conclusion that the nodal stem is a site for CK synthesis that is physiologically relevant to activation of bud outgrowth, and implicate a role of CK transport into axillary buds.

1.6.3 Role of Strigolactone

The earliest investigations on shoot branching indicated that two mobile signals moving in opposite directions might be involved to inhibit bud outgrowth. One of them must be moving down in the stem from shoot apex and the other must be acropetally transported. Later on, the inhibitory signal producing in shoot apex was found to be auxin, whose indirect mode of action confirmed the involvement of another inhibitory signal to act directly on buds to arrest their growth (Snow, 1931; Snow, 1929 and 1932, Le Fanu, 1936; Snow, 1937). Recent identification of strigolactone as an inhibitor of shoot branching (Gomez-Roldan *et al.*, 2008; Umehara *et al*. 2008) supports the previous hypothesis proposed by Snow, as exogenous application of strigolactones suppressed the bushy phenotypes of SL-deficient mutants. These newer studies reported significantly reduced levels of strigolactones in the roots of branching mutants of *Arabidopsis* (*max*), pea (*rms*) and rice (*dwarf*). Previously, SL quantification in different tissues revealed that levels of strigolactones were relatively high in roots as compared to those in other tissue types, such as hypocotyl, stem and leaves (Yoneyama *et al*., 2007). Moreover, expression studies of SL biosynthetic and signalling genes in rice and *Arabidopsis* demonstrated that roots are the sites of SL production and perception (Arite *et al*., 2007; Zou *et al*., 2006; Sorefan *et al*., 2003; Bainbridge *et al*., 2005; Brady *et al*., 2007). In addition, detection of SL in xylem sap of *Arabidopsis* suggests a long distance SL transport from roots (Kohlen *et al*., 2011). This upward transport, strictly from root to shoot and not from shoot to root, has been demonstrated by grafting experiments (Foo and Davies, 2011). These findings confirm strigolactone as another inhibitory signal, suggested in the initial studies on the phenomenon of apical dominance.

Contrary to auxin, the mode of SL action is direct, as direct application of a synthetic SL, GR24 to axillary buds suppresses bud outgrowth (Gomez-Roldan *et al*., 2008; Brewer *et al*., 2009; Braun *et al*., 2012; Dun *et al*., 2012). It has been demonstrated that SLs supply to roots through hydroponics or growth media can arrest bud growth (Gomez-Roldan *et al*., 2008; Umehara *et al*., 2008; Brewer *et al*., 2009; Crawford *et al*., 2010). To explore further the mechanism of SL function in bud outgrowth inhibition, reciprocal grafting experiments were performed using SL-deficient branching mutants and wild-type plants. These grafting studies have shown that root-derived SLs transported through xylem can inhibit bud outgrowth. However, it has also been shown that xylem-transported SLs are not necessary to suppress branching, but local production and perception of SLs in the stem can be sufficient to inhibit bud outgrowth (Napoli, 1996; Beveridge *et al*., 1997a; Beveridge *et al*., 1997b; Turnbull *et al*., 2002; Stirnberg *et al*., 2007). Consistent with this, expression of SL biosynthetic genes *MAX4* and *MAX1*, and a signalling gene *MAX2* have been reported in the *Arabidopsis* nodal stem close to axillary buds (Sorefan *et al*., 2003; Stirnberg *et al*., 2007; Ruyter-Spira*et al*., 2013). Moreover, the recently identified SL transporter PDR1 from petunia has been shown to be expressed in nodal tissues adjacent to leaf axils but not in axillary buds (Kretzschmar *et al*., 2012).

1.6.4 Interplay between Auxin, Cytokinin and Strigolactone

Since the mode of auxin transported basipetally in the stem is indirect as auxin does not enter axillary buds (Hall and Hillman 1975; Morris, 1977), two hypotheses have been proposed to explain auxin indirect regulation of bud activity. According to the canalization theory, auxin transport in the main stem can regulate axillary buds to establish their own polar auxin transport (PAT) streams to export auxin from the buds into the stem (Domagalska & Leyser, 2011). This theory has been supported by these findings that use of auxin transport inhibitors reduces apical dominance (Chatfield *et al*., 2000; Snyder 1949), apically applied auxin does not inhibit bud outgrowth in the presence of auxin transport inhibitors (Chatfield *et al*., 2000), and auxin is exported from the activated buds due to polarization of PIN1 in the buds (Balla *et al*., 2011). In contrast, the second messenger theory suggests that auxin regulates levels of an upwardly mobile signal that enters the bud to control its activity (Sachs & Thimann, 1967). In support of the latter model, cytokinin and strigolactones have been found as good candidates for second messengers that can act directly in buds.

Auxin-Cytokinin Crosstalk: The auxin-cytokinin relationship comes from the studies exploring the mechanisms underlying interactions between auxin and CK in the control of shoot branching. Firstly, it was shown that decapitation of bean (*Phaseolus vulgaris*) resulted in increased CK levels in xylem sap transported from roots (Bangerth, 1994) and application of synthetic auxin NAA (1-naphthylacetic acid) blocked this increased CK transport (Li *et al*., 1995). It was thought that auxin might control CK supply to buds through regulation of CK synthesis. In support of this view, increase in CK levels was observed in the actively growing buds after decapitation (Turnbull *et al*., 1997) and auxin-overproducing lines

showed low CK levels (Eklöf *et al*., 1997). Nordström *et al*. (2004) also showed a significant reduction in cytokinin biosynthesis in *Arabidopsis* seedlings treated with auxin. These findings suggest that auxin action could prevent the activation of buds indirectly through down-regulation of local CK production and/or cytokinin export from roots. Contrary to this, auxin has been found to upregulate expression of *AtIPT5* and *AtIPT7* genes in *Arabidopsis* roots (Miyawaki *et al*., 2004).

More evidence for an antagonistic relationship between auxin and cytokinin came from a report of Tanaka and his colleagues (Tanaka *et al*., 2006) who showed that after decapitation of pea plants, expression of cytokinin biosynthetic genes *PsIPT1* and *PsIPT2* are increased transiently in the nodal stem. The excised nodal stem segments (with increased mRNA levels of *PsIPT2*) were incubated in media with or without IAA. Northern blotting analysis revealed that levels of *PsIPT2* mRNA were decreased with IAA treatment whereas no change was observed in them in IAA-free media. In another experiment, levels of *PsIPT2* mRNA were initially undetectable in the excised nodal stem segments but increased due to IAA-depletion. In addition, *PsIPT2* expression was not only in response to auxin level but also due to the basipetal auxin transport in the stem, as indicated by use of auxin transport inhibitors. Application of IAA in lanolin to the decapitated stump suppressed up-regulation of *PsIPT2* gene. On the other hand, upregulation of *PsIPT2*was induced by application of TIBA in lanolin to the internode above the second node. These findings in pea plants suggest that auxin negatively regulates CK biosynthesis to control bud outgrowth. The *PsIPT2* expression level was found to be very low in roots of intact pea seedlings. Therefore, the *PsIPT2* contribution to CK biosynthesis is under the control of auxin in the nodal stem only. The molecular mechanism controlling bud outgrowth was also explored in transgenic *Arabidopsis* plants carrying a *PsIPT2* promoter -GUS reporter gene. The GUS expression, which was observed before IAA treatment, was completely depleted by IAA treatment (Tanaka *et al*., 2006). This auxin-mediated cytokinin synthesis appeared to be regulated through AXR1/AFB signalling pathway, as a loss-of-function*axr1* mutant exhibited reduced effect of exogenous auxin on cytokinin production (Nordström *et al*., 2004).

Endogenous CK levels are partly controlled by inactivation of CKs, catalyzed by CKX enzymes. Of the two *CKX* genes (*PsCKX1* and *PsCKX2*) isolated from pea stem, *PsCKX2* expression was higher than *PsCKX1* in the stem. Therefore, *PsCKX2* contributes more to regulation of CK levels in this tissue. *PsCKX2* transcripts were undetectable from three to nine hours after decapitation and then increased rapidly after nine hours. Stem treated with TIBA in lanolin showed a similar expression pattern of *PsCKX2* gene. Before and after decapitation, expression patterns of *PsIPT2* and *PsCKX2* were opposite to each other in the stem. In pea stem, *PsCKX2* mRNA is strongly induced by auxin, indicating that auxin positively regulates *PsCKX2* expression. After twelve hours, decreased CK levels in decapitated stem might be caused by both downregulation of *PsIPT2*gene expression and upregulation of *PsCKX2* gene (Tanaka *et al*., unpublished data presented in Shimizu-Sato *et al*., 2009). Apically derived auxin may regulate CK levels in the stem to control shoot branching in two ways; (1) promoting CK degradation through regulation of *CKX* expression

and (2) suppressing CK production through regulation of *IPT* expression, as shown in Fig. 1.8.

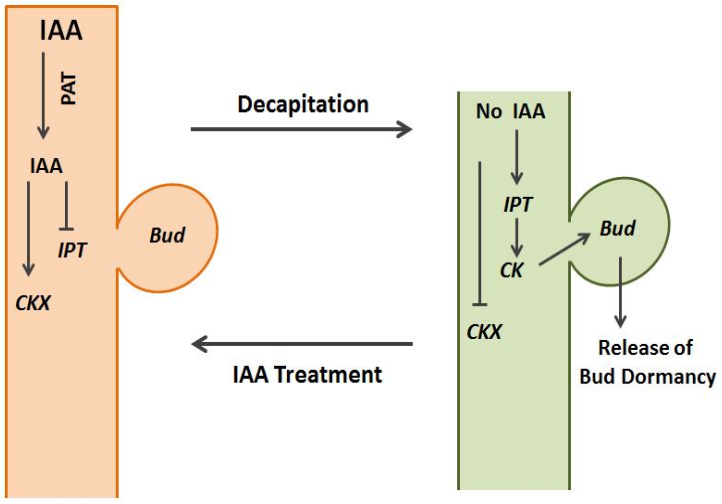

Figure – 1.8: A Model of Interaction between Auxin and Cytokinin *(Adapted and modified from Shimizu-Sato et al., 2009). Auxin downregulates cytotkinin biosynthetic genes IPTs and upregulates CKX genes involved in cytokinin degradation at the node to regulate CK levels, which are increased at the node and in the bud on decapitation (removal of auxin source), indicating that newly synthesized cytokinins at the node are transported to the bud.*

Auxin-Strigolactone Crosstalk: A very close relationship between auxin and strigolactone has been proposed as the explanation for part of the auxin second messenger model. First of all, it has been shown that apically applied auxin does not inhibit branching in *Arabidopsis max* mutants (Sorefan *et al*., 2003; Bennett *et al*., 2006), indicating that the MAX pathway of strigolactone action is a prerequisite for auxin-mediated inhibition of bud outgrowth. Strong supporting evidence is increased auxin transport capacity in the stem of *max* mutants by modulation of levels of PIN auxin efflux carriers (Bennett *et al*., 2006), suggesting that SL regulates auxin flow in the main stem. Consistent with previous findings, it has been shown in *max* mutants that there is an accumulation of PIN1 protein and upregulation of expression of other auxin transporters (Lazar and Goodman, 2006). Also consistent with this finding, recently strigolactone has been found to trigger PIN1 depletion from plasma membrane of xylem parenchyma cells in the stem, within 10 minutes of strigolactone treatment (Shinohara *et al*., 2013). Interestingly, increased auxin transport capacity is correlated with increased shoot branching. Therefore, it is postulated that if increased auxin transport is reduced back to WT capacity, the characteristic branching phenotype would be restored to WT. This can be tested chemically by use of transport inhibitors or genetically in *pin1* mutant background, and indeed the auxin transport inhibitor NPA (1-N-Naphthylphthalamic acid) can restore wild-type auxin response of *max* mutant buds (Bennett *et al*., 2006).

These findings correlate increased auxin transport with increased shoot branching. This paradox can be explained by a model, which proposes a new mode of action for apically derived auxin to suppress bud outgrowth that depends on competition for limited auxin transport capacity in the main stem (Fig. 1.9A). Auxin transport capacity by limited PIN protein levels in the main stem is rapidly and fully saturated with apically-derived auxin. Therefore, other auxin sources like axillary buds are not able to establish their own PAT streams to export auxin into the main stem. In contrast, PINs and other auxin transporters in *max* mutants are over-accumulated, as a result of which auxin transport capacity in the stem is not saturated. This facilitates the axillary buds to export auxin into the main stem, consequently breaking bud dormancy to develop into new branches, the characteristic *max* phenotype. This additional mode of auxin action is independent of AXR1/AFB pathway, as auxin transport capacity is same in *axr1* mutants and wild-type; as well as*axr1*mutant in *max* background shows additive effects on *max* phenotypes (Bennett *et al*., 2006).

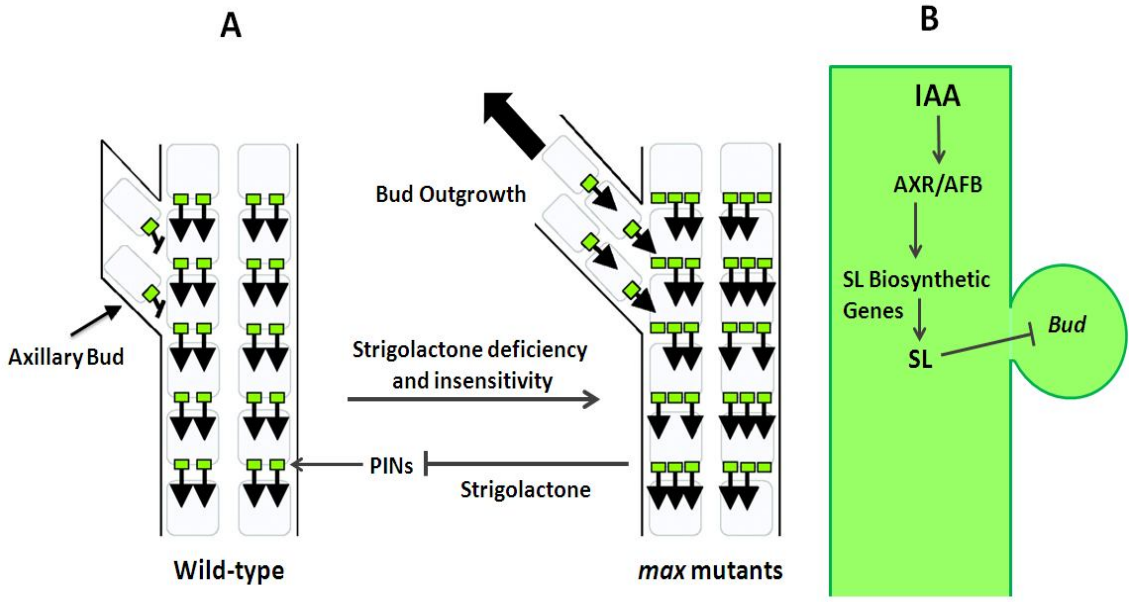

Figure – 1.9: A Model of Interaction between Auxin and Strigolactone *(Adapted and modified from Ongaro and Leyser, 2008, and Domagalska and Leyser, 2011). (A) Auxin transport capacity is modulated by strigolactone through regulation of auxin transporter proteins (PINs), which are downregulated by strigolactone in the wild-type stem. Therefore, capacity of auxin transport in the stem is restricted and saturated by auxin produced in shoot apex. As a result, buds cannot export auxin to grow out. In max mutants, PIN proteins are accumulated, increasing auxin transport capacity in the stem. Outgrowth of buds happens due to export of auxin from the buds. Auxin transporter proteins are represented by green squares and black arrows down the green squares represents auxin transport down in the stem. (B) Auxin upregulates strigolactone biosynthetic genes encoding carotenoid cleavage dioxygenases (CCD7 and CCD8). This results in increased strigolactone levels to inhibit bud outgrowth.*

Regardless of the degree of independence between the two auxin-related pathways, the AXR1/AFB pathway clearly regulates the MAX pathway. In *Arabidopsis*, auxin was shown to upregulate a *MAX4::GUS* in root tip and hypocotyl, depending on AXR1/AFB signalling pathway (Bainbridge *et al*., 2005). It was also found that auxin mediates SL synthesis(Fig. 1.9B) by transcription of *MAX3 and MAX4* genes, as decapitation resulted in decreased expression of strigolactone biosynthetic genes, thereby reducing SL production (Foo *et al*., 2005; Hayward *et al*., 2009; Sorefan *et al*., 2003). In pea, auxin-mediated regulation of *RMS1* and *RMS5* expression has been reported using qRT-PCR (Quantitative real-time PCR) in stem segments (Foo *et al*., 2005; Johnson *et al*., 2006). Removal of auxin source by decapitation caused reduction in basal expression levels of *RMS1*, whereas addition of auxin to decapitated stump maintained *RMS1*transcript levels.

Cytokinin-Strigolactone Crosstalk: As compared with interactions of auxin with cytokinin and strigolactone, little is known about interactions between cytokinin and strigolactone. Recently, it was found in SL-deficient mutant (*rms1*) and SL-insensitive mutant (*rms4*) of pea, that levels of *PsIPT1* expression are increased in nodes and internodes of the shoot (Dun *et al*., 2012). Response of *rms1* mutants to CK supplied to the vasculature or to the bud was found to be more sensitive than wild type, such that even lower CK levels can induce bud outgrowth in *rms1* plants than in wild type. These findings suggest an antagonistic relationship between cytokinin and strigolactone. Furthermore, application of GR24 combined with cytokinin reduces the effect of cytokinin on bud growth in *rms1* but not in *rms4* mutants, indicating that the SL-mediated effect on cytokinin is through the RMS4 signalling pathway. Antagonism between strigolactone and cytokinin maye stablish through their common target, the strigolactone-responsive TCP transcription factor *PsBRC1* (Braun *et al*., 2012; Dun *et al*., 2012). It has already been reported that bud growth is negatively correlated with *PsBRC1* expression (Aguilar-Martínez *et al*., 2007), which is upregulated by GR24 treatment and downregulated by cytokinin application. Therefore, a model was suggested where interaction between strigolactone and cytokinin converges through *BRC1* (Braun *et al*., 2012; Dun *et al*., 2012).

Although cytokinin and strigolactone fulfill criteria for second messenger molecules to act directly in axillary buds, their activities can also be fitted well into the auxin transport canalization model. For example, strigolactone decreases PIN1 in a MAX2-dependent manner, resulting in reduced auxin transport (Crawford *et al*., 2010; Lin *et al*., 2009). Therefore, strigolactone might block auxin export from axillary bud, by limiting the capacity of auxin transport in the main stem (Prusinkiewicz *et al*., 2009). Similarly, cytokinin application to dormant buds induces upregulation and polarization of PIN1, suggesting that cytokinin might activate axillary buds through auxin export from the buds (Kalousek *et al*., 2010). Evidently, it seems that both second messenger hypothesis and canalization-based auxin transport model are coordinated to regulate shoot branching. The interplay between auxin, cytokinin and strigolactone to control shoot branching is depicted in Figure 1.10.

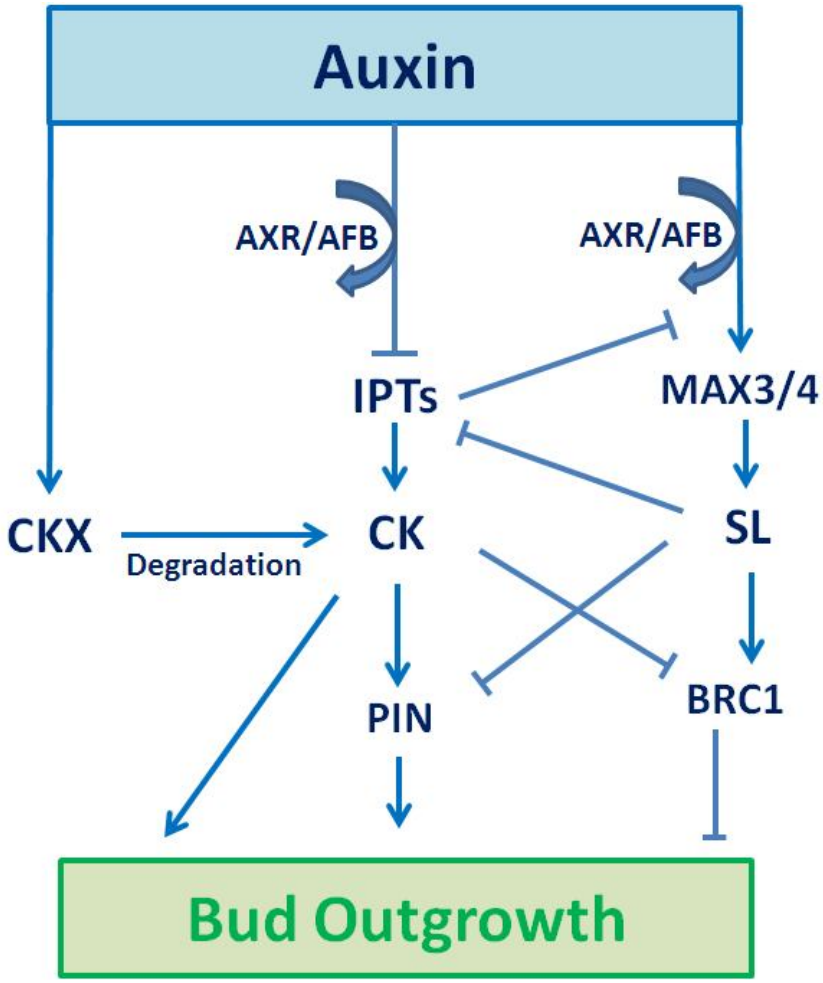

Figure – 1.10: A Summarized Model of Interactions between Auxin, Cytokinin and Strigolactone in controlling Axillary Bud Outgrowth and consequently Shoot Branching, based on Second Messenger and Canalization Hypotheses. *The cytokinin levels are decreased through AXR/AFB dependent downregulation of IPT genes and through increased CK degradation catalyzed by upregulation of CKX genes. Auxin also mediates SL levels by upregulation of SL biosynthetic genes through AXR/AFB pathway. Both auxin-mediated suppression of CK levels and promotion of SL levels are resulted in bud growth inhibition. Cytokinin and strigolactone interaction regulates axillary bud outgrowth. SL inhibits bud outgrowth by decreasing CK synthesis through downregulation of IPT genes, and by regulation of transcription factor BRC1, which acts downstream of strigolactone. Cytokinin suppresses auxin-mediated regulation of strigolactone biosynthetic genes and BRC1 transcription to promote branching. Bud outgrowth is also controlled by auxin export from bud through auxin transporter PINs, which are accumulated by CK and depleted by SL.*

In pea and *Arabidopsis*, strigolactone regulates cytokinin levels through a feedback signal that can move from shoot to roots (Foo *et al*., 2007). It has been found that cytokinin flux is significantly reduced in xylem saps of *rms* and *max* mutants, and can be mediated by a shoot-derived mobile signal, as the grafts between scions of SL-deficient *rms* mutants and WT rootstocks have shown low xylem sap CKs moving from roots (Beveridge, 2000). Interestingly, the *rms2* mutant, showing the characteristic branching phenotypes of *rms* mutants, instead has wild-type CK levels in the xylem sap. This has led to the proposal that *RMS2*is in some way required for the action of this downwardly mobile feedback signal (Beveridge *et al*., 1997a; Beveridge, 2000; Foo *et al*., 2007).

There is a possibility that the feedback signal is novel, but an alternative viewpoint is that this signal is, in fact, auxin. According to this hypothesis, *RMS2* would be predicted to be a part of auxin signalling in some way. Arguments against auxin as a feedback signal have been raised. The *rms2* mutant lacks feedback regulation and has higher IAA levels than the other *rms* mutants (Beveridge *et al*., 1996; Morris *et al*., 2001). However, if *rms2* like *axr1* is involved in auxin signalling, this feature would be expected. In addition, auxin levels in other *rms* mutants are near wild-type (Beveridge, 2000). Rate of auxin transport is not affected in *rms* or *max* mutants, but capacity is affected in both (Beveridge, 2000; Bennett *et al*., 2006). However, transport capacity in *axr1* and *rms2*is similar to WT.

It is important to mention that one key difference between *axr1* and *rms2* mutants is that shoot branching in *rms2*scions grafted to WT roots is restored to wild-type (Morris *et al*., 2001). In contrast, *axr1* scions cannot be rescued by WT roots (Booker *et al*., 2003). This difference along with apparently WT auxin responses of *rms2* mutants in some assays, demonstrates significant differences between the two mutants. Questions still remain unanswered regarding the exact mechanisms regulating xylem CKs with respect to CK and strigolactone interaction.

1.7 Hypothesis: Based on the above discussions, the central hypothesis for this study is, "CKs synthesized in shoot are transported to root via phloem and those synthesized in roots are transported to shoot via xylem. Strigolactone may regulate CK biosynthetic genes *AtIPTs*."

1.8 Aims: To test this hypothesis, the specific aims of the PhD were as follows:

1- To characterize *atipt* mutants (*atipt3,5, atipt3,7, atipt5,7*, *atipt3,5,7*) in *max2* and *max4* backgrounds for phenotypes such as shoot branching.
2- To study spatial expression of *AtIPTs* in *max* mutants by GUS promoter-reporter system.
3- To quantify CK levels in roots and shoot, phloem and xylem of *max* lines, as well as *atipt* mutants (*atipt3,5, atipt3,7, atipt5,7*, *atipt3,5,7*) in *max2* and *max4* backgrounds.

Chapter 2

General Materials and Methods

2.1 Genotypes and Growth Conditions of *Arabidopsis thaliana*

All the genotypes (Table 2.1) used in the research were provided by Dr. Colin Turnbull, Imperial College London.

Table - 2.1: List of Genotypes of *Arabidopsis thaliana*

No.	Genotype	Description	Reference
1	**Col-0**	Columbia ecotype of *A. thaliana* used as WT	
2	***CaMV-35S::GUS***	Col-0 with 35S promoter from CaMV to generate 35S::GUS line in WT	Dr. Jose Botella UQ, Australia
3	***IPT3::GUS IPT5::GUS***	Ws ecotype of *A. Thaliana* in which a gene for GUS was fused to a promoter of each *AtIPT1, AtIPT3, AtIPT5* and *AtIPT7* genes to generate single promoter::GUS genotypes	Miyawaki*et al*., 2004
4	***atipt1,3,5,7***	Quadruple knockout mutant in Col-0 for 4 *IPT* genes *AtIPT1*, *AtIPT3*, *AtIPT5* and *AtIPT7* through T-DNA insertions	Miyawaki*et al*., 2006
5	***max1-1* and *max2-1***	*max1-1* allele induced in En-2 ecotype was introduced in Col-0 through backcrossing and *max2-1* isolated from M2 resulted from EMS mutagenesis in Col-0	Stirnberg*et al*., 2002
6	***max3-9***	*max3-9* was screened from EMS mutagenized population in Col-0 and used for characterization after three back crosses with Col-0	Booker *et al*., 2004
7	***max4-1***	*max4-1* contains single transposon insertion in first intron	Sorefan *et al*., 2003

For tissue culture, seeds were surface sterilized with 70% ethanol for 30 sec and 1% bleach (domestic grade) for 10 min and then rinsed 5 times with sterile water (sterilize by autoclaving at 121^{o}C for 15 minutes). The sterilized seeds were then placed with the help of

sterilized forceps or 200µl tips on plates (120 × 120 square petri dishes) filled with solidified medium (pH= 5.7-5.8) containing half strength MS (Murashige and Skoog, 1962) salts, 0.6 % phytagel and 1% sucrose. Then all plates were sealed with paraffin film, and stratified by keeping in darkness at 4°C for 2-3 days. Plates were then placed vertically in growth room under long day light treatment (16h light at about 100-120 µmol/m²/s and 8h dark) at 23°C.

For cultivation in soil, 2-3 seeds were placed with the help of forceps or pipette (200µl tip) onto the mixture (4:1) of compost (Levington - F2 compost, fine grade peat with sand, N 150, P 200, K 200 g/m3 - pH 5.3 - 5.7) and vermiculite (Sinclair - vermiculite (mica mineral), medium grade, 2-5mm). The compost mixture was filled in P24 or P40 trays (24 or 40 cells in standard 35 x 23 cm trays) or small pots. The filled trays or pots were pre-soaked in intercept (for pest control) solution (0.2g/L) for 30 min. After sowing seeds, the trays or pots were covered with aluminium foil and placed in dark at 4°C for 2-3 days to stratify before incubation in a growth chamber under the same light and temperature condition as stated above or on short day (8hours light at about 100-120 µmol/m²/s and 16 hours dark) in case of plants grown for xylem and phloem sap collection. For this purpose, the seeds are set to germinate at very low light for more than a week. In the growth room, the trays were covered to increase the humidity for a week. In case of planting with the help of pipette, seeds are soaked in water and chilled at 4°C to break seed dormancy.

For hydroponics (Araponics), the seed/plant holders (from the top to bottom: A 2cm diameter collar designed with a small handle for hanging the seed-holder on the cover and to facilitate manipulation of the seed-holder, a tubular body filled with agar dips into the nutrient solution, providing a soft interface between the seed and the solution, a cross-shaped extension of the tubular part which guides the root towards the solution) were filled with 0.67% agar (Melford), on which 2-3 pre-chilled seeds were placed using pipette. Then these holders were kept in tray fitted in tank that was filled with nutrient solution (GHE flora series; FloraGro, FloraMicro and FloraBloom) at 1ml/2Litres. The hydroponics were kept under short day light treatment (10h light at about 100-120 µmol/m²/s and 14h dark) at 23°C.

2.2 Crossing Technique for Mutant Lines Production

To make crosses, from female parent a suitable flower (near to an open flower of which anthers did not shed pollen grains) was selected and all flower parts including sepals, petals and stamens (that include filaments and anthers) were removed with the help of forceps under a dissecting microscope, leaving the carpel intact. After 2-3 days when the stigma of the emasculated flower become receptive, open flower (with shedding anthers) from the male parent was removed by squeezing it close to the base with the forceps to spread out sepals and petals separating the anthers which were then brushed with the receptive stigma on the female parent under the microscope just to observe the pollens on the stigma. The crosses were labeled with different coloured sewing threads w. r. t. different male parent genotypes. After 3-4 days of crossing, elongated siliques were the sign of successful crosses made. When

the siliques of crosses turned yellow, those were harvested before drying in labeled eppendorf tubes just to make sure not to lose the seeds of crosses. The harvested siliques were dried in desiccator containing silica gel at room temperature for 2 weeks before seed sowing.

2.3 Statistical Analysis

Significance of data was determined by using statistical analyses including One-way ANOVA followed by Tukey's post hoc test, Student's t-test and Chi-square. Segregation of genes during screening of mutants (Chapter 3 & 6) was tested with Chi-square analysis performed with Microsoft Excel statistical function. One-way ANOVA with Tukey's post hoc test was used to analyze data on phenotyping (Chapter 3) and hormone quantification (Chapter 5) with more than two genotypes, to determine statistically significant differences between genotypes. One-way ANOVA with Tukey's post hoc test was performed using Minitab 16 trial version available online (http://www.minitab.com/en-GB/products/minitab/default.aspx). Student's t-test was used to compare percentages of aborted seeds within siliques using a trial version of a calculator downloaded from (http://www.statpac.com/statistics-calculator/percents.htm). To analyze a large dataset of cytokinin quantification, principal component analysis (PCA) was used to find patterns between genotypes and different tissues. PCA was performed using Excel Stat tool installed from (http://www.statistixl.com/downloads/download.aspx).

2.4 Bioinformatics Tools

For the research, many web-based bioinformatics tools were used in context of information and functions as given in Table 2.2.

Table - 2.2: Web Links of Bioinformatics Tools used in the Research

Purpose	Web Links of Tools
Germplasm and Lines	http://www.*Arabidopsis*.org http://signal.salk.edu/cgi-bin/tdnaexpress
Genes	http://www.ncbi.nlm.nih.gov/ http://www.*Arabidopsis*.org/servlets/sv
Primer designing	http://www.ncbi.nlm.nih.gov/tools/primer-blast/index.cgi http://signal.salk.edu/tdnaprimers.2.html
Blast	http://www.*Arabidopsis*.org/Blast/index.jsp http://www.ncbi.nlm.nih.gov/genome/seq/BlastGen/BlastGen.cgi?taxid=3702
Gene Expression	https://www.genevestigator.com/gv/plant.jsp
Restriction Enzyme	http://rna.lundberg.gu.se/cutter2/

Chapter 3

Characterization Of Mutants

3.1 Introduction

3.1.1 Shoot Branching

Shoot branching, a key determinant of plant architecture, is the formation of side shoots from main shoot of a plant (Evers *et al*., 2011). During postembryonic development after germination, primary axis of growth is laid down in the form of primary shoot and root apical meristems on the opposite sides. Shoot apical meristem (SAM) produces the main shoot and leaf primordia. Secondary axes of growth are established when new meristems, known as axillary meristems (AMs), are formed from primary shoot apical meristem in the axils of leaves. During vegetative growth, axillary meristems give rise to several leaf primordia, developing into axillary buds (Aguilar-Martínez *et al*., 2007; Schmitz and Theres, 2005). After formation of a few unexpanded leaves, axillary buds become dormant. The arrest of axillary bud growth is partly due to an inhibitory dominant effect of the main shoot apex. This effect of primary shoot over lateral branches is termed as apical dominance (Mouchel and Leyser, 2007; Schmitz and Theres, 2005).

Two prime processes in shoot branching are breaking of bud dormancy and subsequent branch outgrowth, on which branching patterns and overall shoot architecture depend. The key developmental decision, whether an axillary bud remains dormant in the axils of leaves or that grow out to give a branch, is controlled by internal and external stimuli perceived by the plant (Horvath *et al*., 2003). This whole control mechanism gives potential to a plant for adjustment to changing growth conditions (Ongaro and Leyser, 2008). The operating systems of internal and external factors are not independent of each other, but integrate in complex

ways with feedback loops at the levels of cell, organ and whole plant, even up to plant population (Evers *et al*., 2011). Regarding internal factors, shoot branching is controlled by a network of plant hormones. Three plant hormones auxin, cytokinin and strigolactones are known to function in regulating shoot branching and are influential on each other in various ways (Leyser, 2009).

3.1.2 Hormonal Control of Shoot Branching

For more than 100 years, the phenomenon of apical dominance (an inhibitory effect of the main shoot apex on the activity of axillary buds) has been focal research by scientists to understand the control of axillary bud outgrowth (Domagalska and Leyser, 2011). It was known that removal of apex initiated process of branching through activation of dormant axillary buds (Snow, 1929). The first experiment conducted by Thimann and Skoog (1933) showed a link between apical dominance and auxin, as application of auxin on decapitated stump of a plant imitated the shoot dominance effect by suppressing growth and development of lateral buds into branches.

Auxin, synthesized mainly in young expanding leaves of primary shoot apex (Ljung *et al*., 2001), moves down the shoot apex basipetally in a polar manner by active transport, preventing upward movement into axillary buds. Hence it is widely accepted that auxin in this PAT (Polar auxin transport) stream has indirect effects on bud outgrowth (Booker *et al*, 2003; Blakeslee *et al*., 2005; Petrásek and Friml, 2009). Investigations on the indirect mode of auxin action have led to two hypotheses on regulation of bud activity. One hypothesis (Auxin transport-based theory) proposes that polar auxin transport in the main shoot induces PAT streams in axillary buds to export auxin from them, thus inhibiting bud outgrowth (Li and Bangerth, 1999). According to the second hypothesis (Second messenger theory), auxin regulates another mobile signal that can move into buds and control its activity (Snow, 1929 and 1932, Le Fanu, 1936). The inhibition of an axillary bud may depend on a second messenger whose production site is located at opposite end to the main source of auxin (Snow, 1937). Both hypotheses were not convincingly supported, so the mystery behind auxin-mediated bud growth inhibition remained unresolved leaving a number of questions e.g. what is the relationship between auxin and the unknown second signal(s)?

During past two decades, identification and characterization of shoot branching mutants in *Arabidopsis* (*max1, max2, max3* and *max4*), in pea (*rms1, rms2, rms3, rms4* and *rms5*) and in petunia (*dad1, dad2* and *dad3*) (Beveridge *et al*., 1994, 1996, 1997b; Napoli, 1996; Morris *et al*., 2001; Stirnberg *et al*., 2002; Booker *et al*., 2004, 2005; Sorefan *et al*., 2003; Snowden *et al*., 2005; Simons *et al*., 2007) facilitated to unfold the story of a mysterious second messenger involved in the inhibition of axillary bud outgrowth. A candidate for an upwardly mobile long-distance signal as a branch inhibitor was found to be strigolactone (Umehara *et al*., 2008 and Gomez-Roldan *et al*., 2008) that acts downstream of auxin, which also controls transcript levels of strigolactone biosynthetic genes (Foo *et al*., 2005 and Brewer *et al*., 2009).

One and only candidate, which acts directly at axillary bud to activate its outgrowth is cytokinin (Sachs and Thimann, 1967). Cytokinin produced in both root and shoot (Chen *et al*., 1985) can move acropetally in the xylem transpiration stream (Ongaro and Leyser, 2008) and its levels in root xylem sap and in nodal stem have been found to be controlled by auxin (Tanaka *et al*., 2006 and Shimizu-Sato *et al*., 2009). Biosynthesis of both SL and CK are modulated by auxin to suppress bud outgrowth. However, mechanisms of interaction between strigolactone and cytokinin to control bud outgrowth in shoot branching are still unclear.

3.1.3 Aims

This chapter deals with the strategy and approaches to study an interaction between cytokinin and strigolactone in *Arabidopsis thaliana*. Mainly this work is aimed to generate mutants by knocking out cytokinin biosynthetic genes and genes related to SL synthesis and perception by crossing loss-of-function mutants of cytokinin and strigolactone, and to characterize the mutants on phenotypic basis.

3.2 Material and Methods

3.2.1 Growth Conditions

The conditions to grow plants on media plates and in soil were similar to section 2.1.2.

3.2.2 Outcrossing of Genotypes

New combinations of genotypes were created through crossing of parent mutant lines according to section 2.2.

3.2.3 Molecular Techniques

3.2.3.1 Quick DNA Preparation

Genomic DNA was isolated according to a method mentioned in a laboratory manual of *Arabidopsis* (Weigel and Glazebrook, 2002). From 3-4 weeks old plant, 2-3 small leaves were taken in eppendorf tubes, flash frozen, dried using freeze drier (Hetro Drywinner-model DW-1.060e). The dried leaves were crushed using metal beads (Qiagen, Cat. No. 69989) in a tissue lyser II (Qiagen, Cat. No. 85300) for 2 min. Extraction buffer (200mM Tris-Cl pH 7.5, 25mM EDTA pH 8.0, 250mM NaCl, 0.5% SDS) equal to 400µl was added into each sample. The samples were vortexed and centrifuged in a microcentrifuge (Eppendorf 5415R) at 15493×g for 5 min at 4°C. Supernatant (300 µl) was transferred to new autoclaved micro-centrifuge tubes to which 300 µl of 2-propanol were added and mixed by shaking. The samples were again centrifuged as above and the supernatant was discarded.

The pellet (greenish) was washed by adding 1ml of 70% ethanol and centrifuging (15493×g for 1 min). Ethanol was removed, the pellet air dried at room temperature and redissolved in 100 µl of TE buffer (10 mM Tris-Cl, pH 7.5, 1mM EDTA-Na, pH 8.0). After mixing briefly, 1-2 µl was used for a PCR.

3.2.3.2 Amplification of Genomic DNA by Polymerase Chain Reaction (PCR)

DNA polymerase (Promega Cat. No. M3171 and Fermentas Cat. No. EP0702) was used in PCR reaction to amplify a DNA fragment. All primers (Table 3.1) were purchased from Invitrogen.

Table – 3.1: Oligonucleotide Primers

No.	Name	Primer Sequence	Reference
1	**AtIPT1G-LP**	5′ – AAAAACTCTCTCTCCATGCCG – 3′	Signal Salk
2	**AtIPT1G-RP**	5′ – GCTTCAAACGTCGTCAAAGAG– 3′	
3	**AtIPT3G-LP**	5′ – TGGAGAGATTCGCCATGTGACAG– 3′	Miyawaki *et al.*, 2006
4	**AtIPT3G-RP**	5′-CCAACTTGTCGTATATCATTCGTACAGTG- 3′	
5	**AtIPT5G-LP**	5′ – ATTAATCCAGCAGGGGAAGTTAAAGGA– 3′	
6	**AtIPT5G-RP**	5′ –TGACCAACGATCTCTCTCTTAAACCTGAC– 3′	
7	**AtIPT7G-LP**	5′ – CTCTCGGGGTAAATGTCACAC– 3′	Signal Salk
8	**AtIPT7G-RP**	5′ – TTGACAACTCACGACTCGTTG– 3′	
9	**LB_6313R**	5′ – TCAAACAGGATTTTCGCCTGCT– 3′	
10	**LBa1**	5′ – TGGTTCACGTAGTGGGCCATCG– 3′	
11	**AtIPT3-T**	5′-CAACACGTGGGTTAATTAAGAATTCAGTAC-3′	Miyawaki *et al.*, 2006
12	**BAR-F**	5′-CAGGAACCGCAGGAGTGGA -3′	
13	**BAR-R**	5′- CCAGAAACCCACGTCATGCC-3′	
14	**MAX2-F**	5′- TGGAAGAGATTAGGATCAAGATA-3′	
15	**MAX2-R**	5′- TGGAAGAGATTAGGATCAAGATA-3′	

The total volume of a PCR reaction was 50µl including 0.2-0.4µl of DNA polymerase (5U/µl), 1x PCR buffer, 1.5 mM $MgCl_2$ (Buffer and $MgCl_2$ were provided by supplier Promega or Fermentas along with DNA polymerase), dNTP mixture (final concentration was 0.2mM for each nucleotide: dATP, dCTP, dGTP and dTTP), 1µl of 10µM forward primer, 1µl of 10µM reverse primer and 1-2µl template DNA and sterile distilled water that was added to make a final volume up to 50µl. A master mixture was prepared in more than required number of PCR reactions and was aliquoted into PCR tubes. The tubes were placed in thermo cycler (GeneAmp PCR System 9700; Applied Biosystems Veriti 96-well) and PCR program was set as follows: an initial denaturation step at 95°C for 5min and 35 subsequent cycles of 95°C for 30s (denaturation), from 57 to 65°C for 1min (primer annealing) and 72°C for 1-2min (extension time varies according to product size). The final extension step was performed at 72°C for 5min. PCR program was changed when the standard procedure did not produce a required optimum amplification.

3.2.3.3 Agarose Gel Electrophoresis

Agarose gel electrophoresis separates DNA fragments according to their sizes. Gel (1-1.2% w/v) was prepared by dissolving agarose (BDH, supplied by VWR) in Tris-acetate-EDTA buffer (TAE; 40mM Tris-acetate, 1mM EDTA pH = 8.0) and then adding 5µl/100ml SYBR® Safe DNA gel stain (Invitrogen, Cat.No.S33102). Samples were prepared by adding DNA samples and 6x loading dye in the ratio of 1µl:1µl and loaded in the wells of gel (loading dye was not added in case of green coloured buffer used in PCR). Gel was run in TAE-buffer at 80-100 V in a horizontal GEL system (Bio-Rad Sub-Cell GT). DNA fragments were visualized by using a UV transilluminator and photographs were taken through computer attached. To estimate the size of unknown DNA fragments a DNA marker was loaded in one lane of agarose gel. All DNA ladders used are given in Table 3.2.

Table – 3.2: DNA Ladders

Name	Supplier	Cat. No.	Description
1Kb plus	Invitrogen	10787-018	composed of 20 double stranded DNA bands spanning 100 base pairs to 12,000 base pairs
1Kb	Promega	G5711	contains the fragments (in kb): 10.0, 8.0, 6.0, 5.0, 4.0, 3.0, 2.5, 2.0, 1.5, 1.0, 0.75, 0.5, and 0.25
GeneRuler 100bp Plus	Fermentas	SM0321	Comprised of 14 bands: 10 bands from 100bp to 1000bp in 100 bp increments and 4 bands including 1.2kb, 1.5kb, 2kb and 3kb

3.2.4 Phenotypic Studies

A manual approach was used for phenotypic analyses i.e. measurement of rosette diameter, fresh and dry weights of shoot, stem height and counting of axillary branches. For dry weight, samples were wrapped in aluminium foil and placed in an oven set on 105^{o}C till constant weight.

3.3 Strategies and Approaches to generate Mutant Lines

In *Arabidopsis,* nine genes (*AtIPT1-AtIPT9*) identified are responsible for cytokinin synthesis (Miyawaki *et al*., 2006; Kakimoto, 2001; Takei *et al*., 2001; Golovko *et al*., 2002). *AtIPT* genes expressed in the vegetative phase are *AtIPT1*, *AtIPT3*, *AtIPT5* and *AtIPT7* among which *AtIPT1* is expressed at a very low level. Other *AtIPT* genes are barely detectable in vegetative organs (Miyawaki *et al*., 2004). Expression levels of *AtIPT* genes in different plant tissues, previously reported by Takei *et al* (2004a), revealed that transcript levels of *AtIPT1* found to be extremely low, but more abundant in flowers than other tissues. *AtIPT3* expression was detected in all organs, but at lower levels in the reproductive organs (flowers or siliques) and more abundantly in photosynthetic organs (rosette and cauline leaves) than in roots. Two genes *AtIPT5* and *AtIPT7* appeared to be strongly and predominantly expressed in roots.

Expression pattern of *AtIPT* genes during the life cycle of *A. thaliana* was analyzed using Genevestigator Development tool (https://www.genevestigator.com/gv/) (Hruz *et al*., 2008). This tool showed overall *AtIPT1* expression to be low at all developmental stages. The highest levels of *AtIPT3* expression found at mature rosette stage (Figure 3.1).

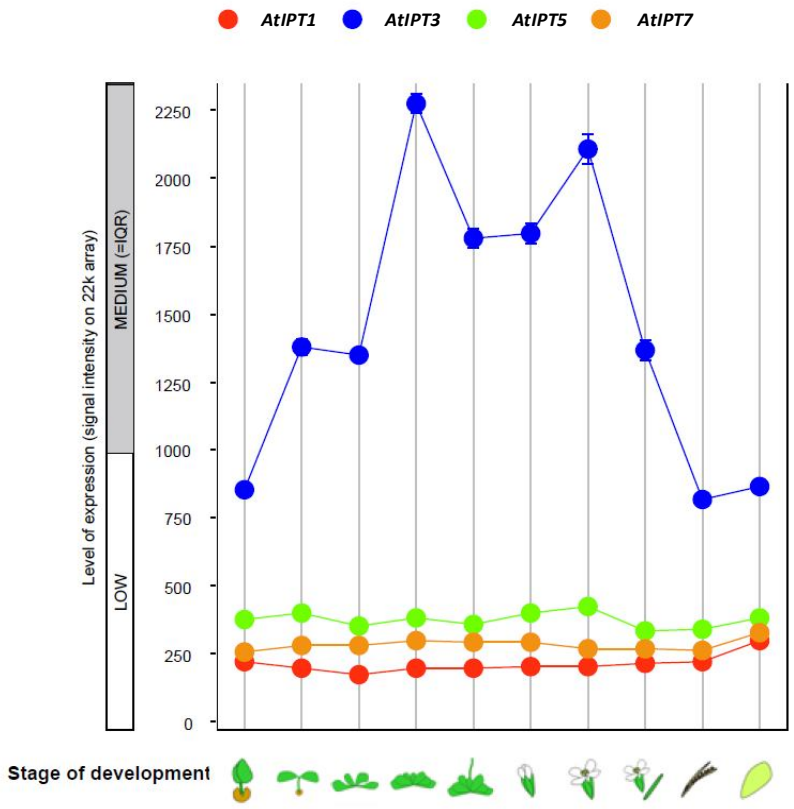

Figure - 3.1: Output Display obtained from Development Tool Interface of Genevestigator Database. *The output shows expression levels of AtIPT1, AtIPT3, AtIPT5 and AtIPT7 at different developmental stages from Affymetrix experimental data stored in the Genevestigator database.*

An exploration for expression levels of *AtIPT1, AtIPT3, AtIPT5* and *AtIPT7* across different tissues using Genevestigator Anatomy tool (Hruz *et al*., 2008) corroborated the previous findings (Takei *et al*., 2004a), as shown in Figure 3.2.

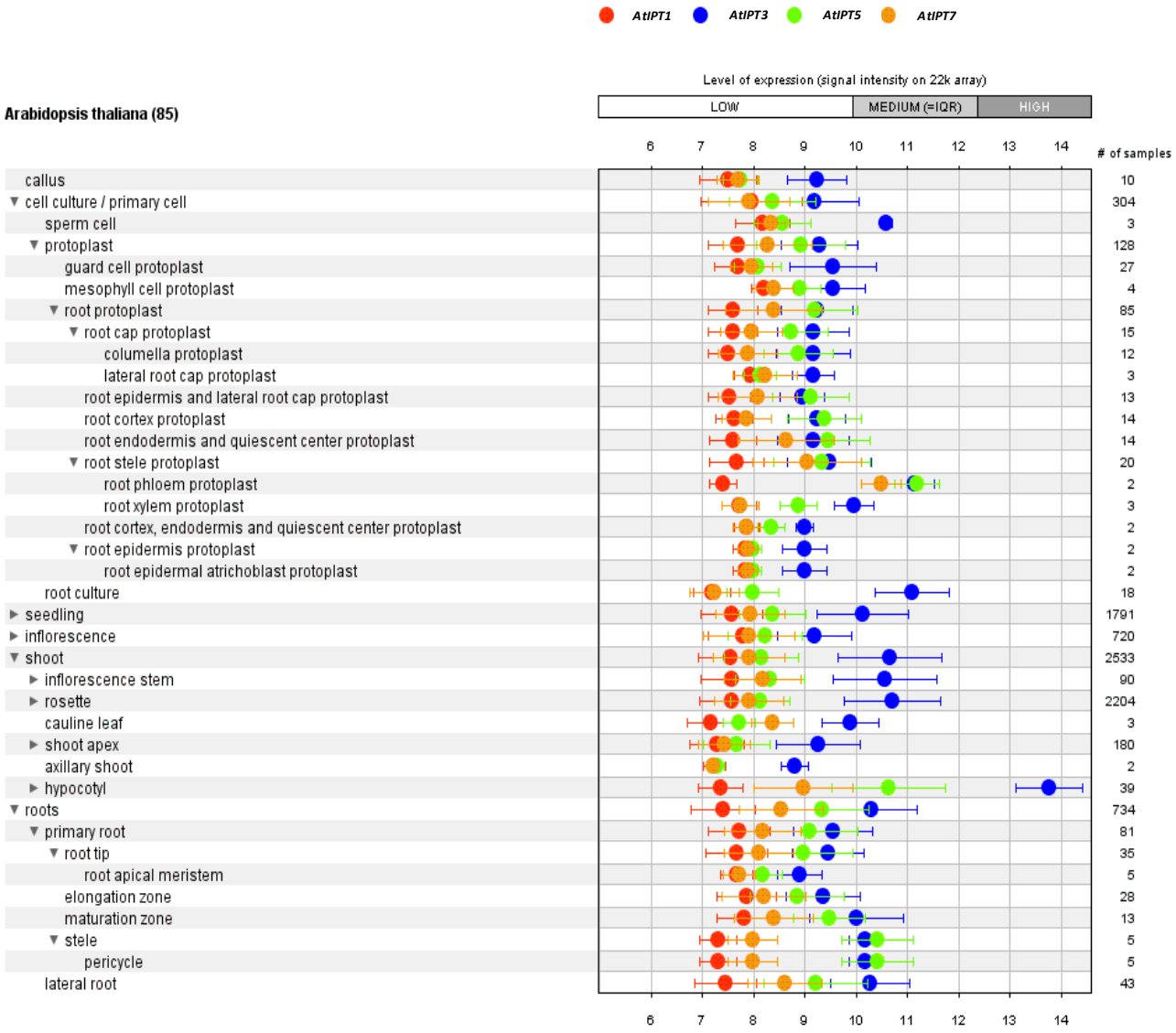

Figure - 3.2: Output Display exported from Anatomy Tool Interface of Genevestigator Database. *The output shows expression pattern of AtIPT1, AtIPT3, AtIPT5 and AtIPT7 in different tissues from Affymetrix experimental data stored in the Genevestigator database.*

Four *MAX* genes (*MAX1-MAX4*) identified in *Arabidopsis* are known to be involved in strigolactone biosynthesis and perception. Three of these genes (*MAX1*, *MAX3* and *MAX4)* are responsible for strigolactone production (Booker *et al*., 2005; Sorefan *et al*., 2003), while *MAX2* is a signalling gene (Stirnberg *et al*., 2002).

As described above, among the four *AtIPT* genes expressed in vegetative phase of plant growth, *AtIPT1* is expressed at a very low level throughout the life cycle of *A. thaliana*, whereas the three other genes (*AtIPT3, AtIPT5* and *AtIPT7*) were shown to be redundant in function (Miyawaki *et al*., 2006).

Keeping all this information in mind, decisions were made on which *atipt* knockout mutants in wild-type and *max* background would be the most informative to explore the interactive role of cytokinin and strigolactone in controlling shoot branching. *AtIPT1* was considered to be of lesser importance due to its low expression and was excluded from the set of *atipt* double mutants. Table 3.3 shows a list of all designated mutant required for the study of role of individual *AtIPT* gene in *max* background.

Table – 3.3: List of Required *atipt* mutants in wild-type, *max2* and *max4* Backgrounds

Wild-type	*max2*	*max4*
atipt5,7	***atipt5,7,max2***	***atipt5,7,max4***
atipt3,5	***atipt3,5,max2***	***atipt3,5,max4***
atipt3,7	***atipt3,7,max2***	***atipt3,7,max4***
atipt3,5,7	***atipt3,5,7,max2***	***atipt3,5,7,max4***

The **approach** used to generate all required mutants (listed in Table 3.3) was to isolate them from F2 segregating population of crosses of quadruple *atipt1,3,5,7* with *max2* and *max4*.

Phenotypes of Parental Lines: The phenotype of *atipt1,3,5,7* has been reported as a very small rosette, prolonged plastochron and delayed flowering (Miyawaki *et al*., 2006). Soon after germination, *max2* is very distinguishable due to long hypocotyls and round rough leaves along with profound branching at later stage of development (Stirnberg *et al*., 2002). At early stages, *max4* does not show a very apparent phenotype but later round edges of leaves and increased branching make it readily distinguishable (Sorefan *et al*., 2003).

The F2 seeds of four individual crosses of *atipt1,3,5,7*, including two crossed with *max2* and two with *max4*, were provided by Dr. Colin Turnbull. A large number of F2 seeds were planted for screening of mutants. Information on crosses and number of plants grown from F2 of each cross is given in Table 3.4.

Table – 3.4:Crosses of *atipt1,3,5,7* with *max2* and *max4*

No.	Female ♀	Male ♂	Cross Code	No. of plants grown
1	***max2***	***atipt1,3,5,7***	**A**	248
2	***max2***	***atipt1,3,5,7***	**B**	216
3	***max4***	***atipt1,3,5,7***	**C**	328
4	***max4***	***atipt1,3,5,7***	**D**	208

Phenotyping and Genotyping: From segregating population, the plants exhibiting branching phenotypes like *max2*, *max4* and very small rosette like *atipt1,3,5,7* were observed and recorded as in Figure 3.3. Small leaves were harvested from each plant to genotype them by PCR for *AtIPT* genes and T-DNA insertions.

1	**2** ***max***	**3** ***max***	**4**	**5** ***max***	**6**
7	**8**	**9**	**10**	**11** ***max***	**12**
13	**14**	**15**	**16**	**17** ***max***	**18** ***max***
19 ***max***	**20**	**21**	**22**	**23**	**24**

Figure - 3.3: A Model Layout of Growth Tray. *It was used to score phenotypes of plants from segregating population of crosses w.r.t. a P24 tray in which 24 plants were grown.*

3.4 Results

3.4.1 Genotyping of *AtIPT* Genes

Miyawaki *et al.* (2006) created a quadruplemutant*atipt1,3,5,7* by combining all four mutant alleles of *ATIPT1*, *ATIPT3*, *ATIPT5* and *ATIPT7* from single T-DNA insertion lines of these genes. They obtained those insertion lines from *Arabidopsis* Biological Resource Center (www.biosci.ohio-state.edu/~plantbio/Facilities/abrc/abrchome.htm) and Kazusa DNA Research Institute (www.kazusa.or.jp/ja2003/english). These *AtIPT* genes have no intron and T-DNA insertions are exonic, that are predicted to represent null alleles. Columbia-0 (Col-0) ecotype was used to create the null alleles of *atipt1* (SALK_020112), *atipt3-2* (KG21969), *atipt5-2* (SALK_133407), *atipt7-1* (SALK_001940) (Miyawaki *et al.*, 2006). The locus of *ATIPT1* (AT1G68460) and *ATIPT5* (AT5G19040) is on chromosome 1 and 5 respectively, whereas *ATIPT3* (AT3G63110) and *ATIPT7* (AT3G23630) are on chromosome 3.

PCR amplification of a genomic fragment with gene-specific primers (LP+RP) and a junction fragment with T-DNA left border (LB) primer and gene-specific right border (RP) primer identified T-DNA insertion in *AtIPT* genes of control plants (Figure 3.4), which are wild-type Col-0 and *atipt1,3,5,7 KO* mutant. This protocol was used to genotype the F2 population of crosses (see Table 3.3). Primers used for *AtIPT* genes and T-DNA are given in Table 3.1.

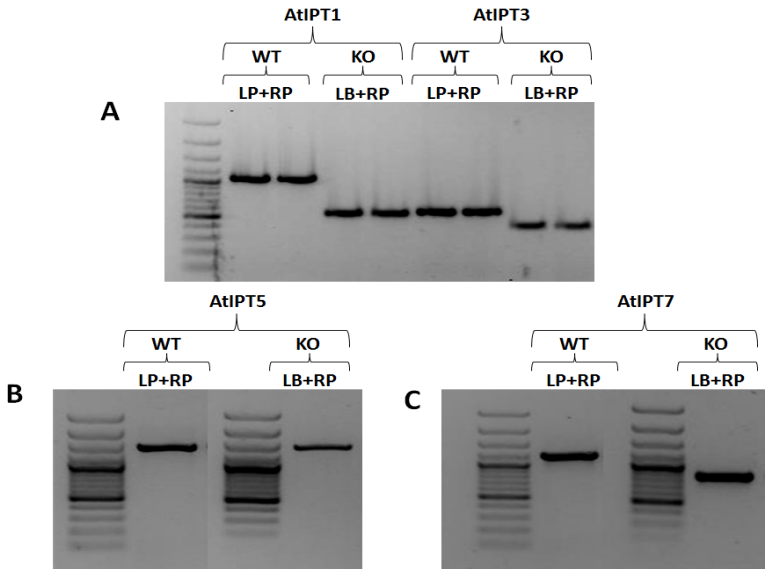

Figure – 3.4: Genotyping of AtIPTs. *Using gene-specific primers (LP+RP), a fragment of 1033bp of AtIPT1, 549bp of AtIPT3 (A), 1406bp of AtIPT5(B) and 1212bp of AtIPT7(C) was amplified from WT control by PCR (35 cycles). T-DNA insertion in each gene was identified in atipt1,3,5,7 (KO) using genomic and T-DNA primer pairs (LB+RP). 8 µl of a sample was loaded in each lane of 1.2% agarose gel. DNA ladder used is 100 bp plus (10 fragments are with the increment of 100bp, and then 1200bp, 1500bp, 2000bp and 3000bp).*

3.4.2 Genotyping of *MAX2* and *MAX4* Genes

Strigolactone signalling mutant *max2* was generated from an ethyl methane sulphonate (EMS) mutagenesis. A mutant allele *max2-1* has a single base change from G to A in the coding region, changing an amino acid from aspartate to asparagine at position 581 (Stirnberg *et al*., 2002). It was impossible to identify this single base mutation with a simple PCR amplification. Therefore, mapping of mutated *MAX2* gene for restriction enzyme cut site using an online tool of web cutter version 2.0 (http://rna.lundberg.gu.se/cutter2/) was done. An ApoI enzyme cut site was found at the point mutation of *max2-1* allele (Appendix II-A). Primers (Table 3.1) across mutation were designed in such a way that gave only one restriction cut site for ApoI enzyme. Enzyme digestion of a PCR product gives one band of 488bp in case of WT and two bands equal to 167bp and 321bp in case of *max2-1,* as shown in Figure 3.5 (A and B).

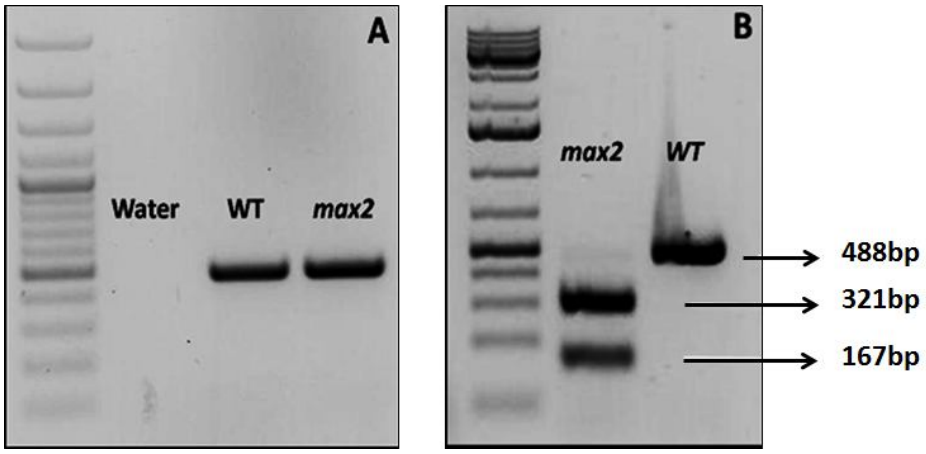

Figure – 3.5: Genotyping of max2-1 allele. *ApoI restriction enzyme digestion of a PCR (35 cycles) product of 488bp amplifying max2-1 allele was performed in WT and max2 mutant. Before digestion, both WT and max2 mutant have same size of product bands (A) but on digestion presence of two bands of 167bp and 321 bp confirms max2-1 allele (B). 6ul (A) and 12ul (B) of a sample was loaded in each lane of 1.2% agarose gel. First left lane is 100 bp plus DNA ladder.*

The strigolactone synthesis mutant *max4-1* was isolated from Sainsbury Laboratory *Arabidopsis* Transposant (SLAT) collection (Tissier *et al*., 1999). *MAX4* genomic DNA consists of five introns, and *max4-1* mutation was caused by a transposon insertion in the first intron of *MAX4* (Sorefan *et al*., 2003). A T-DNA construct used in the SLAT lines contains a defective *Spm* (d*Spm*) element carrying a *BAR* gene (phosphinothricin (PPr) resistance gene), which is used to select for T-DNA incorporation (Tissier *et al*. 1999). PCR amplification of a DNA fragment using *BAR* gene-specific primers (Table 3.1) was used to detect the presence or absence of T-DNA insertion (Figure 3.6) and phenotypic recordings of soil grown plants were performed to screen for homozygous *max4-1* mutant plants.

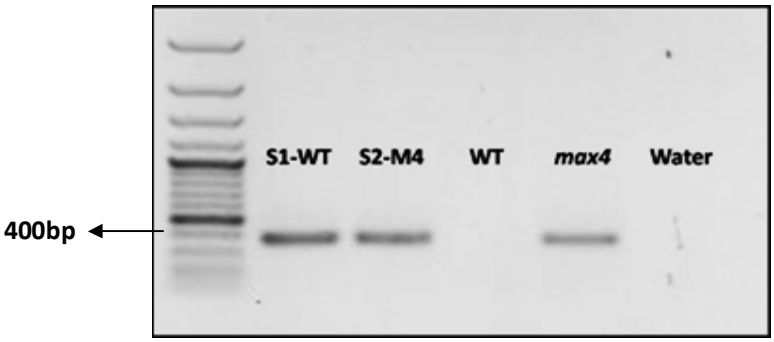

Figure - 3.6: Genotyping of max4-1 allele. *Using BAR gene-specific primers, a product of 370 bp was amplified from WT, max4 and two samples S1-WT and S2-M4 by PCR (35 cycles). The samples were taken from the population segregating for max4-1 allele. S1-WT is a plant with WT phenotype and S2-M4 is a plant with max4 phenotype. The WT phenotype and presence of BAR gene shows that S1-WT is heterozygous for max4-1 allele. 10 µl of a sample was loaded in each lane of 1.2% agarose gel. First left lane is 100 bp plus DNA ladder.*

After genotyping of F2 population segregating for five genes including four *AtIPTs* and one of *MAX2* or *MAX4* gene, plants were selected with 1-2 heterozygous genes.

3.4.3 Screening for*atipt5,7* in WT and *max* backgrounds

Knockout (KO) mutant for *AtIPT5* and *AtIPT7* genes in WT background was designated as *atipt5,7* and in *max4* and *max2* background as *atipt5,7,max4* and *atipt5,7,max2*, respectively. For screening of these mutants, three selected plants from F2 genotyping were genotyped again to confirm genotypic assessments (Table 3.5).

Table – 3.5: Genotyping Score of Plants knockout for *AtIPT5* and *AtIPT7*Genes

F2 Genotyping			
Gene	**P1-D** *atipt5,7*	**P2-C** *atipt5,7,max4*	**P3-B** *atipt5,7,max2*
AtIPT1	**WT**	**WT**	**Ht**
AtIPT3	**WT**	**WT**	**Ht**
AtIPT5	***atipt5***	***atipt5***	***atipt5***
AtIPT7	***atipt7***	**Ht**	***atipt7***
MAX	**WT**	***max4***	***max2***

"P" represents plant and P1- P3 are plant numbers selected. B, C and D corresponds to cross code given in Table-3.4.WT means homozygous for dominant alleles of a gene and Ht means heterozygous for both WT and recessive mutant alleles of a gene. Scoring of IPT genes is PCR based whereas MAX gene is scored on observed phenotype, therefore, WT phenotype of P1-D can be heterozygous for recessive max4 allele.

For further genotyping, F3 seeds of P1-D, P2-C and P3-B were grown and phenotyped. The plant P1-D was segregating for *MAX4* gene as WT and *max4* phenotypes were observed in F3 population. Eight plants out of 36 exhibited branching phenotypes (Chi square; $X^2 < X^2_{0.05} = 0.148 < 3.841$; $p > 0.05 = 0.700$), hence confirmed *max4* knockout genotype. To find *atipt5,7* in a WT background, 36 plants were genotyped with BAR gene. The absence of BAR gene in 11 plants ($X^2 < X^2_{0.05} = 0.593 < 3.841$; $p > 0.05 = 0.442$) confirmed wild-type genotype from population segregating for *max4* allele. Both mutants *atipt5,7* and *atipt5,7,max4* were confirmed from P1-D plant in F3. Therefore, plant P2-C was not considered for further screening. F3 descendants of plant P3-B were genotyped for genes *AtIPT1* and *AtIPT3* as these two genes were heterozygous in that plant. In the case of independent assortment of unlinked genes located on different chromosomes, 1 out of 16 is the expected ratio to be a double homozygous for WT alleles and 2 out of 24 plants ($X^2 < X^2_{0.05} = 3.556 < 3.841$; $p > 0.05 = 0.059$) were found to be homozygous for both *AtIPT1* and *AtIPT3* WT alleles.

3.4.4 Screening for*atipt3,5, atipt3,7* and *atipt3,5,7* in WT and *max4* backgrounds

For screening of double *atipt* mutants *atipt3,5* and *atipt3,7* and triple mutant *atipt3,5,7* in WT and *max4* background, six plants were selected for each mutant from genotyping of F2 population of crosses A-D (Table - 3.4). After critical reviewing and screening based on PCRs and other factors, selection of one plant segregating for only one gene was the best option (Table - 3.6) to find each double, triple and quadruple mutant. Reconfirmation of genotyping of the selected individuals was made by PCR.

Table – 3.6: Genotyping Score of Plants knockout for *AtIPT3, AtIPT5* and *AtIPT7*Genes

F2 Genotyping						
Gene	**P4-C** *atipt3,5*	**P5-C** *atipt3,7*	**P6-A** *atipt3,5,7*	**P7-C** *atipt3,5,max4*	**P8-C** *atipt3,7,max4*	**P9-C** *atipt3,5,7,max4*
AtIPT1	**Ht**	**WT**	**WT**	**WT**	**WT**	**WT**
AtIPT3	***atipt3***	***atipt3***	**Ht**	***atipt3***	**Ht**	***atipt3***
AtIPT5	***atipt5***	**WT**	***atipt5***	***atipt5***	**WT**	**Ht**
AtIPT7	**WT**	**Ht**	***atipt7***	**Ht**	***atipt7***	***atipt7***
MAX	**WT**	**WT**	**WT**	***max4***	***max4***	***max4***

P4-P9 are selected plants. A and C corresponds to cross code given in Table -3.4. WT means homozygous for dominant alleles of a gene and Ht means heterozygous for both WT and recessive mutant alleles of a gene. Scoring of IPT genes is PCR based whereas MAX gene is scored on distinct branching phenotype; therefore, WT phenotype of P4-P6 can be heterozygous for recessive max4 and max2 alleles w.r.t a specific cross.

Selection of plant P6-A was based on genotyping of *MAX2* by restriction enzyme digestion of PCR product which was found to be WT. The plants P4-P9 were grown and observed for their phenotypes. There was no *max4* plant in the F3 populations from plant P4-C and P5-C, confirming WT genotype for *MAX4*. The selected F3 plants (Table - 3.6) were genotyped as those were heterozygous for one of the *AtIPT* genes.

For isolation of the *atipt3,5* mutant, plant P4-C was genotyped for *AtIPT1* to find WT allele. The number of plants expected to be homozygous for WT allele of *AtIPT1* is 1 out of 4 and two plants were found out of 12 plants screened ($X^2 < X^2_{0.05} = 0.444 < 3.841$; $p > 0.05 = 0.505$). For the generation of *atipt3,7* mutant, 24 descendants of plant P5-C were genotyped for *AtIPT7* gene to isolate knock out for that gene and ten plants were found homozygous for the *atipt7* mutant allele ($X^2 < X^2_{0.05} = 3.556 < 3.841$; $p > 0.05 = 0.059$).

Triple mutants designated as *atipt3,5,7* and *atipt3,7,max4* were isolated from F3 populations of plants P6-A and P8-C (Table -3.6)respectively, by genotyping of *AtIPT3* gene which was heterozygous in the F2. One *atipt3,5,7* out of 40 plants ($X^2 > X^2_{0.05} = 10.8 > 3.841$; $p < 0.05 = 0.001$) and two *atipt3,7,max4* out of 80 plants ($X^2 > X^2_{0.05} = 21.6 > 3.841$; $p < 0.05 = 0.000$) were found to be homozygous for mutant alleles of *ATIPT3* gene.

Plant P7-C (Table - 3.6) was segregating for *AtIPT7* gene, making it possible to find both triple mutant *atipt3,5,max4* and quadruple mutant *atipt3,5,7,max4* from single plant (P7) descendants. Their genotyping was scored 10 WT *AtIPT7*plants out of 24 ($X^2 < X^2_{0.05} = 3.556 < 3.841$; $p > 0.05 = 0.059$) and no homozygous *atipt7* mutant allele that correlates to no plant showing phenotype like *atipt3,5,7* i.e. very small plant as it was expected in case of *atipt3,5,7,max4* mutant. Three plants, which were heterozygous for *AtIPT7*, were selected from the F3 population of P7 and grown as F4 with 120 from each one. From these plants, the quadruple *atipt3,5,7,max4* was found in the ratio of approximately 1:3, as 74 out of 327 showed the expected very small phenotypes ($X^2 < X^2_{0.05} = 0.980 < 3.841$; $p > 0.05 = 0.322$).

After screening all required mutants, final confirmation of mutants was made to find phenotypic and genotypic errors as well as seed contamination during harvesting. For this purpose, two plants corresponding to each mutant were selected for seed collection, and approximately 40 seeds per plant were grown on media plates for 6 days. Seedlings of each plant were bulked to harvest DNA for PCR based genotyping of *AtIPT* and *MAX* genes (Figure – 3.7 and 3.8). Bulk seeds only from “clean” plants were labeled and stored for further experiments.

3.4.5 Screening for*atipt3,5, atipt3,7 and atipt3,5*,7 in *max2* background

Screening of double *atipt* mutants *atipt3,5* and *atipt3,7* and triple mutant *atipt3,5,7* in *max2* background was not successful. No plant homozygous for both *atipt3* and *max2* was found in F2 and F3 populations. It was impossible to knockout *AtIPT3* gene from *max2* and vice versa. Both *MAX2* and *AtIPT3* genes are located on chromosome 2 and 3 respectively, hence are unlinked and expected to be assorted independently. Detailed study of the interaction between these two genes is given in Chapter 6.

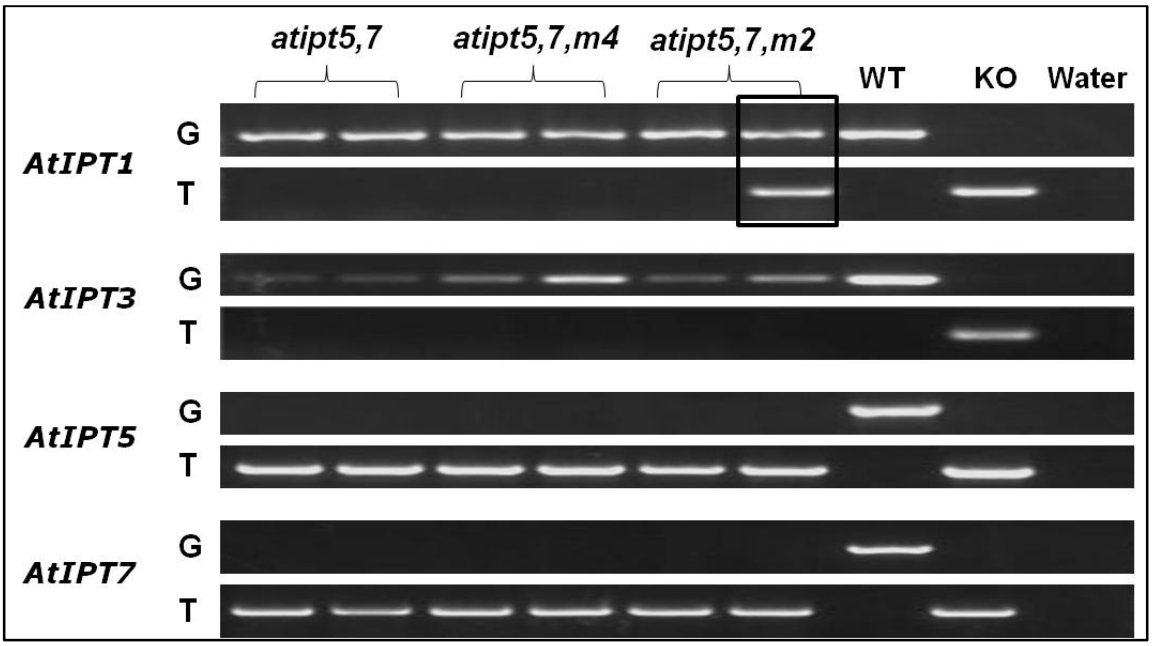

Figure – 3.7: Genotyping of atipt5,7 in WT and max backgrounds. *PCR (35 cycles) with two primer pairs (LP + RP and LB + RP) was performed to identify genomic band or T-DNA insertion in AtIPT1, ATIPT3, AtIPT5 and AtIPT7 genes. KO indicates AtIPT1,3,5,7 whereas G and T stands for genomic and T-DNA, respectively. m2 and m4 represent max2 and max4. Black box locates contamination. 8ul of a sample was loaded in each lane of 1.2% agarose gel.*

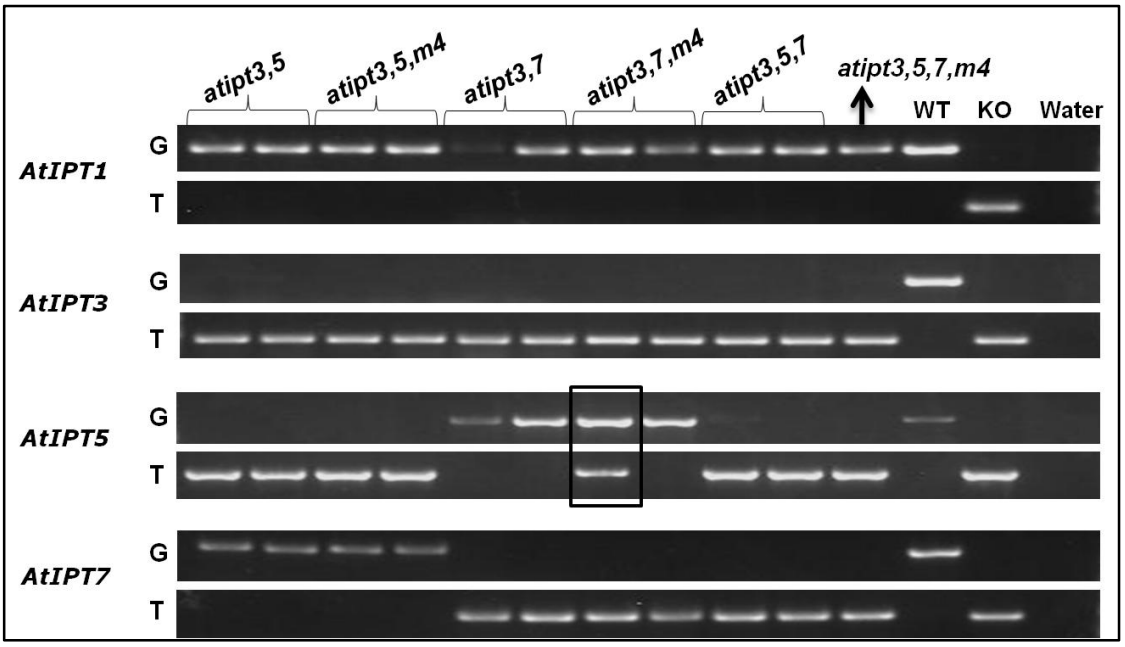

Figure – 3.8: Genotyping of atipt3,5, atipt3,7 and atipt3,5,7 in WT and max4 backgrounds. *PCR (35 cycles) with two primer pairs (LP + RP and LB + RP) was performed to identify genomic band or T-DNA insertion in AtIPT1, ATIPT3, AtIPT5 and AtIPT7 genes. KO indicates AtIPT1,3,5,7 whereas G and T stands for genomic and T-DNA, respectively. max4 is represented as m4. Black box locates contamination. 8ul of a sample was loaded in each lane of 1.2% agarose gel.*

3.4.6 Phenotypic Characterization of Mutants

3.4.6.1 Rosette Morphology

All homozygous mutants generated were fertile and produced viable seeds. After germination the growth and development of triple mutant *atipt3,5,7* and quadruple mutant *atipt3,5,7,max4* was slow, somewhat like *atipt1,3,5,7*. Under normal growth conditions at 3-weeks of age, the rosettes of double *atipt* mutants designated as *atipt5,7, atipt3,5* and *atipt3,7* displayed no differences from wild-type, as evident from fig. 3.9 (A-C). Rosettes of *atipt5,7,max2* were similar to *max2* and those of *atipt5,7,max4* were slightly smaller than *max4* (Fig. 3.9-A). It was noted that triple mutants *atipt3,5,max4* and *atipt 3,7,max4* differed in size, with rosettes (Fig. 3.9- B & C) of mutant plants appearing to be slightly smaller than *max4*. Mutants *atipt3,5,7* and *atipt3,5,7,max4* exhibited very small rosettes, therefore, those were readily distinguishable from wild-type and *max4* but comparatively bigger than *atipt1,3,5,7*(Figure 3.9 D & E).

3.4.6.2 Rosette Diameter

The rosette diameter of 3-weeks old plants grown under long days were measured manually (a ruler was used to measure the longest diameter of 10 plants of each genotype). The rosettes of *max2* and *max4* were found to be significantly bigger than wild-type (see Fig. 3.10-A). The rosette of *atipt5,7* is similar to *max4* and hence the difference of *atipt5,7* from wild type is significant. The rosettes of *atipt5,7,max2* and *atipt5,7,max4*are reduced to wild type size. However, the difference of *atipt5,7,max2* from *max2* is insignificant whereas *atipt5,7,max4* and *max4* are significantly different from each other, as shown in Fig. 3.10 (A). Figure – 3.10 (B & C) shows that rosettes of *atipt3,5, atipt3,7, atipt3,5,7*, *atipt3,5,max4*, *atipt3,7,max4* and *atipt3,5,7,max4* are significantly smaller than both wild-type and *max4* except *atipt3,7* and *atipt3,7,max4*, which are similar to wild-type. As shown in Fig. 3.10 (C), the quadruple mutant *atipt1,3,5,7* exhibits the smallest rosette that is significantly different from *atipt3,5,7* and *atipt3,5,7,max4,* which are similar to each other in diameter.

3.4.6.3 Rosette Dry Weight

The rosettes, used for diameter measurements, were oven dried at 105^{o}C till constant weight. Figure – 3.10 (D) shows significant differences among wild-type, *max2* and *max4,* with *max2* highest and wild-type lowest in rosette dry weights. The dry weights of *atipt5,7,max2* and *atipt5,7,max4* are significantly lowered from *max2* and *max4*, respectively (Fig. 3.10-D). In case of *atipt5,7*, the dry weight is significantly greater that wild-type, as shown in Fig. 3.10 (D). The dry weights of *atipt3,5,max4* and *atipt 3,7,max4* are significantly reduced as compared with *max4.* The dry weight of *atipt3,5* is significantly lower than wild-type, whereas that of *atipt3,7* is similar to wild-type (Fig. 3.10-E). The rosette dry weights of *atipt3,5,7*, *atipt1,3,5,7* and *atipt3,5,7,max4* are highly and significantly reduced in comparison with both wild-type and *max4*. The mutants of *atipt3,5,7* and *atipt3,5,7,max4* showed to have same levels of dry weights but significantly greater than *atipt1,3,5,7* (Fig. 3.10-F).

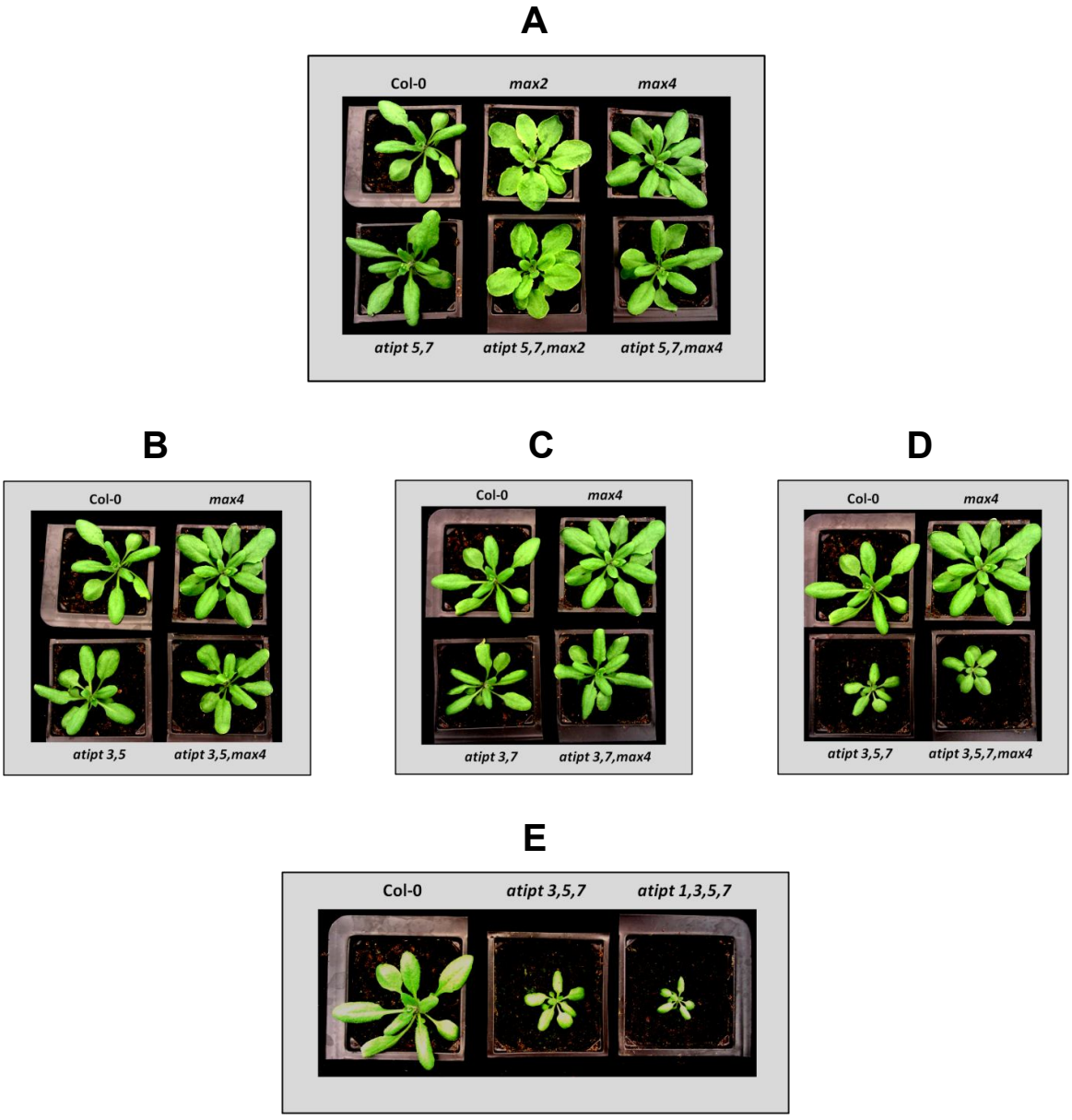

Figure – 3.9: Rosette Morphology of atipt knockout mutants in WT and max backgrounds. *The rosettes of 3-weeks old plants grown under long-day conditions are shown. Mutant and control plants are indicated in the images (A-E). Two mutants designated as atipt3,5,7 and atipt3,5,7,max4 exhibiting very small rosettes (D & E), are highly distinguishable from control plants. Control plants are Col-0, max2, max4 and atipt1,3,5,7. Wild type: Col-0, Colombia-0.*

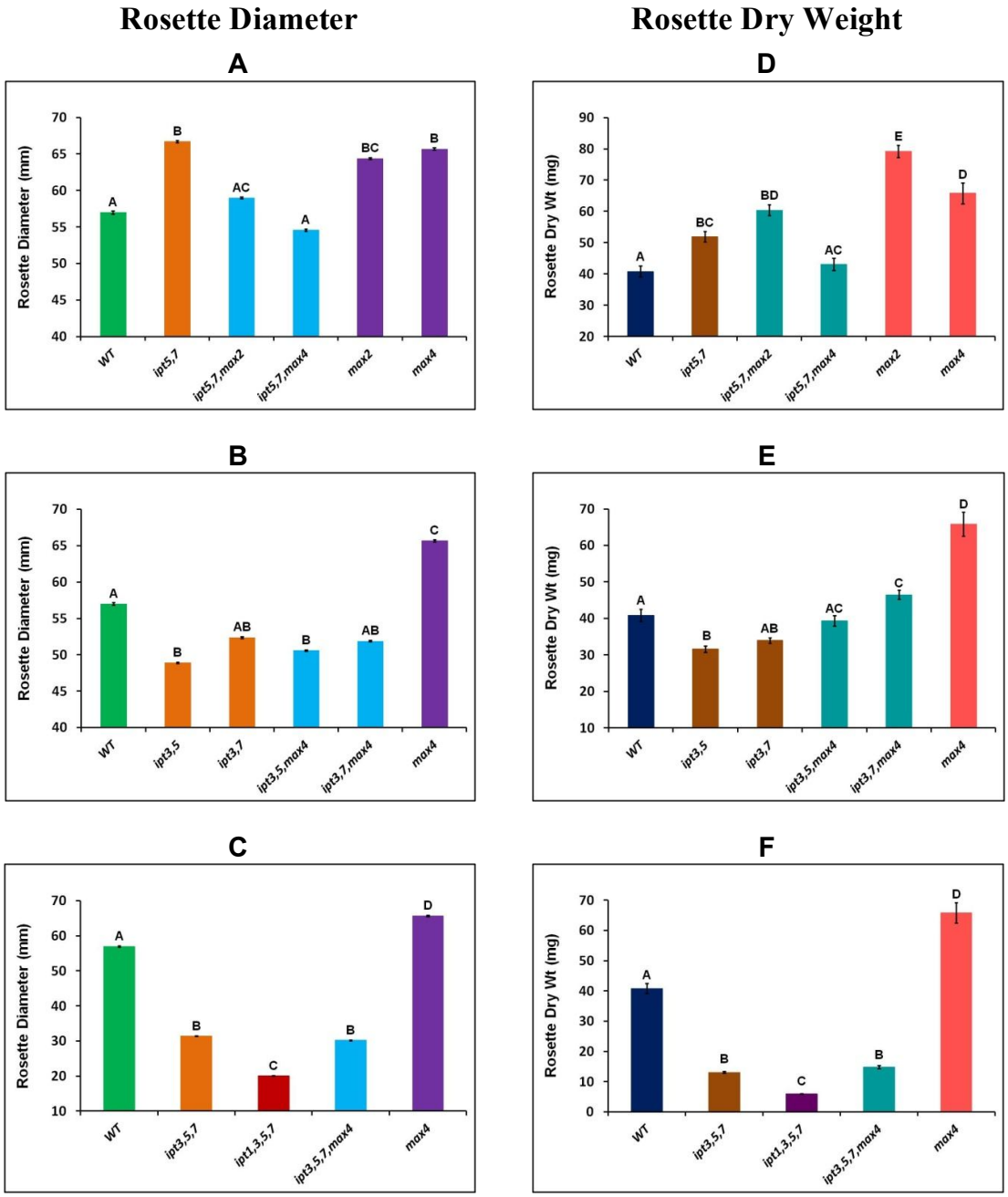

Figure – 3.10: Rosette Diameter and Rosette Dry Weight of atipt knockout mutants in WT and max backgrounds*. Rosettes of 3-weeks old plants grown under long day were used for both parameters. Control plants are WT (Col-0), max2, max4 and atipt1,3,5,7. The rosette diameter was measured manually and the same rosettes were oven dried till constant dry wt. Data from one experiment is represented as three graphs with the same controls. Graphs indicate genotypes at x-axis. Bars shown are means ± SE (n=10) for rosette diameter (A-C) and (n=7) for rosette dry weight (D-F). Means that do not share a letter are significantly different as determined by One-way ANOVA with Tukey's post hoc test ($p \leq 0.05$).*

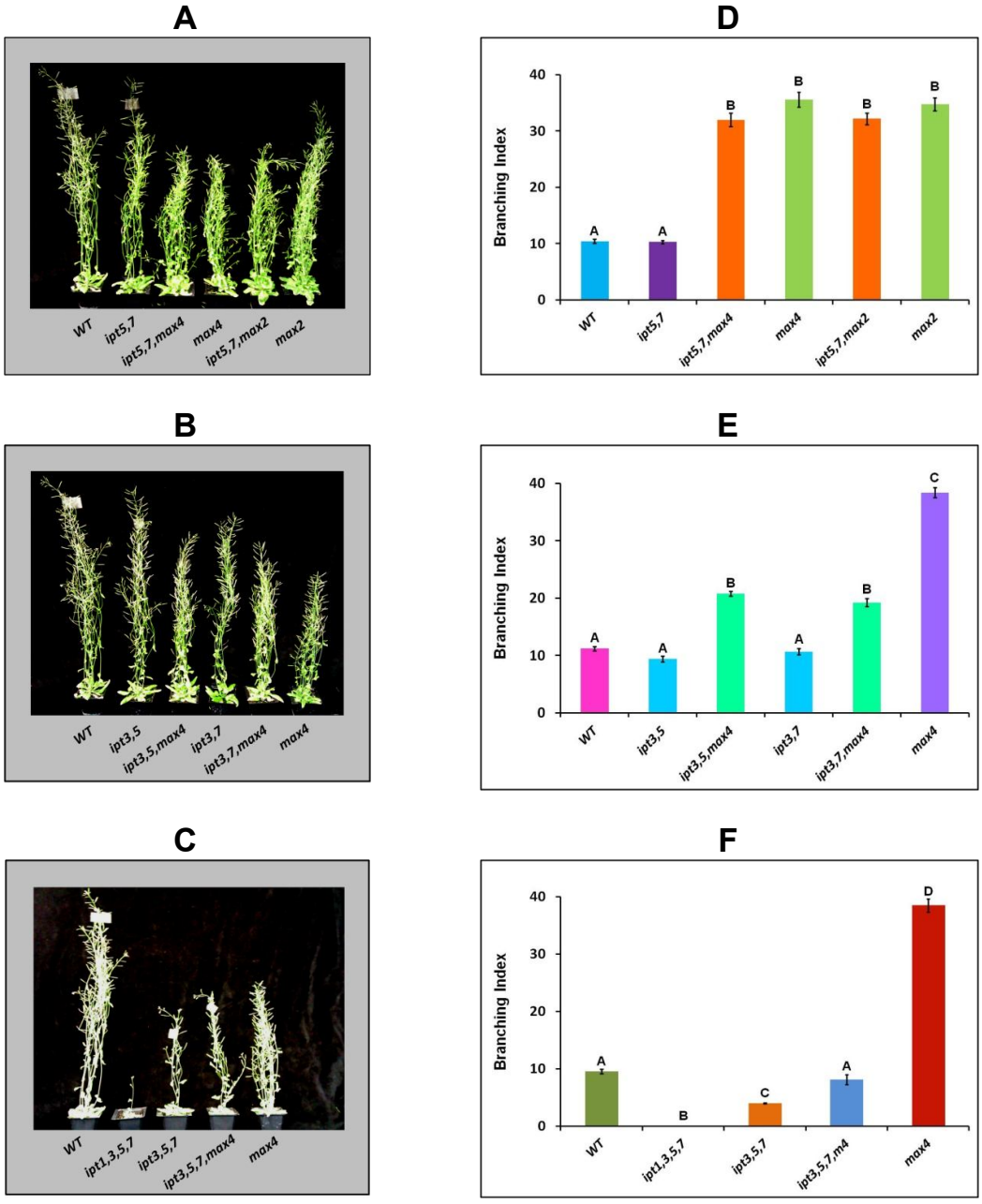

Figure – 3.11: Branching Phenotypes and Branching Index of atipt knockout mutants in WT and max backgrounds*. Mature plants grown under long day were used to measure stem height and to count lateral branches. Controls are WT (Col-0), max2, max4 and atipt1,3,5,7. Branching index was calculated with a formula (number of later branches divided by stem height). Images (A-C) show branching phenotype of each genotype. Data from three independent experiments is represented as graphs (D-F), which indicate mutants at x-axis. The mutants atipt3,5,max4, atipt3,7,max4, atipt3,5,7 and atipt3,5,7,max4 exhibit dramatic reduction in number of lateral branches (B,C,E & F). Bars shown are means ± SE (n=20). Means that do not share a letter are significantly different as determined by One-way ANOVA with Tukey's post hoc test ($p \leq 0.05$).*

3.4.6.4 Shoot Branching

Branching index of *atipt5,7* was same as of wild-type, whereas *atipt5,7,max4* and *atipt5,7,max2* displayed branching phenotype, with number of branches similar to *max4* and *max2*, respectively (Figure 3.11- A and D). Branching in case of *max2* and *max4* is significantly increase by 20% in comparison with wild-type. Branching phenotypes of *atipt3,5* and *atipt3,7* were not different from wild-type, but *atipt3,5,max4* and *atipt3,7,max4* exhibited about 50% reduction in number of branches, as compared with *max4* (Figure 3.11 B and E). Branching is dramatically reduced in case of *atipt3,5,7* and completely suppressed in *atipt1,3,5,7*, as compared with wild-type. The *atipt3,5,7,max4* mutant was also found to have decreased branching index as compared to *max4* but the number of branches were not different from wild-type (Figure 3.11- C & F).

3.5 Discussion

3.5.1 Screening of Mutants

To investigate the interactive role of cytokinin and strigolactone in controlling shoot branching in *Arabidopsis*, the double and triple knockout mutants for *ATIPT3*, *AtIPT5* and *AtIPT7* genes in WT, *max2* and *max4* background were screened from segregating population of two crosses of quadruple *atipt1,3,5,7* with *max2* and *max4*. All mutant combinations (Table-3.3) were isolated successfully apart from *atipt3,5,max2, atipt3,7,max2, atipt3,5,7,max2* due to the reason that double knockout of *AtIPT3* and *MAX2* genes was found to be lethal and seeds were aborted. As these genes are located on different chromosomes, so it may be an effect of *atipt3* and *max2* alleles or due to loss of a function crucial for reproduction (see detail in Chapter 6). Two genes *ATIPT3* and *AtIPT7* are located on the same chromosome 3 at a distance more than half length of chromosome (5.56 Kb). Therefore, it is expected that these genes should segregate independently. However, a greater number of plants were screened to find out recombination event between *atipt3* and *atipt7*.

3.5.2 Rosette Growth

Growth of mutants was observed visually and in the form of rosette diameter and rosette dry weight, taken as indicative growth parameters. The rosette diameters are differentially dependent on maximum leaf size and growth reflecting overall size and growth of the shoot. The double *atipt* mutant *atipt5,7* exhibited bigger rosette than wild type (Fig. 3.10-A). The phenotype of *atipt5,7* was previously reported as wild type. However, this was concluded on a visual basis and not from any detailed phenotypic analyses (Miyawaki *et al*., 2006). The enhanced rosette growth of *atipt5,7* could be due to change in expression of other *IPT* genes especially *AtIPT3* that is highly expressed at the age of mature rosette before bolting (Takei *et al*., 2004a; Genevestigator database, Figure-3.1 & 3.2). No such information on *AtIPT* gene

expression in *atipt5,7* is available. However, iP and tZ-type CK levels were found to be normal (Miyawaki *et al*., 2006). Those CK levels were quantified from whole seedlings, but tissue-specific CK levels have not been reported. Detailed analyses on leaf morphology and size, CK quantification from shoot and phloem and expression profiles of *AtIPT* genes in *atipt5,7* background are required before further explanations can be proposed. The idea of overexpression of *AtIPT3* in *atipt5,7* is also supported from a report showing that plants overexpressing *AtIPT3* have 70% greater leaf size compared with wild type and this was a result of increased cell number (Galichet *et al*., 2008).

The rosettes of SL-deficient mutants *max2* and *max4* are bigger than wild-type (Fig. 3.10-A). Unlike the findings on *max2* rosette size in the present study, *max2* mutant leaves were previously shown to have a reduced area based on detailed morphometry measurements using parameters of leaf length and width, and petiole length (Stirnberg *et al*., 2002). The overexpression of *AtIPT* genes and subsequent CK synthesis in *max2* and *max4* may be the reason for the bigger rosettes as it has been found in pea that transcripts of *PsIPT1* in *rms* (SL mutants in pea) mutants were increased (Dun *et al.*, 2012). However, it is also reported that application of GR24 (synthetic strigolactone) decreased leaf size in *max4* due to reduced auxin levels, deduced from reduced intensity of expression of the auxin reporter DR5::GUS in young expanding rosette leaves (Ruyter-Spira *et al.*, 2011), and because a reduction in leaf size is a known consequence of decreased auxin content (Ljung *et al*., 2001). Therefore the rosette phenotypes of *max* mutants could be the outcome of increased CK levels or elevated IAA levels (Beveridge *et al*., 1997b; Ruyter-Spira *et al*., 2011) or both. The rosettes of *atipt5,7* in *max2* and *max4* were smaller than *max2* and *max4,* respectively but *atipt5,7,max2* was similar to *max2* (Fig. 3.10-A). The reduced rosette size of *atipt5,7,max4* was unexpected as compared with *atipt5,7* and *max4*. In addition to all the reasons discussed above, the variation among genotypes (Fig. 3.10-A) may be as a result of different seed quality (See Appendix II-C, showing whole trays of plants).

Triple null mutant for *AtIPT3, AtIPT5* and *AtIPT7* genes in WT and *max4* backgrounds showed reduced shoot growth in the form of their readily distinguishable very small rosette size, and resembled *atipt3,5,7* and *atipt1,3,5,7* reported by Miyawaki *et al.* (2006). Similar phenotypes were recorded in case of *CKX* overexpressor lines having low CK levels due to increased degradation in tobacco (Werner *et al*., 2001) and in *Arabidopsis* (Werner *et al*., 2003 and 2010) as well as in a triple knockout mutant for cytokinin receptors, *ahk2 ahk3 cre1* (Nishimura *et al*., 2004) which have greatly impaired CK perception. These phenotypes of mutant shoots were correlated to reduced shoot meristem size (Werner *et al*., 2001 and 2003; Nishimura *et al*., 2004; Miyawaki *et al*., 2006), which plays a critical role in normal shoot growth and development. The rosette size of *atipt3,7* in both WT and *max4* backgrounds was close to WT and slightly bigger than *atipt3,5 and atipt3,5,max4,* which in turn were smaller than WT. This suggests a possible role for *AtIPT5* in determining shoot size. Although *AtIPT5* is highly expressed in roots (Miyawaki *et al*., 2004 and Takei *et al*., 2004a), root cytokinin can play a role in controlling shoot development as reported in tomato (Ghanem *et al*., 2011). It is noteworthy that knockout of *AtIPT3, AtIPT5* and *AtIPT7* genes in *max4* in any double and triple combinations resulted in reduced shoot size compared with *max4*. This

somewhat contradicts the previous report suggesting high levels of redundancy between *AtIPTs* (Miyawaki *et al*., 2006).

The trends from rosette dry matter measurements support the data on rosette diameter, except for *AtIPT5,7* dry weight (DW) being greatly decreased compared with *max2*, but still higher than WT. This could be due to the difference in growth in the form of number of leaves as obvious from rosette visual phenotypes (Fig 3.9-A). Likewise, *max4* has smaller leaves, correlating with lower weight than *max2*.

3.5.3 Branching Index

Normal branching phenotypes of *atipt5,7, atipt3,5* and *atipt3,7*are similar to those reported by Miyawaki *et al*. (2006) who found phenotypes similar to WT in all *atipt* double mutant combinations. Reduction in CK synthesis in *atipt3,5,max4* and *atipt3,7,max4* subsequently resulted in about 50% decrease in numbers of branches, suggesting that *AtIPT5* and *AtIPT7* in *max4* background could not rescue the CK deficiency resulting from absence of *AtIPT3*.The importance of *AtIPT3* was further shown by it being sufficient for the maintenance of *max2* and *max4* branching phenotypes in both*atipt5,7,max2* and *atipt5,7,max4*. The role of *AtIPT5* and *AtIPT7* genes is very interesting as their expression is higher in roots and very low in shoot (Takei *et al*., 2004a). These spatial and temporal expression differences lead to the proposal that either root-derived CKs play a role in shoot branching or their low levels in shoot are sufficient for the promotion of branching. The latter hypothesis is supported in a report that the overexpression of *AtIPT* genes only in roots neither elevated cytokinin levels in the shoot nor increased shoot branching in non-transgenic scions of grafted plants (Faiss *et al*., 1997). Contrary to this, the over accumulation of CK in shoots of *HS::IPT* (*IPT* gene under the control of heat shock promoter) transgenic tobacco plants as an outcome of increased CK transport from the localized induction of *IPT* gene expression in roots strengthens the concept of root-CK involvement in shoot signalling (Vysotskaya *et al.,* 2010). In favour of CK as a local signal for shoot branching is another finding in pea where low xylem- CKs come from the roots of *rms* mutants (Foo *et al.*, 2007). Therefore, shoot branching phenotypes of *rms* mutants can be the consequence of CKs synthesized locally in their shoots. Although the branching index of *atipt3,5,7,max4* was equal to wild-type but overall branch growth and stem height is greatly reduced relative to wild-type (Figure 3.11- C & F). Therefore, CK is not involved only in breaking the bud dormancy to promote branching but also in the subsequent branch growth, as CK levels increase in activated buds (Turnbull *et al*., 1997 and Emery *et al*., 1998).

Results of rosette size and shoot branching, collectively suggest that the branching phenotypes of *max* mutants require CK availability and *ATIPT3* is a key gene for CK synthesis. Likewise, complete recovery of *atipt3,5,6,7*mutant growth by *AtIPT3p::AtIPT3-GFP*(Miyawaki*et al.,* 2006)validates this finding. Recently, levels of *PsIPT1* expression are found to be increased in nodes and internodes of the shoots of SL-deficient mutants (*rms1*)

and SL-insensitive mutants (*rms4*) of pea (Dun *et al*., 2012). It indicates that strigolactone downregulate *IPT* gene(s) to inhibit axillary bud outgrowth.

The severely reduced shoot growth of triple (*atipt3,5,7*) and quadruple mutants (*atipt1,3,5,7* and *atipt3,5,7,max4*) indicates that *AtIPT1* does not play a great role in plant growth. As *AtIPT1* is the least expressed gene (Takei *et al*., 2004; Genevestigator database, Figure-3.1 & 3.2) and Miyawaki *et al*. (2006) has reported that *AtIPT1* has the least effect on *atipt* knockouts.

3.6 Conclusions

1- Phenotype of *max* mutants depends on cytokinin supply.

2- Mutation in *AtIPT3* cause reduced growth and shoot branching in *max* mutants.

3- *AtIPT1* does not play a significant role in growth.

Chapter 4

Regulation of Cytokinin Biosynthetic Genes (AtIPTs)

4.1 Introduction

This chapter explores interaction and relationship between cytokinin and strigolactone, investigating regulation of cytokinin biosynthetic genes *AtIPTs* by strigolactone in the shoot and roots of *Arabidopsis thaliana*.

As described in Chapter 3, two prime processes of shoot branching including activation of axillary bud and subsequent bud growth into a branch are regulated by hormonal signals and mediated by a complex interplay between three hormone players namely, auxin, cytokinin and strigolactones. The network of interacting hormones moves systemically through a plant to control competition between apical dominance and branching (Muller and Leyser, 2011). This section briefly describes the molecular mechanisms underlying the interactions between three above mentioned actors in the control of shoot branching (Shimizu-Sato *et al*., 2009).

4.1.1 Interaction between Auxin and Cytokinin

The classical view of apical dominance control in plants, first proposed many decades ago, is that auxin inhibits branching by suppressing activation of axillary buds whereas cytokinin promotes bud outgrowth and hence shoot branching. However, the mechanism of interaction between auxin and cytokinin is still unresolved (Shimizu-Sato *et al*., 2009). In this context, indirect action of auxin is in contrast to direct effect of cytokinin (Ongaro and Leyser, 2008).

Application of exogenous auxin (NAA) decreases cytokinin biosynthesis, mediated by the auxin signalling pathway involving *AXR1*, as no effect of exogenous auxin on cytokinin production is found in a truly auxin-insensitive *axr1* mutant (Nordström *et al.*, 2004). Increased branching of same *axr1* mutant and resistance of its axillary buds to the inhibitory effects of apically applied auxin (Lincoln *et al.*, 1990; Stirnberg *et al.*, 1999) suggest that auxin signal transduction is involved in suppression of branching. More evidence is consistent with the model that apical auxin regulates cytokinin synthesis. For example, it has been reported in pea that auxin reduces CK levels by down-regulating expression of CK biosynthetic genes (IPT) in the nodal stem (Tanaka *et al.*, 2006). After decapitation, accumulation of CKs transported from roots has been found in the buds of chickpeas (Mader *et al.*, 2003). Increase in levels of CK transported from roots has been observed in pea and bean after decapitation but can be restored by auxin application to decapitated stump (Li *et al.*, 1995; Bangerth, 1994; Bangerth *et al.*, 2000). Thus the level of cytokinin from sources of stem and root correlates with activity of axillary bud.Collectively these observations and reports suggest that auxin reduces and inhibits lateral bud outgrowth by down regulating CK production and limiting CK supply to axillary bud (Ongaro and Leyser, 2008).

4.1.2 Interaction between Auxin and Strigolactone

After identification and characterization of branching mutants (*max1, max2, max3* and *max4*) in *Arabidopsis* (Stirnberg *et al*., 2002; Booker *et al*., 2004, 2005; Sorefan *et al*., 2003), a close connection between auxin and the MAX pathway has been proposed based on various studies. Buds of *max* mutants are substantially insensitive to auxin (Sorefan *et al*., 2003; Bennett *et al*., 2006), suggesting that auxin is dependent on the MAX pathway. In addition, modulation of levels of PIN auxin efflux carriers (Bennett *et al*., 2006) and up-regulation of transcripts of auxin transporters (Lazar and Goodman, 2006) in *max* mutants caused an increase in auxin transport capacity in the stem of mutants (Bennett *et al*., 2006), resulting in increased shoot branching. The distinctive bushy phenotype of *max* mutants is restored to wild-type, either chemically with addition of transport inhibitors or genetically in *pin1* mutant background. As well as, wild-type auxin response has been observed in *max* mutant buds by applying auxin transport inhibitor NPA. Hence, this strong evidence leads to the conclusion that the MAX pathway operates by regulating auxin transport in the stem (Bennett *et al*., 2006). After confirmation that the signal involved in the MAX pathway was strigolactone (Umehara *et al*., 2008 and Gomez-Roldan *et al*., 2008), studies on the interactive role of auxin and strigolactone revealed that auxin increases expression levels of *MAX3* and *MAX4*genes leading to increased strigolactone production that suppresses bud outgrowth (Hayward *et al*., 2009) and that strigolactone acts downstream of auxin to control apical dominance (Brewer *et al*., 2009).Both models (auxin transport-based and second messenger based) for axillary bud outgrowth are not mutually exclusive and may be coordinated to regulate shoot branching.

4.1.3 Interaction between Cytokinin and Strigolactone

There is strong evidence in pea that cytokinin levels are regulated by strigolactone, as low levels of cytokinin has been observed from xylem sap of *rms* branching mutants (*rms1, rms3, rms4 and rms5*) compared with wild-type (Foo *et al*., 2007). Grafting experiments reveal that WT scion to *rms4* or *rms3* rootstocks can restore normal CK levels in xylem sap. Therefore, a mobile signal moving from shoot to roots mediates cytokinin levels (Beveridge, 2000). Similar reduced levels of cytokinin have been shown in xylem sap of *max* mutants (Foo *et al*., 2007). However, many questions related to regulatory mechanism of interaction between cytokinin and strigolactone are still unanswered.

4.1.4 Strategies and Approaches to study Regulation of *AtIPTs*

Spatial expression of *AtIPTs* was analyzed using transgenic *Arabidopsis* plant seedlings expressing a gene for *beta glucuronidase* (GUS) or green fluorescent protein (GFP) fused to regulatory sequence of each *AtIPT* gene. These analyses of promoter::reporter constructs of *AtIPT* genes suggest that CK synthesis is restricted to specific tissues and organs. For example, activity of*AtIPT3::GUS* is localized to phloem throughout the plant with similar patterns of strong GUS staining shown in transverse sections of leaf petiole and root. Likewise, fluorescence of *AtIPT3::GFP* is shown in the phloem companion cells throughout the whole seedling. Staining for *AtIPT5::GUS* is found in columella root caps of primary and lateral roots as well as in xylem-radius pericycle cells presumably giving rise to primary and lateral root primordia, stem of lateral buds, base of young inflorescence and fruit abscission zone. In the case of *AtIPT5::GFP*, gene expression is also seen in lateral root primordia, pericycle and emerging lateral roots (Miyawaki *et al*., 2004; Takei *et al*., 2004a).

Lines of *AtIPT3::GUS* and *AtIPT5::GUS* provided by Dr. Tatsue Kakimoto were used in the current study. To test the hypothesis 'Strigolactone regulates CK biosynthetic genes', crosses of *AtIPTs::GUS* with *max2* and *max4* were generated to observe change in expression of these *AtIPT* genes in *max* backgrounds.

4.2 Material and Methods

4.2.1 Growth Conditions and Crossing

The growth conditions for plants on media plates and in soil were similar to section 2.1.2. New crosses were created from parental lines according to section 2.2.

4.2.2 Hormone Treatment

Seedlings on media plates were treated with 10 ml of 0.02% acetone, 1µm GR24, NAA and BAP for 24 hours on shaker (Biometra WT12) at the speed of 30 rotations/min, under same growth conditions. Synthetic hormones were dissolved in 0.02% acetone.

4.2.3 Histochemical Staining for GUS Activity

The modified form of the method described by Jefferson *et al.* (1987) was used to stain GUS lines histochemically (Miyawaki, 2004). Individual seedlings (10-days old)or required tissue and organ from plants were taken and transferred into 2ml eppendorf tubes already containing 1ml of GUS solution (1mM X-GlucA, 0.1% (w/v) Triton X-100, 0.5mM $K_3Fe(CN)_6$ (ferricyanide), 0.5mM $K_4Fe(CN)_6.3H_2O$ (ferrocyanide), 10mM Na_2EDTA and 50mM PO_4 buffer pH 7.0). All samples were vacuum infiltrated to allow solution to fully enter tissues and then incubated at 37°C until activity could be detected in GUS lines. The duration of incubation depended on promoter activity. The GUS solution was removed and the samples were washed with 70% ethanol twice, left over night in 70% Ethanol in the dark to remove chlorophyll to make them ready for visualization. Samples are mounted on slides to capture their images using a Zeus Axioplan 2 microscope attached to computer based software (Axiovision) for image acquisition.

4.3 Results

4.3.1 Expression Analysis of *AtIPT* Genes using Genevestigator

In order to gain insight into the interactions between cytokinin and strigolactone, gene expression analysis was carried out using Genevestigator; a microarray database coupled with expression data analysis tools (Hruz *et al.*, 2008; Zimmermann *et al.*, 2004).

The Genevestigator "samples" and "perturbation" search tools were used to look at the expression levels of four *AtIPTs* (see Appendix III) but only analysis for *AtIPT3* (blue) and *AtIPT5* (red) in *max* mutants and after strigolactone treatment are shown in Figures 4.1 & 4.2. The expression of *AtIPT3* is down-regulated in *max4* hypocotyls and in *max3-9* seedlings on addition of strigolactone.

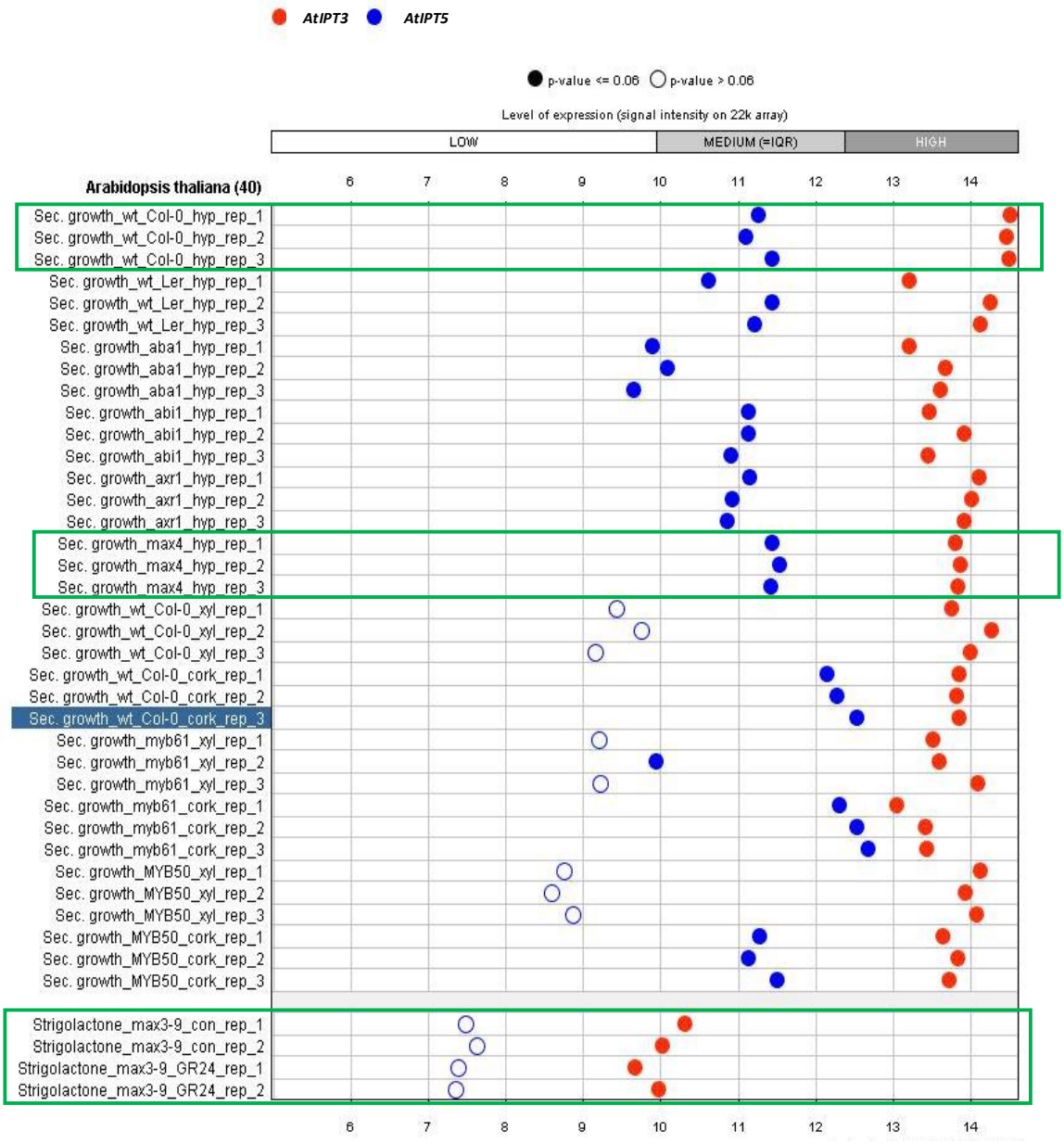

Figure – 4.1: Output Display obtained from Sample Tool Interface of Genevestigator Database.

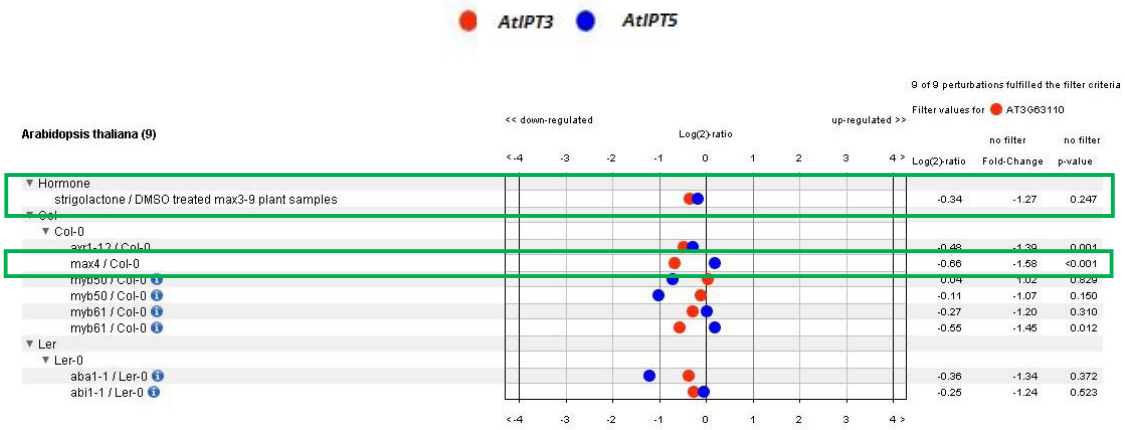

Figure - 4.2: Output Display exported from Perturbation Tool Interface of Genevestigator Database.

4.3.2 Crosses

At the start of project, the available lines were *AtIPT3::GUS,max4* (F2 seeds), *AtIPT5::GUS,max2* (double homozygous seeds). All other required crosses (*AtIPT3::GUS* × *max2* and *AtIPT5::GUS* × *max4*) were made and F2 seeds were harvested.

4.3.3 Screening for *AtIPT5::GUS* Line in *max2* and *max4* backgrounds

The available double homozygous line *AtIPT5::GUS*, *max2* was confirmed by GUS staining. All seedlings grown on plates (24 seeds per plate) showed expression in root primordia and columella root cap of main and lateral roots. All 48 seeds grown in soil displayed *max2* phenotype with long hypocotyls, increased shoot branching and rough leaves. The GUS expression and shoot branching therefore confirmed a double homozygous state for *AtIPT5::GUS* and *max2* mutation.

F2 seeds of a cross between *AtIPT5::GUS* and *max4* were grown in soil. From population segregating for *max4* branching phenotype, F3 seeds of wild-type and branching *max4* plants were harvested and tested for *GUS* expression in roots by growing on plates. Through microscopic scoring, two *max4* lines, exhibiting 100% GUS staining in root cap and lateral root primordial, were selected for further analysis.

4.3.4 Screening for *AtIPT3::GUS* Line in *max2* and *max4* backgrounds

F2 seeds of *AtIPT3::GUS* crossed with *max2* and *max4* were checked for segregation. Plants with increased branching phenotype and also some with wild-type phenotype were selected for *GUS* expression analysis. The plants of *max2* and *max4* exhibiting GUS activity in all

phloem networks in leaves were selected and theirF3 seeds were grown to test homozygosity of *AtIPT3::GUS*. If all F3 plants grown from single plant show GUS activity, then the parent plant is double homozygous. One out of nine was found to be double homozygous mutant for *AtIPT3::GUS* and *MAX2* genes. A double homozygous line *AtIPT3::GUS*,*max4*was selected with the same strategy.

4.3.5 Expression of *AtIPT5::GUS*

The roots and shoots of twelve seedlings were analyzed for analysis of *AtIPT5::GUS* expression and Figures 4.3- 4.6 show the images of their representatives. Figure 4.3 shows that the expression of *AtIPT5::GUS* is reduced in roots of *max2* and *max4* as compared with wild-type expression under control conditions. After application of GR24 (Strigolactone analogue), *GUS* expression is restored in *max4* but not in *max2*. There is no noticeable change in *GUS* expression in wild-type roots treated with GR24 from untreated control wild-type roots (Figure 4.3). Roots of all genotypes including wild-type, *max2* and *max4* when treated with auxin in the form of NAA, show greatly induced expression of *AtIPT5::GUS* in comparison with untreated controls, as shown in Figure 4.4. Application of synthetic cytokinin BAP decreases GUS staining in roots of wild-type. This negative regulation is more noticeable in vascular tissues than in root caps whereas BAP treatment restores wild-type *AtIPT5::GUS* expression in *max2* and *max4*, as evident from Figure 4.5.

Under control conditions, expression of *AtIPT5::GUS* is downregulated in shoots of *max2* and *max4*, as shown in Figure 4.6. Application of GR24 and NAA restores *AtIPT5::GUS* expression in *max4* only whereas it does not change expression patterns in *max2* compared with untreated *max2*. Addition of BAP causes recovery of *AtIPT5::GUS* expression in both *max2* and *max4* mutants. It is noteworthy that the differences among hormone treatments seen in mutants are not obvious in wild-type (Figure 4.6).

4.3.6 Expression of *AtIPT3::GUS*

Under control conditions, levels of *AtIPT3::GUS* expression are elevated in the phloem throughout *max2* and *max4* mutant seedlings in comparison with wild-type expression, as shown in Figure 4.7 and 4.8. Both root and shoot treated with GR24 show reduction in expression of *AtIPT3::GUS* in *max4* compared with untreated *max4* but GR24 does not alter the increased *AtIPT3::GUS* expression in *max2* (Figure 4.7 and 4.8). Addition of NAA decreases expression of *AtIPT3::GUS* in root and shoot of *max4* but *AtIPT3::GUS* expression remains unchanged in *max2* background after NAA treatment, a similar expression pattern to that observed following GR24 application (Figure 4.7 and 4.8). Wild-type root and shoot do not show obvious changes in wild-type expression patterns of *AtIPT3::GUS* following GR24 and NAA application. Application of BAP down-regulates expression *AtIPT3::GUS* in both root and shoot of all genotypes, but is more obvious in roots than in shoots (Fig. 4.7 and 4.8).

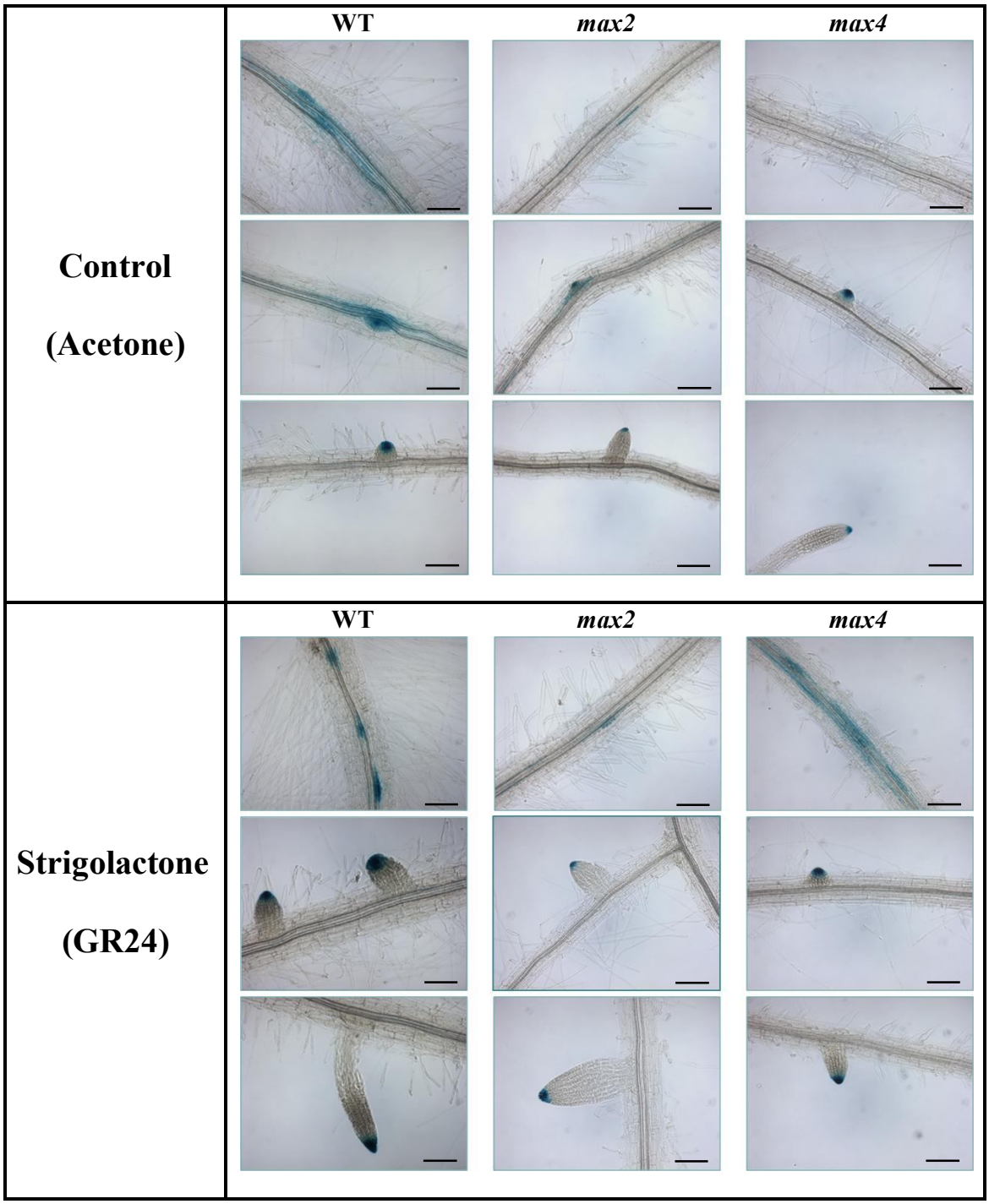

Figure – 4.3: Spatial Expression of AtIPT5::GUS in Roots following GR24 Treatment. *Expression of AtIPT5::GUS is located at primary and lateral roots cap and primordia. Seedlings of WT, max2 and max4 treated with 10 ml of 0.02% acetone (control) and 1µm of GR24 for 24 hours were incubated O/N in GUS staining solution at 37°C. Bar = 380 µm.*

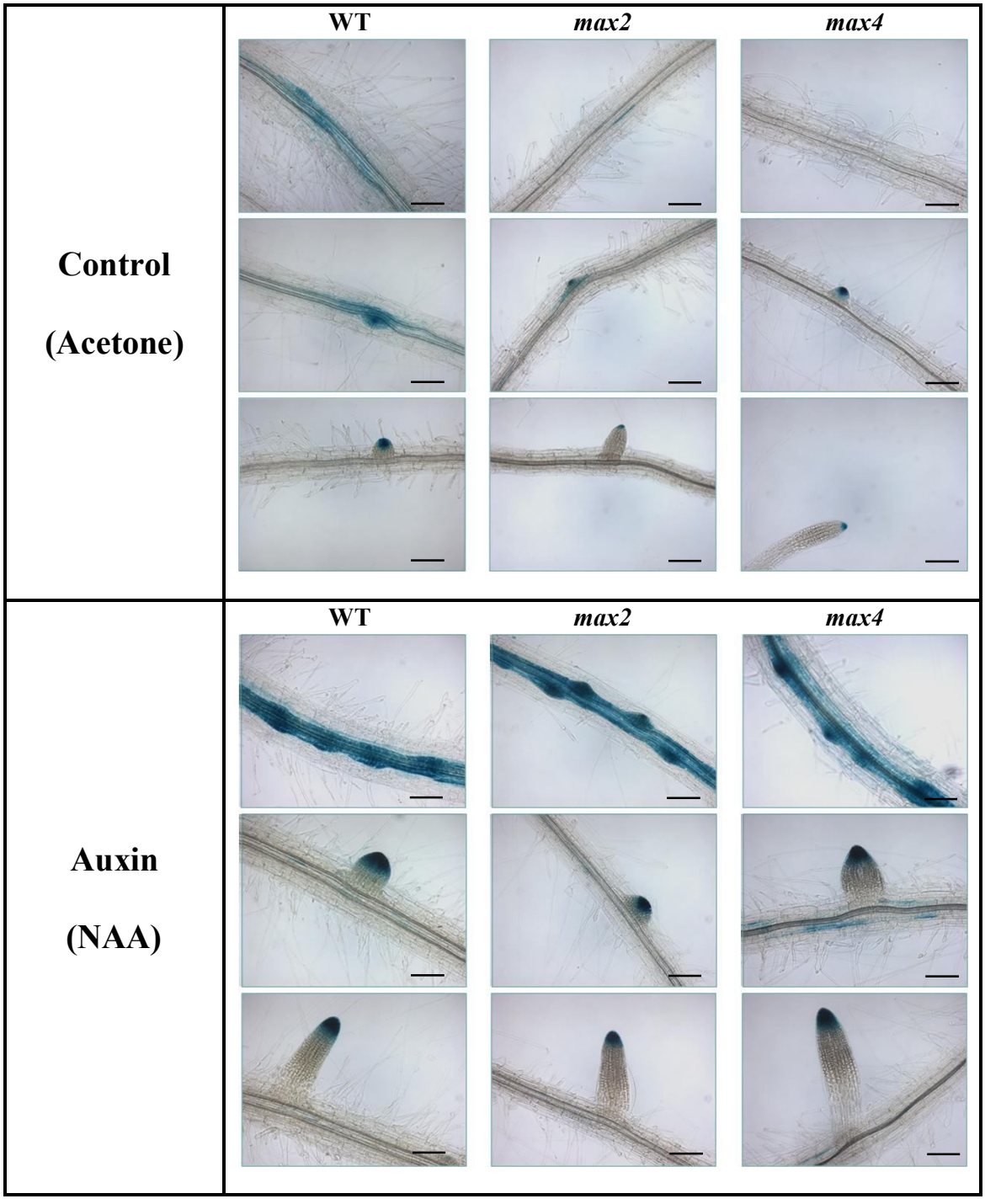

Figure – 4.4: Spatial Expression of AtIPT5::GUS in Roots following NAA Treatment. *Seedlings treated with 10 ml of 0.02% acetone (control) and 1µm of NAA for 24 hours were incubated O/N in GUS staining solution at 37°C. Bar = 380 µm.*

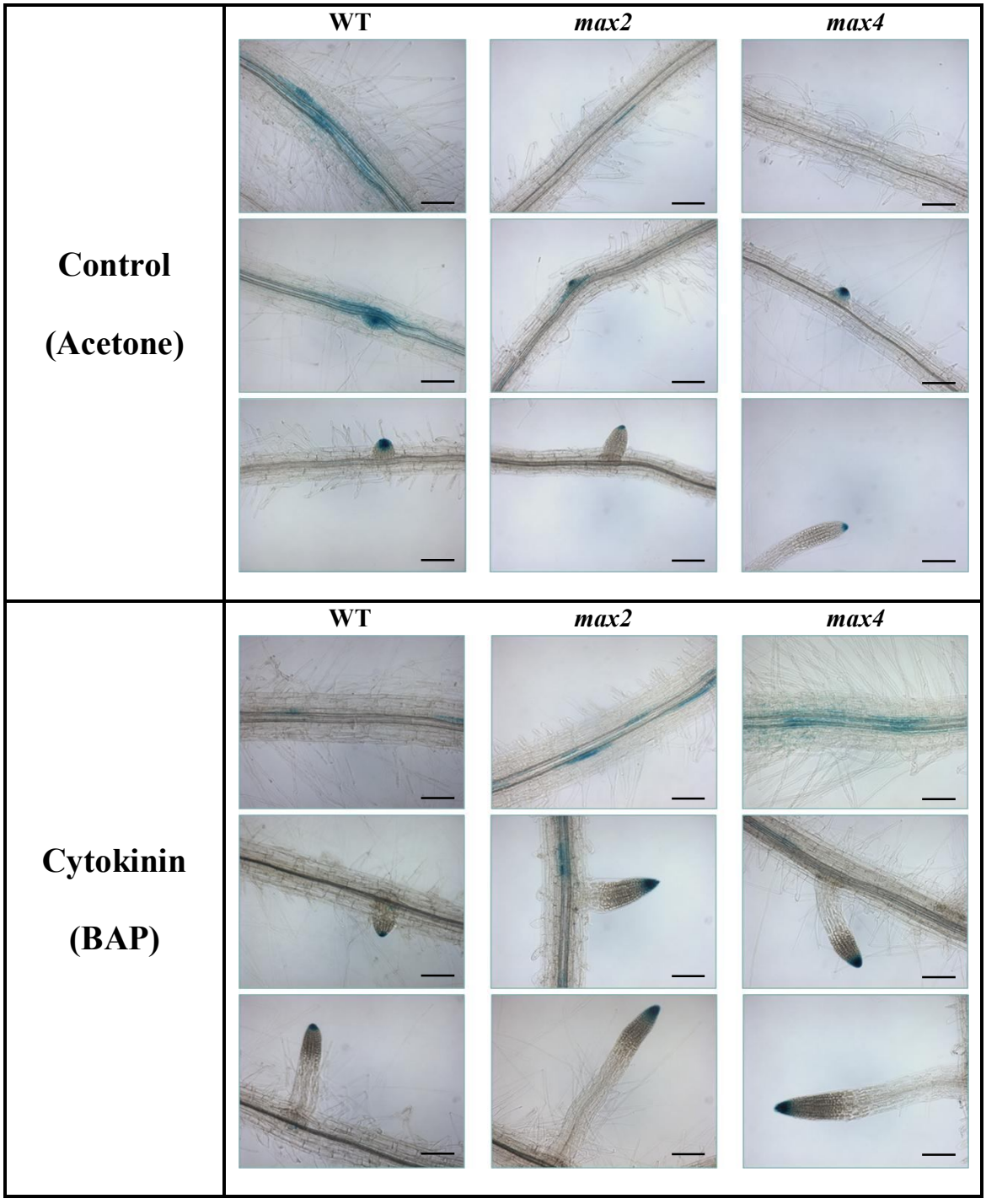

Figure – 4.5: Spatial Expression of AtIPT5::GUS in Roots following BAP Treatment. *Seedlings treated with 10 ml of 0.02% acetone (control) and 1µm of BAP for 24 hours were incubated O/N in GUS staining solution at 37°C. Bar = 380 µm.*

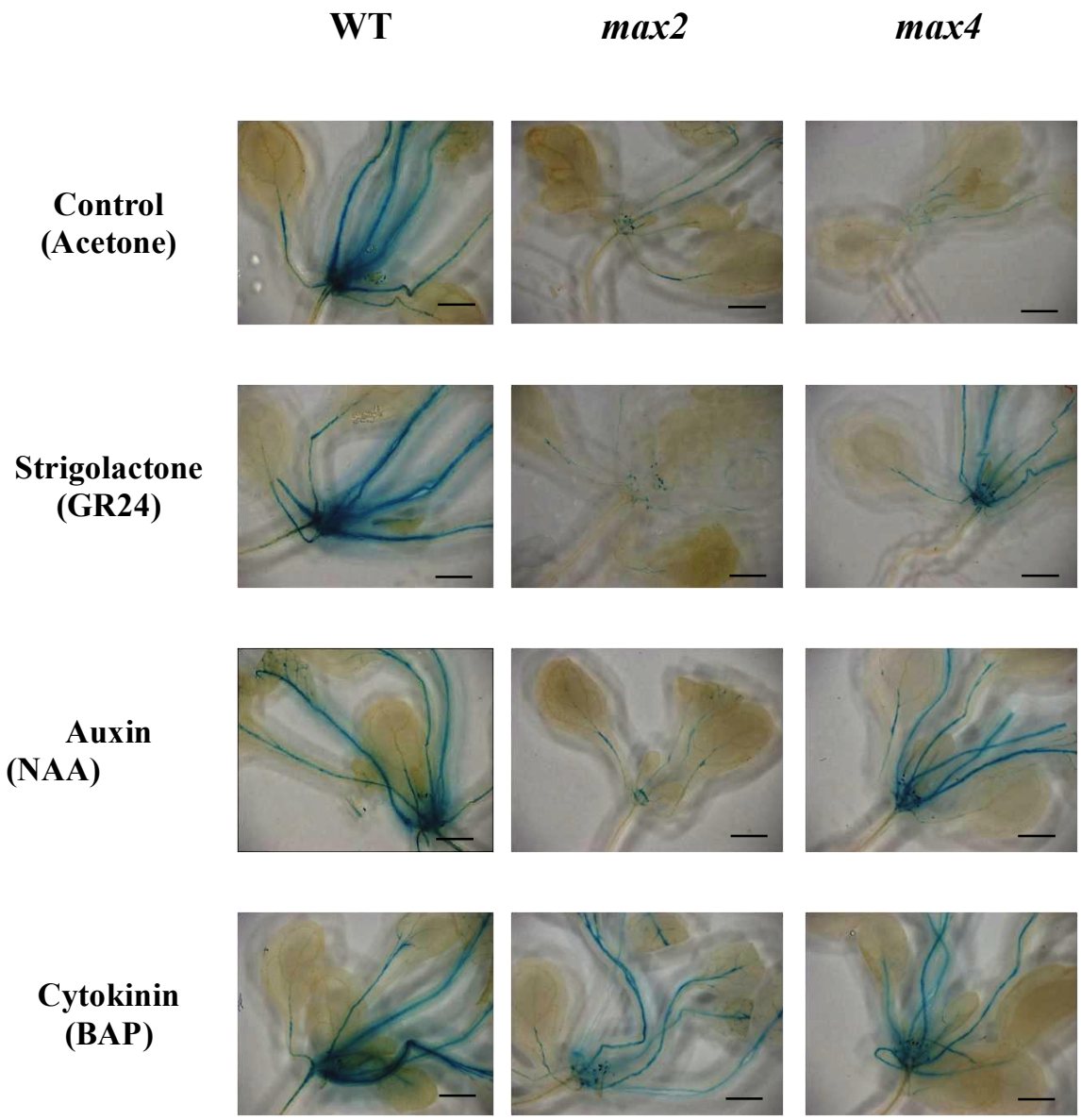

Figure – 4.6: Spatial Expression of AtIPT5::GUS in Shoot. *Expression of AtIPT5::GUS is located at meristematic region extending to leaf vasculature. Seedlings treated with 10 ml of 0.02% acetone (control) and 1µm of GR24, NAA and BAP for 24 hours were incubated O/N in GUS staining solution at 37°C. Bar = 800 µm.*

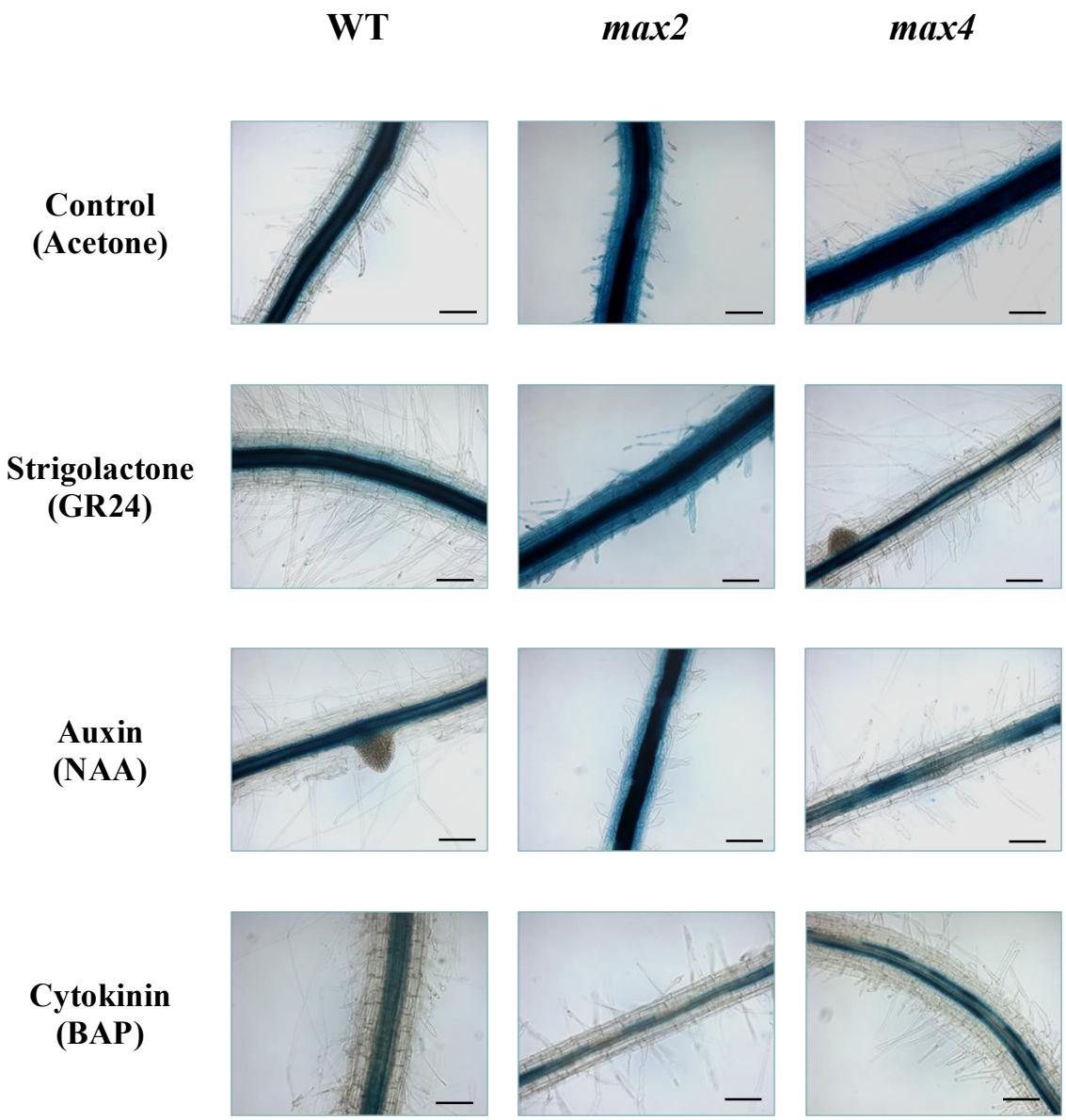

Figure – 4.7: Spatial Expression of AtIPT3::GUS in Roots. *Expression of AtIPT3::GUS is located in phloem of roots. Seedlings treated with 10 ml of 0.02% acetone (control) and 1µm of GR24, NAA and BAP for 24 hours were incubated for an hour in GUS staining solution at 37°C. Bar = 380 µm.*

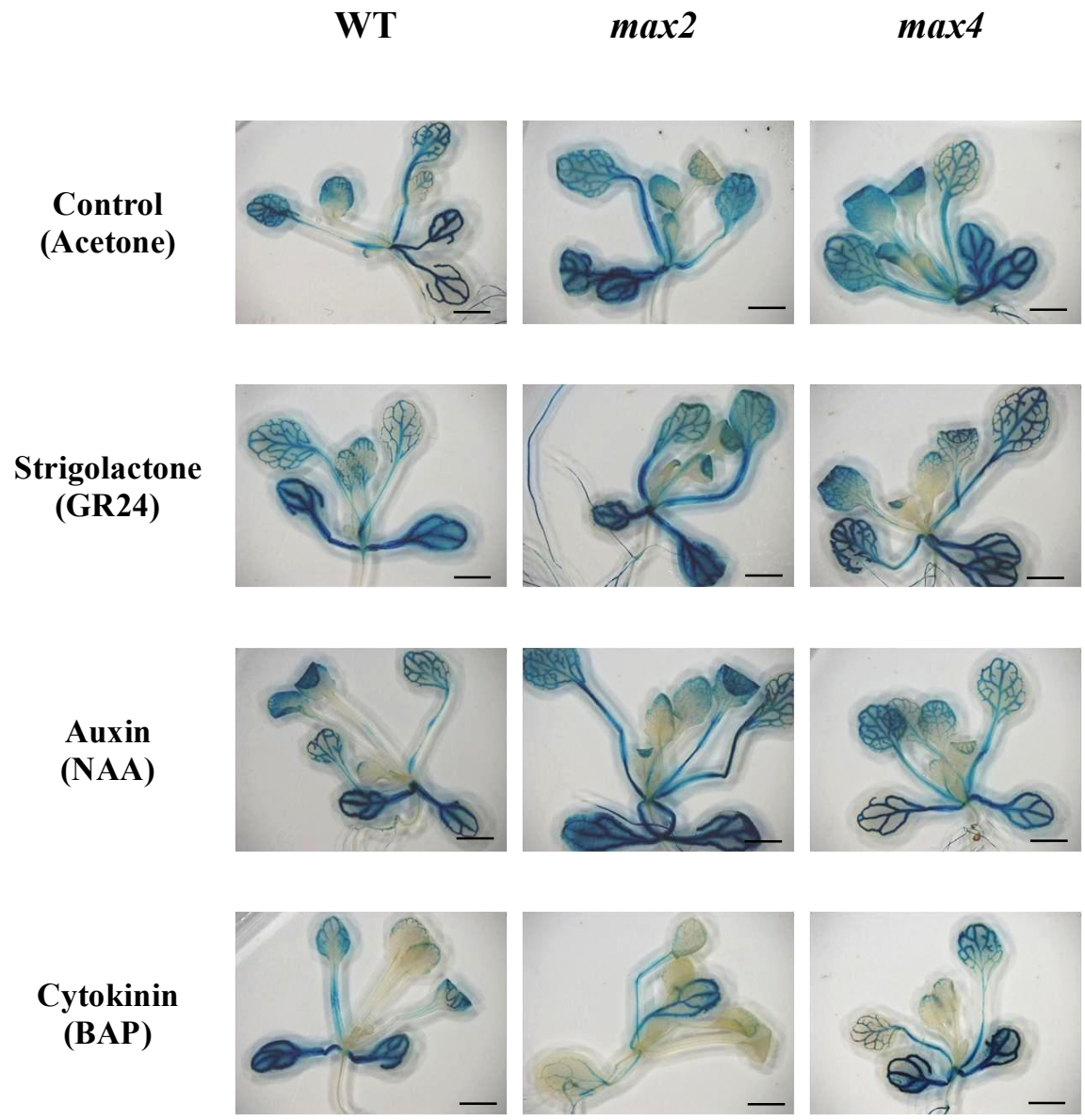

Figure – 4.8: Spatial Expression of AtIPT3::GUS in Shoot. *Expression of AtIPT3::GUS is located in phloem of shoot. Seedlings treated with 10 ml of 0.02% acetone (control) and 1µm of GR24, NAA and BAP for 24 hours were incubated for an hour in GUS staining solution at 37^{o}C. Bar = 1.4mm.*

4.4 Discussion

4.4.1 Online Expression Analysis of *AtIPTs*

In Genevestigator database, there is limited informative microarray data available to check expression of *AtIPT* genes in *max* mutants and under treatment of synthetic strigolactone GR24. Indeed only two experiments have been uploaded in the online database. One experiment was done in *max3* background but without wild-type control and other compared wild-type and *max4* hypocotyls only. Therefore, absence of control in one experiment and tissue specificity in the other experiment does not provide very conclusive information about *AtIPT* gene expression.

4.4.2 Tissue-Specific Expression of *AtIPT5*

It was observed that *AtIPT5::GUS* in wild-type background is expressed in shoot meristematic region extending to leaf vasculature (Figure 4.6). Such tissue-specific expression of *AtIPT5* gene was not previously reported (Miyawaki *et al*., 2004). Therefore, this can now be included as an additional site of CK production catalyzed by *AtIPT5* gene. Expression of *AtIPT5::GUS* has been reported already in root caps, lateral root primordia, stem of lateral buds, base of young inflorescence and fruit abscission zone. In previous work to study expression of *AtIPT* genes, no GUS activity for any of the *AtIPTs* was reported in the shoot meristematic region (Miyawaki *et al*., 2004).This is somewhat surprising because shoot meristem is thought to be a site for biosynthesis of cytokinin (Letham, 1994), which plays an important role in growth and development of shoot meristem. For example, examination of longitudinal sections from shoot meristems of wild-type and *35S::ATCKX* overexpressor lines revealed alterations in morphology of the shoot meristem in *35S::ATCKX* line. Overexpression of *AtCKX1* resulted in decreased cytokinin content and caused a significant reduction in the diameter and height of the meristem as a consequence of significantly decreased number and size of meristematic cells across the epidermal layer of shoot meristem in *35S::AtCKX1* (Werner *et al*., 2003).

Recently, it has been shown using *AtIPT5::GUS* reporter lines (generated by Cheng *et al*., 2012) that *AtIPT5* is expressed at around the edges of a non-induced *Arabidopsis* callus. Following incubation of callus in SIM (cytokinin-rich shoot induction medium), *AtIPT5*expression disappeared gradually from all regions except future pro-meristems. Ultimately, the activity of *AtIPT5::GUS* was found to be restricted to the pro-meristem region. Furthermore, mutations in *AtIPTs* caused significant reduction in frequency of shoot regeneration, which was much lower in double mutant *atipt5,7* and triple mutant *atipt3,5,7* than in wild type or single mutants. These findings from molecular and genetic analyses suggest *AtIPT*-dependent cytokinin biosynthesis during formation of shoot meristem and subsequent shoot regeneration (Cheng *et al*., 2012). Likewise, highly reduced shoot growth has been reported in *atipt3,5,7* and *atipt1,3,5,7* (Miyawaki *et al*., 2006). Collectively, previous reports support the finding of *AtIPT5::GUS* expression in the merstematic region of shoot.

4.4.3 Strigolactone-mediated Regulation of *AtIPT3* and *AtIPT5*

Qualitative *GUS* expression analysis indicates that *AtIPT3::GUS* is upregulated in root (Figure 4.7) and shoot (Figure 4.8) of *max2* and *max4*. Recently, it has been shown that transcript levels of *PsIPT1* in pea are significantly elevated in stem tissue segments of *rms4* and *rms5* but *PsIPT2* is unchanged (Dun *et al*., 2012). The increased *AtIPT3::GUS* staining corresponding to elevated *AtIPT3* gene expression in *max2* and *max4* mutants is similar to increased transcript levels of *PsIPT1* in *rms* mutant stem.

Figure 4.3 and 4.6 shows that *AtIPT5::GUS* is downregulated in root and shoot of *max2* and *max4*. Switching off *AtIPT5* gene function in shoot and roots of *max2* and *max4* may be under control of strigolactone directly or due to negative regulation of cytokinin biosynthesis as a consequence of upregulated *AtIPT3* gene. However, application of synthetic SL (GR24) recovers expression of *AtIPT5::GUS* in *max4*but not in the SL-insensitive *max2* suggests direct SL-dependent regulation of *AtIPT5*.

Application of GR24 does not affect the activity of *AtIPT5::GUS* and *AtIPT3::GUS* in *max2* (Figure 4.3-4.8) because *MAX2* is involved in the perception of strigolactone. Therefore, this evidence confirms that SL/GR24 response requires *MAX2*-dependent signalling pathway. Addition of GR24 does not affect expression of *AtIPT5::GUS* and *ATIPT3::GUS* in wild-type roots and shoots. This is consistent with the lack of impact of GR24 on *PsIPT1* or *PsIPT2* expression patterns in wild-type peas (Dun *et al*., 2012). It has also been shown that overexpression of *MAX4* under the control of 35S promoter in wild-type plants has no obvious effect on wild-type phenotype. This suggests that either *MAX4* is not involved in the rate-limiting step in SL synthesis or strigolactone cannot inhibit branching below WT levels (Sorefan *et al*., 2003).

4.4.4 Auxin-mediated Regulation of *AtIPT3* and *AtIPT5*

AtIPT5::GUS and *AtIPT3::GUS* shows different patterns of auxin-mediated regulation compared with each other as well as between root and shoot tissues. NAA treatment up-regulates *AtIPT5::GUS* expression in roots of wild-type, *max2* and *max4* (Figure 4.4), suggesting this regulation is SL-independent. For wild-type, this finding is in line with the previous report that auxin upregulates *AtIPT5* expression in roots of *Arabidopsis* (Miyawaki *et al*., 2004). On the other hand, auxin displays SL-dependent regulation of *AtIPT5* in shoots, as no change in expression is observed in NAA-treated *max2* shoots (Figure 4.7) compared with *max2* controls.

The unchanged expression of *AtIPT5::GUS* in *max2* shoot and that of *AtIPT3::GUS* in root and shoot of *max2* on treatment with NAA suggest that strigolactone works as a second messenger for auxin. This is consistent with previous findings that strigolactone acts downstream of auxin to control shoot branching (Brewer *et al*., 2009). The restored expression levels of *AtIPT5::GUS* in *max4* shoot and that of *AtIPT3::GUS* in root and shoot

of *max4* on the application of NAA are surprising and indicate that other mechanisms are involved.

According to Kohlen *et al*. (2011), some orobanchol is still produced in *max4-1*, indicating that either *max4-1* is leaky or another less active pathway, separated from the MAX pathway, is involved in strigolactone biosynthesis. The enhanced bushy phenotype of *max4-5*compared with that of *max4-1* (Bennett *et al*., 2006) suggests that the *max4-1* mutant retains some catalytic activity. The presence of alternative SL biosynthetic pathways is also possible that would explain the reason why *MAX2* over-expression in SL biosynthetic mutant backgrounds can partially inhibit the increased branching phenotypes (Stirnberg *et al*., 2007). Multiple biosynthetic pathways for other hormones including auxin (Zhao, 2010) and cytokinins (Sakakibara, 2006) have been reported.

It has been shown that auxin increases expression level of *MAX4* leading to increased strigolactone production (Hayward *et al*., 2009). Therefore, auxin may also induce expression of the mutant *MAX4-1* gene. However, both proposals of leaky allele or alternate SL biosynthetic pathway are not supported from the results of this chapter, because if *max4-1* has some catalytic activity or if there is another pathway of SL synthesis, it would be predicted to show differences in the expression of *AtIPT5::GUS* and *ATIPT3::GUS* between *max2* and *max4* under control conditions. However, the actual expression patterns found are same in both mutants.

4.4.5 Regulation of *AtIPTs* by Cytokinin

Cytokinin treatment in the form of BAP application negatively regulates *AtIPT* biosynthetic genes. Similar regulation of *AtIPTs* by cytokinin has been reported to occur through A-type *Arabidopsis* response regulator (Type-A ARR) proteins, which are involved in negative regulation of CK signalling, forming a negative feedback loop (To *et al*., 2004). The upregulation of *AtIPT5* by cytokinin in *max* mutants is unexpected and there is no simple and easy explanation for it. Further investigation is required to confirm this finding.

4.5 Conclusions

1- *AtIPT3* is upregulated and *AtIPT5* is downregulated in *max2* and *max4* mutants.
2- Auxin-mediated upregualtion of *AtIPT5* in roots is SL-dependent but in shoot is MAX2-dependent.
3- Regulation of *AtIPT3* by auxin in root and shoot is MAX2-dependent.

Chapter 5

Regulation of Cytokinin Levels and Transport

5.1 Introduction

This chapter presents an investigation of cytokinin status in shoot and root tissues and distribution through phloem and xylem. The main objective of this work was to elucidate the regulation of cytokinin levels and transport by strigolactone using *Arabidopsis AtIPT* knockout mutants in *max* and wild-type backgrounds.

5.1.1 Cytokinin Biosynthesis and Translocation

As described in Chapter 1, seven isopentenyltransferase (AtIPT) enzymes are responsible for catalyzing the first step of the adenine-derived pathway through which iP-type and tZ-type cytokinins are synthesized (see section 1.3.3, Fig. 1.2). The corresponding genes of AtIPT enzymes (Kakimoto, 2001; Takei *et al*., 2001a) are differentially and spatially expressed (see section 1.3.4) in *Arabidopsis* (Miyawaki *et al*., 2004; Takei *et al*., 2004a). Four genes including *AtIPT1, AtIPT3, AtIPT5* and *AtIPT7* are expressed during vegetative phase. CKs are synthesized initially in the form of iP-type CKs and then are converted to tZ-type CKs by activity of CYP735As (see section 1.3.3, Fig. 1.2), which are expressed abundantly in roots (Takei *et al*., 2004b). Consistent with this, xylem sap contains tZ-type cytokinins, mainly tZR (Beveridge *et al*., 1997; Takei *et al*., 2001b), which are translocated to the shoot. In contrast, iP-type cytokinins are transported through phloem sap (Corbesier *et al*., 2003) to roots. The main forms of iP-type CKs in phloem sap are iPRP, iPR and iP. From these findings, it is clear that different types of CKs are found in xylem and phloem (see section 1.3.6, Figure 1.3) but the biological role of this differential translocation is yet unknown. *AtIPT5* is highly whereas *AtIPT7*and *AtIPT3* are moderately expressed in roots (Takei *et al*., 2004a), it can be concluded that iP-type CKs are synthesized locally in roots. It is still unclear whether

CYP735As utilize locally synthesized iP-type CKs and/or phloem-derived iP-type CKs.

5.1.2 Regulation of Cytokinin Levels and Translocation by Strigolactone

In 2008, two reports demonstrated strigolactone as a novel plant hormone involved in suppression of shoot branching, using shoot branching mutants in *Arabidopsis,* pea and rice (Gomez-Roldan *et al*., 2008; Umehara *et al*., 2008). Although shoot branching mutants were correlated with strigolactone for the first time in 2008, these mutants had been reported for a long time. Cytokinin was known to promote shoot branching (Sachs and Thimann, 1967; Turnbull *et al*., 1997; Emery *et al*., 1998) and considered mainly to be synthesized in roots, supplying cytokinin to shoot via xylem sap. The role of xylem-CKs in shoot branching control remained controversial as evidence was in favour of and against xylem-derived CKs, playing a role in controlling shoot branching (Bangerth, 1994; Li *et al*., 1995; Faiss *et al*., 1997; Böhner & Gatz, 2001). In this context, shoot branching mutants of pea (*rms*) were investigated for function of xylem-CKs in conferring their distinctive phenotypes. It was found that xylem cytokinin levels were extremely low (40-fold) in pea *rms1 and rms5* mutants as compared with wild-type plants (Beveridge *et al*., 1997b; Morris *et al*., 2001) and only *rms2* exhibited a significant increase in xylem CKs (Beveridge *et al*., 1997b). Grafting experiments using *rms4* and wild-type plants revealed that a feedback mobile signal coming from the shoot was responsible for decreased transport of CKs in xylem (Beveridge *et al*., 1997a).

There is a hypothesis that proposes auxin as a long-distance feedback signal that controls xylem transport of CKs (Beveridge, 2000; Foo *et al*., 2007). Reduced xylem-CKs might be correlated with high auxin levels or enhanced auxin response. However, *rms2* mutant shoots have elevated IAA levels and other *rms* mutants do not have increased IAA content (Beveridge *et al*., 1996; Morris *et al*., 2001). On the other hand, enhanced auxin response is thought unlikely to be responsible for inducing the increased branching phenotype. Instead, auxin application could not inhibit branching in *rms* mutants (Beveridge, 2000; Bennett *et al*., 2006). Feedback regulation was found to be conserved, as shoot branching mutants of *Arabidopsis* (*max*) also had highly decreased xylem-CKs (Foo *et al*., 2007). When shoot branching mutants were linked with the absence of a shoot branching inhibitor, strigolactone (Gomez-Roldan *et al*., 2008; Umehara *et al*., 2008), new questions were raised regarding interactions between strigolactone and cytokinin in controlling shoot branching. An antagonistic relationship between strigolactone and cytokinin was proposed on the basis of previous findings, but it is still unresolved how strigolactone regulates xylem cytokinin? Here, it is hypothesized that xylem-CKs are controlled by strigolactone through regulation of CK biosynthetic genes (*AtIPTs*) in root and shoot. To test this hypothesis *atipt* double (*atipt5,7; atipt3,5* and *atipt3,7*) and triple (*atipt3,5,7*) mutants are created in wild-type and *max* backgrounds, as described in chapter 3 (section 3.3). Levels of CKs were quantified by LCMS in shoot and root tissues as well as in xylem and phloem saps, and analyzed by principal component analysis to find patterns of CK distribution in different tissue types.

5.1.3 Principal Component Analysis (PCA)

In life sciences, various techniques are used to collect data for many more variables per sample than actual number of samples analyzed. For example, microarrays, mass spectrometers (MS), high pressure liquid chromatography (HPLC) and HPLC coupled with MS (LCMS) can quantify levels of thousands of variables in hundreds of samples. Due to such high-dimensionality of samples, it is hard to readily visualize the data. Moreover, the number of variables and their many possible relationships make exploration of the data very challenging (Ringner, 2008).

For a large number of variables, multivariate statistical methods are commonly used to analyze diversity irrespective of data set (biochemical, hormonal, molecular markers or morphological data). In multivariate analyses, ordination methods (that is used in exploratory data analysis rather than in hypothesis testing) categorize objects across values from multiple variables; hence, similar objects are located closer to each other while different objects are at a distance from each other. Such related and unrelated correlations (relationships between objects) on several axes (one for each variable), are characterized numerically and presented graphically to assess information and explanation of data easily. At present, the most commonly used ordination technique is principal component analysis (PCA) as a "pattern finding method" to complement cluster analysis (Mohammadi and Prasanna, 2003).

Principal component analysis, based on a mathematical algorithm, reduces dimensionality of data by decreasing number of variables while retaining most of the variation present in whole set of data. This reduction of variables is accomplished due to consideration of some redundancy in the variables (redundancy means that some of variables are correlated with one another, possibly because they are measuring the same construct). This redundancy makes it possible to reduce observed variables into a smaller number of artificial variables by identifying their directions, called principal components (PCs), along which most of variance in observed variables is accounted. By using significant components, each sample can be characterized by a few numbers relative to the values for a large number of variables. Samples can then be plotted along two axes of PCs. This graphical presentation makes it possible to visualize assessment of similarities and differences between samples and to determine samples together in a group (Ringner, 2008).

PC1 calculated in a PCA captures the maximum amount of total variation in observed variables. Under classic conditions, this means that PC1 will be correlated with some of the observed variables or may be correlated with many. PC2 calculated has two important qualities. First, this component captures the maximum amount of variation in the data set that was missed by PC1. Again under classic conditions, this means that PC2 will be correlated with some of observed variables that did not display strong correlations with PC1. The second key attribute of PC2 is that it will be uncorrelated with PC1. Correlation between PC1 and PC2 would be zero. Remaining PCs that are computed in the analysis display the same two features. A principal component analysis continues in this manner, with each next PC

accounting for gradually smaller and smaller amounts of variation. That is why only the first few significant PCs (Conventionally, if the Eigen value is greater than 1, PC is significant) are usually displayed and interpreted. On completion of PCA, resulting components will display varying degrees of correlations with observed variables (Mohammadi and Prasanna, 2003).

5.2 Materials and Methods

5.2.1 Growth Conditions

The genotypes were grown in compost, hydroponics and on plates according to section 2.1.2.

5.2.2 Root and Shoot Tissues Harvest

The genotypes were grown in hydroponics on short-day photoperiod (in some case after two weeks transferred to long-day photoperiod). Before bolting, roots and shoots were harvested to quantify cytokinins in roots and shoots separately. Therefore, fresh root and shoot tissues of three plants were bulked, weighed 1g (0.5g in case of tissue culture seedlings) and frozen immediately in liquid nitrogen after wrapping in aluminium foil. These flash frozen samples were stored at –80°C.

5.2.3 Phloem Sap Collection

Phloem sap was collected according to method described by Corbesier *et al*. (2003). Seven mature leaves from 2-month old plants grown at short-day photoperiod were harvested and placed in a 2-ml eppendorf tube containing 1.5ml of 10 mM EDTA (pH 8.5) for 12-16 hours. Twelve (12) plants were used in each independent experiment. The tubes containing the harvested leaves were kept in airtight chambers with increased humidity to avoid evaporation of EDTA solution during sap collection time. The chambers were kept on same conditions in which plants were grown. Therefore, leaves during exudation were subjected to the same light–dark cycle as for intact plants. Collected leaf exudates were stored at –20°C or –80°C until quantification.

5.2.4 Xylem Sap Collection

Syringe-suction method was used to collect xylem sap from *Arabidopsis* plants, as described by Beveridge *et al*. (1997a) with minor modifications. Plants were grown on short-day photoperiod for two months. After germination, plants were kept covered with translucent plastic lid for two weeks to get quite long hypocotyls. One day before sap collection, plants were properly watered. Rosettes were decapitated above the hypocotyl. A flexible silicon tube (of different diameter according to need fitting with different widths of hypocotyls) attached to a 5-mL syringe was placed over stump (decapitated hypocotyl) and tied tightly in place. Syringe plunger was pulled out and held at that position to create a vacuum in the

syringe. About 50-100 µl of xylem sap per plant was collected under vacuum into the syringe for about 120 minutes. Samples of xylem sap were then frozen in liquid nitrogen and stored at −80°C until CK quantification on LCMS.

5.2.5 Extraction of Cytokinin

5.2.5.1 Extraction from Root and Shoot Tissues

The tissue was ground to powder in liquid N_2 with the help of pestle and mortar While still frozen, 10 ml per gFW tissue of cold (4°C) extraction solvent (methanol/formic acid/water, 60:5:35 including 35 mg/L 5'AMP. Sigma A2252) were added. Internal standard (Deuterium (^{2}H) labelled cytokinins, (OlChemIm, Olomouc, Czech Republic, a list and chromatogram of D-standards is given in Appendix IV-A) was added at the conentration of 10ng each compound per gFW tissue. Grinding was continued to make fine slurry, poured into 15ml falcon tube and kept for 10 min or o/n in the cold room (set at 4°C). The tube was centrifuged at 10000 g for 10 min at 4°C and supernatant was transferred into new 15 ml tube. The pellet was redissolved in 5 ml extraction solvent per gFW with vigorous mixing and kept for 10 mins in the cold room. These tubes were centrifuged again and supernatant was added to first one. The extract was passed through (pre-wetted with 5 ml methanol) Sep Pak C18 "Vac 500mg 6ml" or "Plus 400mg" cartridge (Waters p/n WAT036790 open column or WAT036810 syringe fitting) to remove hydrophobics (lipid, pigments) and collected in a glass tube. The extract was evaporated to nearly 1ml (water only present, no methanol) in Jouan concentrator at maximum 40°C or no heat. Then it can be stored -20°C if needed.

The Oasis MCX 150mg 30µm cartridge (Waters p/n 186000256) was pre-washed with 5 ml 1 M formic acid. The 1 ml sample was diluted with 4 ml 1 M formic acid and loaded onto Oasis cartridge which was washed with 5 ml 1 M formic acid and then with 5 ml methanol (fraction contains IAA and ABA) Now the sample was eluted with 5 ml 0.35 M NH_4OH (contains CK nucleotides) and then eluted again with 5 ml 0.35 M NH_4OH in 60% Methanol (contains all other CKs). Both eluates were evaporated to dryness at 40°C.

5.2.5.1 Extraction from Leaf Exudates

At the end of phloem sap collection (section 5.2.3), leaves in batches from each tube were weighed. For CK quantification, samples from two tubes were bulked, and hence 6 replications were used. Volume of EDTA solution containing leaf exudates was measured. Based on total fresh weight of each biological replication, total volume of each biological replication and transpiration as µl/leaf; µl/leaf/h; µl/g/h, the calculation was made to take volume of EDTA equivalent to 0.5-1g weight of leaf (g tissue represented by each pooled ml of exudates). The C18 cartridges were prepared by flushing with 5 ml methanol and with then 5 ml H_2O. Sample were loaded onto cartridges, D-labelled standard (5-10 ng each compound) was added. The loaded samples were allowed to pass through and collected all in a tube-A. The cartridges were washed with 4 ml H_2O and also collected into tube-A which was stored

until LCMS is run, because it is possible that tube-A might have some phloem-CKs, especially tZRP and cZRP. The CKs from cartridges were eluted with 4 ml 70% Methanol and samples were dried on Jouan concentrator with no heat.

5.2.6 Sample Preparation for LC-MS Analysis

The pellet (from section 5.2.5.1and 5.2.5.2) was re-dissolved in 100 µl HPLC grade Methanol, in same glass tube by vigorous vortexing and transferred to 1.5 ml eppendorf tube. The glass tube was rinsed with 100µl 50% HPLC methanol in milliQ water and added into same eppendorf which was centrifuged for 10 minutes at full speed (>10000 g). Now the sample from eppendorf tube was filtered through 0.45 µm 4mm diameter syringe filter into autosampler vial (Chromacol vial Cat. No. 3-FISV, 12x32 mm having 300 µl fused glass insert). The syringe was rinsed with 100 µl HPLC grade 100% methanol and filtered. The liquid in the autosampler vials evaporated completely on the Jouan concentrator without using heat. The sample was dissolved in solvent compatible with LCMS. Firstly, 10 µl of HPLC acetonitrile was added. This helps to dissolve especially the less soluble CKs like iP. Then 190 µl of ammonium acetate buffer (10 mM, ~pH3.3) was added and vortexed thoroughly.

For quantification of CKs in xylem sap, root exudates from three plants were bulked. The standard mixture (5-10ng of each compound) was added to 200 µl xylem sap taken into a syringe attached to filter (0.45 µm 4mm diameter syringe filter). The sample was filtered into autosampler vial (as described in previous paragraph). The syringe was rinsed with 50 µl H_2O and filtered through. The samples are now ready for analysis by LCMS.

5.2.7 LC-MS Analysis

LC-MS analyses were carried out largely as described by Foo *et al*. (2007), using a solvent gradient of acetonitrile in 10 mM ammonium acetate, pH 3.4 (solvent A as 5% acetonitrile in 10 mM ammonium acetate, solvent B as 95% acetonitrile in water with 0.1% formic acid for a solvent program: initially 5% for 4 min, rising to 14% at 20 min and 32% at 25 min (this is programmed as 0% solvent B, then 15% B, then 35% B); at rate of 200 µL min-1. The C18 column (Phenomenex Luna, 3-µm, 100 × 32 mm) was used in HPLC (Agilent 1100 Binary LC system), coupled to mass spectrometer (Applied Biosystems Q-Trap hybrid mass spectrometer) fitted with a Turbo Ion spray (electrospray) source operating in positive ion multiple reaction monitoring (MRM) mode with dwell time 30 mins for each MS-MS ion pair. The injected volume ranges from 10 – 100 µl depending on CK levels.

After running on LC-MS, the cytokinins were quantified according to the following formula:

ng (Analyte) = (peak area of analyte/peak area of standard) × 10

Then each analyte concentration in ng was converted into pmoles.

5.3 Results

5.3.1 Quantification of Cytokinins

Levels of ribotides, ribosides and free base cytokinins were measured through LC-MS-MS following the protocol (see section 5.2.5, 5.2.6 and 5.2.7) from shoot tissues, phloem sap, root tissues and xylem sap of *max1, max2, max3* and *max4* mutants. A chromatogram of d-labeled cytokinin mixture is given in Appendix IV-A.

5.3.2 CK Levels in *max* mutants

5.3.2.1 Shoot-CKs: Quantified compounds in shoots (2- months old grown hydroponically under short-days) of wild-type plant and *max* mutants are iPRP, iPR, iP, ZRP, tZR, tZ, DZRP, cZRP, cZR, cZ. Fig. 5.1 shows that levels of iPRP, ZRP and cZ are higher than other compounds quantified in wild-type. ZRP is the most abundant (28 pmoles/gFW) in wild-type shoot and it is 3-fold higher than iPRP. Levels of ZRP, tZR and tZ are highly decreased in all four *max* genotypes (*max1, max2, max3* and *max4*) as compared to wild-type. ZRP is decreased by about 4-6 fold (6-fold in case of *max1*). In the case of tZR, approximately a 7-fold reduction was observed in *max1*, 5-fold in *max2* while 3-fold in *max3* and *max4*. tZ is reduced by about 1.5-2.5 fold. In case of all other CK compounds (iP-type, cZ- and DZ-type CK metabolites), the *max* mutants are not significantly different from wild-type, as evident from Fig. 5.1.

5.3.2.2 Phloem-CKs: Phloem sap was collected from leaves of *max* genotypes (*max1, max2, max3* and *max4*) which were grown hydroponically under a short-day photoperiod. The CK compounds; iPRP, iPR and cZR were detected in the phloem sap of *max* mutants.

As shown in Fig. 5.2, iPR is found abundantly in phloem sap of wild-type, and is about 10-fold higher than iPRP. Levels of iPRP are significantly increased in all *max* genotypes as compared with wild-type (~ 17-fold in *max1*, 12-fold in *max2* and 8-9 fold in *max3* and *max4*) but *max3* and *max4* exhibit lower levels than *max1* and *max2* mutants, as can be seen from fold change. In the case of iPR levels, *max1* and *max4* are similar to wild-type whereas *max2* shows significant reduction (~ 4-fold) in levels and *max3* shows significant increased (~ 3-fold) levels, as compared with the wild-type. All *max* mutants are similar to wild-type in the case of cZR, except *max2* that exhibits a significant decrease (Fig. 5.2).

5.3.2.3 Root-CKs: Roots of three plants (2-month old grown hydroponically under short-days) per replication per genotype were pooled to measure levels of cytokinins compound. The detectable compounds in roots of *max* mutants include iPRP, iPR, iP, ZRP, tZR, tZ, DZRP, cZRP, cZR, cZ. For all CK compounds quantified, the *max* mutants are not significantly different from wild-type, as evident from Fig. 5.3.

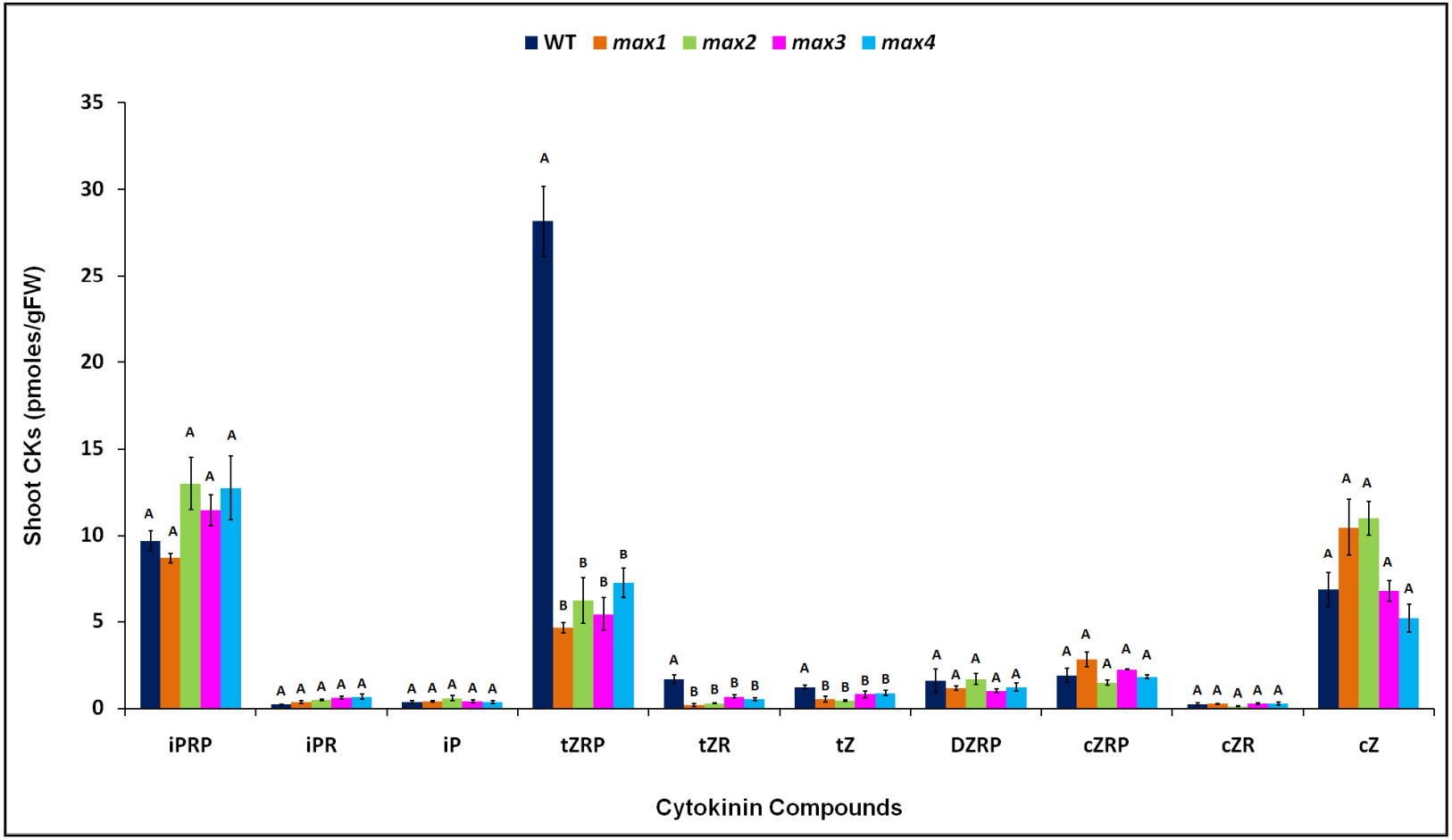

Figure – 5.1: Cytokinin Levels in Shoot Tissues of Col-0 and max Genotypes. *The genotypes were grown hydroponically under short-day photoperiod.1g sample from bulk of three shoots (2-months old) per replication per genotype was analyzed. Col-0 is a wild-type genotype used as a control. Bars shown are means ± SE (n=6). Means that do not share a letter are significantly different as determined for each compound by One-way ANOVA with Tukey's post hoc test ($p \leq 0.05$).*

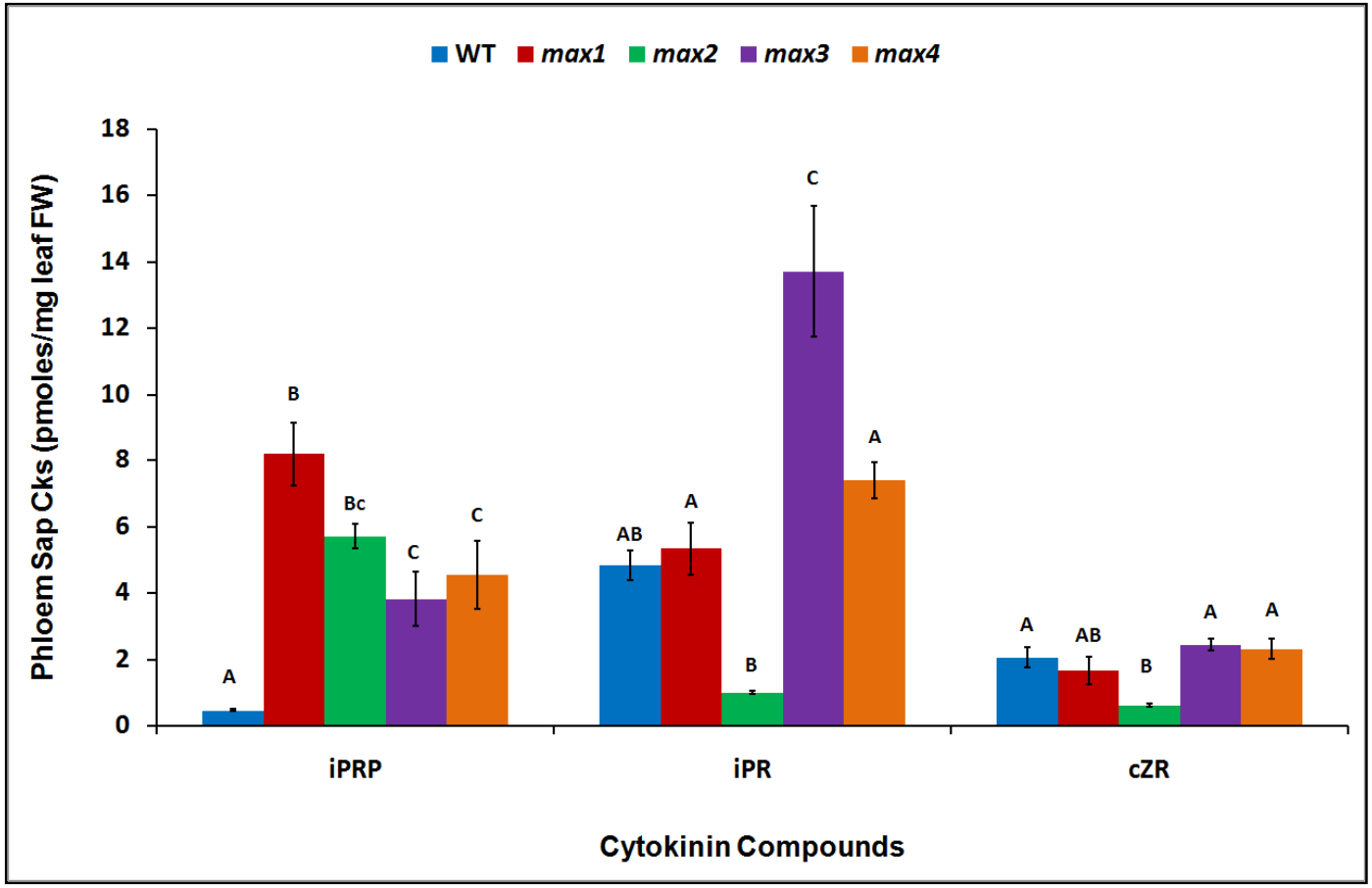

Figure – 5.2: Cytokinin Levels in Phloem Sap of Col-0 and max Genotypes. *The genotypes were grown hydroponically under short-day photoperiod. The phloem sap from leaves of 2-months old plants was collect in 10mM EDTA. Col-0 is a wild-type control. Bars shown are means ± SE (n=6). Means that do not share a letter are significantly different as determined for each compound by One-way ANOVA with Tukey's post hoc test ($p \leq 0.05$).*

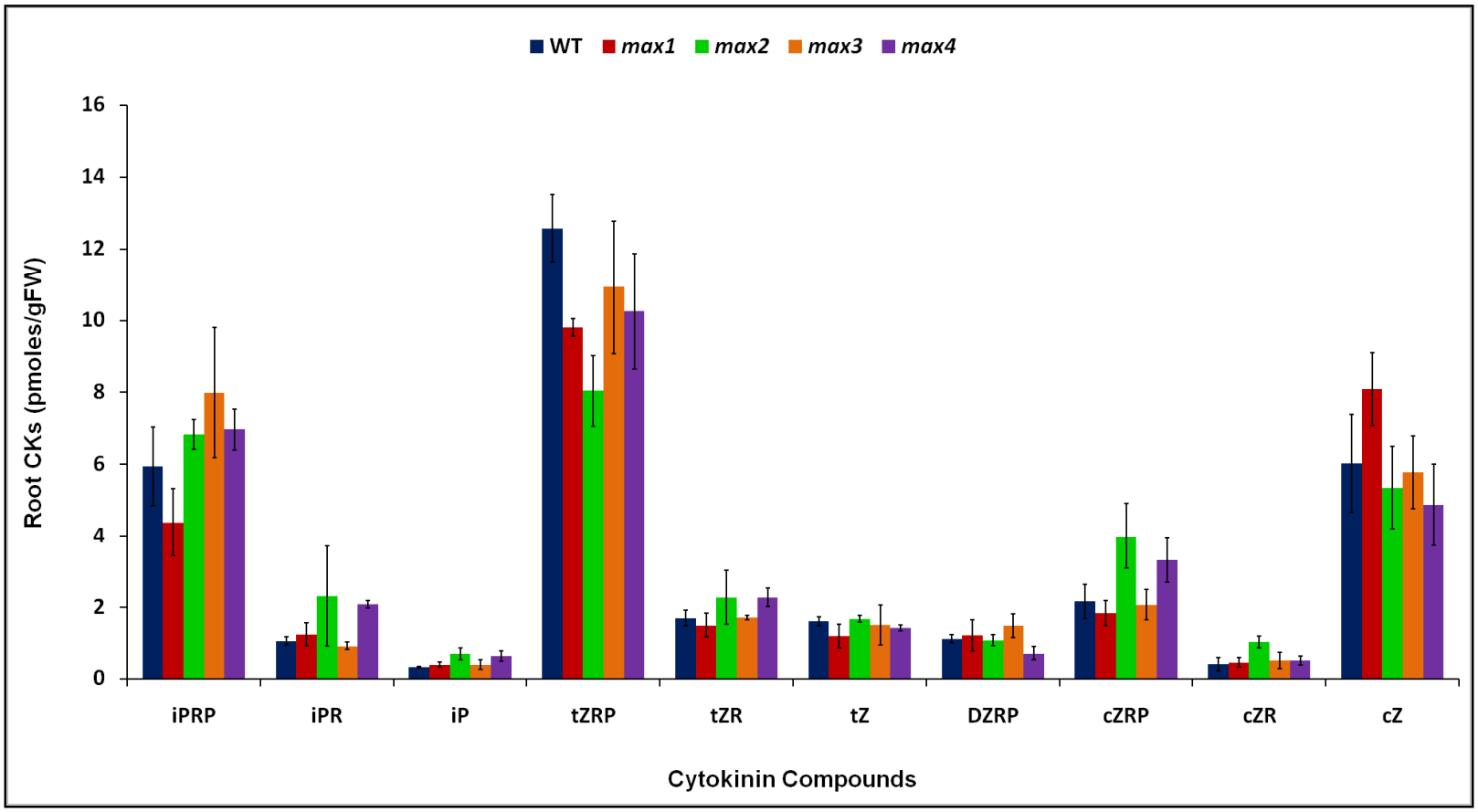

Figure – 5.3: Cytokinin Levels in Root Tissues of Col-0 and max Genotypes. *The genotypes were grown hydroponically under short-day photoperiod for 2 months.1g from bulk of three roots per replication per genotype was analyzed. Col-0 is a wild-type control. Bars shown are means ± SE (n=6). Means are not significantly different as determined for each compound by One-way ANOVA ($p \leq 0.05$).*

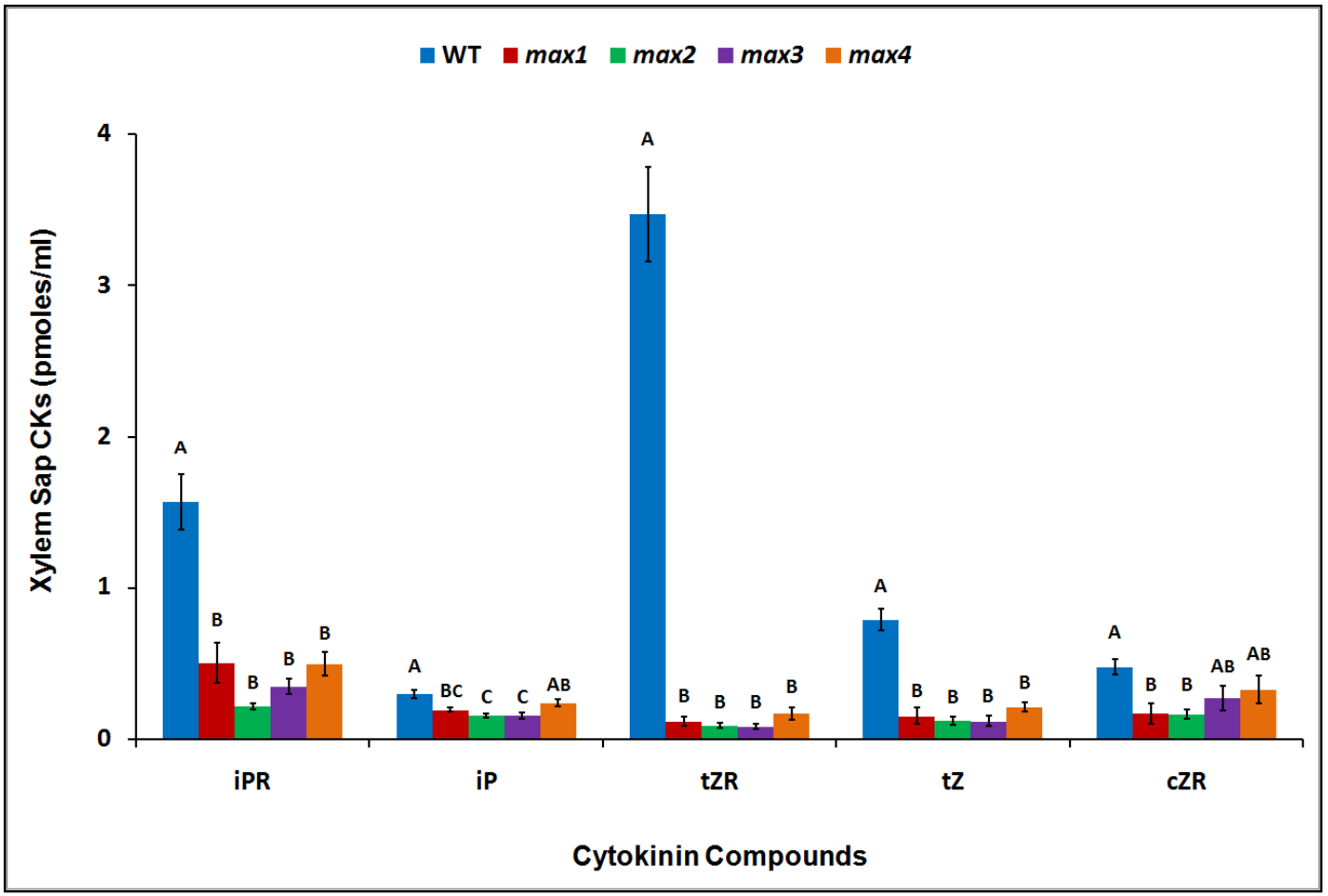

Figure – 5.4: Cytokinin Levels in Xylem Sap of Col-0 and max Genotypes. *The shoots of 2-months old genotypes grown in soil under short-day photoperiod were cut and tubing was attached with hypocotyls to collect xylem sap by syringe-suction for 2 hours. Control is wild-type Col-0. Bars shown are means ± SE (n=7). Means that do not share a letter are significantly different as determined for each compound by One-way ANOVA with Tukey's post hoc test ($p \leq 0.05$).*

5.3.2.4 Xylem-CKs: The xylem sap from three plants per replication per genotype was used for quantification of cytokinin compounds. In the xylem sap, the detected CK compounds were iPR, iP, tZR, tZ and cZR, out of which levels of tZR, tZ and iPR are higher in wild-type, as shown in Fig. 5.4. The most abundant is tZR, which is increased by 2-fold as compared with iPR. Levels of iPR, tZR and tZ are significantly reduced in all *max* genotypes as compared with wild-type. Xylem-iPR is decreased by 3-fold in *max1* and *max4*; 7-fold in *max2* and 4.5 fold in *max3*. Levels of tZR are highly decreased (40-fold in case of *max2* and *max3*), whereas tZ levels are decreased by 3-6-fold in all *max* mutants. Fig. 5.4 shows that iP levels are very low but are significantly reduced in all *max* mutants, except *max4* that is similar to wild-type. Levels of cZR are significantly reduced in *max1* and *max2* but those in *max3* and *max4* are not different from wild-type levels.

5.3.3 CK Levels in *atipt* mutants in WT and *max* backgrounds

Levels of cytokinin species (ribotides, ribosides and free-bases) were measured from *atipt* double and triple mutants in wild-type and *max* backgrounds. Detail of CK levels in each tissue of genotypes is given as follows:

5.3.3.1 Cytokinin Levels of Shoot Tissues

Genotypes were grown hydroponically under short-day (8 hours) photoperiod and after two weeks plants were transferred to long-day (16 hours) photoperiod. Three shoots (one and half month old) per replication per genotype were bulked to quantify cytokinin compounds.

Double mutant *atipt5,7* shows no difference from wild-type and similarly triple mutants *atipt5,7,max2* and *atipt5,7,max4* are not different from their respective controls *max2* and *max4* for iP-type CK compounds (iPRP, iPR and iP), as shown in Figure 5.5 (A). However, as compared to *atipt5,7,max2* and *atipt5,7,max4*, levels of iPR are significantly increased in *atipt5,7* (Fig. 5.5-A) and this genotype also has significant elevation in tZRP levels relative to wild-type. Significantly higher levels of tZRP in *atipt5,7,max2* and *atipt5,7,max4* than *max2* and *max4* are shown in Fig,5.5(A). Double mutant *atipt5,7* in wild-type and *max* backgrounds do not show difference from their respective wild-type and *max* controls for tZR and tZ levels, with the only exception that *atipt5,7* has slightly but significantly increased tZ levels compared with wild-type (Fig. 5.5-A).

Figure 5.5(B) shows that *atipt3,5* and *atipt3,7* in wild-type and *max4* backgrounds have significantly lower levels of iP-type CKs, as compared with their corresponding controls wild-type and *max4*. Double mutant *atipt3,5* is similar to *atipt3,5,max4*, and *atipt3,7* is comparable to *atipt3,7,max4*. For iPRP, *atipt3,5* and *atipt3,7* show about 1.5 and 5 fold decrease from wild-type, respectively and same fold decrease is found in *atipt3,5,,max4* and *atipt3,7,max4* as compared with *max4*. Therefore, *atipt3,7*and *atipt3,7,max4* mutants show consistently and significantly lower (~3-fold) of iP-type compounds than the corresponding *atipt3,5* and *atipt3,5,max4* (Fig. 5.5B). Compared with iPRP, levels of tZRP are increased

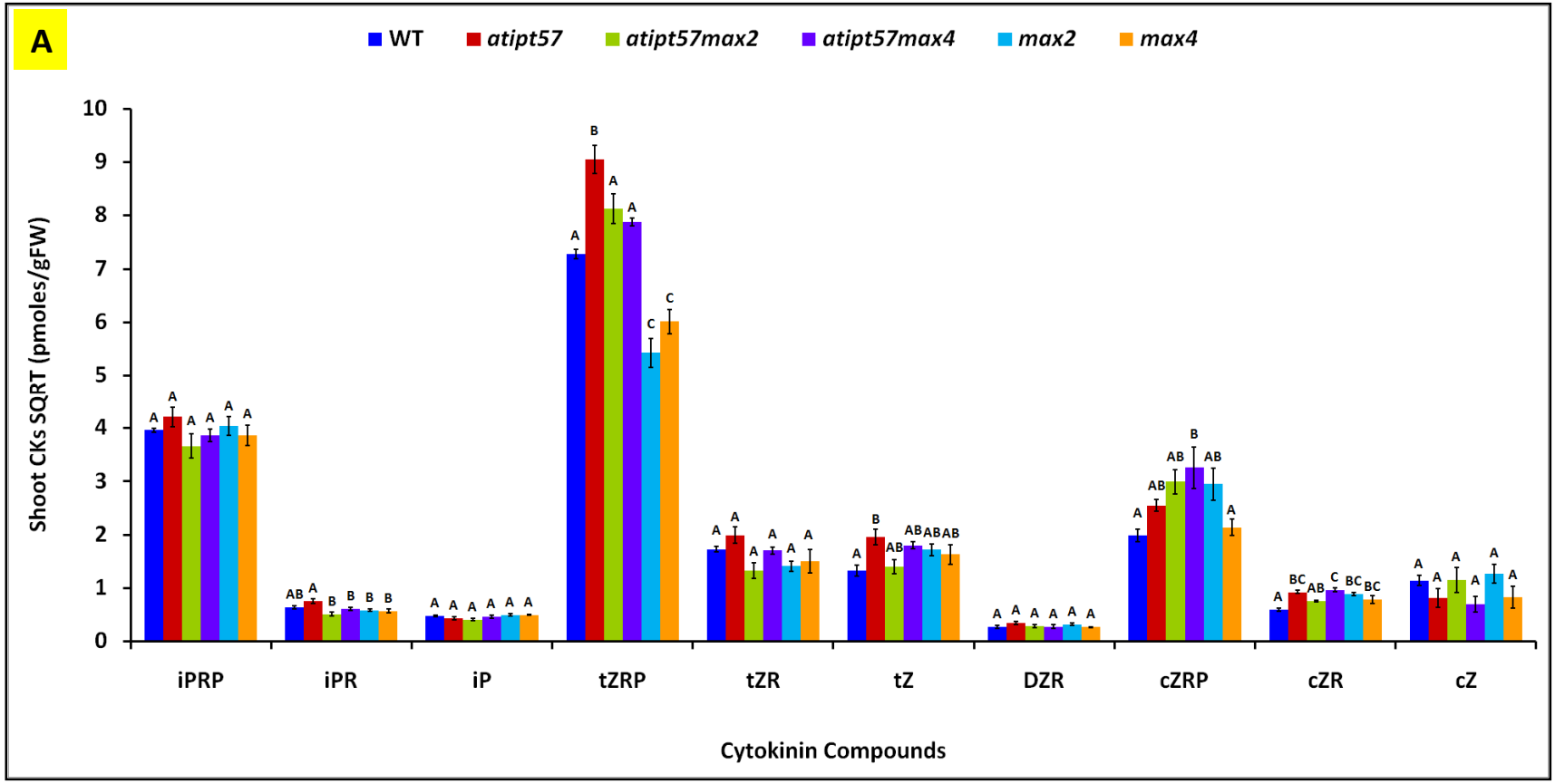

Figure – 5.5 (A): Cytokinin Levels in Shoot Tissues of atipt5,7 in WT and max Backgrounds. *The genotypes were grown in hydroponics.1g from bulk of three shoots per replication per genotype was used to quantify cytokinin levels. Col-0 (wild-type genotype), max2 and max4 are controls. Bars shown are square root transformed means ± SE (n=5). Means that do not share a letter are significantly different as determined for each compound by One-way ANOVA with Tukey's post hoc test ($p \leq 0.05$).*

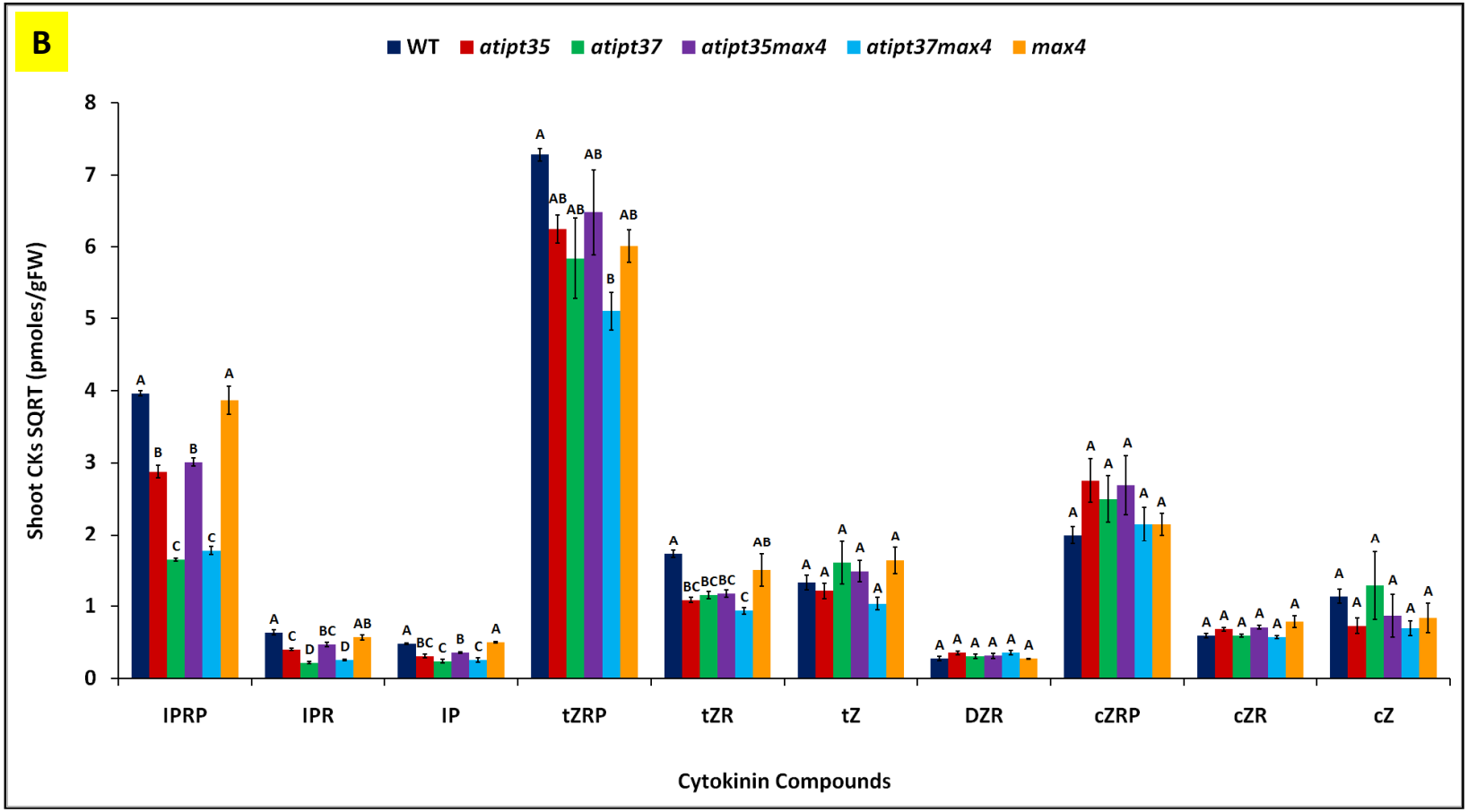

Figure – 5.5 (B): Cytokinin Levels in Shoot Tissues of atipt3,5 and atipt3,7 in WT and max4 Backgrounds. *The genotypes were grown in soil.1g from bulk of three shoots per replication per genotype was used to quantify cytokinin levels. WT (Col-0) and max4 are controls. Bars shown are square root transformed means ± SE (n=5). Means that do not share a letter are significantly different as determined for each compound by One-way ANOVA with Tukey's post hoc test ($p \leq 0.05$).*

by ~ 3.5-fold in wild-type. Double mutants *atipt3,5* and *atipt3,7* are like wild-type and *atipt3,5,max4* and *atipt3,7,max4* are not different from *max4*, which is also similar to wild-type. Similar pattern is shown in Fig. 5.5 (B) for tZ levels, while for tZR, *atipt3,5* and *atipt3,7* have significantly reduced levels compared with wild-type. Compared with *max4*, tZR levels in *atipt3,5,max4* is not changed, but *atipt3,7,max4* shows a significant reduction (Fig. 5.6B).

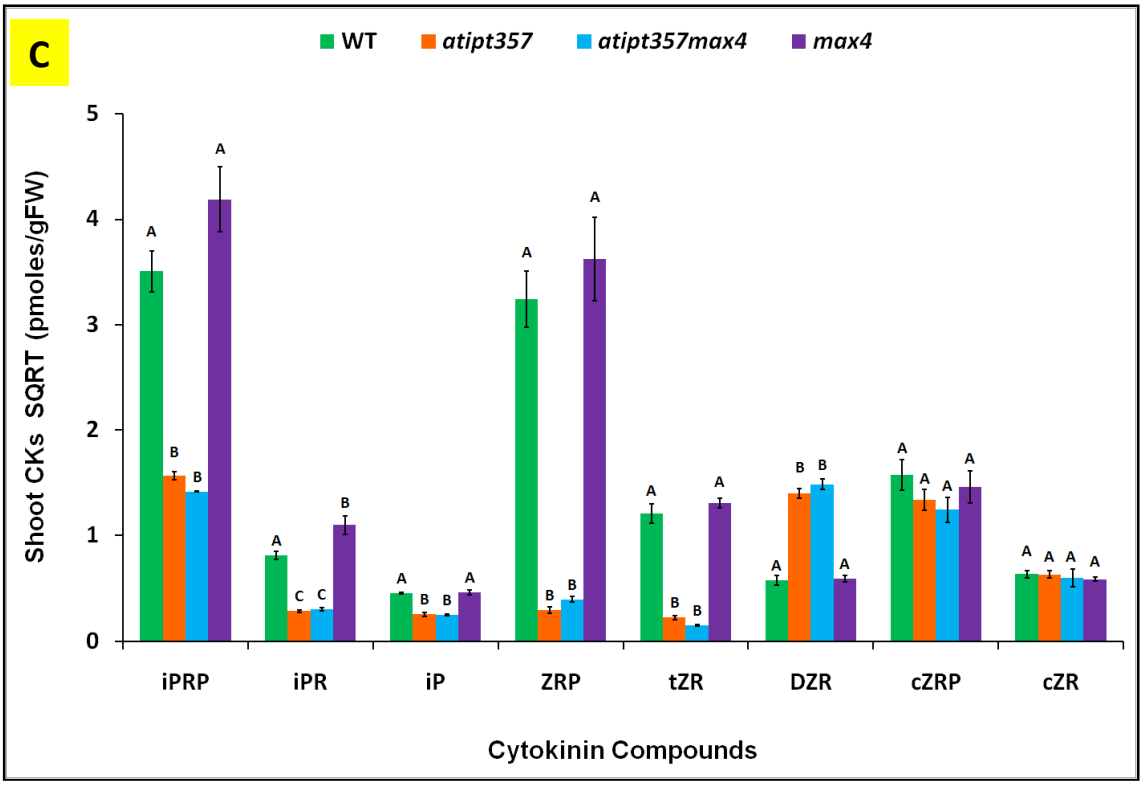

Figure – 5.5 (C): Cytokinin Levels in Shoot Tissues of atipt3,5,7 in WT and max4 Backgrounds. *The genotypes were grown on MS media plates for 2-weeks. Bulked shoots (equal to 1 g) per replication per genotype were used. Col-0 (WT) and max4 are controls. Bars shown are square root transformed means ± SE (n=5). Means that do not share a letter are significantly different as determined for each compound by One-way ANOVA with Tukey's post hoc test ($p \leq 0.05$).*

As evident from Fig. 5.5 (C), triple mutant *atipt3,5,7* and quadruple mutant *atipt3,5,7,max4* are alike having remarkable reduced levels of iP and tZ-type CKs as compared with the corresponding wild-type and *max4*controls. Multiple mutants *atipt3,5,7* and *atipt3,5,7,max4* show about 5 and 9 fold decrease in iPRP levels compared with wild-type and *max4*, respectively. Levels of iPR were much lowered (8-fold in *atipt3,5,7* and 13-fold in *atipt3,5,7,max4)*. However, approximately 118-fold lower tZRP levels was found in *atipt3,5,7* than wild-type and 85-fold in *atipt3,5,7,max4* than *max4*. Genotypes *atipt3,5,7* and *atipt3,5,7,max4* have about 28- and 75-fold reduced tZR levels as compared with corresponding controls.

Levels of cZ-type CKs are not changed among all *atipt* mutants in both *max* and non-*max* backgrounds (Fig. 5.5 A,B & C), apart from a few exceptions that *atipt5,7,max4* is significantly different from *max4* for higher cZRP levels and *atipt5,7* from wild-type for increased cZR levels, shown in Fig. 5.6 (A). There is no difference among double *atipt* genotypes in wild-type and *max* backgrounds. However, levels of DZR are significantly greater in *atipt3,5,7* and *atipt3,5,7,max4* than wild-type and *max4*, respectively (Fig. 5.5-C).

5.3.3.2 Phloem Cytokinin Levels

Levels of iPRP are significantly elevated in *atipt5,7,max2* and *atipt5,7,max4* compared with wild-type, as shown in Fig. 5.6(A), and these levels are more increased in *max2* and *max4* but difference from *atipt5,7,max2* and *atipt5,7,max4* is not significant. Double mutant *atipt5,7* also exhibited slight increase in iPRP levels than wild-type. Levels of iPR and cZR are significantly decreased in all genotypes than WT (Fig. 5.6-A).

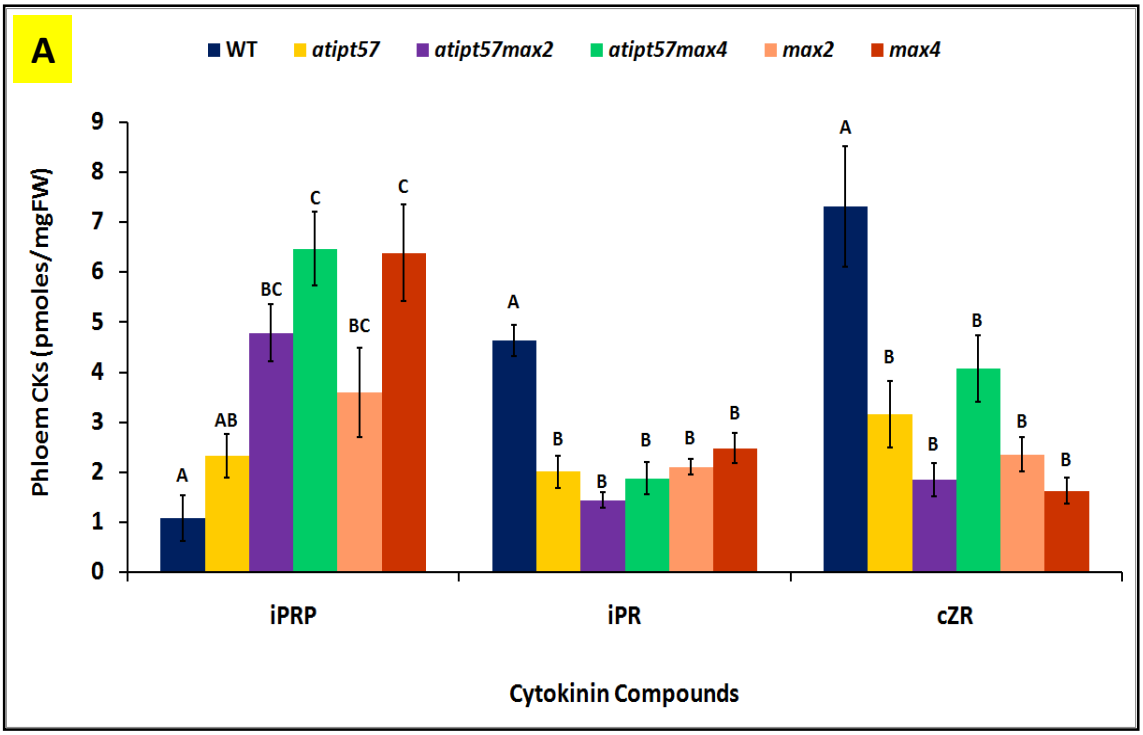

Figure – 5.6 (A): Cytokinin Levels in Phloem Sap of atipt5,7 in WT and max Backgrounds. *The phloem sap from leaves of 2-months old soil-grown genotypes was collected in 10mM EDTA. Col-0 (WT), max2 and max4 are control plants. Bars shown are means ± SE (n=5). Means that do not share a letter are significantly different as determined for each compound by One-way ANOVA with Tukey's post hoc test ($p \leq 0.05$).*

As shown in Fig. 5.6 (B), iPRP are significantly reduced in all genotypes compared with *max4*. Levels of iPRP are decreased by about 10-fold in *atipt3,5* and *atipt3,5,max4* whereas approximately 100-fold in *atipt3,7* and *atipt3,7,max4* compared with *max4*. Regarding iPR, double mutants *atipt3,5* and *atipt3,7* in wild-type and *max4* backgrounds have lower levels as compared with the corresponding controls wild-type and *max4*. In case of cZR levels, there is no difference among genotypes (Fig. 5.6-B).

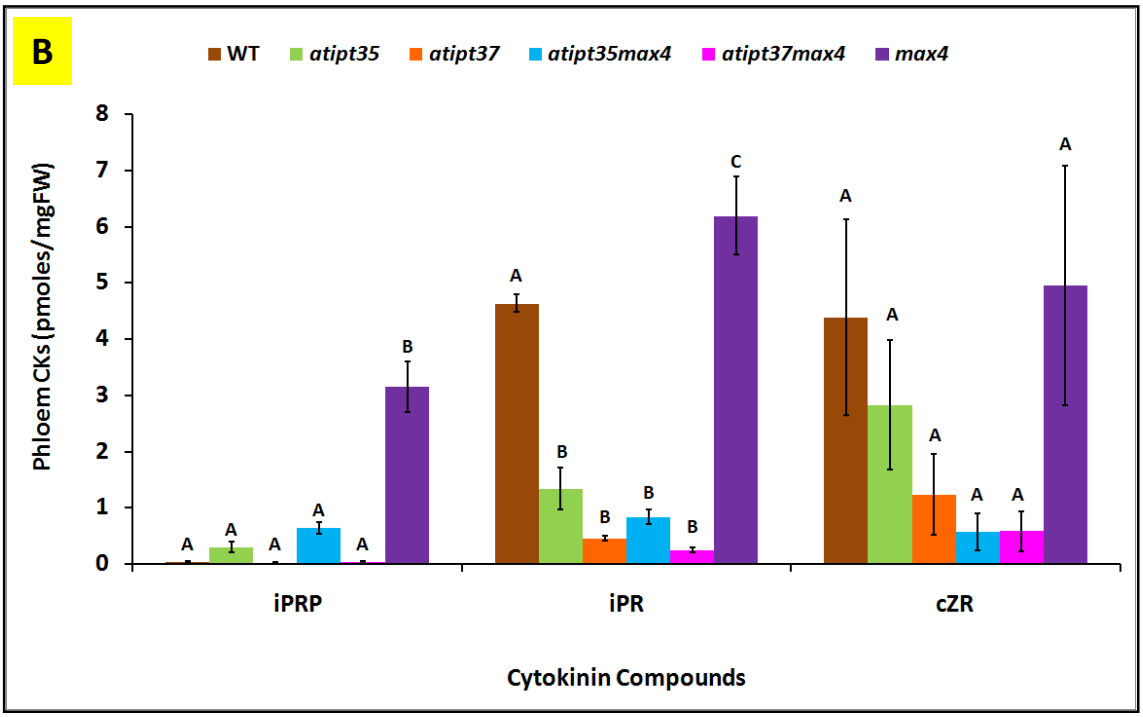

Figure – 5.6 (B): Cytokinin Levels in Phloem Sap of atipt3,5 and atipt3,7 in WT and max Backgrounds. *The leaf exudates were collected from 2-months old soil-grown genotypes. Wild-type (Col-0) and max4 are control plants. Bars shown are means ± SE (n=5). Means that do not share a letter are significantly different as determined for each compound by One-way ANOVA with Tukey's post hoc test ($p \leq 0.05$).*

5.3.3.3 Cytokinin Levels in Roots

Levels of iP and tZ-type CK compounds are significantly decreased in *atipt5,7,max2* and *atipt5,7,max4* as compared with *max2* and *max4*. Double mutant *atipt5,7* show significant reduction in levels of iP-type CKs (iPRP, iPR and iP) as compared with wild-type but *atip5,7* and wild-type are not different from each other for levels of tZ-type compounds (Fig. 5.7-A). The levels of cZ-type compounds do not show difference among genotypes, as shown in Fig 5.7 (A).

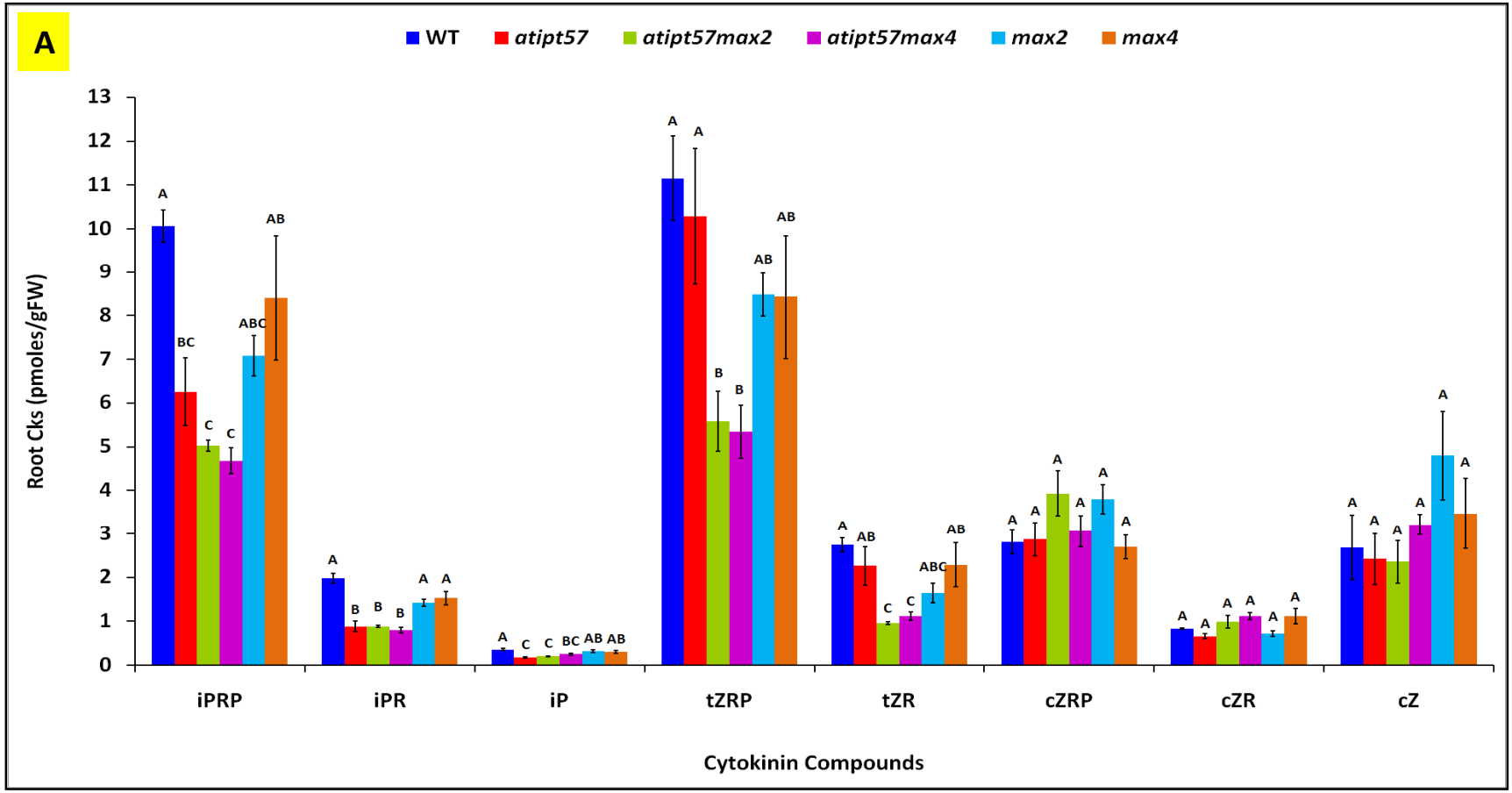

Figure – 5.7 (A): Cytokinin Levels in Root Tissues of atipt5,7 mutants in WT and max Backgrounds. *The genotypes were grown in hydroponics.1g from bulk of three roots per replication per genotype was used to quantify cytokinin levels. Col-0 (WT), max2 and max4 are controls. Bars shown are means ± SE (n=5). Means that do not share a letter are significantly different as determined for each compound by One-way ANOVA with Tukey's post hoc test ($p \leq 0.05$).*

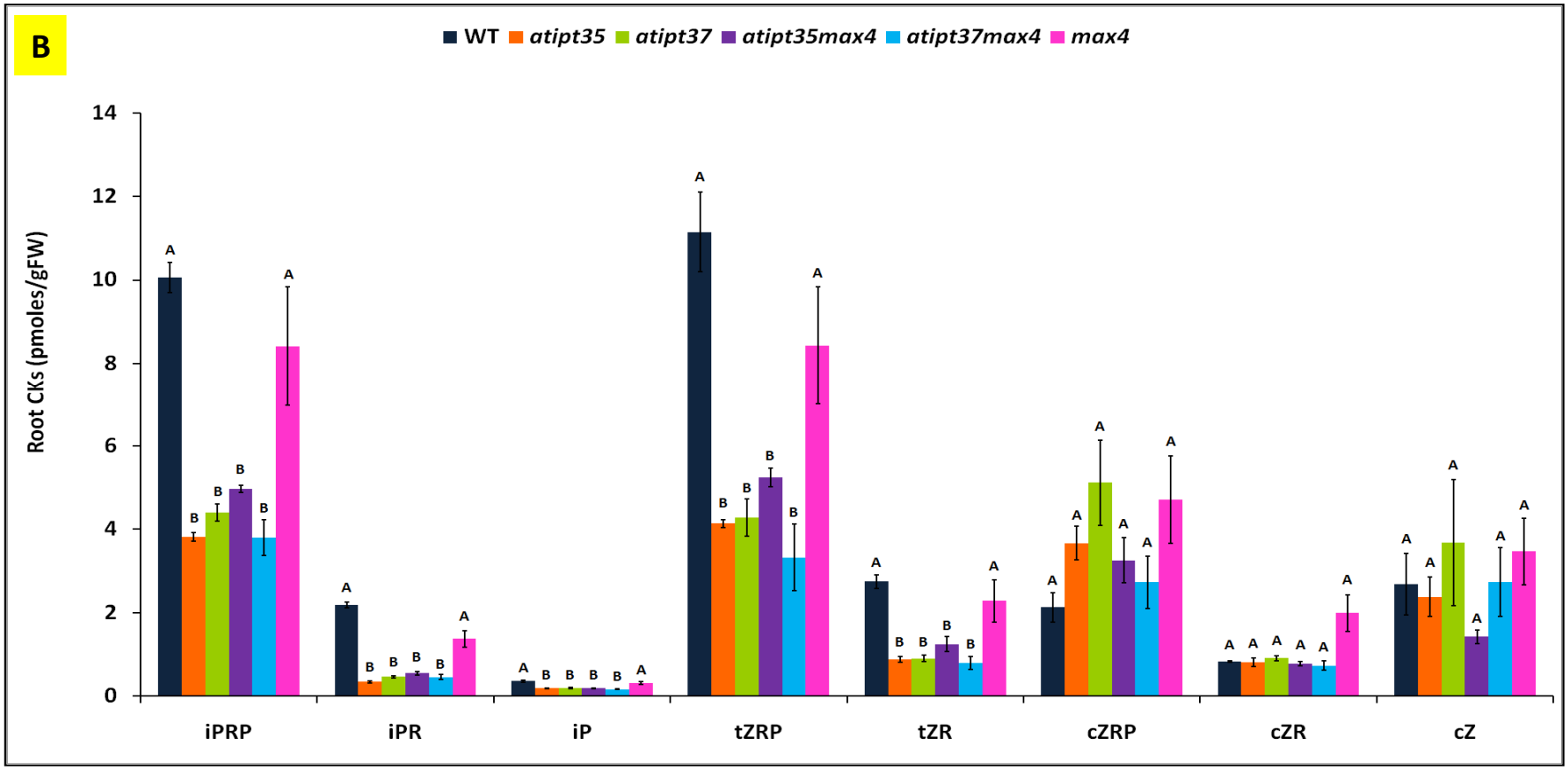

Figure – 5.7 (B): Cytokinin Levels in Root Tissues of atipt3,5 and atipt3,7 in WT and max Backgrounds. *The genotypes were grown in hydroponics.1g from bulk of three roots per replication per genotype was taken to quantify cytokinin levels. WT and max4 are control plants. Bars shown are means ± SE (n=5). Means that do not share a letter are significantly different as determined for each compound by One-way ANOVA with Tukey's post hoc test ($p \leq 0.05$).*

Double mutants *atipt3,5* and *atipt3,7* in wild-type and *max4* backgrounds exhibit significant reduction in iP-and tZ-type CK compounds as compared with wild-type and *max4* (Figure 5.7-B). No difference among genotypes is shown in Figure 5.8-B for cZ-type compounds.

As shown in Figure 5.7 (C), levels of iP- and tZ-type CK species are highly reduced in roots of *atipt3,5,7* and *atipt3,5,7,max4* as compared with WT and *max4*. Levels of tZRP are decreased by about 60-fold in *atipt3,5,7* and approximately 70-fold in *atipt3,5,7,max4* as compared with wild-type and *max4*, respectively. Triple mutant *atipt3,5,7* and quadruple mutant *atipt3,5,7,max4* have almost 13-fold reduction in tZR levels from the corresponding controls wild-type and *max4*. The genotypes do not differ from each other for DZ and cZ-type CKs.

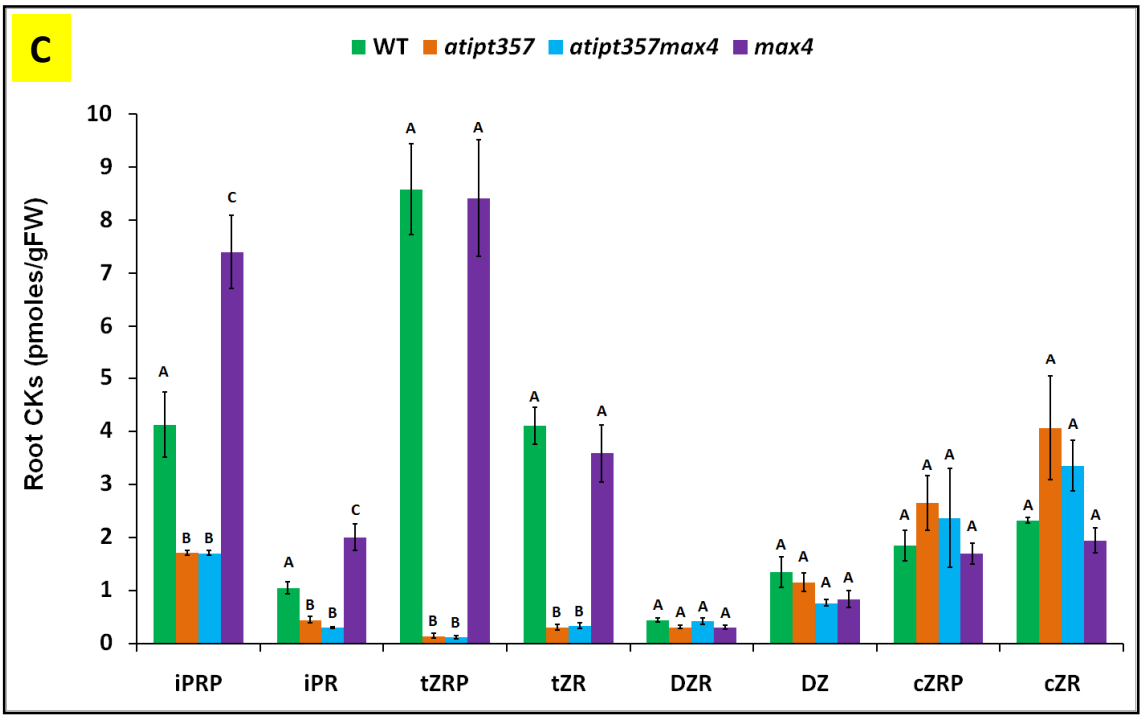

Figure – 5.7 (C): Cytokinin Levels in Root Tissues of atipt3,5,7 in WT and max4 Backgrounds. *The genotypes were grown on MS media plates for 2-weeks on long-day photoperiod. The bulked roots (equal to 0.5g) per replication per genotype were used. WT and max4 are control plants. Bars shown are means ± SE (n=5). Means that do not share a letter are significantly different as determined for each compound by One-way ANOVA with Tukey's post hoc test ($p \leq 0.05$).*

5.3.3.4 Xylem Cytokinin Levels

For collection of xylem sap, the plants were grown at normal growth conditions in short-days but kept covered with translucent plastic covers for 2 weeks to induce shade avoidance response that elongates the hypocotyl. Long hypocotyls of *Arabidopsis* plants are somewhat easier to tie with tubing to collect xylem sap. Previously, plants were grown under very low

light in short-days for the same purpose. The hypocotyl was found to be very elongated but its width was much reduced. However, new growth conditions reduce time to grow plants with having elongated hypocotyls of wider girth.

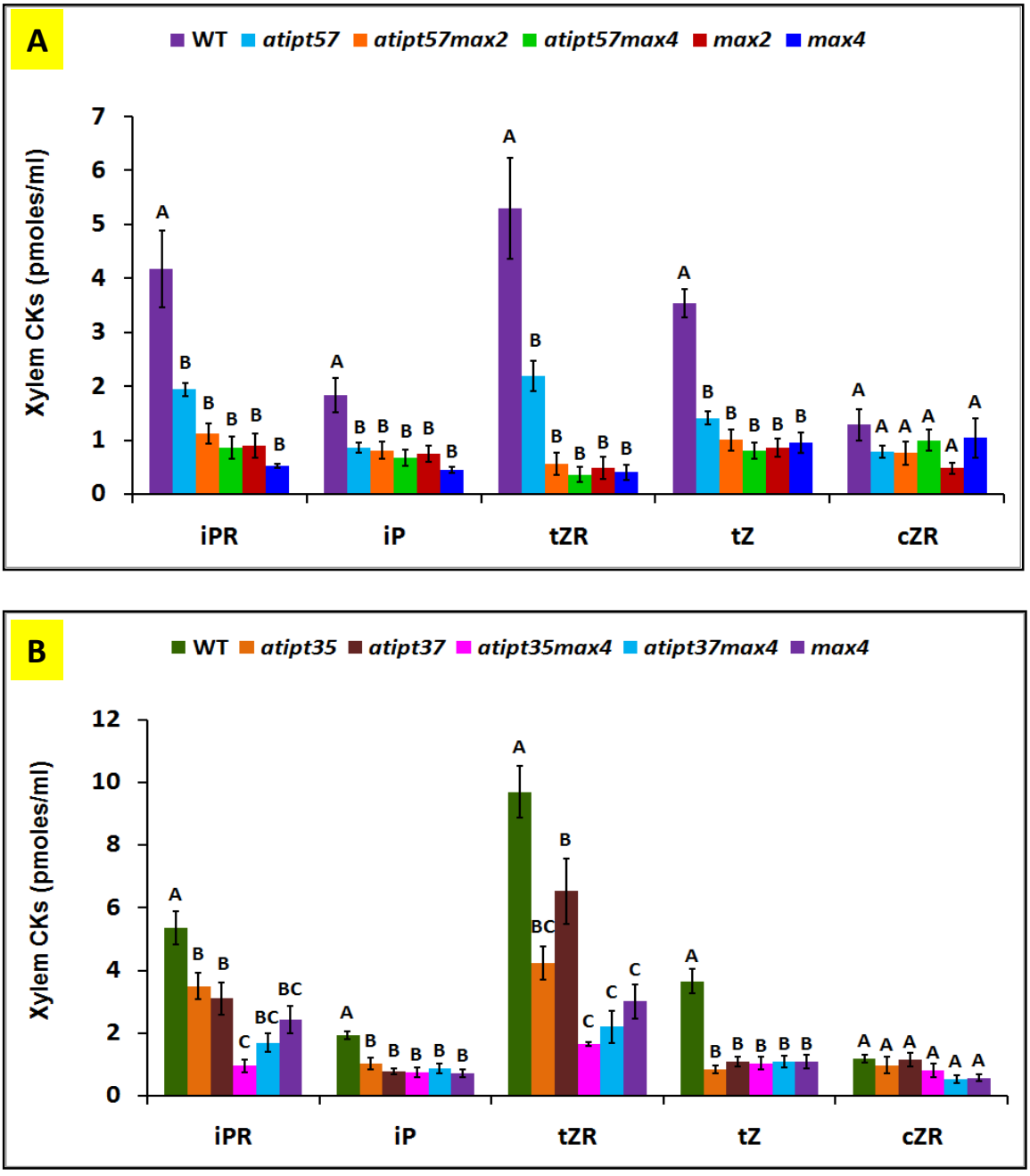

Figure – 5.8: Cytokinin Levels in Xylem Sap of atipt mutants in WT and max Backgrounds. *The rosettes of 2-months old genotypes grown in soil at short-day photoperiod were decapitated and xylem sap was collected by suction for 2 hours. WT, max2 and max4 are control plants. Data from two experiments is represented as two graphs (A & B). Bars shown are means ± SE (n=5). Means that do not share a letter are significantly different as determined for each compound by One-way ANOVA with Tukey's post hoc test ($p \leq 0.05$).*

Levels of iPR, iP, tZR and tZ in xylem sap of *atipt5,7, atipt3,5* and *atipt3,7* in wild-type and *max* backgrounds are significantly reduced compared with WT, but are similar to *max2* and *max4*(Fig. 5.9 A and B). Again cZR levels are not different across genotypes (Fig. 5.8 A& B).

5.3.4 PCA for CK Levels

5.3.4.1 PCA for shoot, phloem, root and xylem CKs of *max* genotypes

PCA was performed to see the collective pattern of all CK data quantified in shoot, root, phloem and xylem saps of wild-type and *max* genotypes. Scree plot (see Appendix IV-D) of all PCs computed indicates that the first three principal components (PC1, PC2 and PC3) are significant (Eigen value $\geq$ 1). Therefore, biplot of CK variables and ordination plot of genotypes are shown along PC1 and PC2 axes (Fig. 5.9) and PC1 and PC3 axes (Fig. 5.10).Although Figures 5.9 and 5.10 show that the genetic and hormonal variability are separated by tissue types, Figure 5.11 exhibits overlapping clusters for root and shoot tissues across genotypes.

Along axes of PC1 and PC2, the root and shoot tissues are overlapped and genotypes are closer to each other due to CK variables (iPRP, ZRP, cZRP, DZRP, tZR, tZ and cZ) as shown in Fig 5.9 (A & B). It means there is no variation among genotypes for CK variables in roots and shoot. But along axes of PC1 and PC3 (Fig. 5.10 A & B), *max* genotypes in shoot tissues are separated from wild type for tZ-type CK variables, shown clustered in opposite directions. This relates to tZ-type CKs being reduced in *max* genotypes, but tZ-type CKs show no variation among genotypes in root tissues and are grouped with root tissues.

CK-ribotides variables (iPRP, tZRP and cZRP) are not present in xylem sap, therefore, their vectors are in opposite direction from xylem tissues, as plotted in Fig. 5.9 (A & B) and Fig. 5.10 (A & B). The *max* genotypes are separated from wild-type due to reduced iP and tZ-type CK variables (iPR, iP, tZR and tZ) whose allocated vectors are in the opposite direction from *max* genotypes (Fig. 5.10 A& B). The tZ-type CK variables are reduced in shoot tissues and xylem sap of *max* genotypes as compared with wild-type. Therefore, the vectors of those variables are on the plane between WT-shoot and WT-xylem, but away from *max* genotypes for both tissue types, as shown in Fig. 5.10 (A & B). The genotypes have variations among themselves for iPR and cZR CK variables and *max2* is separated from other genotypes due to reduced iPR and cZR in phloem sap and highest in *max3*. This explains why*max3* is placed near vectors of iPR and cZR. These vectors are also along with iP vector, although iP was not detected in phloem sap (Fig. 5.9A& B). The profiles for iP become clearer in the plot of PC1 and PC3, where it shows a slightly different direction than cZR and IPR (Fig. 5.10A& B). The iP variable vector is close to *max* genotypes for xylem sap due to strength of similarity among genotypes for iP compounds but separated from wild-type xylem iP compound (5.10 A & B).

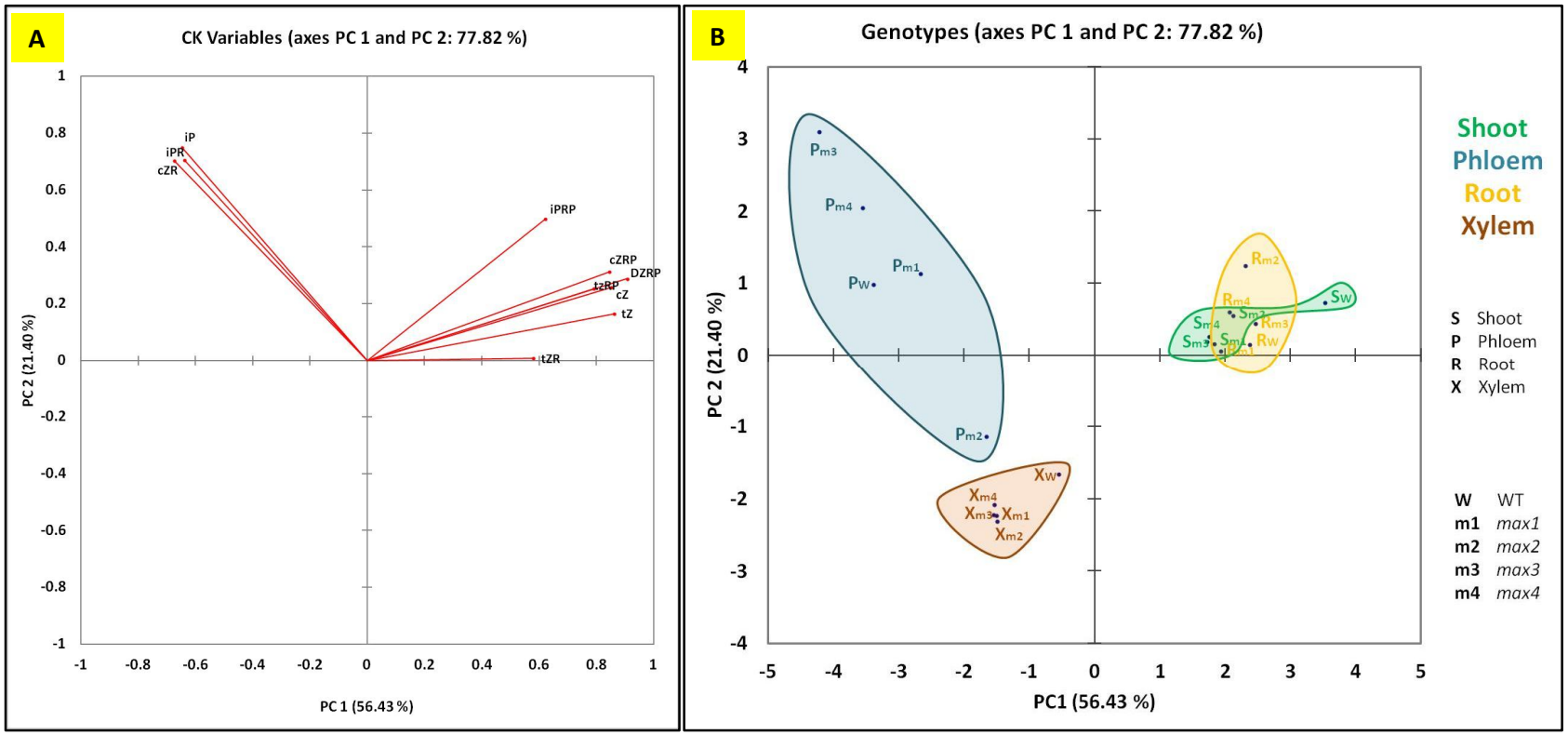

Figure – 5.9: Two Axes (PC1, PC2) of a Principal Components Analysis of max genotypes for Shoot, Phloem, Root and Xylem. *(A) Loading plot showing CK compounds vectors (iPRP, iPR, iP, tZRP, tZR, tZ, DZRP, cZRP, cZR, cZ, indicated by arrows) and (B) Score plot showing the position of genotypes variables (denoted by abbreviations) for shoot, phloem, root and xylem variables (shown by abbreviations as well as different colours). Arrows represent eigen vectors showing the strength by the length of the vector and direction of the CK variable correlation relative to the first two components PC1 and PC2. The colored outlines enclose the tissue variables. PCA was performed at 95% confidence level.*

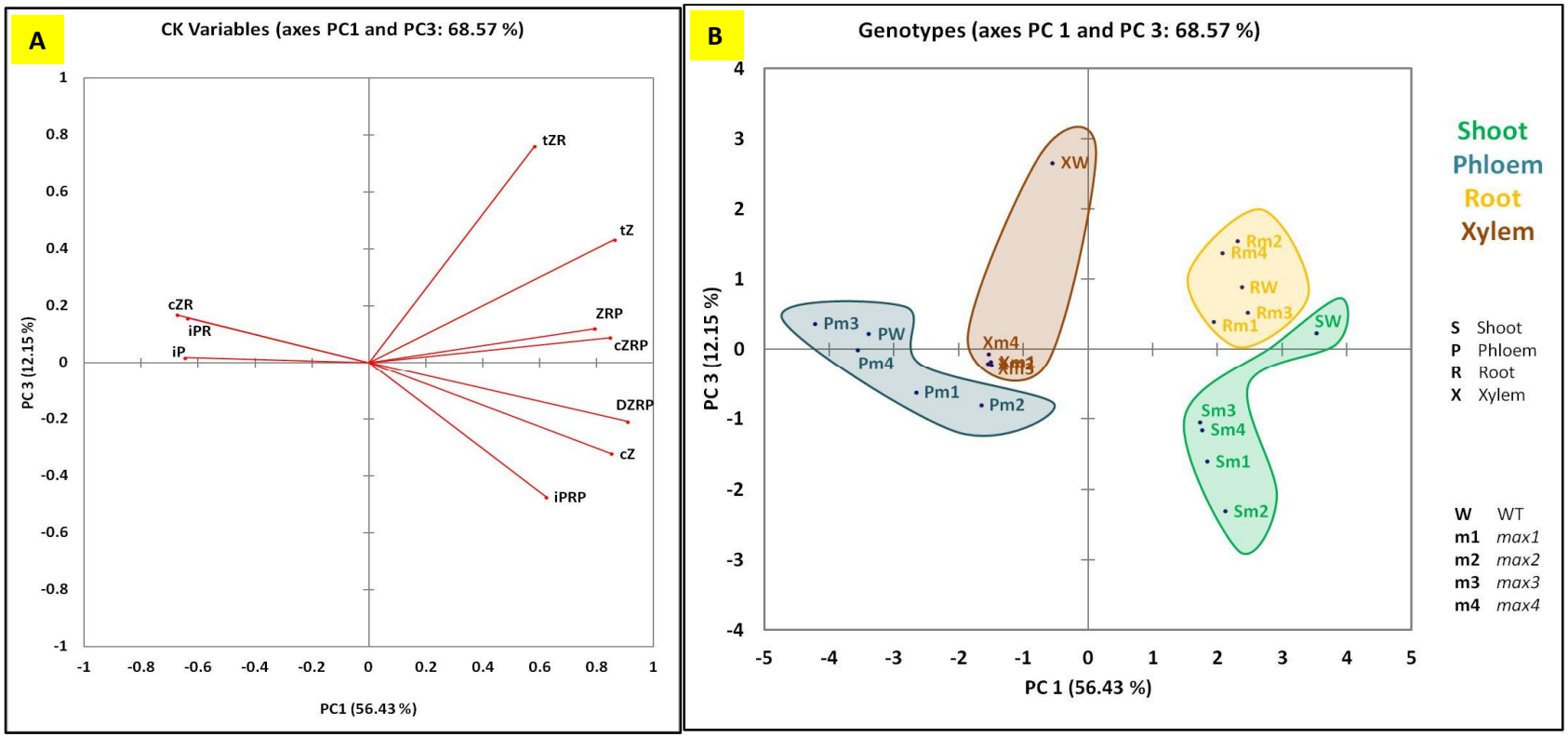

Figure – 5.10: Two Axes (PC1, PC3) of a Principal Components Analysis of max genotypes for Shoot, Phloem, Root and Xylem. *(A) Loading-plot showing CK compounds vectors (iPRP, iPR, iP, tZRP, tZR, tZ, DZRP, cZRP, cZR, cZ, indicated by arrows) and (B) Score plot showing the position of genotypes variables (denoted by abbreviations) for shoot, phloem, root and xylem variables (shown by abbreviations as well as different colours. Arrows represent eigen vectors showing the strength by the length of the vector and direction of the CK variable correlation relative to the first and third components PC1 and PC3. The colored circles enclose the tissue variables. PCA was performed at 95% confidence level.*

5.3.4.2 PCA for shoot, phloem, root and xylem CKs of *atipt* double mutants in WT and *max* backgrounds

As with the previous PCA, all CK compounds measured from tissues of *atipt* double mutants in wild-type and *max* backgrounds were visualized. Scree plot (see Appendix IV-D) indicates that first three principal components (PC1, PC2 and PC3) are significant (Eigen value ≥ 1). Therefore, plots are shown along PC1 and PC2 axes (Fig. 5.11 A) and along PC1 and PC3 axes (Fig. 5.11 B).

Triple mutant *atipt3,5,7* and quadruple mutant *atipt3,5,7,max4* exhibit very small phenotypes and could not be used to collect comparable phloem and xylem sap samples. Therefore, these mutants were excluded from this collective this PCA.

Along axes of PC1 and PC2, the tissue variables are separated from each other, meaning that tissues differ from each other in the patterns of CK variables among the genotypes (Fig. 5.11 A). Fig. 5.11 (B) shows that the phloem and xylem tissues are overlapped on axes of PC1 and PC3, implying that the trends of CK variables are somewhat similar between the phloem and xylem tissues, but genotypes are scattered showing differences among themselves for CK variables.

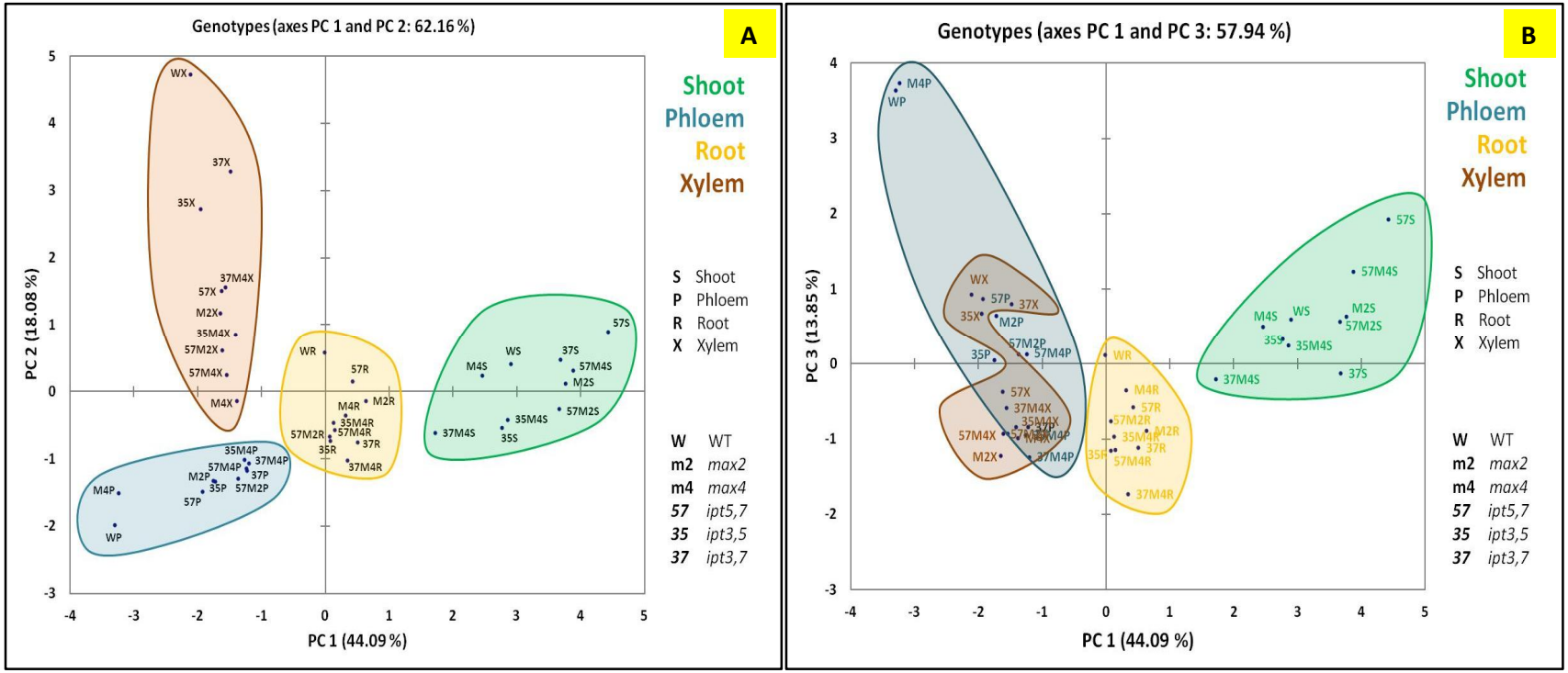

Figure – 5.11: Principal Components Analysis for Shoot, Phloem, Root and Xylem CKs of atipt double mutants in WT and max Backgrounds. *Score plots on PC1 and PC2 axes (A) and PC1 and PC3 axes (B), showing the position of genotypes variables (denoted by abbreviations) for shoot, phloem, root and xylem variables (shown by abbreviations as well as different colours). The colored circles enclose the tissue variables. PCA was performed at 95% confidence level.*

5.3.4.3 PCA for shoot and root CKs of *atipt* triple mutant in WT and *max* backgrounds

Principal component analysis for all CK compounds measured in shoot and roots of triple mutant *atipt3,5,7* and quadruple mutant *atipt3,5,7,max4*, was computed with data from all 5 replications to see the pattern among genotypes as well as variations among replicates. The scree plot (see Appendix IV-D) of all components extracted in PCA shows the first three significant principal components PC1, PC2 and PC3 (Eigen value $\geq$ 1). PC3 is only marginally significant, therefore, biplot of CK compounds is shown together with ordination plot of genotypes only for PC1 and PC2 axes (Fig. 5.12).

Fig. 5.12 shows that the wild-type and *max4* genotypes are separated by quite some distance from *atipt3,5,7* and *atipt3,5,7,max4*. This means that wild-type and *max4* have different overall trends of CK variables compared with *atipt3,5,7*, and *atipt3,5,7,max4*. The genotypes are also separated into root and shoot groups of wild-type with *max4* and *atipt3,5,7* with *atipt3,5,7,max4* (Fig. 5.12), due to different pattern of CK variables. In this case, DZR variable is very important in shoots of *atipt3,5,7* and *atipt3,5,7,max4*, with DZR being increased in these genotypes compared with wild-type and *max4*. As shown in Fig. 5.15, the iP and tZ-type CK variable vectors are in the direction of wild-type and max4 and away from roots and shoot of *atipt3,5,7* and *atipt3,5,7,max4*, reflecting the decrease in iP-and tZ-type CKs in shoot and roots of *atipt3,5,7* and *atipt3,5,7,max4*. There is much less variations among replicates of each genotypes, indicating high uniformity of sampling.

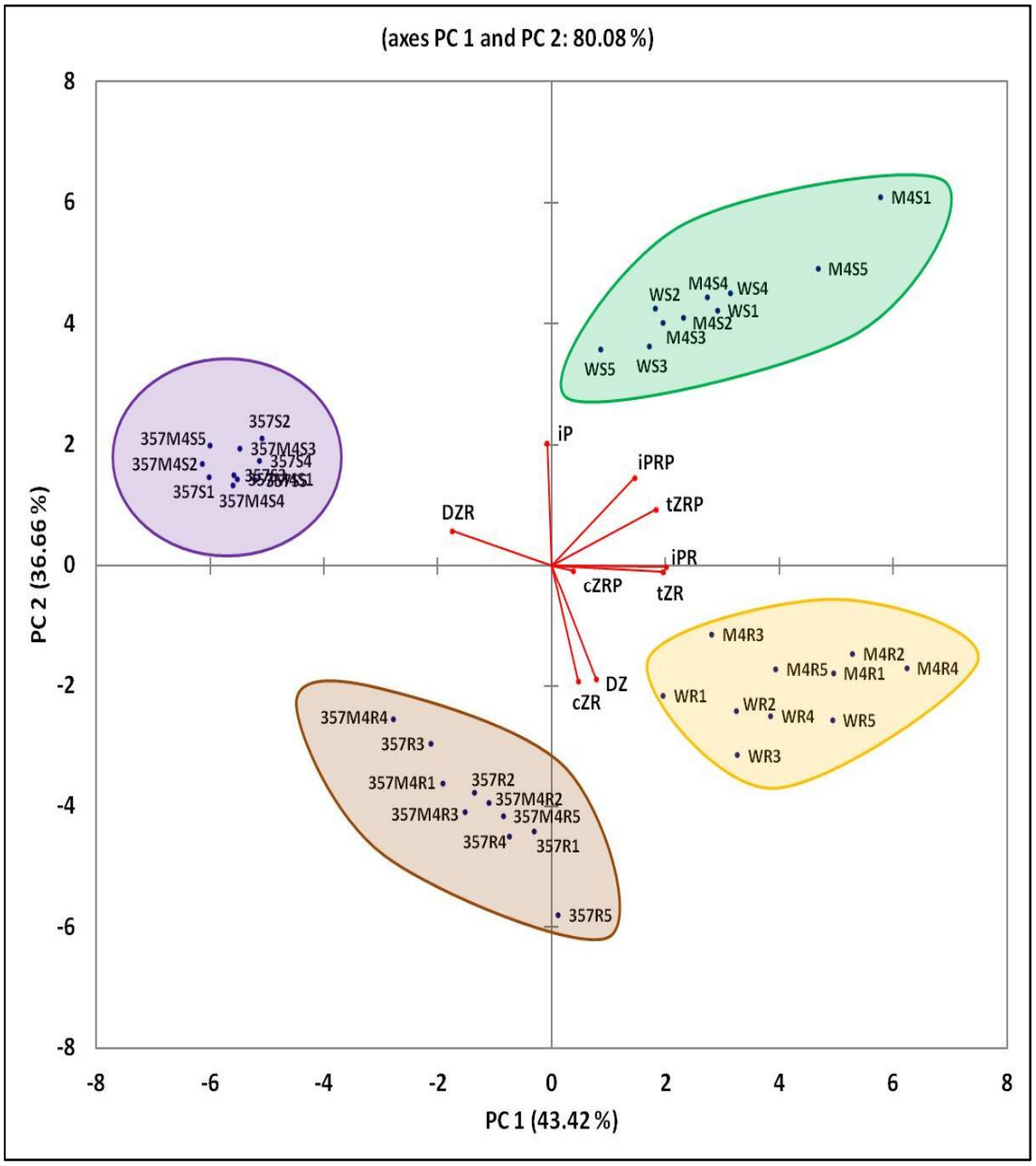

Figure – 5.12: Principal Components Analysis for Shoot and Root CKs of atipt triple mutant in WT and max Backgrounds. *Bi-plot showing CK compounds vectors (iPRP, iPR, iP, tZRP, tZR, DZR, DZ, cZRP, cZR, represented by arrows) and the position of genotypes variables (denoted by abbreviations) for shoot and root variables (shown by abbreviations as well as different colors) with replication variables (indicated by numbers). Arrows represent eigen vectors showing the strength by the length of the vector and direction of the CK variable correlation relative to the first two components PC1 and PC2. The colored circles enclose the root and shoot tissue variables as well as those variables that fall into the same cluster (95% confidence level). Abbreviations for the variables are: S, shoot; R, root; W, wild-type; M4, max4; 357,atipt3,5,7; 357M4, atipt3,5,7,max4.*

5.4 Discussion

5.4.1 Principal Component Analysis

Biochemical data such as measurements of hormonal levels among a large number of genotypes and tissue types cannot be easily analyzed by simple statistical analysis of variance (ANOVA) and tests of significance like LSD, Tukey's test etc. Therefore, PCA was used to analyze variations and diversity among a large number of variables in form of CK species, genotypes and tissue types. PCA allowed detection and visualization of patterns among different tissues for CK distribution. PCA of CK data shows the presence of similar and different patterns of CK and genotype variables among types of tissues (Fig. 5.11, 5.12, 5.14 and 5.16). The tissue-specific variation in CK profiles is discussed in detail in the following sections.

5.4.2 Synthesis of iP-type Cytokinins

The *ipt5,7* mutant has unchanged levels of iP-type CKs in its shoot but noticeably decreased levels in its roots, in comparison with equivalent wild-type tissues (Fig. 5.5A and 5.7A). This result is consistent with the previous (RT-PCR) data showing spatial distinct *AtIPT* expression patterns where both *AtIPT5* and *AtIPT7* is higher in roots than shoots (Takei *et al*., 2004), together with *AtIPT3* being highly expressed in mature rosette leaves (Takei *et al*., 2004a; Genevestigator database, Figure-3.1 & 3.2). It can, therefore, be concluded that pools of iP-type CKs in the shoots of *atipt5,7* remain unchanged due to presence of the *AtIPT3* gene, but are affected in roots due to absence of *AtIPT5* and *AtIPT7* genes.

Levels of iP-type CKs are significantly decreased in shoot and root of *atipt3,5* and *atipt3,7* double mutants (Fig. 5.5 B) and more extremely reduced in a triple mutant *atipt3,5,7* (Fig. 5.5 C). These results are in line with the previous findings of greatly reduced iP-type CKs in these mutants (Miyawaki *et al*., 2006). Reduction in levels appears to be predominantly due to absence of the *AtIPT3* gene as *atipt3*was the only single mutant that exhibited decreased levels of iP-type cytokinins (Miyawaki *et al*., 2006). Likewise there is reduced accumulation of nitrogen-induced CKs in the *atipt3* mutant (Takei *et al*., 2004b). Collectively, it is suggested that *AtIPT3* is a major gene for the primary step of iP-type CK synthesis.

5.4.3 Synthesis of tZ-type Cytokinins

Wild-type levels of tZ-type CKs in shoots of double mutants *atipt5,7, atipt3,5* and *atipt3,7* (Fig 5.5A & B) indicates the presence of iPRP-independent tZ biosynthesis, as there is low supply of iPRP in case of *atipt3,5* and *atipt3,7* (Fig. 5.7 B, Miyawaki *et al*., 2006). In plants, tZ biosynthesis takes place through two possible pathways. One is the iPRP-independent that produces tZRP directly by IPT enzyme using a hydroxylated side-chain precursor (Astot *et al*., 2000) and the other is iPRP-dependent that is catalyzed by two enzymes, CYP735A1 and CYP735A2. CYP735A genes are predominantly expressed in roots as compared with weak

expression in shoot (based on quantification of transcript levels), suggesting roots as a major site of tZ-type CK production (Takei *et al*., 2004b). Therefore, synthesis of tZ-type CKs locally in shoot is somewhat surprising, as activity of CYP735A is very much low in shoot. Another possibility is that tZ-type CKs are transported from root via xylem but tZ-nucleotides are not found in xylem sap (Beveridge *et al*., 1997; Foo *et al*., 2007), which is also confirmed from xylem-CK profiles (Figure 5.4 and 5.8). The conversion of xylem-derived tZR into tZRP is also possible but levels of tZR in double mutants *atipt5,7, atipt3,5* and *atipt3,7*are also reduced compared with wild-type (Figure 5.8). However, strongly reduced tZ-type CKs in shoots of *atipt3,5,7* does not support the proposal of tZRP synthesis independent of iPRP because the supply of iPRP is greatly decreased (8-fold) in *atipt3,5,7* but comparatively tZRP is highly (~100 fold) reduced (Figure 5.5 C). That also suggests that *AtIPT1* is not involved in the alternate biosynthetic pathway of tZ-type CKs. It can be predicted that both iPRP-dependent and iPRP-independent pathways work alongside in shoot. Decreased levels of tZ-type CKs in roots of double and triple *atipt* mutants, corresponding to low levels of iP-type CKs (Figure 5.7 A, B & C), are consistent with the idea that most of or all tZ-type CKs come from iPRP-dependent pathway in roots (Takei *et al*., 2004b).

5.4.4 Synthesis of DZ- and cZ-type Cytokinins

No alteration in cZ-type cytokinin was observed in shoot, phloem, root and xylem of all *max* mutants, nor in *atipt* mutant genotypes in wild-type and *max* backgrounds. This supports the existence of another pathway for biosynthesis of cZ-type CKs through tRNA prenylation that is catalyzed by tRNA-IPT genes (tRNA-IPT2 & 9). Prenylated-tRNA has a *cis*-hydroxyl group, thus degradation of prenylated tRNA generates cZ-type CKs (Kamada-Nobusada and Sakakibara, 2009). The single knockout mutants for either *tRNA-IPT* genes in *Arabidopsis*, *atipt2* or *atipt9*, have been shown to have decreased levels of cZ-type cytokinins, and cZ-type cytokinins could not be detected in the *atipt2,9* double mutant, indicating that *AtIPT2* and *AtIPT9* are absolutely required for cZ-type cytokinin production. The lack of cZ-type cytokinin in *atipt2,9* also suggests an absence of isomerization of tZ to cZ. Overall, the decrease in cZ-type cytokinin levels in *atipt2,9* double mutants supports the idea that cZ-type cytokinins are synthesized from modified tRNAs (Miyawaki *et al*., 2006).

The shoots of *atipt3,5,7* mutant in both wild-type and *max4* background exhibit an increase in DZR levels (Fig. 5.5 C and 5.15). This is quite unexpected due to very low supply of tZ-type CKs in these mutants because DZ is formed from Zeatin due to conversion by a NADPH-dependent zeatin reductase (Martin *et al*., 1989), and production of DZRP and DZR from tZRP and tZR, respectively, has also been predicted (Kamada-Nobusada and Sakakibara, 2009). Another possibility is that the conversion between *cis*- and *trans*-isomers of zeatin catalyzed by the enzyme *cis-trans* zeatin isomerase (Bassil *et al*., 1993) can be a source of zeatin supply for DZ-type cytokinin in *atipt3,5,7* and *atipt3,5,7,max4* mutants.

5.4.5 Phloem and Xylem Cytokinins

Cytokinin compounds are transported to roots through phloem and to shoot via xylem. The predominant forms in phloem sap are iPRP and iPR (Corbesier *et al*., 2003; Hirose *et al*., 2008), whereas the major form of cytokinin in xylem sap are tZR and tZ (Beveridge *et al*., 1997b; Takei *et al*., 2001b; Hirose *et al*., 2008). The phloem and xylem CK data presented in this chapter (see Fig. 5.2, 5.4, 5.6 A &B, and 5.8 A & B) agree with the previous findings of dominant iP- and tZ- type CK forms in phloem and xylem sap, respectively.

Hydroxylation activity of CYP735A1 and CYP735A2 enzymes, predominantly found in roots, utilize iPRP as a substrate but not the iPR and iP forms of CKs (Takei *et al*., 2004b). Wild-type phloem exudates shows reduced levels of iPRP (~10-fold; Fig. 5.2) compared to iPR levels (Fig. 5.2 and 5.6 A & B), indicating a minor role of phloem iPRP in synthesis of tZ-type cytokinin in roots. This idea is also supported by results of a grafting experiment with *atipt1,3,5,7* mutant, which was shown to have decreased pool of both iP- and tZ-type cytokinins than wild-type plant (Miyawaki *et al*., 2006). Normal levels of iP-type cytokinins were observed in the mutant root-stocks grafted with wild-type scions, whereas only partial recovery of tZ-type cytokinins was found in the same graft (Matsumoto-Kitano *et al*., 2008). There is a slight increase in iPRP levels in phloem sap of *atipt5,7* (Fig. 5.7A), but decreased iPRP in root resulting in reduced synthesis of tZRP (Figure 5.7A) and reduced xylem transport (Figure 5.9 A) of tZ-type cytokinins in *atipt5,7*. Taken together, all these findings further support the proposal that tZ-type cytokinin in the roots is dependent on locally synthesized iP-type CKs rather than phloem derived ones. According to a previously proposed model (Kudo *et al*., 2010), iP-type CKs are transported to roots, where these are converted into tZ-type CKs. However, the CK data obtained from phloem, root and xylem tissues do not support this model.

Double mutants *atipt3,5* and *atipt3,7* exhibit remarkable decreases in phloem and xylem CKs (Fig. 5.6 B and 5.7 B) as compared with wild-type. This can be explained by spatial and temporal expression of *AtIPT3*. It is reported that *AtIPT3* is expressed in phloem (Miyawaki *et al*., 2004) and is highly expressed at the stage of mature rosette (Takei *et al*., 2004a; Genevestigator database, Figure-3.1 & 3.2). Therefore, loss of *AtIPT3* function causes reduction in tissue-specific synthesis and transport of CKs, as explained in previous discussion sections of this chapter (see section 5.4.1 and 5.4.2).

5.4.6 Effect on Cytokinin Content due to *max* mutation

The *max* mutations do not change the profile of iP-type CKs in shoot and roots of wild-type nor in the backgrounds of *atipt5,7, atipt3,5, atipt3,7* and *atipt3,5,7* but result in altered patterns of tZ-type CKs (Fig. 5.1, 5.3, 5.5 ABC, and 5.7 ABC). The wild-type levels of tZ-type CKs in shoots of *atipt3,5, atipt3,7atipt3,5,max4* and *atipt3,7,max4* (Fig. 5.5 B) supports their iPRP-independent synthesis (Astot *et al*., 2000)rather than being xylem-derived tZ CKs, as *atipt3,5* and *atipt3,7* in both wild-type and *max* backgrounds also exhibit low xylem-CKs

(Fig. 5.8B). This also reflects that absence of two *AtIPT* genes does not affect iPRP-independent CK synthesis in shoot. This hypothesis is supported by the normal wild-type phenotypes of *atipt* double mutants (Miyawaki *et al*, 2006). A major conclusion is that the trends of tZ-type CKs in shoots and roots of *atipt* double and triple mutants in *max* backgrounds are parallel to those in wild-type background.

The *max* mutations also have effects on phloem and xylem CK species. The iPRP levels are highly increased (8-17 fold) in phloem sap of *max* genotypes as compared with wild-type (Fig. 5.2), whereas tZR content is highly decreased (upto 40-fold) in xylem sap of *max* mutants (Fig. 5.4). The xylem CK data are in line with the previous findings of Foo *et al*. (2007). The *atipt5,7* mutants in *max* and wild-type backgrounds show interesting trends of CK species in phloem, root and xylem. The *max2* and *max4* mutations in *atipt5,7* background show increased iPRP levels in phloem sap as compared with wild-type and *atipt5,7* (Fig. 5.7A). This increase may be due to up-regulation of *AtIPT3* in phloem (Miyawaki *et al*., 2004) and this is supported by enhanced *AtIPT3::GUS* expression in *max2* and *max4* (Figure 4.5 and 4.6). Similarly, elevated levels of *PsIPT* genes have been reported in *rms* mutants of pea (Dun *et al*., 2012). However, the increased iPRP levels in the phloem sap of *atipt5,7,max2* and *atipt5,7,max4* does not change the tZ-type CKs in roots, rather the trend is parallel to those of iP-type CK supply from roots of the same mutants (Figure 5.7 A). Although the iPRP levels in phloem sap of *max* genotypes are significantly higher than in wild-type, tZ-type CKs in roots of *max* genotypes are equal to wild-type (Fig. 5.2 and 5.3). However, levels of tZ-type CKs are decreased in roots of *atipt5,7,max2* and *atipt5,7,max4* (Fig. 5.8A). Collectively, all these findings suggest that phloem-derived iPRP is not utilized to synthesize tZ-type CKs in roots (discussed in section 5.4.3). Contrary to increased iPRP levels in phloem of *atipt5,7,max2* and *atipt,5,7,max4*, the xylem CKs are decreased in these genotypes as compared with wild-type and *atipt5,7* (Fig. 5.8A). One possible interpretation is that phloem-derived iPRP might be used as a feedback signal to inhibit xylem transport of CKs from root to shoot and might be involved in other mechanisms of CK metabolism. Consistent with this, it is reported that the feedback signal that inhibits xylem CK comes from the shoot (Beveridge *et al*., 1997a). Further investigations are required to discover how xylem transport is blocked to stop transport of tZ-type CKs.

5.7 Conclusions

1- iPRP-independent pathway of CK synthesis exists in shoots.
2- Phloem-derived iPRP may not be utilized in iPRP-dependent pathway of tZ synthesis in roots.
3- Phloem-derived iPRP might be a feedback signal that blocks transport of CKs via xylem.
4- Synthesis of cZ-type cytokinins is independent of iPRP.

Chapter 6

Identification of Lethal Mutants

6.1 Introduction

6.1.1 Lethality

Lethality is recognized as non-viability of an organism with loss of function of essential genes, required for normal growth and development. The lethality may occur due to mutation in a single or multiple essential genes. If a mechanism is controlled by duplicated genes that encode essential proteins with redundant functions, a single knockout of such genes will not be detected by phenotype and would require appropriate multiple mutants to be generated. Synthetic lethality is termed when a genotype fails to survive only due to mutations in distinct non related genes whose functional interaction is required for the survival of that genotype. Normally, it is considered that lethal mutants cannot be explored because it is hard to generate and/or maintain them. But it is possible to some extent to study the role of essential genes either in their heterozygous mutant forms or by use of weak alleles. Lethality reflects the importance of a gene function in metabolic, cellular or developmental mechanisms and can act at the stage of gamete formation (male and/or female) or embryo development. The gametophytic and embryonic lethals may provide valuable information on developmental interactions during the reproductive phase of plant life cycle (Meinke *et al*., 2008; Candela *et al*., 2011).

6.1.2 Plant Gametogenesis and Embryogenesis

Unlike animals, plant development is divided into two phases of development; vegetative and reproductive. Therefore, the reproductive organs, stamen (male) and carpel (female) are produced later in plant development. The plant life cycle alternates between sporophytic (diploid) and gametophytic (haploid) generations. The switching is triggered by the initiation of meiosis during the reproductive phase of plant development. During male and female gametogenesis, the process of gamete formation is started in a similar manner with the differentiation of cells and initiation of meiosis (Wilson and Yang, 2004).

A critical step in the life cycle of a plant is embryogenesis, which is a complex developmental process to form a multicellular organism from a single cell (fertilized zygote) by cell division, differentiation and growth. The process of seed development through embryogenesis can be conceptually divided into three steps: (1) the embryo patterning by rapid cell division, (2) cell expansion and (3) synthesis and accumulation of reserves. A viable seed is produced through the coordination between the developments of three seed components: (1) the maternal tissues such as integuments developing into the seed coat, (2) the triploid endosperm and (3) the diploid embryo (Devic, 2008).

6.1.3 Seed Abortion

As a result of the complex processes of gametogenesis and embryogenesis, a viable seed is formed enabling survival of the next generation. A large number of essential genes are expected to be expressed for the production of viable gametes and seeds. Hence mutations in any of these essential genes may cause inability of a plant to produce a normal seed. Normally, the presence of one quarter (1/4) of aborted seeds in the siliques of recessive mutants indicates that lethality is due to disruption of gene functions associated with essential cellular mechanisms, leading to seed abortion. Consequently, a homozygous mutant plant cannot be obtained (Devic, 2008).

6.1.4 Cytokinin and Lethality

Cytokinin is known to be involved in regulation of the cell cycle (Stals and Inzé, 2001). Previous publications on cytokinin related mutants showed a role of cytokinin during the reproductive phase of *Arabidopsis* life cycle, as detailed below:

Cytokinin oxidase/dehydrogenase (AtCKX) enzymes are involved in degradation of cytokinin in plants. The over-expressers (OE) of *AtCKXs* (35S::AtCKX1 and 35S::CKX3) revealed a role for cytokinin in sexual phase of development in *Arabidopsis*. For example, the flowers of OE-AtCKX plants produce low numbers of pollen grains. The siliques of 35S::AtCKX1 and 35S::CKX3 plants were not filled completely and contained about 8 to 20 viable but larger seeds, whereas wild-type siliques had approximately 60 seeds. The seeds in the siliques of 35S::AtCKX1 and 35S::CKX3 did not mature uniformly and some were aborted during development (Werner *et al.*, 2003).

Cytokinin-Independent 1 (CKI1) belongs to a group of plant histidine kinases (AHKs) (Pischke *et al*., 2002) that activate cytokinin signalling via *Arabidopsis* Histidine Phosphotransfer Proteins (AHPs) (Deng *et al*., 2010). T-DNA insertion alleles of *CKI1* appeared to be lethal as no homozygous *cki1* plant was found. Detailed examination of developing female gametophytes by confocal laser scanning microscopy revealed that more than 98% of ovules were defective in female gametophyte development, as the earliest stage of megagametogenesis at which abnormal female gametophytes were observed was the four-nucleate stage. The abnormal female gametophytes showed defects in cell morphology and nuclear position. Compared with the cell polarity typical of a wild-type female gametophyte, nuclei were found to be positioned incorrectly within the cells and relative to other cells. Cell vacuoles were also deformed. Collectively, these observations indicate that the *CKI1* gene product is required for normal cell morphology and nuclear divisions during megagametogenesis, suggesting the role of cytokinin signal transduction via CKI1 in female gametophyte development in *Arabidopsis* (Pinscher *et al*., 2002). Furthermore, the histochemical analysis of GUS activity under the control of the *CKI1* promoter and in situ localization of *CKI1* mRNA revealed that CKI1 expresses at the very early stage of female gametophyte development and its expression continues until fertilization (Hejatko *et al*., 2003).

In *Arabidopsis*, *CYTOKININ RESPONSE FACTORS* (*CRFs*) have been shown to be up-regulated by cytokinin. In addition, the CRF proteins were found to be accumulated rapidly in the nucleus in response to cytokinin, dependent on the AHKs-AHPs signalling pathway, but independent of the RESPONSE REGULATORS (ARRs). Moreover, the CRF proteins were found to regulate the cytokinin responses through the type-B ARRs. Mutations in *CRF* genes revealed that their role in the development of embryos, as the siliques of *crf5_crf5,CRF6_crf6* or *CRF5_crf5,crf6_crf6* mutants were found to have 25% aborted seeds due to embryo arrest at the early heart stage. Transformation of *CRF5* cDNA succeeded to recover the embryo lethal phenotype in a *crf5_crf5,crf6_crf6* double mutant (Rashotte *et al*., 2006).

Kinoshita-Tsujimura and Kakimoto (2011) have reported that three cytokinin receptors CRE1/AHK4, AHK2 and AHK3 in the haploid cells are required for the development of male and female gametophytes. The triple mutants *(cre1-12,ahk2-2tk,ahk3-3)* did not set seed, showing that reproductive growth is retarded. Further investigation revealed that anthers of mutant plants contained only a few pollen grains. A large proportion (78%) of ovules was abnormal and lacked an embryo sac. Reciprocal crosses between the triple mutants and the wild type showed that pollen from mutant plants did not germinate on the wild-type stigmas and vice versa. These results lead to the proposal that cytokinin receptors in the sporophyte play an important role in male and female gametophyte development.

Recently, the role of CK signalling in female gametophyte development has been explored using triple *ahk* mutants (*ahk2–5,ahk3–7,cre1–2*; *ahk2–1,ahk3–1,ahk4–1*; *ahk2–7,ahk3–3,cre1–12)*, suggesting that at least a low level of activity of cytokinin signalling is required

for female gametophyte development. It was also shown in transgenic plants carrying a GUS reporter driven by the promoter of AHK2, AHK3 or CRE1 that the signalling is localized in the chalaza of the ovule. Expression of a female megaspore specific marker (*pFM2*::GUS) was found to disappear in the ovules of triple *ahk* mutants. Collectively, this investigation leads to conclude that cytokinin signalling in the chalaza functions for female megaspore specification in female gametophyte development (Cheng *et al*., 2013).

6.1.5 Strigolactone and Lethality

Strigolactone has recently been added to the list of plant hormones, and is being investigated for its different roles in controlling plant growth and development. There is no strong evidence available yet to show the involvement of strigolactone in the mechanisms of cell cycle and reproduction, but a role for strigolactone was predicted in reproduction on the basis of expression data of strigolactone biosynthetic and signalling genes in different plant species, as detailes below:

Tissue-specific expression of *MAX2* gene was investigated by fusing 3.45 kb of *MAX2* upstream sequence and *MAX2* cDNA, to the *GUS* reporter gene. Expression of *M2p::M2–GUS* was highest in the vasculature of flowers and siliques along with leaves and stems. The funiculi in siliques are connecting tissues between developing seeds and placenta, and were stained particularly strongly. Vascular GUS activity declined when the growth of leaves and stems ceased, but remained high in the funiculi of ripening siliques (Stirnberg *et al*., 2007). The relative expression of *MAX2* by real-time RT-PCR was also detected in flowers and mature seeds (Mashiguchi *et al*., 2009).

In *Arabidopsis*, expression of *MAX3* (AtCCD7) was detected in flowers, siliques and seeds (Booker *et al*., 2004; Mashiguchi *et al*., 2009). In tomato, the highest level of SlCCD7 expression was observed in green immature fruits (Vogel *et al*., 2010). In kiwifruit, the expression of AcCCD7 and AcCCD8 was also detected in young fruit and in seeds from ripened fruit (Ledger *et al*., 2010). In maize, increased ZmCCD8 mRNA levels were observed in shank and ear shoots of female inflorescences (Guan *et al*., 2012). Expression of genes related to strigolactone has been detected in reproductive organs but the actual function of strigolactone in the reproduction, seed setting and fruit development is unclear and needs to be explored.

Until now, CCD7 activity, involved in strigolactone biosynthesis, has never been shown to affect reproduction, but in *L. japonicus*. Reduced flower, fruit and seed numbers were observed in *L. japonicas* as a result of LjCCD7 silencing by RNA interference (Liu *et al*., 2013). It has already been reported that flowering in petunia dad1/ccd8 mutant is delayed and flowers were found to be smaller than in the wild type (Snowden *et al*., 2005). In SlCCD8-silenced tomato plants, floral organs, fruits and seeds were smaller, and 60% reduction in seed number was found relative to controls (Kohlen *et al*., 2012). The size of ear and shank was significantly decreased in maize ZmCCD8 mutants (Guan *et al*., 2012). These reports

suggest possible roles for strigolactone in controlling different mechanisms of reproduction. However, essential functions of strigolactone in plant survival have not yet been defined, and no strigolactone related lethality has been reported.

6.1.6 Aims

This chapter deals with the identification of lethality due to double mutations in the cytokinin biosynthetic gene *AtIPT3* and the strigolactone signalling gene *MAX2*. Despite considerable efforts, the double homozygous recessive mutant could not be obtained from reciprocal crosses between single *atipt3* and *max2* mutants.

6.2 Materials and Methods

6.2.1 Genotypes

***atipt3*:** The single knockout mutant *atipt3* was isolated from the F2 segregating population of cross between *atip1,3,5,7* and *max2* (see Table 3.4).

***max2-1*:** This is ethyl methane sulphonate (EMS) mutagenic allele of *MAX2* gene (see section 3.4.2, Stirnberg *et al.,* 2002).

Δ max2: This mutant line is taken from Salk Institute of Biological Sciences (Salk_092836, N680512), which was created by T-DNA insertion in the exon of *MAX2* gene.

6.2.2 Growth Conditions

The conditions to grow plants in the soil were similar to section 2.1.2.

6.2.3 Crossing

The reciprocal crosses between *atipt3* and *max2* were made according to section 2.2.

6.2.4 Genotyping of *AtIPTs* and *MAX2* Genes

The genotyping of *AtIPTs* and *MAX2* genes were performed according to section 3.2.3, 3.4.1 and 3.4.2.

6.2.5 Seed Mapping

Mapping of distribution of aborted seeds within siliques was performed according to method in which a silique grid drawn on a paper is utilized to map the positions of aborted seeds (Meinke, 1982), as shown in Fig. 6.1. This method provides a record of seed number and positions within individual siliques. The data then can be used to calculate segregation ratios and to determine whether the distribution of mutant seeds in bottom and upper halves of siliques is random or non-random.

For seed mapping, 20 individual siliques of each genotype were harvested and dissected with the help of a syringe needle under a microscope. The seeds were counted and mapped starting from base of the silique and recorded on each silique grid accordingly.

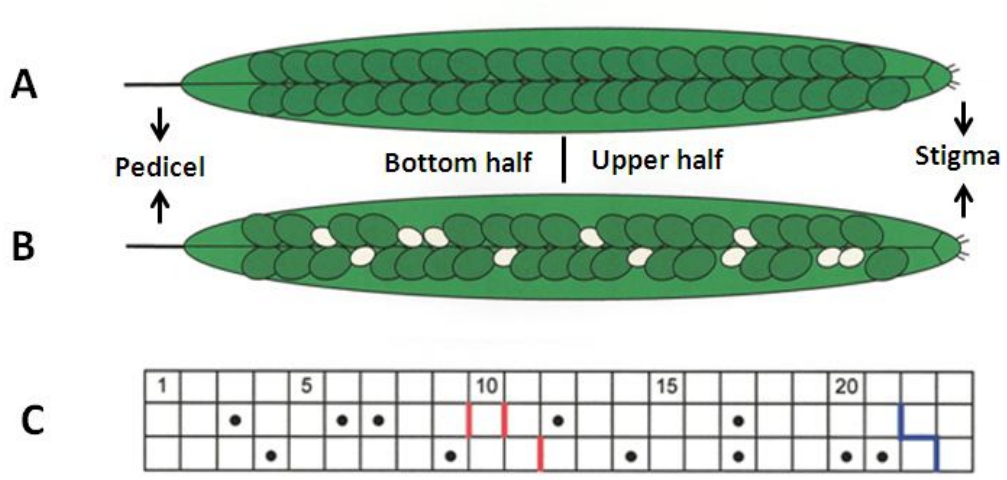

Figure – 6.1: Seed Mapping within Silique of Arabidopsis thaliana. *(A) Internal view of a wild-type silique. (B) A silique of heterozygous mutant plant containing white aborted seeds. (C) A silique grid for mapping seed positions. A seed within a silique is represented by each grid square, in which a dot corresponds to a mutant aborted seed. The tip closest to stigma surface is shown on right side and base closest to pedicel is on left side of the map grid.*

6.3 Results

6.3.1 Screening for*atipt3,5, atipt3,7 and atipt3,5*,7 in *max2* background

For the screening for double *atipt* mutants *atipt3,5* and *atipt3,7* in *max2* background, the plants (see Table 6.1) were selected from F2 population of two crosses between *max2* and *atipt1,3,5,7,* coded as A & B (see Table 3.4). The selection was based on genotyping of five genes segregating in the F2 population. The reconfirmation of genotyping of the selected individuals was made by PCR and their F3 seeds were grown for further selection.

Forty eight seeds (F3) of each plant from P10-P17 (Table 6.1) were sown in the soil. After a week of germination, not a single plant with the*max2*-like long hypocotyl phenotype was observed. This was quite unexpected and surprising. Two weeks later, all plants continued to display wild- type characteristics, and no small phenotype like *atipt1,3,5,7* was noted. It was concluded that either genotyping of these plants for *MAX2* gene by PCR followed by enzyme digestion (See section 3.4.2) had not worked correctly or had been interpreted wrongly. All of the selected plants were segregating for two or three genes. Therefore, it was decided to genotype more F2 plants, which had already been scored as *max2* phenotypes, from cross A (Table 3.4). The reconfirmation of genotyping of *AtIPT* genes (as double heterozygous) made it possible to select two plants P18 and P19, from which attempts were made to isolate *atipt3,5* and *atipt3,7* homozygous mutants in *max2* background, respectively.

As shown in Fig. 6.2 (A & C), the descendants of P18A and P19A were genotyped for *AtIPT5* and *AtIPT7* genes, respectively, with the genomic primers to find these genes knockouts. The single knock outs for *ATIPT5* and *AtIPT7* were further amplified for *AtIPT3* gene with genomic and T-DNA primers to isolate double mutants (Fig. 6.2 B &D). It was observed that the segregation of *AtIPT5* was normal (1:3) but that of *AtIPT7* was not normal with knockouts of *AtIPT7* present at very low frequency (see Table 6.2). All single knockouts for *ATIPT5* (9 in number) and *AtIPT7* (3 in number) genes were segregating for wild-type and mutant alleles of *AtIPT3* gene (Fig. 6.2 B & D). As a result, no double homozygous mutants of *atipt3,5* and *atipt3,7* were found in *max2* backgrounds of P18 and P19, respectively. The 48 plants (F3) of P18 and 40 plants (F3) of P19 were genotyped for their corresponding segregating *AtIPT* genes. Therefore, it was thought that this small number of plants was insufficient for detection of double homozygous mutants and the decision was made to screen a large number of F3 plants from P18 and P19.

Table – 6.1: Genotyping Score of F2 Plants for *AtIPTs and MAX2* Genes

F2 Genotyping										
Gene	**P10-A** *atipt3,5*	**P11-A** *atipt3,5*	**P12-A** *atipt3,5*	**P13-A** *atipt3,5*	**P14-A** *atipt3,7*	**P15-A** *atipt3,7*	**P16-A** *atipt3,7*	**P17-A** *atipt3,7*	**P18-A** *atipt3,5*	**P19-A** *atipt3,7*
AtIPT1	**Ht**	**Ht**	**WT**	**WT**	**Ht**	**Ht**	**Ht**	**Ht**	**WT**	**WT**
AtIPT3	*atipt3*	*atipt3*	*atipt3*	*atipt3*	*atipt3*	*atipt3*	*atipt3*	*atipt3*	**Ht**	**Ht**
AtIPT5	*atipt5*	*atipt5*	*atipt5*	*atipt5*	**Ht**	**WT**	**Ht**	**Ht**	**Ht**	**WT**
AtIPT7	**Ht**	**Ht**	**Ht**	**Ht**	*atipt7*	*atipt7*	*atipt7*	*atipt7*	**WT**	**Ht**
MAX2	**Ht**	**Ht**	**Ht**	**Ht**	**Ht**	**Ht**	**Ht**	**Ht**	*max2*	*max2*

"P" represents plant and P10- P19 are plant numbers selected. A corresponds to cross code given in Table -3.4. WT means homozygous for dominant alleles of a gene and Ht means heterozygous for both WT and recessive mutant alleles of a gene. The score of AtIPT and MAX2 genes is PCR based whereas MAX2 gene in case of P18 and P19 is also scored on distinct branching phenotype.

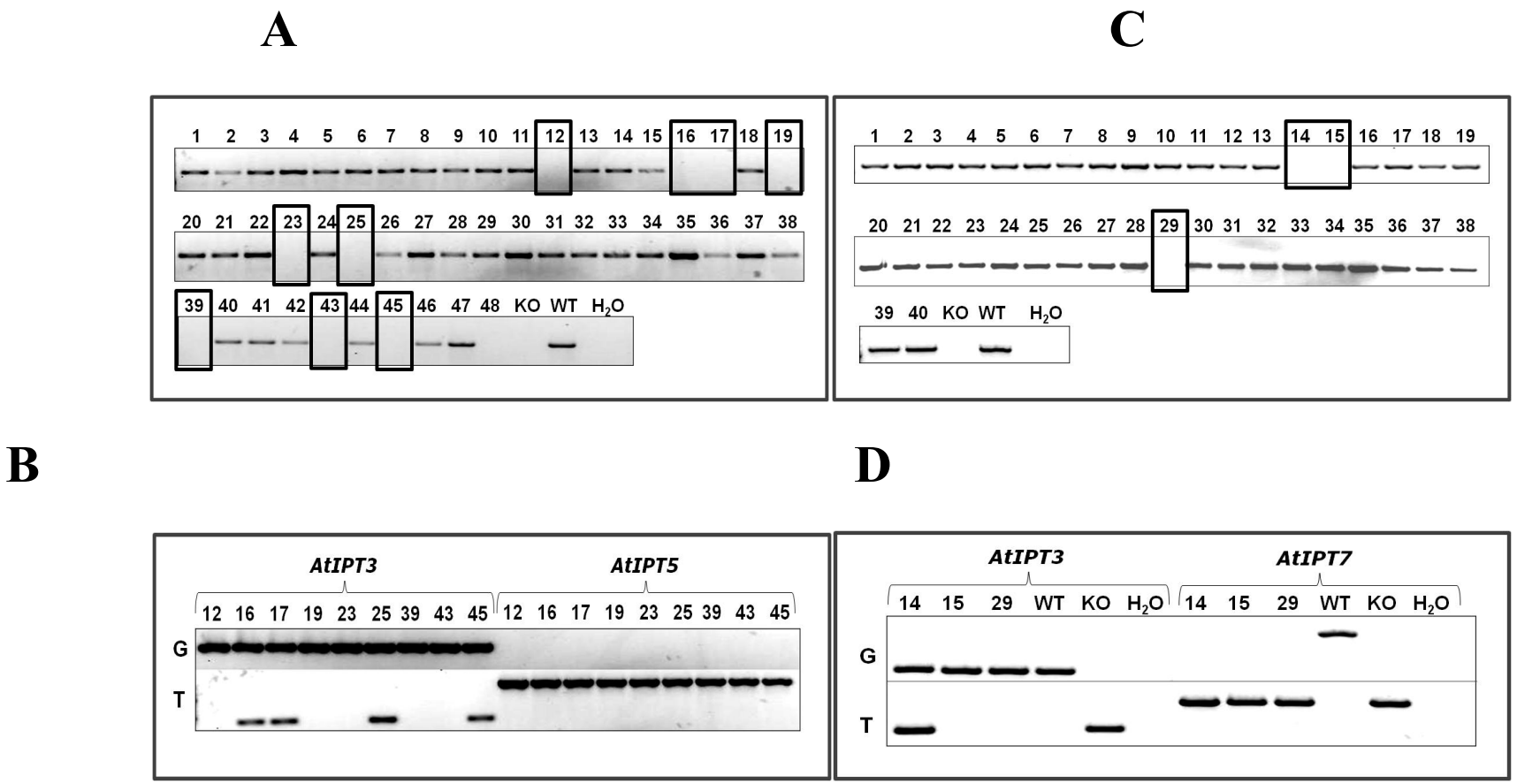

Figure – 6.2: Amplification of AtIPT3, AtIPT5 and AtIPT7 genes.*PCR (35 cycles) with genomic primer pairs (LP + RP) was performed to identify absence and presence of genomic bands for AtIPT5 (A) and AtIPT7 (C) genes in F3 progeny from P18A and P19A F2 plants. The samples with no genomic band were further amplified with two primer pairs (LP + RP and LB + RP) to identify genomic band or T-DNA insertion in ATIPT3 and AtIPT5 (B), or AtIPT3 and AtIPT7 (D) genes. KO symbolize atipt1,3,5,7 whereas G and T stands for genomic and T-DNA, respectively. H_2O is a negative control for PCR reaction. Black boxes indicate absence of genomic band. 8ul of a sample was loaded in each lane of 1.2% agarose gel.*

For the extended re-screening, 120 F3 seeds of each P18 and P19 were sown and small leaves of 2-weeks old plants were harvested to isolate their DNA for genotyping. The 87 and 120 descendants of P18 and P19, respectively, were genotyped for *AtIPT3* gene with the genomic primers and as a result, no single knock out for *AtIPT3* gene was identified, indicating distortion of normal segregation (see Table 6.2). All samples showed amplification of genomic band, some of which are shown in Fig. 6.3 (A & B).

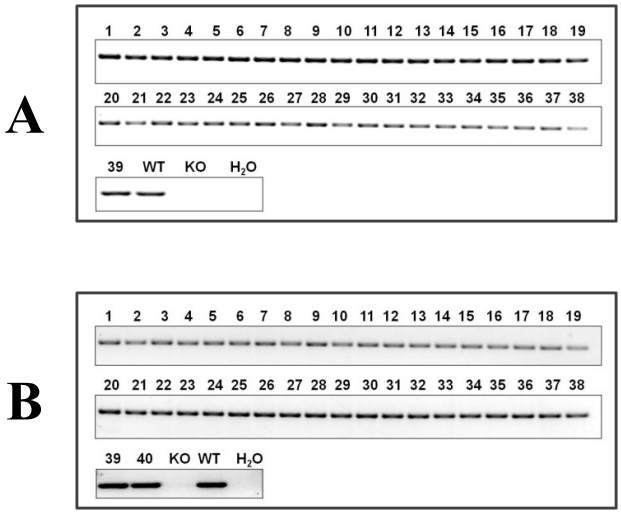

Figure – 6.3: ***Amplification of AtIPT3 gene:*** *PCR (35 cycles) with genomic primer pairs (LP + RP) was performed to identify absence and presence of genomic band for AtIPT3 from plant P18A (A) and P19A (B). KO symbolizes atipt1,3,5,7 whereas WT stands for wild-type. H_2O is a negative control for PCR reaction.*

Table – 6.2: Segregation Ratios of *AtIPT3*, *AtIPT5* and *AtIPT7* in Plants P18 and P19

Plant. No.	**Genes**	**Genotypes**		**Goodness of fit to ratio 1:3**	
		AtIPT	***atipt***	***Calculated X^2***	$X^2_{0.05}$
P18	*AtIPT5*	38	9	0.858	3.841
	AtIPT3	87	0	> 26.0	3.841
P19	*AtIPT7*	36	3	6.231	3.841
	AtIPT3	120	0	> 26.0	3.841

AtIPT represents wild-type score including homozygous and heterozygous alleles
atipt corresponds to mutant knockout homozygous alleles
X^2 is calculated value of Chi-Square Goodness-of-Fit test
$X^2_{0.05}$ is critical value to accept and reject null hypothesis
If X^2 is greater than $X^2_{0.05}$, it rejects null hypothesis and if X^2 is lower than $X^2_{0.05}$, it accepts null hypothesis. Rejection and acceptance means that data fits the segregation ratio tested or not.

Table – 6.3: Genotyping Score of F2 Plants for *AtIPTs* Genes and Phenotypic Score of *max2* and *max4*

F2 Genotyping								
Genes	**P20-B**	**P21-B**	**P22-B**	**P23-B**	**P24-B**	**P25-C**	**P26-C**	**P27-C**
AtIPT1	**WT**	**WT**	**WT**	**WT**	**WT**	**WT**	**WT**	**WT**
AtIPT3	**Ht**	**Ht**	**Ht**	**Ht**	**Ht**	***atipt3***	***atipt3***	***atipt3***
AtIPT5	***atipt5***	***atipt5***	***atipt5***	***atipt5***	***atipt5***	***atipt5***	***atipt5***	***atipt5***
AtIPT7	***atipt7***	***atipt7***	***atipt7***	***atipt7***	***atipt7***	**Ht**	**Ht**	**Ht**
MAX	***max2***	***max2***	***max2***	***max2***	***max2***	***max4***	***max4***	***max4***

Further, an F3 population from plant P3-B (See Table 3.5) was used for the screening of *atipt3,5,7* in *max2* background. The plant P3-B was already used to identify *atipt5,7* mutants in *max2* background, as the P3-B was segregating for the wild-type and mutant alleles of *AtIPT1* and *AtIPT3* genes but homozygous for recessive mutant alleles of *AtIPT5*, *AtIPT7* and *MAX2* genes. The five plants P20-P24 (Table 6.3) were selected from the F3 population of P3-B. The selected plants carried homozygous dominant wild-type alleles of *AtIPT1* and were segregating only for *AtIPT3*, as shown in Table 6.3. For comparison, three plants (P25-P27) segregating for *AtIPT7* gene were selected from the F3 population derived from P7-C (Table 3.6), which was previously used to isolate *atipt3,5* and *atipt3,5,7* in *max4* background. One hundred and twenty (120) F4 seeds from each of P20-P27 were sown for further screening. The phenotypic data was recorded in order to find plants exhibiting very small rosettes similar to *atipt3,5,7* (reported in Miyawaki, 2006) in this F4 population.

The descendants of plants P20-P24 were collectively taken as one population in *max2* background and those of plants P25-P27 as one population in *max4* background. In total, 600 and 360 seeds were sown for the screening of *max2* and *max4* populations, respectively. In case of *max4* population, 327 plants survived (90.83%), out of which 74 plants displayed a small phenotype similar to *atipt3,5,7*,consistent with a Mendelian ratio of 1:3, approximately ($X^2 < X^2_{0.05}$ = 0.980 < 3.841; $p > 0.05$ = 0.322). In contrast, only 13 plants showing small phenotypes were observed out of 480 surviving plants from the *max2* population of 600 sown. The expected number of plants was 120 out of 480. It was observed that 120 seeds did not germinate. It leads to the suggestion that the expected number of 150 plants out of 600 were not found in the *max2* population. Further confirmation was made by genotyping the 13 small plants from this population, as those were still segregating between wild-type and mutant recessive alleles of *AtIPT3* gene, but none were double homozygous *atipt3,max2*. Therefore, their phenotype was not due to a genetic outcome but can be attributed to environmental factors and growing conditions.

6.3.2 Seed Abortion Percentage

The work described above shows that isolation of *atipt* mutants *atipt3,5*, *atipt3,7* and *atipt3,5,7* in *max2* background was not successful. The problems during screening of a large number of plants prompted the checking of seed setting in the siliques of plants with *AtIPT3_atipt3,atipt5_atipt5,max2_max2* and *AtIPT3_atipt3,atipt7_atipt7,max2_max2* genotypes, which were isolated from the screening of F3 descendants of plants P18 and P19, as given in Table 6.1. Before drying and dehiscence, the mature siliques of these plants were harvested and stored in 70% ethanol. Ethanol treatment was used for the de-pigmentation of the siliques. Image acquisition of cleared pods under a microscope was used to assess seed setting. Seed set was observed to be reduced in the pods of both these lines, as compared with nearly 100% seed setting in the wild-type Col-0 and *max2* pods (Fig 6.4).

Figure – 6.4: Seed Setting in the Mature Siliques. *The genotypes of siliques are wild-type Columbia-0 (Far Left), max2 (Far Right), AtIPT3_atipt3, atipt5_ atipt5,max2_max2 (Middle Left), and AtIPT3_atipt3, atipt7_ atipt7,max2_max2 (Middle Right). Bar = 1.98cm.*

For calculation of seed abortion percentage, 10 dry pods of *AtIPT3_atipt3, atipt5_ atipt5,max2_max2* and *AtIPT3_atipt3, atipt7_ atipt7,max2_max2* were harvested before dehiscence. Seeds within the pods categorized as normal (light brown) and shrunken (dark brown or black) were counted from each pod under the microscope. It was found that **23.14%** and **15.74%** seeds were aborted (see Table 6.4 for segregation ratios) in case of *AtIPT3_atipt3, atipt5_ atipt5,max2_max2* and *AtIPT3_atipt3, atipt7_ atipt7,max2_max2,* respectively.

Table – 6.4: Segregation Ratios of Aborted Seeds in Dry Pods before Dehiscence

Genotypes	Seeds			Goodness of fit to ratio 1:3		
	Total	***Normal***	***Aborted***	***Calculated X^2***	***$X^2_{0.05}$***	***p value***
AtIPT3_atipt3, atipt5_ atipt5, max2_max2	363	279	84	0.669	3.841	0.413
AtIPT3_atipt3, atipt7_ atipt7, max2_max2	362	305	57	16.534	3.841	0.000

Significant = $X^2 > X^2_{0.05}$ and $p < 0.05$

6.3.3 Screening for *max2* mutant in *atipt3* background

The successful identification of *atipt5,7* mutant in *max2* background and absence of *atipt3* knockout in *max2* backgrounds of *atipt3,5*, *atipt3,7* and *atipt3,5,7* during the major screening experiments, lead to the conclusion that there is a problem in the isolation of double knockout mutants for *AtIPT3* and *MAX2* genes. Therefore, a plant P28 was selected to confirm interaction between *ATIPT3* and *MAX2* genes. The plant P28-A was homozygous for recessive alleles of *AtIPT3* gene and for wild-type alleles of *AtIPT1*, *ATIPT5* and *AtIPT7* genes (Fig. 6.5 A). The phenotype of P-28 was wild-type, and heterozygous status for *MAX2* gene was confirmed by PCR followed by ApoI enzyme digestion, (Fig. 6.5 B). The F3 seeds of plant P-28 were sown and tested for segregation ratio of *max2* phenotype along with control plants including Col-0 and *max2*. It was observed that all plants exhibited wild-type phenotypes (Fig. 6.5 C). This surprising observation was consistent with the wild type phenotypes of all F3 descendants of P10-P17 (Table 6.1), which were likewise segregating for *MAX2* gene.

A

F2 Genotyping	
Gene	**P28-A**
AtIPT1	WT
AtIPT3	*atipt3*
AtIPT5	WT
AtIPT7	WT
MAX2	Ht

B

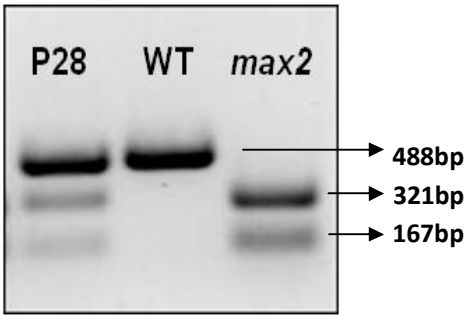

C

Figure – 6.5: Genotype and Phenotype of atipt3-atipt3,MAX2_max2. *(A) Genotypic score based on PCR of AtIPTs and MAX2, (B) The product of MAX2 gene PCR followed by ApoI enzyme digestion, run on 1.5% agarose gel, and (C) Phenotypes of wild-type Col-0 (Left), max2 (Right) and atipt3-atipt3,MAX2_max2 (Middle).*

When *MAX*2 was knocked out, it appeared impossible to find knock out for *AtIPT*3 and vice versa. Therefore, it was decided to select a plant P-29, which was homozygous for wild-type dominant alleles of *AtIPT1*, *ATIPT5* and *AtIPT7* genes, but segregating for both *AtIPT*3 and *MAX*2 genes. Two hundred and forty (240) seeds of plant P-29 were sown to allow accurate scoring of segregation ratios. It was observed that 62 plants showed *max2* phenotypes and 121 exhibited wild-type phenotypes, whereas 57 seeds did not germinate. The expected ratio of 1:3 ($X^2 > X^2_{0.05} = 7.696 > 3.841$; $p < 0.05 = 0.005$) appears to be modified into 1:2 ($X^2 < X^2_{0.05} = 0.025 < 3.841$; $p > 0.05 = 0.875$), which is a ratio known to be associated with (recessive) lethality.

6.3.4 Mapping of Aborted Seeds within Siliques

Genotyping of F3 plants of P-29 identified individuals with heterozygous genotypes for one or other of the two genes, i.e. *AtIPT3_atipt3,max2_max2* and *atipt3_atipt3,MAX2_max2*. The siliques of these plants were dissected to show aborted seeds (Fig. 6.6).

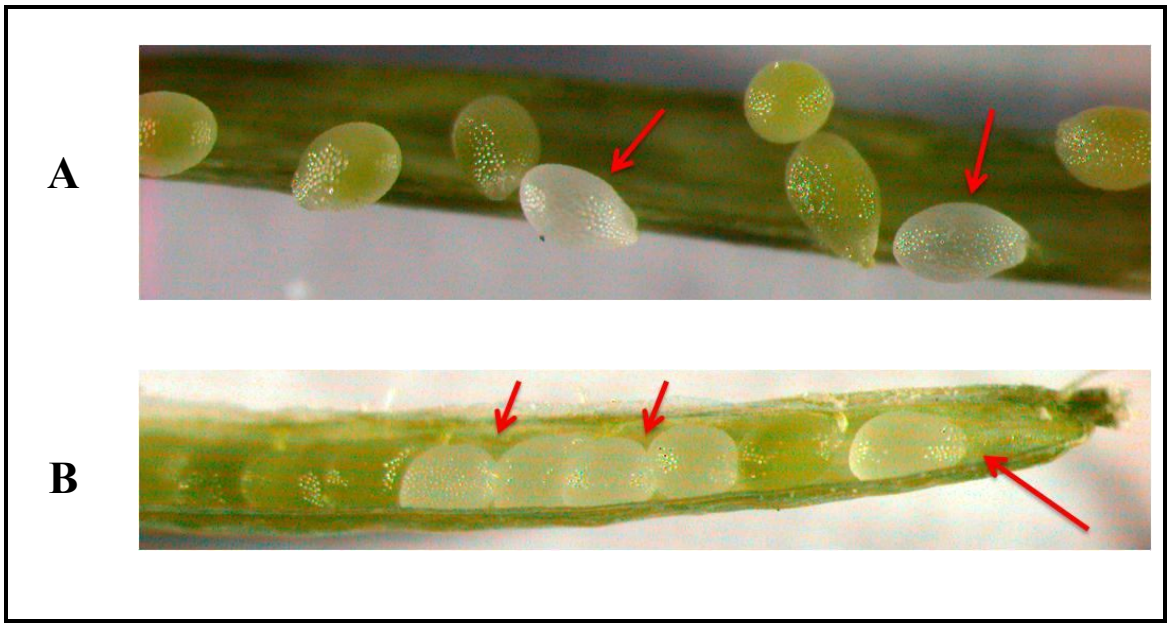

Figure – 6.6: Aborted Seeds in Siliques. *Siligues of AtIPT3_atipt3,max2_max2 (A) and atipt3_atipt3,MAX2_max2 (B), red arrows shows white aborted seeds in the pods of genotypes.*

To find the physical distribution of aborted seeds in heterozygous genotypes of *AtIPT3_atipt3,max2_max2* and *atipt3_atipt3,MAX2_max2,* seed mapping was performed using 20 siliques of each genotype. It was found that approximately 17% of seeds were aborted in siliques of both genotypes and distribution of aborted seeds was non-random (see Fig. 6.7). Approximately 75% and 70% of aborted seeds were located in the top half of the siliques in case of *AtIPT3_atipt3,max2_max2* and *atipt3_atipt3,MAX2_max2,* respectively. This higher abortion percentage in the upper half is significantly different ($p< 0.05 = 0.000$) from random distribution (50%). Abortion percentage in these two genotypes was low and significantly different from 25% of aborted seeds (see Table 6.5).

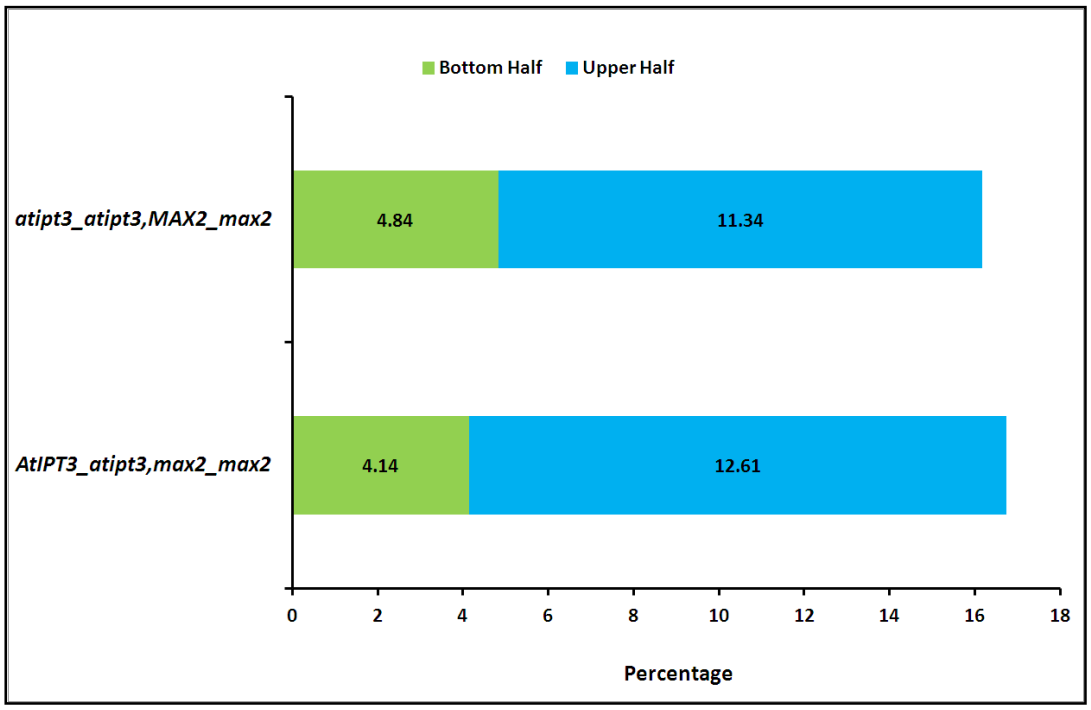

Figure – 6.7: Seed Abortion Percentage in Bottom and Upper Halves of Silique at Mature Embryo Stage. *According to grid mapping method, 20 siliques of two heterozygous individuals AtIPT3_atipt3,max2_max2 and atipt3_atipt3,MAX2_max2, were used to count number of aborted seeds and their positions along the length of the siliques. Most of siliques from both genotypes contained a greater number of aborted seeds in the upper half of the silique.*

Table – 6.5: Segregation Ratios of Aborted Seeds in Siliques at Mature Embryo Stage

Genotypes	Seeds			Goodness of fit to ratio 1:3		
	Total	*Normal*	*Aborted*	*Calculated* X^2	$X^2_{0.05}$	*p value*
AtIPT3_atipt3, max2_max2	967	805	162	> 26.0	3.841	0.000
atipt3_atipt3, MAX2_max2	1032	865	167	> 26.0	3.841	0.000

Significant = $X^2 > X^2_{0.05}$ and $p< 0.05$

6.3.5 Genotyping Score of *AtIPT3* and *MAX2* genes

The F3 Population of P-29 (*ATIPT3_atipt3,MAX2_max2*) was genotyped for *AtIPT3* and *MAX2* to score the segregation ratios of both alleles. The scores are given in Table 6.6 in the form of four different expected genotypes. The recessive *atipt3* allele segregated in a 1:3 ratio ($X^2 < X^2_{0.05} = 0.296 < 3.841$; $p > 0.05 = 0.586$), but segregation of *max2* allele deviated significantly from the expected 1:3 ratio ($X^2 > X^2_{0.05} = 10.667 > 3.841$; $p < 0.05 = 0.001$), instead fitting well with a 1:2 ratio ($X^2 < X^2_{0.05} = 2.250 < 3.841$; $p > 0.05 = 0.133$).

Table – 6.6: Genotype Frequencies from Progeny of a Plant Heterozygous for both *AtIPT3* and *MAX2* genes

Genotype	Score
AtIPT3_MAX2_	26
AtIPT3_max2max2	30
atipt3p3MAX2_	16
atipt3atipt3max2max2	0

6.3.6 Reciprocal crosses between *atipt3* and *max2*

In all the work described above, the mutant allele *max2-1* generated from an ethyl methane sulphonate (EMS) mutagenesis was used as a female parent to cross with *atipt1,3,5,7*. To test for other possible independent mutations in the genetic background, it was decided to use another allele of *max2* to cross with *atipt3*. For this purpose, Salk_092836 (N680512), which was created by T-DNA insertion in the exon of *MAX2*, was selected. The reciprocal crosses were made between *atipt3* and both alleles of *MAX2* (*max2-1* and Salk_092836). From the F2 population of these crosses, the phenotypic data is given in Table 6.3 and 6.4. All crosses exhibited *max2* phenotype in 1:2 ratios rather in 1:3 ratios.

Table – 6.7: Segregation Ratios from F2 Population of Crosses between *atipt3* and *max2*

Cross. No.	Parents		Phenotypes		Goodness of fit to ratios		
	Female	***Male***	***WT***	***max2***	X^2 ***for 1:3***	X^2 ***for 1:2***	$X^2_{0.05}$
1	*atipt3*	*max2-1**	101	65	17.743	2.533	3.841
2	*max2-1**	*atipt3*	78	39	4.333	0.000	3.841
3	*atipt3*	Δ *max2*	113	64	11.753	0.636	3.841
4	Δ *max2*	*atipt3*	120	67	11.695	0.524	3.841

*EMS mutagenic allele of *MAX2,* Δ T-DNA insertion allele of *MAX2*

Significant = $X^2 > X^2_{0.05}$ and $p < 0.05$

6.4 Discussion

Creation of double knockout lines for *ATIPT3* and *MAX2* genes was not successful. This type of interaction between a cytokinin biosynthetic gene and a strigolactone signalling gene was quite unexpected and still unresolved from the results available from the current research. Existence of single knockout mutants for *ATIPT3* and *MAX2* genes suggests that both supplement each other to control some essential role in the reproductive phase of development.

Previously, the lines generated by overexpression of *AtCKX* genes, and by mutations in cytokinin signalling genes *CKI1*, *CRFs* and *AHKs* suggested a wide range of cytokinin functions from gametogenesis to embryogenesis (Werner *et al*., 2003; Pischke *et al*., 2002; Deng *et al*., 2010; Hejatko *et al*., 2003; Rashotte *et al*., 2006; Kinoshita-Tsujimura and Kakimoto, 2011; Cheng *et al*., 2013), as detailed in section 6.1.6. However, no lethal mutant has been reported as a result of strigolactone deficiency. Therefore, a role of strigolactone in reproduction was predicted on the basis of expression patterns found for genes related to strigolactone. Previous reports showed expression of CCD7 and CCD8 in reproductive organs of *Arabidopsis*, Tomato, Maize and Kiwifruit (Booker *et al*., 2004; Mashiguchi *et al*., 2009; Vogel *et al*., 2010; Ledger *et al*., 2010; Guan *et al*., 2012). It is also found that *MAX2* is expressed in flower, siliques and mature seeds (Stirnberg *et al*., 2007; Mashiguchi *et al*., 2009). On the other hand, *AtIPT3* have been shown to be expressed at a very low level in flower and siliques (Takei *et al*., 2004a). However, further investigation is required to explore actual functions of *AtIPT3* and *MAX2* during reproduction as well as how lethality is caused by strigolactone.

It has also been shown that only *AtIPT7* is expressed in pollen tube whereas expression of *AtIPT3* during reproductive phase of development was not observed (Miyawaki *et al*., 2004). On the other hand, *MAX2*is expressed in stamen filament, stigma (Shen *et al*., 2007)and siliques (Stirnberg *et al*., 2007). Localization of MAX2 was found to be in the nucleus, suggesting that MAX2 may function to degrade nuclear protein(s) such as transcriptional regulator(s) (Stirnberg *et al*., 2007). It was also reported that farnesylation (addition of a 15-carbon isoprenoid called a farnesyl group to proteins bearing a CaaX motif: a four-amino acid sequence at the carboxyl terminus of a protein) of AtIPT3 relocated the protein in the nucleus/cytoplasm, whereas the nonfarnesylated AtIPT3 protein was localized in the plastids. It can be predicted that both proteins together may be involved in controlling cell cycle during reproductive development, as cytokinin is already known to be involved in cell cycle progression (Riou-Khamlichi *et al*., 1999).

If there is an interaction between cytokinin and strigolactone, then *atipt3* KO should not be isolated in *max4* background. One possible explanation is that *max4-1* is not a true null allele, as discussed in chapter 4 (4.4.4). More profound branching phenotype of *max4-5* than that of *max4-1* (Bennett *et al*., 2006) has been observed, suggesting that *max4-1* mutant retains some catalytic activity. Indeed, Kohlen *et al*. (2011) detected production of some orobanchol in

max4-1, indicating that either *max4-1* is leaky or another strigolactone biosynthetic pathway is present, apart from the reported MAX pathway.

Existence of single knockout mutants for *ATIPT3* and *MAX2* genes suggests that both genes control same essential role in reproductive phase of development. Numbers of aborted seeds in heterozygous genotypes are significantly greater in upper halves of siliques. It was suggested by seed mapping in siliques that the significantly biased distribution of aborted seeds towards stigma in upper halves of siliques is a consequence of defective male gametophyte. In addition, abortion percentage in this case is expected to be lower than 25%, because wild-type pollen tubes can compete with mutant pollen tubes to fertilize ovules in the ovary (Meinke, 1982). Indeed, it was found that abortion percentage in *AtIPT3_atipt3,max2_max2* and *atipt3_atipt3,MAX2_max2* is about 17%, significantly different from 25%. The consequence may be due to low transmission of mutant alleles. It reveals that interaction between *AtIPT3* and *MAX2* genes causes lethality in male gametophyte. Segregation of *atipt3* allele is found to be normal (1:3) but that of *max2-1* allele is a 1:2 ratio. Phenotyping data of *AtIPT3_atipt3,MAX2_max2* using two different *max2* alleles, *max2-1* allele and T-DNA insertion allele confirmed previous finding that *max2* allele segregates in 1:2 ratio. All findings suggest that there is segregation distortion from Mendelian ratios and both *AtIPT3* and *MAX2* might be interacting during development and germination of pollens.

The reciprocal crosses of *AtIPT3_atipt3,max2_max2*, *atipt3_atipt3,MAX2_max2*and *ATIPT3_atipt3,MAX2_max2* with the wild-type as well as detailed examination of male and female organs and gametophytes in these genotypes is required to give insight into the interaction of cytokinin and strigolactone in controlling aspects of the reproductive phase of development in *Arabidopsis*.

6.5 Conclusions

1- Double mutation in *AtIPT3* and *MAX2* is lethal.

2- Lethality may be caused by defects in male gametophyte.

Chapter 7

General Discussion

Shoot branching, a key determinant of plant architecture, plays a pivotal role in the development of aboveground plant form and structure (Evers *et al*., 2011). Therefore it is considered a major plant character to improve crop yield (see section 1.1). Shoot branching is partly controlled by three plant hormones; auxin, cytokinin (CK) and strigolactone (SL). Auxin and strigolactone are known as repressors of shoot branching. On the other hand, cytokinin is the only candidate to promote branching; hence it is antagonistic in function to auxin and strigolactone (Ongaro and Leyser, 2008). Previous reports (Beveridge *et al*., 1997b; Morris *et al*., 2001; Foo *et al*. 2007) have shown low levels of cytokinin in xylem sap of strigolactone deficient mutants, which are known as *max* mutants in *Arabidopsis thaliana* (Thale cress) and *rms* mutants in *Pisum sativum* (Pea).

The research presented in this thesis was designed to explore possible mechanisms behind low xylem-cytokinin levels in *max* mutants, which represents an interaction between cytokinin and strigolactone. The first step in synthesis of iP-type and tZ-type cytokinins is catalyzed by isopentenyltransferases (IPTs) (Fig. 1.2) which are encoded by nine *IPT* genes in *Arabidopsis* (Kakimoto, 2001; Takei *et al*., 2001a). Study of spatial expression of *AtIPT* genes suggests that cytokinin synthesis is restricted to specific tissues and organs in shoot and roots (Miyawaki *et al*., 2004; Takei *et al*., 2004a). CKs synthesized in shoot are transported to roots through phloem where both phloem-derived and root-derived iP-type CKs are converted by CYP735As (Takei *et al*., 2004b) to tZ-type CKs, which are then transported to the shoot through xylem (Fig. 1.3).Therefore, it is hypothesized that strigolactone may modulate xylem-CKs by regulating CK biosynthetic genes (*AtIPTs*) in root and shoot. This hypothesis was tested by creating *atipt* mutants in wild-type and *max* backgrounds. These mutants in both backgrounds were characterized by phenotypic studies and cytokinin quantification. Regulation of *AtIPT* genes by strigolactone was studied by generating *AtIPT::GUS* lines in *max* background. The next section of this chapter presents discussion of main results on which basis final conclusion is given and future work is proposed.

7.1 Screening for *atipt* mutants in wild-type and *max* backgrounds

Completion of *Arabidopsis* genome sequencing has made it possible to analyze gene function by reverse genetics approach, which is commonly in use for isolation of insertion mutant alleles in the gene of interest. Contrary to forward genetics, reverse genetics starts with the gene sequence rather than the gene function in the form of a phenotype, which often cannot be identified in case of redundancy. In the reverse genetics approach, mutagenesis is based on the insertion of foreign DNA into the gene of interest, using either transposable elements or T-DNA. The foreign DNA alters the expression of the gene into which it is inserted, as well as it acts as a marker for identification of mutation. Hence, a researcher simply identifies an insertion line and subsequently analyzes the line for effects of the disrupted gene (Krysan *et al*., 1999). Multiple members of a gene family can be knocked out by crossing single insertion lines. In this way, a triple *atipt3,5,7* and a quadruple *atip1,3,5,7* mutant were created to investigate the role of these four genes, which are expressed in the vegetative phase of *Arabidopsis* (Miyawaki *et al*., 2004; Takei *et al*., 2004a). Both mutants exhibited severely reduced growth with short and thin aerial parts, but the phenotype of *atip1,3,5,7*tended to be more severe (Figure 3.9 and 3.11; Miyawaki *et al*., 2006). However, it indicates that the levels of *AtIPT1* do not play a great role in plant growth. It has already been reported that *AtIPT1* is the least expressed of these four genes (Takei *et al*., 2004a; Genevestigator database, Figure 3.1 & 3.2). Therefore, it was decided to generate *atipt* mutant combinations, considering *AtIPT1* to have a minor role. Hence the role of individual genes was studied by double mutants like *atipt5,7*, *atipt3,7* and *atipt3,5* and triple *atipt3,5,7*. These mutants were generated in wild-type and *max* backgrounds by crossing a quadruple mutant *atip1,3,5,7* with *max2* and *max4*. From F2 populations of these crosses, all required mutant combinations were successfully screened except *atipt3,5,max2, atipt3,7,max2* and *atipt3,5,7,max2*, because it was found impossible to knockout *AtIPT3* and *MAX2* genes together. Double knockouts cannot be found as a result of linked genes located on the same chromosome. However, these genes are not linked, being located on different chromosomes and hence are expected to be assorted independently. Instead, double homozygote was found to be lethal, which may be an effect of *atipt3* and *max2* alleles or due to loss of an essential function during reproduction (see next section 7.3).

7.2 Double mutation of *AtIPT3* and *MAX2* is lethal

Isolation of the double mutant *atipt3,max2* proved impossible, as combined mutations in *AtIPT3* and *MAX2* was lethal and seeds of *atipt3,max2* were aborted. The interaction between *AtIPT3* and *MAX2* was previously unknown and unexpected. Survival of both single mutant *atipt3* and *max2* indicates that both proteins are involved in controlling the same essential function in reproduction. If any interaction between cytokinin and strigolactone exists, it would also be impossible to knock out *ATIPT3* in *max4/ccd8* background, but that cross was successful. There are two possibilities that either *max4-1* is not a true null allele or alternate biosynthetic pathway is involved in production of strigolactone. Relevant to first point, some strigolactone (orobanchol) has been reported in *max4-1* (Kohlen *et al*., 2011). This is

consistent with more profound branching phenotype of *max4-5* as compared with *max4-1* (Bennett *et al*., 2006).

Previously gametophytic and embryo lethal mutants have been correlated with the deficiency of cytokinin (Werner *et al*., 2003; Pischke *et al*., 2002; Deng *et al*., 2010; Hejatko *et al*., 2003; Rashotte *et al*., 2006; Kinoshita-Tsujimura and Kakimoto, 2011; Cheng *et al*., 2013), but not with lack of strigolactone. However, a role for strigolactone is predicted in reproduction based on gene expression data. Expression of AtCCD7 (*Arabidopsis*), SlCCD7 (Tomato), ZmCCD8 (Maize), AcCCD7 and AcCCD8 (Kiwifruit) have been reported in reproductive organs (Booker *et al*., 2004; Mashiguchi *et al*., 2009; Vogel *et al*., 2010; Ledger *et al*., 2010; Guan *et al*., 2012). Very low levels of transcripts of *AtIPT3* have been found in flower and siliques (Takei *et al*., 2004b). On the other hand, *MAX2* expression is found in flower, siliques and mature seeds (Stirnberg *et al*., 2007; Mashiguchi *et al*., 2009). However, actual functions of *AtIPT3* and *MAX2* in reproduction are unclear. Reduced flower and seed number has been reported in *L. japonicas* due to CCD7 silencing (Liu *et al*., 2013) and also in CCD8-silenced tomato (Kohlen *et al*., 2012).

Abortion percentage in siliques of *AtIPT3_atipt3,max2_max2* and *atipt3_atipt3,MAX2_max2* was about 17% (significantly different from 25%). It indicates that transmission of mutant alleles is reduced. Seed mapping of heterozygous genotypes reveals that numbers of aborted seeds are significantly higher in the upper half of siliques (towards stigma). According to Meinke (1982), such distribution of aborted seeds suggests lethality due to defects in male gametophyte. In this case, the abortion percentage is expected to be lower than 25%, as wild-type pollen tubes out-compete mutant pollen tubes to fertilize ovules. In *Arabidopsis*, only *AtIPT7* is expressed in pollen tube (Miyawaki *et al*., 2004). Therefore, *AtIPT3* gene function in male gametophyte was unforeseen. On the other hand, *MAX2::GUS* expression appeared to be in stamen (Shen *et al*., 2007; Stirnberg *et al*., 2007) and MAX2 protein is localized in nucleus, suggesting that MAX2 functions in regulation of transcription. It was also shown that farnesylated AtIPT3 protein was translocated to nucleus/cytoplasm. Therefore, it can be predicted that both proteins may interact to control cell cycle during reproductive phase. Cytokinin is well known to be involved in cell cycle progression (Riou-Khamlichi *et al*., 1999).

Genotyping of double heterozygous *AtIPT3_atipt3,MAX2_max2* shows that segregation of *atipt3* allele is normal in 1:3 ratio but *max2* allele is segregating in 1:2 ratio. It indicates that transmission frequency of *max2* through male gametophyte is higher than *atipt3*. Phenotyping of *AtIPT3_atipt3,MAX2_max2* demonstrates that both alleles, EMS mutagenic *max2-1* allele and T-DNA insertion allele, are present in 1:2 ratio. All findings suggest that the segregation ratio is distorted from Mendelian ratio and both *AtIPT3* and *MAX2* interact during pollen development and germination. Further experiments are required to explore how both genes interact to control essential functions during reproduction.

7.3 Deficiency of cytokinin has depletion effect on shoot branching of *max4* mutant

SL-deficient mutant *max4* and SL-insensitive mutant *max2* are readily distinguishable with their profoundly increased branching as compared with wild-type. Double *atipt* mutants *atipt5,7, atipt3,5* and *atipt3,7,* exhibit normal wild-type branching patterns and levels, confirming already reported wild-type phenotypes of these mutants (Miyawaki *et al*., 2006). But increased branching due to *max4* mutation is suppressed by approximately 50% in *atipt3,5*and *atipt3,7* backgrounds and by about 80% in *atipt3,5,7* background. This significant reduction is correlated with decreased cytokinin synthesis. The presence of *AtIPT5* and *AtIPT7*genes in *max4* background could not rescue the deficiency in branching resulting from the absence of *AtIPT3* expression, as *AtIPT3* alone was enough for the maintenance of *max2* and *max4* like branching phenotypes in case of *atipt5,7,max2* and *atipt5,7,max4,* respectively. Therefore, it is suggested that bushy phenotype of *max* mutants is dependent on CK supply and *ATIPT3* gene is mainly responsible for CK production. It is also validated by complete growth recovery of *atipt3,5,6,7* mutant in which *AtIPT3p::AtIPT3-GFP* was incorporated (Miyawaki*et al.,* 2006).

In the case of *atipt3,5,7,max4,* stem height was highly reduced and axillary branch growth was very suppressed as compared with *max4*. Therefore, it suggests that CK is involved in releasing axillary buds from dormancy to promote branching as well as in the subsequent branch growth and development, as increased CK levels in activated buds have been reported (Turnbull *et al*., 1997 and Emery *et al*., 1998). The arrest of axillary bud outgrowth is attributed to reduction in the rates of cell division and cytokinin was discovered as a promoter of cell division (Miller *et al*., 1955). At completion of each cycle of cell division, newly formed cells either enter a new cell cycle or remain quiescent at G1 phase (Anderson *et al*., 2001). Therefore, vegetative bud dormancy is initiated prior to S-phase of cell cycle. For example, the growth of dormant potato tuber meristems is blocked in G1 phase (Campbell *et al*., 1996). The cell cycles in proliferating and dormant axillary buds of pea were characterized by mRNA levels of cell-cycle-related genes e.g. cyclins (cell cycle regulators). Transcripts of these genes were markedly low in quiescent axillary buds, whereas expression was greatly enhanced in axillary buds after decapitation (Devitt and Stafstorm, 1995; Shimizu and Mori, 1998). Length of the G1 phase of cell cycle is modulated by D-type cyclins, which are often described as rate limiting to cell division in plants (Dewitte *et al*., 2007). Transcription of D-type cyclin *CycD3* has been shown to be upregulated with a high level of cytokinin in *Arabidopsis* (Riou-Khamlichi *et al*., 1999). Therefore, cytokinin is required for both events release of axillary bud inhibition and promotion of bud outgrowth.

7.4 *AtIPT5::GUS* is expressed in meristematic region of shoot

In this work, *AtIPT5::GUS* expression was detected in the meristematic region of shoots. This expression site of *AtIPT5::GUS* was not previously reported, had been shown in root caps, lateral root primordia, stem of lateral buds, base of young inflorescence and fruit abscission

zone. In fact, no expression of any *AtIPT* gene was noted in the meristematic region (Miyawaki *et al*., 2004), an unexpected finding because it has been suggested that cytokinin is synthesized in shoot meristems (Letham, 1994). It has also been shown that cytokinin is involved greatly in growth and development of shoot meristem (Werner *et al*., 2003).

SHOOTMERISTEMLESS (STM) gene encodes a protein that belongs to a class of Knotted1-like homeobox (KNOX) proteins, which are transcription factors required for meristem maintenance and precise patterning of organ initiation. The KNOX genes have been reported to be expressed exclusively in the meristem (Long *et al*., 1996; Hake *et al*., 2004). It has been shown that the division and maintenance of undifferentiated stem cells in the shoot meristem is a consequence of increased cytokinin activity in the central regions of meristem (Veit, 2009), where KNOX proteins are responsible for activating CK biosynthetic genes and CK response genes. The significant increase in transcript levels of *AtIPT5, AtIPT7* and *ARR5* was found in response to induction of STM activity (Jasinski *et al*., 2005). The function of shoot meristem is correlated with cell division, which is promoted by CK (as discussed in previous section). Miller and Skoog (1957) reported that new shoot meristems in culture are stimulated by cytokinins. In support of cytokinin function in meristem initiation, the activity of *pAtIPT5::GUS* has been found to be restricted to pro-meristem regions in an induced callus (Cheng *et al*., 2012). Taken together, all data are consistent with the finding that *AtIPT5::GUS* expression is localized to the meristematic region of shoot.

7.5 Lack of strigolactone synthesis and perception results in upregulation of *AtIPT3* and downregulation of *AtIPT5*

Mutation in either *MAX2* or *MAX4* resulted in upregulation of *AtIPT3::GUS* expression in the phloem throughout root and shoot. Consistent with this, Dun and co-workers (2012) recently reported that *rms4* and *rms5* showed significant increase in transcript levels of *PsIPT1* in stem segments of pea. Contrary to upregulated *AtIPT3::GUS* expression, root and shoot of *max2* and *max4* mutants exhibited downregulation of *AtIPT5::GUS*, which may be regulated directly by strigolactone. Alternatively, high cytokinin levels as a consequence of upregulated *AtIPT3*may negatively regulate *AtIPT5*. Following application of GR24 (synthetic SL analogue), expression of both *AtIPT3::GUS* and *AtIPT5::GUS* are restored but in *max4* only. MAX2 is known to be involved in perception of strigolactone, therefore, expression patterns of *AtIPT5::GUS* and *AtIPT3::GUS* in *max2* are not altered after addition of GR24. It suggests that regulation of *AtIPT3* and *AtIPT5*by strigolactone is strictly MAX2-dependent.

Auxin-mediated regulation of *AtIPT5::GUS* and *AtIPT3::GUS* is found in a MAX2-dependent manner similar to the strigolactone responses, except for upregulation of *AtIPT5::GUS* expression in roots of wild-type, *max2* and *max4* following NAA treatment. This indicates MAX2-independent regulation of *AtIPT5*. Previously, *AtIPT5* has been reported to be upregulated by auxin in wild-type roots of *Arabidopsis* (Miyawaki *et al*., 2004). MAX2-dependent regulation of *AtIPT5::GUS* in shoot and *AtIPT3::GUS* in root and shoot is

consistent with the previous findings that strigolactone acts downstream of auxin, suggesting strigolactone as a second messenger for auxin action (Brewer *et al.*, 2009).

Expression of *AtIPT5::GUS* and *AtIPT3::GUS* is restored in *max4* only after application of NAA, which is somewhat surprising. It indicates that either *max4-1* is leaky (discussed in section 7.2) or an alternative SL biosynthetic pathway is present, as *MAX2* over-expression in SL biosynthetic mutants *max1, max3* and *max4* can partially inhibit their increased branching phenotypes (Stirnberg *et al.*, 2007). It is reported that auxin upregulates *MAX4* resulting in increased SL production (Hayward *et al.*, 2009). Therefore, some catalytic activity (deduced from limited orobanchol production) of *max4-1* may be increased due to induced expression of the mutant *MAX4-1* gene by auxin. If *max4-1* retains some catalytic activity or if there is an alternate SL biosynthetic pathway, it could show some expression of *AtIPT5::GUS* and *ATIPT3::GUS* in *max4* under control conditions. But the actual expression patterns of *AtIPT5::GUS* and *ATIPT3::GUS* are found to be same in both *max2* and *max4* backgrounds. Figure 7.1 demonstrates different mechanisms of *AtIPTs* regulation by Auxin.

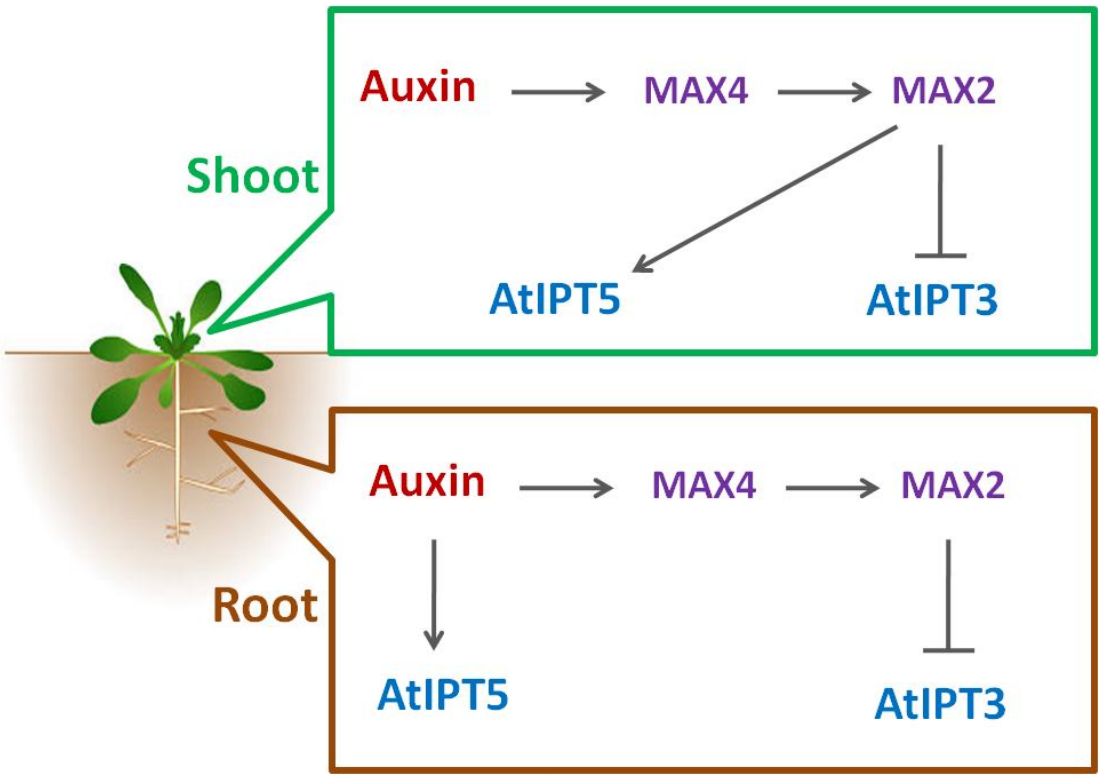

Figure - 7.1: Auxin-mediated Regulation of AtIPTs. *Based on AtIPT::GUS results, it is shown that auxin regulates AtIPT3 and AtIPT5 in shoot in a MAX2-dependent manner but in roots auxin mediates MAX2-dependent regulation of AtIPT3 and SL-independent regulation of AtIPT5.*

7.6 *AtIPT3* is a key gene for biosynthesis of iP-type CKs

From discussion in Chapter 5, it was found that *AtIPT3*, which is involved in the primary step of CK production, is a main gene for synthesis of iP-type CKs. Shoot and root of both *atipt3,5* and *atipt3,7* show significant reductions in levels of iP-type CKs, which were more extremely reduced in root and shoot of triple mutant *atipt3,5,7*. Similar findings were previously reported by quantification of iP-type CK levels in the seedlings of these double and triple mutants, whereas among single mutants, only *atipt3* has reduced levels of iP-type CKs (Miyawaki *et al*., 2006). Therefore, *AtIPT3* appears to be predominantly responsible for the production of iP-type CKs. Likewise, normal wild-type type levels of iP-type CKs are observed in the shoot of *atipt5,7* but levels are significantly reduced in the roots of *atipt5,7*. This finding is parallel to the reported expression patterns of *AtIPT5* and *AtIPT7*. It has been shown by real-time PCR that *AtIPT5* and *AtIPT7* are significantly expressed in roots but at a very low level in shoots. The highest expression levels of *AtIPT3* are found at the mature rosette developmental stage (Takei *et al*., 2004a) and this is also confirmed by Genevestigator database. Therefore, *AtIPT3* is a main gene for synthesis of iP-type CKs in shoot but acts with *AtIPT5* and *AtIPT7* in roots.

The profiles of iP-type CKs in shoot and roots of wild-type, *atipt5,7*, *atipt3,5*, *atipt3,7* and *atipt3,5,7* are not changed in presence of *max* mutations. From Chapter 4 (see also section 7.4), it is evident that *max2* and *max4* mutations cause upregulation of *AtIPT3* and downregulation of *AtIPT5* in wild-type background. On this basis, levels of iP-type CKs in *atipt5,7,max2* and *atipt5,7,max4* are expected to be increased (due to presence of upregulated *AtIPT3*) and those in *atipt3,7,max4* are predicted to be decreased (due to presence of downregulated *AtIPT5*). As*AtIPT3* is expressed in phloem (Miyawaki *et al*., 2004),there is a possibility that increased levels of iP-type CKs in *atipt5,7,max2* and *atipt5,7,max4* are not detected in shoot tissues as they may be transported to roots via phloem sap. Cytokinin measurement from phloem sap of *atipt5,7,max2* and *atipt5,7,max4* can potentially clarify this notion. However, compared with *atipt3,7*, levels of iP-type CKs are not reduced in *atipt3,7,max4,* even though *AtIPT5* is predicted to be downregulated in *max4*. This is somewhat unexpected and not in line with the finding from *AtIPT5::GUS* results. Currently, it is not known whether transcript levels of *AtIPT5* may change in wild-type and *max* mutants due to disruption of other *AtIPTs*, especially *AtIPT3*.

7.7 Synthesis of tZ-type CKs is iPRP-independent in shoot and iPRP-dependent in root

It has been reported that tZ-type CKs are synthesized in a two-step pathway dependent on iPRP, which is the first metabolite produced through the adenine-derived pathway, in which this initial step is catalyzed by IPT enzymes (Kakimoto, 2001; Takei *et al.*, 2001a). The second step involves hydroxylation of iPRP into tZRP by cytochrome P450 enzymes (CYP735A1 and CYP735A2). Both *CYP735As* are found to be expressed predominantly in roots (Real-time based quantification of transcript levels). Therefore, it indicates that tZ-type

CKs are mainly synthesized in roots (Takei *et al*., 2004c). It has also been shown that tZRP is directly produced by the activity of IPT enzymes in *Agrobacterium* and *Arabidopsis* (Åstot *et al*., 2000), suggesting iPRP-independent synthesis of tZ-type CKs.

The presence of an iPRP-independent pathway is also supported by quantification of tZ-type CKs presented in Chapter 5, from which it has been found that shoots of double mutants *atipt5,7, atipt3,5* and *atipt3,7* show no difference from wild-type in levels of tZ-type CKs. As the decreased supply of iPRP does not reduce the wild-type levels of tZRP in case of *atipt3,5* and *atipt3,7,* there is either iPRP-independent synthesis of tZRP involved or rapid conversion of iPRP into tZRP by CYP735As. *CYP725A1* has been found to be expressed only at a very low level in the rosette leaves (Takei *et al*., 2004b), pointing to the existence of an iPRP-independent pathway for the synthesis of tZ-type CKs in shoot. It is also possible that both pathways (iPRP-independent and iPRP-dependent) work side by side. Another possibility is that tZ-type CKs found in shoot are translocated from root in xylem stream but the detected CKs in xylem sap do not include tZRP (Beveridge *et al*., 1997b; Foo *et al*., 2007), which may be found in shoot due to conversion from tZR and/or tZ transported to the shoot through xylem sap. Shoots of triple mutant *atipt3,5,7*have extremely reduced levels of tZ-type CKs, indicating that either *AtIPT1* is not involved in direct synthesis of tZRP or that the extremely low levels of *AtIPT1* are not enough for iPRP-independent synthesis of tZRP. Roots of *atipt5,7, atipt3,5,atipt3,7* and *atipt3,5,7* have been found to have reduced levels of tZ-type CKs, suggesting dominance of the iPRP-dependent pathway in roots, consistent with the low levels of iPRP also shown in the roots of these mutants.

Levels of tZ-type CKs in shoots of *max4, atipt3,5,max4* and *atipt3,7,max4* are not significantly changed from those in wild-type and *atipt3,5* and *atipt3,7*. This again suggests synthesis of tZ-type CKs through iPRP-independent pathway in shoot (Astot *et al*., 2000). Double mutants *atipt3,5* and *atipt3,7* in wild-type and *max* backgrounds have low CK levels in xylem sap. On this basis, unchanged tZ-type CKs in shoots of *atipt3,5,max4* and *atipt3,7,max4* from *atipt3,5* and *atipt3,7* and *max4*is more likely to be due to direct synthesis tZ-type CKs rather than contribution of xylem derived CKs(as discussed already in case of *atipt3,5* and *atipt3,7*). Overall, therefore, the pattern of tZ-type CKs in shoots and roots of double and triple *atipt* mutants in *max* backgrounds is similar to those in WT background.

7.8 Biosynthesis of cZ-type CKs occurs through alternate pathway independent of adenine-derived pathway

Synthesis of cZ-type CKs has been found to take place through breakdown of prenylated tRNA containing *cis*-hydroxyl group attached to it (Vreman *et al*., 1978). Prenylation of tRNA is catalyzed by two tRNA-IPT enzymes (AtIPT2 and AtIPT9) in *Arabidopsis* (Kakimoto, 2001; Takei *et al*., 2001a; Golovko *et al*., 2002). Both single mutants *atipt2* and *atipt9* showed decreased levels of cZ-type CKs, which were undetectable in double mutant *atipt2,9*. This finding suggests synthesis of cZ-type CKs from modified tRNAs through an independent pathway. Measurement of cZ-type CKs in shoot and root tissues as well as in

phloem and xylem saps shows changes in levels neither among *max* genotypes nor among double and triple *atipt* mutants in wild-type and *max* backgrounds. As *AtIPT2* and *AtIPT9* genes are not disrupted in these mutants, therefore, cZ-type CKs are normally synthesized independently via the alternate pathway.

7.9 Shoot-derived iPRP is not hydroxylated in roots

It has been reported that hydroxylation activity of CYP735As is restricted to root zone, as genes encoding these enzymes are highly and predominantly expressed in roots. These enzymes utilize iPRP only (not iPR and iP) as a substrate to convert it into tZRP (Takei *et al*., 2004b). Phloem sap of wild-type plants was found to have very low levels of iPRP as compared to iPR levels, indicating that the pool of iPRP to be converted into tZRP may be synthesized locally in the root by the activity of *AtIPT5* and *AtIPT7*. Reciprocal grafting of *atipt1,3,5,7* with wild-type corroborated this hypothesis. Both iP-type and tZ-type CKs are extremely decreased in *atipt1,3,5,7* as compared with wild-type plant. Mutant rootstocks grafted with wild-type scions showed normal wild-type levels of iP-type whereas same grafts partially recovered tZ-type CKs in the mutant rootstocks (Matsumoto-Kitano *et al*., 2008). Levels of iPRP in phloem sap of *atipt5,7* are slightly increased, but apparently did not contribute greatly to the pool of iPRP in roots of *atipt5,7*, which has decreased iPRP levels compared with wild-type roots (discussed in section 7.6). Therefore, reduced iPRP may have resulted in reduced synthesis of tZ-type cytokinins in *atipt5,7* roots leading to reduced xylem CKs. This finding supports the idea that tZ-type cytokinins in roots depend on local synthesis of iPRP rather than shoot-derived iPRP translocated through phloem (Figure 7.2).

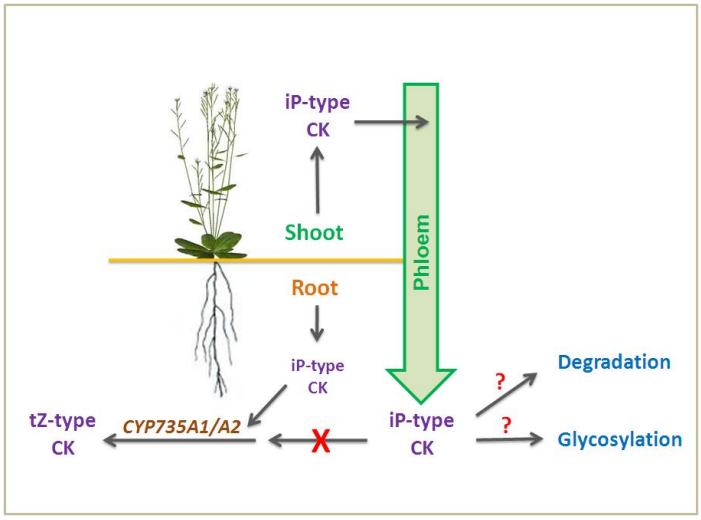

Figure – 7.2: A Scheme representing Non-Hydroxylation of Shoot-derived CKs in Roots: *The iP-type CKs synthesized in shoot are translocated to roots where those CKs are not converted into tZ-type CKs (shown with red cross symbol), rather those might be involved in other CK metabolisms like degradation or glycosylation that is not yet confirmed (shown with red question marks). The hydroxylation enzymes CYP735A1/A2 utilize the locally synthesized iP-type CKs in the roots.*

7.10 iPRP is a feedback signal to limit transport of tZ-type CKs in xylem

Quantification of CKs in phloem and xylem saps of *max* mutants reveals that these mutants have increased iP-type cytokinins in phloem sap but decreased tZ-type CKs in xylem sap. Foo *et al*. (2007) has already reported highly reduced xylem CKs in *max* and *rms* mutants. The profiles of CK compounds in phloem sap, root tissues and xylem sap of *ipt5,7* mutants in *max* and wild-type backgrounds provide a plausible explanation for low xylem CKs in *max* mutants. Levels of iPRP are increased in phloem sap of *atipt5,7,max2* and *atipt5,7,max2* as compared with iPRP levels of wild-type and *atipt5,7*. This elevation in iPRP levels may be due to upregulation of *AtIPT3* gene in phloem of *max2* and *max4* (discussed in section 7.5). In agreement with this, increased transcript levels of *PsIPT1* have been found in *rms* mutants (Dun *et al*., 2012). However, increased iPRP levels in phloem saps of *atipt5,7,max2* and *atipt5,7,max4* does not provide for synthesis of tZ-type CKs in roots of *atipt5,7,max2* and *atipt5,7,max4*(discussed in section 7.7). Although *max* genotypes have significantly higher levels of iPRP phloem sap than wild-type, levels of tZ-type CKs in roots of *max* genotypes are equal to wild-type. Roots of *atipt5,7,max2* and *atipt5,7,max4* show significant reduction in levels of tZ-type CKs. Therefore, it implies that CYP735As may not utilize phloem-derived iPRP for synthesis of tZ-type CKs in roots (discussed in section 7.9). In contrast to higher phloem iPRP levels, xylem CKs are decreased in *atipt5,7,max2* and *atipt,5,7,max4* as compared with wild-type and *atipt5,7*. All findings lead to the proposal that that phloem-derived iPRP might be used as a feedback signal to limit xylem transport of CKs from root to shoot. Indeed a feedback signal has been reported from grafting experiments using *rms4* and wild-type plants where the signal that prevents transport of CKs in xylem comes from shoot (Beveridge *et al*., 1997a).

If iPRP transported to roots through phloem is not utilized by CYP735As to be converted into tZRP, where does this iPRP go in roots? There are two possibilities of CK metabolism to maintain CK levels either by glycosylation or by degradation. For glycosylation, activity of LOG enzymes in roots is first required to convert iPRP into iP, which then glycosylated as iP9G. Degradation in roots is more likely, as AtCKX1 has been reported to prefer CK-nucleotides (iPRP and tZRP) and iP9G as a substrate (Kowalska *et al*., 2010) and *AtCKX1::GUS* expression was found to be localized in pericycle (pericycle is adjacent to phloem)around the junction of growing lateral root with primary root. Therefore, it is predicted that high levels of iPRP in phloem may be degraded in the pericycle by AtCKX1 enzyme activity. However, it is still not clear how xylem transport is blocked to stop transport of tZ-type CKs.

7.11 Schematic illustration to explain translocation of xylem cytokinins

A schematic model is developed from the results of this thesis to explain regulation of xylem CKs in *max* mutants. Fig. 7.3 represents that both *max2* and *max4* mutations result in upregulation of *AtIPT3* gene in the phloem of mutants. As a consequence, the production of iPRP is increased in phloem sap transported to the mutant roots where iPRP may function as a feedback signal to control translocation of cytokinins via xylem.

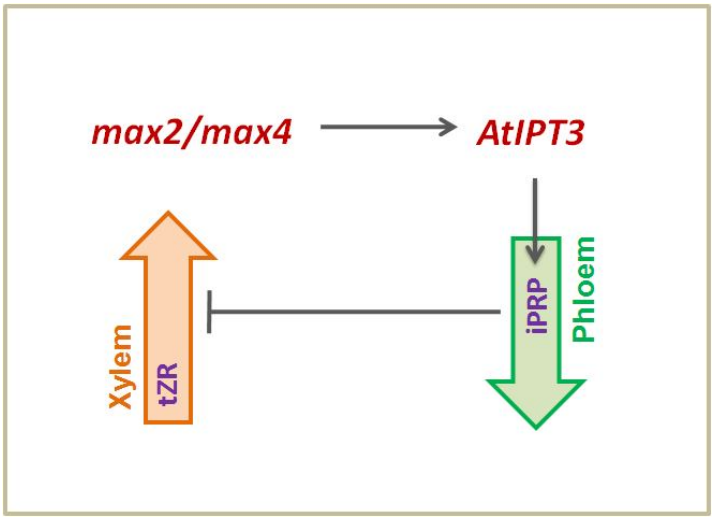

Figure – 7.3: Regulation of Cytokinin Transport by Strigolactone: *AtIPT3 is upregulated in max2 and max4. This results in increased production of iPRP that is transported to mutant roots to inhibit transport of xylem CKs. Therefore, iPRP is suggested as a feedback signal.*

7.12 Conclusions

It can be concluded from the current study that *AtIPTs* are regulated by strigolactone and play an important role in branching phenotype of *max* mutants. Mutation in *AtIPT3* gene causes reduction in branching of *max4*. Therefore, the bushy phenotype of *max* mutants is partly dependent on CK supply in shoot. Both positive and negative MAX2-dependent regulatory components are present because strigolactone downregulates *AtIPT3* and upregulates *AtIPT5*. Two *max* mutants, *max2* and *max4,* exhibited upregulation of *AtIPT3*in the phloem of mutants, which correlates with increased iPRP levels in the phloem sap. Translocation of these high levels of iPRP do not contribute to increase synthesis of tZ-type CKs in roots and their subsequent xylem transport in *max2* and *max4* mutants. Therefore, iPRP may serve as a feedback signal to regulate xylem transport of tZ-type CKs in *max* mutants.

7.13 Future Work

Based on the findings presented in this thesis, future work is proposed as follows:

1- Lethality due to double mutation in AtIPT3 and MAX2 genes can be investigated by crossing of heterozygous genotypes (*AtIPT3_atipt3,max2_max2; atipt3_atipt3, MAX2_max2* and *AtIPT3_atipt3,MAX2_max2*) with wild-type and crossing of other alleles such as *max4-5*, *max3-1* and *d27* with *atipt3,* by examination of stamen, ovary, pollens and ovules in heterozygous genotypes, by in *vitro* and in *vivo* tests of pollen tube germination from pollens of heterozygous genotypes, by analyzing expression of *AtIPT3* and *MAX2* in flowers of *ATIPT3::GUS,max2 and MAX2::GUS,atipt3* and by examination of aborted seeds of heterozygous genotypes to find any defects in developing embryos

2- Effect of strigolactone on root branching can be studied by characterization of *atipt* mutants in wild type and *max* backgrounds with measurement of primary root length and lateral root number.

3- Exact localization of *AtIPT5::GUS* expression in shoot can be determined by sectioning of meristematic region and leaf petioles. Morphology of shoot meristem in wild-type *max2* and *max4* can be explored by measuring size and height of meristem and counting cell numbers in meristem.

4- Strigolactone-mediated regulation of *AtIPT3* and *AtIPT5* can be confirmed by quantification of transcript levels of these genes in *max2* and *max4*.

5- Transcript levels of *AtIPT* genes in double *atipt* mutants in wild-type and *max* backgrounds can be quantified, especially to study possible feedback effects on regulation of expression of *AtIPTs* when other *AtIPT* genes are disrupted.

6- iPRP-independent synthesis of tZ-type CKs in shoot can be investigated by quantifying CK levels in shoot after application of inhibitors of CYP735As and by knocking out *CYP735As* from *atipt* mutants in wild-type and *max* backgrounds.

7- Radiolabelled iPRP can be applied to shoot to confirm the finding that shoot-derived iPRP is not converted into tZRP in roots.

8- CK metabolism can be studied by quantifying expression of LOG and CKX genes in roots, by measuring glycosides and by assaying for CKX activity in roots.

REFERENCES

Aguilar-Martínez, J.A., Poza-Carrión, C. and Cubas, P. 2007.*Arabidopsis BRANCHED1* acts as an integrator of branching signals within axillary buds. Plant Cell.19(2): 458-472.

Akiyama, K., Matsuzaki, K. and Hayashi, H. 2005. Plant sesquiterpenes induce hyphal branching in arbuscular mycorrhizal fungi. Nature. 435: 824-827.

Akiyoshi, D.E., Regier, D.A. and Gordon, M.P. 1987. Cytokinin production by *Agrobacterium* and *Pseudomonas* Spp. J. Bacteriol.169: 4242-4248.

Alder, A., Alder, A., Jamil, M., Marzorati, M., Bruno, M. , Vermathen, M., Bigler, P., Ghisla, S., Bouwmeester, H., Beyer, P. and Al-Babili, S. 2012. The path from β-carotene to carlactone, a strigolactone-like plant hormone. Science.335: 1348-1351.

Allen, M., Qin, W.S., Moreau, F. and Moffatt, B. 2002.Adenine phosphoribosyltransferase isoforms of *Arabidopsis* and their potential contributions to adenine and cytokinin metabolism. Physiol. Plant. 115: 56-68.

Altman, A. 1999.Plant biotechnology in the 21st century: The challenges ahead. EJB.2(2): 51-55.

Anderson, J. V., Chao, W. S. and Horvath, D. P. 2001. A current review on the regulation of dormancy in vegetative buds. Weed Science. 49: 581-589.

Arite, T., Iwata, H., Ohshima, K., Maekawa, M., Nakajima, M., Kojima, M., Sakakibara, H. and Kyozuka, J. 2007.*DWARF10*, an *RMS1/MAX4/DAD1* ortholog, controls lateral bud outgrowth in rice. Plant J. 51: 1019-1029.

Arite, T., Umehara, M., Ishikawa, S., Hanada, A., Maekawa, M., Yamaguchi, S. and Kyozuka, J. 2009.*d14*, a strigolactone insensitive mutant of rice, shows an accelerated outgrowth of tillers. Plant Cell Physiol. 50: 1416-1424.

Åstot, C., Doležal, K., Nordström, A., Wang, Q., Kunkel, T., Moritz, T. and Chua, N. H. 2000.An alternative cytokinin biosynthesis pathway. Proc. Natl. Acad. Sci. USA. 97: 14778-14783.

Auldridge, M.E., Block, A., Vogel, J.T., Dabney-Smith, C., Mila, I., Bouzayen, M., Magallanes-Lundback, M., DellaPenna, D., McCarty, DR. and Klee, H.J. 2006a. Characterization of three members of the *Arabidopsis* carotenoid cleavage dioxygenase family demonstrates the divergent roles of this multifunctional enzyme family. Plant J. 45(6): 982-993.

Auldridge, M.E., McCarty, D.R. and Klee, H.J. 2006b. Plant carotenoid cleavage oxygenases and their apocarotenoid products. Curr.Opin. Plant Biol. 9: 315-321.

Bainbridge, K., Sorefan, K., Ward, S. and Leyser, O. 2005.Hormonally controlled expression of the *Arabidopsis MAX4* shoot branching regulatory gene. Plant J. 44: 569-580.

Bajguz, A and Piotrowska, A. 2009. Conjugates of auxin and cytokinin. Phytochemistry. 70(8): 957-969.

Baker, D.A. 2000. Long-distance vascular transport of endogenous hormones in plants and their role in source: sink regulation. Israel J. Plant Sci. 48: 199-203.

Balla, J., Kalousek, P., Reinohl, V., Friml, J. and Prochazka, S. 2011. Competitive canalization of PIN-dependent auxin flow from axillary buds controls pea bud outgrowth. Plant J. 65: 571-577.

Bangerth, F. 1994. Response of cytokinin concentration in the xylem exudate of bean (*Phaseolus vulgaris* L.) plants to decapitation and auxin treatment, and relationship to apical dominance. Planta. 194: 439-442.

Bangerth, F., Li, C.J. and Gruber, J. 2000.Mutual interaction of auxin and cytokinins in regulating correlative dominance. Plant Growth Regul. 32: 205-217.

Bassil, N.V., Mok, D.W.S. and Mok, M.C. 1993. Partial purification of a *cis-trans*-isomerase of zeatin from immature seed of *Phaseolus vulgaris* L. Plant Physiol. 102: 867-872.

Beaty, J.S., Powell, G.K., Lica, L., Regier, D.A., MacDonald, E.M.S., Hommes, N.G. and Morris, R.O. 1986.*Tzs*, a nopaline Ti plasmid gene from *Agrobacterium tumefaciens*associated with *trans*-zeatin biosynthesis. Mo1. Gen. Genet. 203: 274-280.

Bennett, M.J., Marchant, A., Green, H.G., May, S.T., Ward, S.P., Millner, P.A., Walker, A.R., Schulz, B. and Feldmann, K.A. 1996. *Arabidopsis AUX1* gene: a permease-like regulator of root gravitropism. Science. 273: 948-950.

Bennett, T., Sieberer, T., Willett, B., Booker, J., Luschnig, C. and Leyser, O. 2006. The *Arabidopsis* MAX pathway controls shoot branching by regulating auxin transport. Curr.Opin. Plant Biol. 16: 553-563.

Beveridge, C.A. 2000. Long-distance signalling and mutational analysis of branching in pea. Plant Growth Regul. 32: 193-203.

Beveridge, C.A., Murfet, I.C., Kerhoas, L., Sotta, B., Miginiac, E. and Rameau, C. 1997a. The shoot controls zeatin riboside export from pea roots: evidence from the branching mutant *rms4*. Plant J. 11: 339-345.

Beveridge, C.A., Ross, J.J. and Murfet, I.C. 1994.Branching mutant *rms2* in *Pisum sativun*. Plant Physiol. 104: 953-959.

Beveridge, C.A., Ross, J.J. and Murfet, I.C. 1996.Branching in pea (action of genes *RMS3* and *RMS4*). Plant Physiol. 110(3): 859-865.

Beveridge, C.A., Symons, G.M., Murfet, I.C., Ross, J.J. and Rameau, C. 1997b. The *rms1* mutant of pea has elevated indole-3-acetic acid levels and reduced root-sap zeatin riboside content but increased branching controlled by graft transmissible signal(s). Plant Physiol. 115: 1251-1258.

Bilyeu, K.D., Cole, J.L., Laskey, J.G., Riekhof, W.R., Esparza, T.J., Kramer, M.D. and Morris, R.O. 2001.Molecular and biochemical characterization of a cytokinin oxidase from maize. Plant Physiol. 125: 378-386.

Blakeslee, J. J., Peer, W. A. and Murphy, A. S. 2005. Auxin transport. Curr.Opin. Plant Biol. 8: 494-500.

Böhner, S. and Gatz, C. 2001.Characterisation of novel target promoters for the dexamethasone-inducible/tetracycline-repressable regulator TGV using luciferase and isopentenyltransferase as sensitive reporter genes. Mol. Gen. Genet. 264: 860-870.

Booker, J., Auldridge, M., Wills, S., McCarty, D., Klee, H. and Leyser, O. 2004. *MAX3/CCD7* is a carotenoid cleavage dioxygenase required for the synthesis of a novel plant signalling molecule. Current Biol. 14: 1232-1238.

Booker, J., Chatfield, S. and Leyser, O. 2003. Auxin acts in xylem-associated or medullary cells to mediate apical dominance. Plant Cell.15: 495-507.

Booker, J., Sieberer, T., Wright, W., Williamson, L., Willett, B., Stirnberg, P., Turnbull, C., Srinivasan, M., Goddard, P. and Leyser, O. 2005.*MAX1* encodes a cytochrome P450 family member that acts downstream of *MAX3/4* to produce a carotenoid-derived branch inhibiting hormone. Developmental Cell. 8: 443-449.

Brady, S.M., Orlando, D.A., Lee, J.Y., Wang, J.Y., Koch, J., Dinneny, J.R., Mace, D., Ohler, U. and Benfey, P.N. 2007. A high-resolution root spatiotemporal map reveals dominant expression patterns. Science. 318: 801-806.

Braun, N., de Saint Germain, A., Pillot, J. P., Boutet-Mercey, S., Dalmais, M., Antoniadi, I., Li, X., Maia-Grondard, A., Le Signor, C., Bouteiller, N., Luo, D., Bendahmane, A.,

Turnbull, C. and Rameau, C. 2012. The pea TCP transcription factor *PsBRC1* acts downstream of strigolactones to control shoot branching. Plant Physiol. 158: 225-238.

Brewer, P.B., Dun, E.A., Ferguson, B.J., Rameau, C. and Beveridge, C.A. 2009.Strigolactone acts downstream of auxin to regulate bud outgrowth in pea and *Arabidopsis*. Plant Physiol. 150: 482-493.

Brewer, P.B., Kolta,i H. and Beveridge, C.A. 2013.Diverse roles of strigolactones in plant development. Mol. Plant. 6: 18-28.

Brown, B.T., Foster, C., Phillips, J.N. and Rattigan, B.M. 1979. The indirect role of 2,4-D in the maintenance of apical dominance in decapitated sunflower seedlings (*Helianthus annuus* L.). Planta. 146: 475-480.

Brownlee, B.G., Hall, R.H. and Whitty, C.D. 1975. 3-Methyl-2-butenal: an enzymatic degradation product of the cytokinin N6-(Δ2-isopentenyl) adenine. Can. J. Biochem. 53: 37-41.

Brzobohatý, B., Moore, I., Christofferson, P., Bako, L., Campos, N., Schell, J. and Palme, K. 1993. Release of active cytokinin by a β-glucosidase localized to the maize root meristem. Science. 262: 1051-1054.

Bürkle, L., Cedzich, A., Döpke, C., Stransky, H., Okumoto, S., Gillissen, B., Kühn, C. and Frommer, W.B. 2003. Transport of cytokinins mediated by purine transporters of the PUP family expressed in phloem, hydathodes, and pollen of *Arabidopsis*. Plant J. 34: 13-26.

Candela, H., Pérez-Pérez, J.M. and Mico,l J.L. 2011. Uncovering the post-embryonic functions of gametophytic- and embryonic-lethal genes. Trends Plant Sci. 16: 336-345.

Campbell, M.A., Suttle, J.C. and Sell, T.W. 1996. Changes in cell cycle status and expression of p34cdc2 kinase during potato tuber meristem dormancy. Physiol. Plant. 98: 743-752.

Cambridge, A.P. and Morris, D.A. 1996. Transfer of exogenous auxin from the phloem to the polar auxin transport pathway in pea (*Pisum sativum* L.). Planta. 199: 583-588.

Casimiro, I., Beeckman, T., Graham, N., Bhalerao, R., Zhang, H., Casero, P., Sandberg, G. and Bennett, M. J. 2003. Dissecting *Arabidopsis* lateral root development. Trends Plant Sci. 8(4): 165-171.

Chatfield, S.P., Stirnberg, P., Forde, B.G. and Leyser, O. 2000.The hormonal regulation of axillary bud growth in *Arabidopsis*. Plant J. 24, 159-169.

Chen, C.M. 1997. Cytokinin biosynthesis and interconversion. Physiol. Plant. 101: 665-673.

Chen, C.M. and Eckert, R.L. 1977. Phosphorylation of cytokinin by adenosine kinase from wheat germ. Plant Physiol. 59: 443-447.

Chen, C.M., Ertl, J.R., Leisner, S.M. and Chang, C.C. 1985. Localization of cytokinin biosynthetic sites in pea plants and carrot roots. Plant Physiol. 78: 510-513.

Chen, C.M. and Kristopeit, S.M. 1981a. Metabolism of cytokinin: deribosylation of cytokinin ribonucleoside by adenosine nucleosidase from wheat germ cells. Plant Physiol. 68: 1020-1023.

Chen, C.M. and Kristopeit, S.M. 1981b. Metabolism of cytokinin: dephosphorylation of cytokinin ribonucleotide by 5′-nucleotidases from cytosol. Plant Physiol. 67: 494-498.

Chen C.M. and Petschow B. 1978.Cytokinin biosynthesis in cultured rootless tobacco plants. Plant Physiol. 62: 861-865.

Cheng C.Y., Mathews D.E., Eric Schaller G. and Kieber J.J. 2013.Cytokinin-dependent specification of the functional megaspore in the *Arabidopsis* female gametophyte. Plant J. 73: 929-940.

Cheng, Z.J., Wang, L., Sun, W., Zhang, Y., Zhou, C., Su, Y.H., Li, W., Sun, T.T., Zhao, X.Y., Li, X.G., Cheng, Y., Zhao, Y., Xie, Q. and Zhang, X.S. 2013. Pattern of auxin and cytokinin responses for shoot meristem induction results from the regulation of cytokinin biosynthesis by *AUXIN RESPONSE FACTOR3*. Plant Physiol. 161(1):240-251.

Cho, M., Lee, S. H. and Cho, H. T. 2007. P-glycoprotein4 displays auxin efflux transporter-like action in *Arabidopsis* root hair cells and tobacco cells. Plant Cell. 19: 3930-3943.

Cline, M.G. 1997. Concepts and terminology of apical dominance. Am.J.Bot. 84: 1064-1069.

Cohen, J.E. 2003. Human Population: The Next Half Century. Science.302: 1172-1175.

Corbesier, L., Prinsen, E., Jacqmard, A., Lejeune, P., Van Onckelen, H., Pe´rilleux, C. and Bernier, G. 2003. Cytokinin levels in leaves, leaf exudate and shoot apical meristem of Arabidopsis thaliana during floral transition. J. Exp. Bot. 54: 2511-2517.

Crawford, S., Shinohara, N., Sieberer, T., Williamson, L., George, G., Hepworth, J., Müller, D., Domagalska, M.A. and Leyser, O. 2010. Strigolactones enhance competition

between shoot branches by dampening auxin transport. Development. 137: 2905-2913.

Deng, Y., Dong, H., Mu, J., Ren, B., Zheng, B., Ji, Z., Yang, W.C., Liang, Y. and Zuo, J. 2010. *Arabidopsis* histidine kinase CKI1 acts upstream of histidine phosphotransfer proteins to regulate female gametophyte development and vegetative growth. Plant Cell. 22: 1232-1248.

Devic, M. 2008. The importance of being essential: *EMBRYO-DEFECTIVE* genes in *Arabidopsis*. C. R. Biol. 331(10): 726-736.

Devitt, M.L. and Stafstrom, J.P. 1995. Cell cycle regulation during growth-dormancy cycles in pea axillary buds. Plant Mol. Biol. 29: 255-265.

Dewitte, W. and Murray, J.A.H. 2003. The plant cell cycle. Annu. Rev. Plant Biol. 54: 235-264.

Dietrich, J.T., Kaminek, M., Blevins, D.G., Reinbott, T.M., Morris, R.O. 1995. Changes in cytokinins and cytokinin oxidase activity in developing maize kernels and the effects of exogenous cytokinin on kernel development. Plant Physiol. Biochem. 33: 327-336.

Dixon, S.C., Martin, R.C., Mok, M.C., Shaw. G. and Mok, D.W.S. 1989. Zeatin glycosylation enzymes in *Phaseolus*: isolation of O-glucosyltransferase from *P. lunatus* and comparison to O-xylosyltransferase from *P. vulgaris*. Plant Physiol. 90: 1316-1321.

Doebley, J.F., Gaut, B.S. and Smith, B.D. 2006. The Molecular Genetics of Crop Domestication. Cell. 127(7): 1309-1321.

Domagalska, D.A. and Leyser, O. 2011. Signal integration in the control of plant development. Nat. Rev. Mol. Cell Biol. 12: 211-221.

Doust, A. 2007.Architectural Evolution and its Implications for Domestication in Grasses. Ann. Bot. 100:941-950.

Dun, E.A., Brewer, P.B. and Beveridge, C.A. 2009. Strigolactones: Discovery of the elusive shoot branching hormone. Trends Plant Sci. 14: 364-372.

Dun, E.A., de Saint Germain, A., Rameau, C. and Beveridge, C.A. 2012.Antagonistic Action of Strigolactone and Cytokinin in Bud Outgrowth Control. Plant Physiol. 158(1): 487-498.

Dun, E.A., de Saint Germain, A., Rameau, C. and Beveridge, C.A. 2013.Dynamics of Strigolactone Function and Shoot Branching Responses in *Pisum sativum*. Mol. Plant. 6(1): 128-140.

Edwards, C.A., Armstrong, D.J., Kaiss-Chapman, R.W. and Morris, R.O. 1981. Cytokinin-active ribonucleosides in *Phaseolus* RNA. I. Identification in tRNA from etiolated *Phaseolus vulgpris* L. seedlings. Plant Physiol. 67: 1181-1184.

Eklöf, S., Åstot, C., Moritz, T., Blackwell, J., Olsson, O. and Sandberg, G. (1997).Auxin-cytokinin interactions in wild type and transgenic tobacco. Plant Cell Physiol. 33: 225-235.

El-Showk, S., Ruonala, R. and Helariutta, Y. 2013. Crossing paths: Cytokinin signalling and crosstalk. Development. 140(7): 1373-1383.

Entsch, B. and Letham, D.S. 1979. Enzymic glycosylation of the cytokinin, 6-benzylaminopurine. Plant Sci. Lett. 14: 205-212.

Entsch, B., Parker, C.W., Letham, D.S. and Summons, R.E. 1979. Preparation and characterization using high-performance liquid chromatography of an enzyme forming glucosides of cytokinins. Biochim.Biophys.Acta. 570:1 24-139.

Emery, R.J.N., Longnecker, N.E. and Atkins, C.A. 1998.Branch development in *Lupinus angustifolius*. II. Relationship with endogenous ABA, IAA and cytokinins in axillary and main stem buds. J. Exp. Bot. 49(320): 555-562.

Evers, J.B., van der Krol, A.R., Vos, J. and Struik, P.C. 2011. Understanding shoot branching by modelling form and function, Tren.Plant Sci. 16(9): 464-467.

Faiss, M., Zalubilová, J., Strnad, M. and Schmülling, T. 1997. Conditional transgenic expression of the *ipt* gene indicates a function for cytokinins in paracrine signalling in whole tobacco plants. Plant J. 12: 401-415.

Friml, J. 2003. Auxin transport – shaping the plant.Curr.Opin. Plant Biol. 6: 1-6.

Friml, J. and Palme, K. 2002. Polar auxin transport – old questions and new concepts? Plant Mol. Biol. 49:273-284.

Friml, J., Vieten, A., Sauer, M., Weijers, D., Schwarz, H., Hamann, T., Offringa, R. and Jürgens, G. 2003. Efflux-dependent auxin gradients establish the apical–basal axis of Arabidopsis. Nature. 426: 147-153.

Feldman, L. J. 1979. Cytokinin biosynthesis in roots of com. Planta. 145: 315-321.

Foo, E., Bullier, E., Goussot, M., Foucher, F., Rameau, C. and Beveridge, C.A. 2005. The branching gene *RAMOSUS1* mediates interactions among two novel signals and auxin in pea. Plant Cell. 17: 464-474.

Foo, E. and Davies N.W. 2011. Strigolactones promote nodulation in pea. Planta. 234: 1073-1081.

Foo, E., Morris, S., Parmenter, K., Young, N., Wang, N., Jones, A., Rameau, C., Turnbull, C. and Beveridge, C. 2007. Feedback regulation of xylem cytokinin content is conserved in Pea and *Arabidopsis*. Plant Physiol. 143: 1418-1428.

Frébort, I., Kowalska, M., Hluska, T., Frébortová, J. and Galuszka, P. 2011. Evolution of cytokinin biosynthesis and degradation. J. Exp. Bot. 62(8):2431-2452.

Galichet, A., Hoyerová, K.,Kamínek, M. and Gruissem, W. 2008. Farnesylation Directs AtIPT3 Subcellular Localization and Modulates Cytokinin Biosynthesis in *Arabidopsis*. Plant Physiol. 146(3): 1155-1164.

Galuszka, P., Frébort, I., Šebela, M., Sauer, P., Jacobsen, S. and Peč, P. 2001. Cytokinin oxidase or dehydrogenase?Mechanism of cytokinin degradation in cereals. Eur. J. Biochem. 268: 450-461.

Galuszka, P., Popelková, H., Werner, T., Frébortová, J., Pospíšilová, H., Mik, V., Köllmer, I., Schmülling, T. and Frébort, I. 2007. Biochemical characterization of cytokinin oxidases/dehydrogenases from *Arabidopsis thaliana* expressed in *Nicotiana tabacum* L. J. Plant Growth Regul. 26: 255-267.

Gälweiler, L., Guan, C., Müller, A., Wisman, E., Mendgen, K., Yephremov, A. and Palme, K. 1998. Regulation of polar auxin transport by AtPIN1 in *Arabidopsis* vascular tissue.Science. 82: 2226-2230.

Geisler, M., Blakeslee, J.J., Bouchard, R., Lee, O.R., Vincenzetti, V., Bandyopadhyay, A., Titapiwatanakun, B., Peer, W.A., Bailly, A., Richards, E.L., Ejendal, K.F., Smith, A.P., Baroux, C., Grossniklaus, U., Müller, A., Hrycyna, C.A., Dudler, R., Murphy, A.S. and Martinoia, E. 2005. Cellular efflux of auxin catalyzed by the *Arabidopsis* MDR/PGP transporter AtPGP1. Plant J. 44: 179-194.

Geisler, M. and Murphy, A.S. 2006. The ABC of auxin transport: The role of p-glycoproteins in plant development. FEBS Lett. 580: 1094-1102.

Ghanem, M.E., Albacete, A., Smigocki, A.C., Frébort, I., Pospíšilová, H., Martínez-Andújar, C., Acosta, M., Sánchez-Bravo, J., Lutts, S., Dodd, I.C. and Pérez-Alfocea, F. 2011.

Root-synthesized cytokinins improve shoot growth and fruit yield in salinized tomato (*Solanum lycopersicum* L.) plants. J. Exp. Bot. 62(1): 125-140.

Gilland, B. 2002. World population and food supply: can food production keep pace with population growth in the next half-century? Food Policy. 27: 47-63.

Gillissen, B., Bürkle, L., Andre, B., Kühn, C., Rentsch, D., Brandl, B., Frommer, W.B. 2000. A new family of high-affinity transporters for adenine, cytosine, and purine derivatives in *Arabidopsis*.Plant Cell. 12: 291-300.

Goldwasser, Y., Yoneyama, K., Xie, X. and Yoneyama, K. 2008.Production of strigolactones by *Arabidopsis thaliana* responsible for *Orobanche aegyptiaca* seed germination.Plant Growth Regul. 55: 21-28.

Golovko, A., Sitbon, F., Tillberg, E. and Nicander, B. 2002.Identification of a tRNA isopentenyltransferase gene from *Arabidopsis thaliana*. Plant Mol. Biol. 49: 161-169.

Gomez-Roldan, V., Fermas, S., Brewer, P.B., Puech-Page`s, V., Dun, E.A., Pillot, J., Letisse, F., Matusova, R., Danoun, S., Portais, J., Bouwmeester, H., Be´card, G., Beveridge, C.A., Rameau, C. and Rochange, S.F. 2008. Strigolactone inhibition of shoot branching. Nature. 455: 189-194.

Guan, J.C., Suzuki, M., Wu, S., Latshaw, S.P., Petruff, T., Goulet, C., Klee, H.J., Koch, K.E. and McCarty, D.R. 2012.Diverse roles of strigolactone signalling in maize architecture and the uncoupling of a branching-specific sub-network. Plant Physiol. 160: 1303-1317.

Haberer, G. and Kieber, J.J. 2002.Cytokinins.New Insights into a Classic Phytohormone.Plant Physiol. 128: 354-362.

Hake, S., Smith, H.M., Holtan, H., Magnani, E., Mele, G. and Ramirez, J. 2004. The role of *KNOX* genes in plant development.Annu. Rev. Cell Dev. Biol. 20: 125-151.

Hall, S.M. and Hillman, J.R. 1975. Correlative inhibition of lateral bud growth in *Phaseolus vulgaris* L. Timing of bud growth following decapitation.Planta. 123: 137-143.

Hamiaux, C., Drummond, R.S., Janssen, B.J., Ledger, S.E., Cooney, J.M., Newcomb, R.D. and Snowden, K.C. 2012. *DAD2* is anα/β hydrolase likely to be involved in the perception of the plant branching hormone, strigolactone. Curr. Biol. 22: 2032-2036.

Hayward, A., Stirnberg, P., Beveridge, C.A. and Leyser, O. 2009. Interactions between auxin and strigolactone in shoot branching control. Plant Physiol. 151: 400-412.

Hedden, P. 2003. The genes of the Green Revolution.Trends Genet. 19(1): 5-9.

Hejátko, J., Pernisová, M., Eneva, T., Palme, K. and Brzobohatý B. 2003. The putative sensor histidine kinase CKI1 is involved in female gametophyte development in Arabidopsis. Mol. Genet. Genomics 269: 443-453.

Hirose, N., Makita, N., Yamaya, T. and Sakakibara, H. 2005. Functional characterization and expression analysis of a gene, OsENT2, encoding an equilibrative nucleoside transporter in rice suggest a function in cytokinin transport. Plant Physiol. 138(1): 196-206.

Hirose, N., Takei, K., Kuroha, T., Kamada-Nobusada, T., Hayashi, H. and Sakakibara, H. 2008.Regulation of cytokinin biosynthesis, compartmentalization and translocation. J. Exp. Bot. 59: 75-83.

Hruz, T., Laule, O., Szabo, G., Wessendorp, F., Bleuler, S., Oertle, L., Widmayer, P., Gruissem, W. and Zimmermann, P. 2008. Genevestigator v3: a reference expression database for the meta-analysis of transcriptomes. Adv. Bioinformatics. 2008(article id-420747): 1-5.

Horvath, D. P., Anderson, J. V., Chao, W. S. and Foley, M. E. 2003.Knowing when to grow: signals regulating bud dormancy. Trends Plant Sci. 8(11): 534-540.

Hou, B., Lim, E.K., Higgins, G.S. and Bowles D.J. 2004.N-Glucosylation of cytokinins by glycosyltransferases of *Arabidopsis thaliana*.J. Biol. Chem. 279: 47822-47832

Huang, X., Effgen, S., Meyer, R.C., Theres, K. and Koornneef, M. 2012. Epistatic natural allelic variation reveals a function of *AGAMOUS-LIKE6* in axillary bud formation in *Arabidopsis*. Plant Cell. 24(6): 2364-2379.

Hubbard, L., McSteen, P., Doebley, J. and Hake, S. 2002. Expression patterns and mutant phenotype of *TEOSINTE BRANCHED1* correlate with growth suppression in maize and teosinte. Genetics. 162: 1927-1935.

Hufford, K.M., Canaran, P., Ware, D.H., McMullen, M.D. and Gaut, B.S. 2007. Patterns of Selection and Tissue-Specific Expression among Maize Domestication and Crop Improvement Loci. Plant Physiol. 144(3): 1642-1653.

Humphrey, A.J., Galster, A.M. and Beale, M.H. 2006. Strigolactones in chemical ecology: waste products or vital allelochemicals? Nat. Prod. Rep. 23: 592-614.

Hwang, I. and Sheen, J. 2001. Two-component circuitry in *Arabidopsis* signal transduction. Nature. 413: 383-389.

Hwang, I., Sheen, J. and Müller, B. 2012.Cytokinin Signalling Networks. Ann. Rev. Plant Biol. 63: 353-380.

Inoue, T., Higuchi, M., Hashimoto, Y., Seki, M., Kobayashi, M., Kato, T., Tabata, S., Shinozaki, K. and Kakimoto, T. 2001.Identification of CRE1 as a cytokinin receptor from *Arabidopsis*. Nature 409: 1060-1063.

Ishikawa, S., Maekawa, M., Arite, T., Onishi, K., Takamure, I. and Kyozuka, J. 2005.Suppression of tiller bud activity in tillering dwarf mutants of rice. Plant Cell Physiol. 46: 79-86.

Ito, S., Kitahata, N., Umehara, M., Hanada, A., Kato, A., Ueno, K., Mashiguchi, K., J. Kyozuka, J., Yoneyama, K., Yamaguchi, S. and Asami, T. 2010.A new lead chemical for strigolactone biosynthesis inhibitors. Plant Cell Physiol. 51: 1143-1150.

Ito, S., Umehara, M., Hanada, A., Kitahata, N., Hayase, H., Yamaguchi, S. and Asami, T. 2011.Effects of triazole derivatives on strigolactone levels and growth retardation in rice. PLoS One 6: e21723.

Jasinski, S., Piazza, P., Craft, J., Hay, A., Woolley, L., Rieu, I., Phillips, A., Hedden, P. and Tsiantis, M. 2005. KNOX action in *Arabidopsis* is mediated by coordinate regulation of cytokinin and gibberellin activities. Curr Biol. 15: 1560-1565.

Johnson, X., Brcich, T., Dun, E.A., Goussot, M., Haurogné, K., Beveridge, C.A. and Rameau, C. 2006. Branching genes are conserved across species: genes controlling a novel signal in pea are coregulated by other long-distance signals. Plant Physiol. 142: 1014-1026.

Johnson, A.W., Gowda, G., Hassanali, A., Knox, J., Monaco, S., Razavi, Z. and Rosebery, G. 1981.The preparation of synthetic analogs of strigol. J. Chem. Soc. Perkin Trans. 1: 1734-1743.

Kakimoto, T. 2003. Perception and signal transduction of cytokinins. Annu. Rev. Plant Biol. 54: 605-627.

Kakimoto, T. 2001. Identification of plant cytokinin biosynthetic enzymes as dimethylallyldiphosphate: ATP/ADP Isopentenyltransferases. Plant Cell Physiol. 42: 677-685.

Kakimoto, T. 1996. CK1, a histidine kinase homolog implicated in cytokinin signal transduction. Science. 274: 982-985.

Kalousek, P., Buchtová, D., Balla, J., Reinöhl, V. and Procházka, S. 2010.Cytokinins and polar transport of auxin in axillary pea buds. Magazine Acta Universitatis Agriculturae et Silviculturae Mendeleianae Brunensis. 58: 79-88.

Kamada-Nobusada, T. and Sakakibara, H. 2009.Molecular basis for cytokinin biosynthesis.Phytochemistry. 70(4): 444-449.

Kaminek, M. and Armstrong, D.J. 1990.Genotypic variation in cytokinin oxidase from *Phaseolus* callus cultures. Plant Physiol. 93: 1530-1538.

Kasahara, H., Takei, K., Ueda, N., Hishiyama, S., Yamaya, T., Kamiya, Y., Yamaguchi, S. and Sakakibara, H. 2004. Distinct isoprenoid origins of *cis*- and *trans*-zeatin biosyntheses in *Arabidopsis*. J. Biol. Chem. 279: 14049-14054.

Kende, H. and Zeevaart, J.A.D. 1997. The Five Classical Plant Hormones. P. Cell. 9(1): 197-121.

Khush, G.S. 1987. Rice breeding: Past, present and future. J.Genet. 66: 195-216.

Khush, G.S. 1995. Modern varieties – their real contribution to food supply and equity. Geo J. 35: 275-284.

Khush, G.S. 1999. Green revolution: preparing for the 21st century. Genome. 42: 646-655.

Khush, G.S. 2001.Green revolution-the way forward.Nat. Rev. Genet. 2: 815-822.

Khush, G.S. and Virk, P.S. 2005.IR varieties and their impact. Los Banos (Philippines): International Rice Research Institute. 163p.

Kinoshita-Tsujimura, K. and Kakimoto, T. 2011. Cytokinin receptors in sporophytes are essential for male and female functions in *Arabidopsis thaliana*. Plant Signal Behav. 6**:** 66-71.

Koda, Y. and Okazawa, Y. 1978. Cytokinin Production by Tomato Root: Occurrence of Cytokinins in Staled Medium of Root Culture. Physiol. Plant. 44(4): 412-416.

Kohlen, W., Charnikhova, T., Lammers, M, Pollina, T., Tóth, P., Haider, I., Pozo, M.J., de Maagd, R.A., Ruyter-Spira, C., Bouwmeester, H.J. and López-Ráez, J.A. 2012. The tomato *CAROTENOID CLEAVAGE DIOXYGENASE 8* (SlCCD8) regulates rhizosphere signalling, plant architecture and affects reproductive development through strigolactone biosynthesis. New Phytol. 19: 535-547.

Kohlen, W., Charnikhova, T., Liu, Q., Bours, R., Domagalska, M.A., Beguerie, S., Verstappen, F., Leyser, O., Bouwmeester, H. and Ruyter-Spira, C. 2011. Strigolactones are transported through the xylem and play a key role in shoot architectural response to phosphate deficiency in nonarbuscular mycorrhizal host *Arabidopsis*. Plant Physiol. 155: 974-987.

Kowalska, M., Galuszka, P., Frébortová, J., Šebela, M., Béres, T., Hluska, T., Šmehilová, M., Bilyeu, K.D. and Frébort, I. 2010. Vacuolar and cytosolic cytokinin dehydrogenases of *Arabidopsis thaliana*: heterologous expression, purification and properties. Phytochemistry. 71: 1970-1978.

Krall, L., Raschke. M., Zenk, M. H. and Baron, C. 2002. The Tzs protein from *Agrobacterium tumefaciens*C58 produces zeatin riboside 5-phosphate from 4-hydroxy-3-methyl-2-(E)-butenyl diphosphate and AMP. FEBS Lett. 527: 315-318.

Kretzschmar, T., Kohlen, W., Sasse, J., Borghi, L., Schlegel, M., Bachelier, J.B., Reinhardt, D., Bours, R., Bouwmeester, H.J, and Martinoia, E. 2012. A petunia ABC protein controls strigolactone- dependent symbiotic signalling and branching. Nature.483: 341-344.

Krysan, P.J., Young. J.C. and Sussman, M.R. 1999. T-DNA as an Insertional Mutagen in *Arabidopsis*. Plant Cell 11: 2283-2290.

Kudo, T., Kiba, T. and Sakakibara, H. 2010.Metabolism and long distance translocation of cytokinins. J. Integr. Plant Biol. 52(1): 53-60.

Kurakawa, T., Ueda, N., Maekawa, M., Kobayashi, K., Kojima, M., Nagato, Y., Sakakibara, H. and Kyozuka, J. 2007.Direct control of shoot meristem activity by a cytokinin-activating enzyme.Nature. 445: 652-655.

Kuroha, T., Tokunagaa, H., Kojima, M., Ueda, N., Ishida, T., Nagawa, S., Fukuda, H., Sugimoto, K. and Sakakibara, H. 2009. Functional Analyses of LONELY GUY Cytokinin-Activating enzymes reveal the importance of the direct activation pathway in *Arabidopsis*. Plant Cell. 21(10): 3152-3169.

Laloue, M. and Fox, J.E. 1989.Cytokinin oxidase from wheat.Patrial purification and general properties. Plant Physiol. 90: 899-906.

Laloue, M. and Pethe, C. 1982.Dynamics of cytokinin metabolism in tobacco cells.In PF Wearing, ed. Plant Growth Substances. Academic Press, London, pp. 185-196.

Lazar, G. and Goodman, H. M. 2006.*MAX1*, a regulator of the flavonoid pathway, controls vegetative axillary bud outgrowth in *Arabidopsis*. Proc. Natl. Acad. Sci. USA. 103: 472-476.

Ledger, S.E., Janssen, B.J., Karunairetnam, S., Wang, T. and Snowden, K.C. 2010. Modified *CAROTENOID CLEAVAGE DIOXYGENASE* 8 expression correlates with altered branching in kiwifruit (*Actinidia chinensis*). New Phytol. 188: 803-813.

Le Fanu, B. 1936. Auxin and correlative inhibition.New Phytol. 35: 205-220.

Letham, D.S. 1994. Cytokinins as phytohormones-Sites of biosynthesis, translocation, and function of translocated cytokinin. In: Cytokinins Chemistry, Activity, and Function, eds., D.W.S. Mok and M.C. Mok, CRC Press, Boca Raton, p.57-80.

Leyser, O. 2009.The control of shoot branching: an example of plant information processing. Plant, Cell & Environment.32(6): 694-703.

Leyser, O. 2003.Regulation of shoot branching by auxin. Trends Plant Sci. 8: 541-545.

Li, C. and Bangerth, F. 1999. Autoinihibition of indole acetic acid transport in the shoot of two-branched pea (*Pisum sativum*) plants and its relationship to correlative dominance.Physiol. Plant. 106**:** 415-420.

Li, C.J., Herrera, G.J. and Bangerth, F. 1995. Effect of apex excision and replacement by 1-naphthylacetic acid on cytokinin concentration and apical dominance in pea plants. Physiol. Plant 94: 465-469.

Li, G., Liu, K., Baldwin, S.A. and Wang, D. 2003. Equilibrative nucleoside transporters of *Arabidopsis thaliana*: cDNA cloning, expression pattern and analysis of transport activities. J. Biol. Chem. 278: 35732-35742.

Lin, H., Wang, R., Qian, Q., Yan, M., Meng, X., Fu, Z. , Yan, C., Jiang, B., Su, Z., Li, J. and Wang, Y. 2009. *DWARF27*, an iron-containing protein required for the biosynthesis of strigolactones, regulates rice tiller bud outgrowth. Plant Cell.21: 1512-1525.

Lincoln, C., Britton, J.H. and Estelle, M. 1990. Growth and development of the *axr1* mutants of *Arabidopsis*.Plant Cell. 2: 1071-1080.

Liu, J., Novero, M., Charnikhova, T., Ferrandino, A., Schubert, A., Ruyter-Spira, C., Bonfante, P., Lovisolo, C., Bouwmeester, H.J. and Cardinale, F. 2013. Carotenoid cleavage dioxygenase 7 modulates plant growth, reproduction, senescence, and determinate nodulation in the model legume *Lotus japonicus*. J. Exp Bot. 64(7): 1967-1981.

Ljung, K., Bhalerao, R. and Sandberg, G. 2001. Sites and homeostatic control of auxin biosynthesis in *Arabidopsis* during vegetative growth. Plant J. 28: 465-474.

Ljung, K., Hull, A.K., Celenza, J., Yamada, M., Estelle, M., Normanly, J. and Sandberg, G. 2005.Sites and regulation of auxin biosynthesis in *Arabidopsis* roots.Plant Cell. 17: 1090-1104.

Ljung, K., Hull, A., Kowalczyk, M., Marchant, A., Celenza, J., Cohen, J. D. and Sandberg, G. 2002.Biosynthesis, conjugation, catabolism, and homeostasis of indole-3-acetic acid in *Arabidopsis thaliana*.Plant. Mol. Biol. 49: 249-272.

Long, J.A., Moan, E.I., Medford, J.I. and Barton, M.K. 1996.A member of the KNOTTED class of homeodomain proteins encoded by the *STM* gene of *Arabidopsis*.Nature. 379: 66-69.

Lucas, M., Godin, C., Jay-Allemand, C. and Laplaze, L. 2008. Auxin fluxes in the root apex co-regulate gravitropism and lateral root initiation. J. Exp. Bot. 59(1): 55–66.

Mader, J.C., Turnbull, C.G.N. and Emery, R.J.N. 2003. Transport and metabolism of xylem cytokinins during lateral bud release in decapitated chickpea (*Cicer arietinun*) seedlings. Physiol. Plant. 117: 118-129.

Maher, E.P. and Martindale, S.J.B. 1980. Mutants of *Arabidopsis* with altered responses to auxins and gravity. Biochem.Genet. 18: 1041-1053.

Mähönen, A.P., Bonke, M., Kaupinnen, L., Riikonen, M., Benfey, P.N. and Helariutta, Y. 2000. A novel two-component hybrid molecule regulates vascular morphogenesis of the *Arabidopsis* root. Genes Dev. 14: 2938-2943.

Malito, E., Alfieri, A., Fraaije, M.W. and Mattevi, A. 2004.Crystal structure of a Baeyer–Villiger monooxygenase. Proc. Natl. Acad Sci. USA. 101: 13157-13162.

Martin, R.C., Mok, M.C., Habben, J.E. and Mok, D.W. 2001.A maize cytokinin gene encoding an O-glucosyltransferase specific to *cis*-zeatin.Proc. Natl. Acad. Sci. USA 98: 5922-5926.

Martin, R.C., Mo,k M.C. and Mok, D.W. 1999a. A gene encoding the cytokinin enzyme zeatin O-xylosyltransferase of Phaseolus vulgaris.Plant Physiol. 120:553–558.

Martin, R.C., Mo,k M.C. and Mok, D.W. 1999b. Isolation of a cytokinin gene, *ZOG1*, encoding zeatin O-glucosyltransferase from *Phaseolus lunatus*.Proc. Natl. Acad. Sci. USA. 96: 284-289.

Martin, R.C., Mok, M.C., Shaw, G. and Mok, D.W.S. 1989. An enzyme mediating the conversion of zeatin to dihydrozeatin in *Phaseolus* embryos. Plant Physiol. 90:1630-1635.

Mashiguchi, K., Sasaki, E., Shimada, Y., Nagae, M., Ueno, K., Nakano, T., Yoneyama, K., Suzuki, Y. and Asami, T. 2009.Feedback-regulation of strigolactone biosynthetic genes and strigolactone-regulated genes in *Arabidopsis*.Biosci.Biotechnol.Biochem. 73: 2460-2465.

Matsumoto-Kitano, M., Kusumoto, T., Tarkowski, P., Kinoshita-Tsujimura, K., Va´clavikova´, K., Miyawaki, K. and Kakimoto, T. 2008. Cytokinins are central regulators of cambial activity. Proc. Natl. Acad. Sci. USA. 105: 20027–20031.

Matusova, R., Rani, K., Verstappen, F.W.A., Franssen, M.C.R., Beale, M.H. and Bouwmeester, H.J. 2005. The strigolactone germination stimulants of the plant parasitic *Striga*and *Orobanche*spp. are derived from the carotenoid pathway. Plant Physiol. 139: 920-934.

McGaw, B.A. and Horgan, R. 1983. Cytokinin catabolism and cytokinin oxidase.Phytochemistry. 22: 1103-1105.

McSteen, P. and Leyser, O. 2005. Shoot branching. Annu. Rev. Plant Biol. 56: 353-374.

Medford, J.I., Horgan, R., El-Sawi, Z. and Klee, H.J. 1989.Alterations of endogenous cytokinins in transgenic plants using a chimeric isopentenyl transferase gene. Plant Cell 1: 403-413.

Meinke, D.W. 1982. Embryo-lethal mutants of *Arabidopsis thaliana*: evidence for gametophytic expression of the mutant genes. Theor. Appl. Genet. 63: 381-386.

Meinke, D., Muralla, R., Sweeney C. and Dickerman, A. 2008.Identifying essential genes in Arabidopsis thaliana. Trends Plant Sci. 13(9): 483-491.

Michniewicz, M., Brewer, P. B. and Friml, J. 2007.Polar Auxin Transport and Asymmetric Auxin Distribution.The Arabidopsis Book.ASPB.

Miller, C. O., Skoog, F., Von Saltza, M. H. and Strong, F. 1955.Kinetin, a cell division factor from deoxyribonucleic acid. J. Am. Chem. Soc. 77(5): 1392-1392.

Miyawaki, K., Matsumoto-Kitano, M. and Kakimoto, T. 2004. Expression of cytokinin biosynthetic isopentenyltransferase genes in *Arabidopsis*: tissue specificity and regulation by auxin, cytokinin, and nitrate. Plant J. 37:128-38.

Miyawaki, K., Tarkowski, P., Matsumoto-Kitano, M., Kato, T., Sato, S., Tarkowska, D., Tabata, S., Sandberg, G. and Kakimoto, T. 2006. Roles of *Arabidopsis*ATP/ADP isopentenyltransferases and tRNA isopentenyltransferases in cytokinin biosynthesis.Proc. Nat. Acad. Sci. USA. 103: 16598-16603.

Mockaitis, K. and Estelle, M. 2008. Auxin Receptors and Plant Development: A New Signalling Paradigm. Annu. Rev. Cell Dev. Biol. 24:55-80.

Moffatt, B., Pethe, C. and Laloue, M. 1991. Metabolism of benzyladenine is impaired in a mutant of Arabidopsis thaliana lacking adenine phosphoribosyltransferase activity. Plant Physiol. 95: 900-908.

Mohammadi, S.A. and Prasanna, B.M. 2003.Analysis of Genetic Diversity in Crop Plants-Salient Statistical Tools and Considerations. Crop Sci. 43: 1235-1248.

Mok, M.C. 1994. Cytokinins and plant development-an overview.Mok, D.W.S.; Mok, M.C. Cytokinins-Chemistry, activity, and function. Boca Raton, FL: CRC Press. pp. 155-166.

Mok, M.C., Martin, R.C. and Mok, D.W.S. 2000.Cytokinins: Biosynthesis, Metabolism and Perception. In Vitro Cell. Dev. Biol. Plant. 36: 102-107.

Mok, D.W. and Mok, M.C. 2001. Cytokinin metabolism and action.Annu. Rev. Plant Physiol. Plant Mol. Biol. 52: 89-118.

Morris, D.A. 1977. Transport of exogenous auxin in 2-branched dwarf pea-seedlings (*Pisum sativum* L.)- some implications for polarity and apical dominance. Planta. 136: 91-96.

Morris, S.E., Turnbull, C.G.N., Murfet. I.C. and Beveridge, C.A. 2001.Mutational analysis of branching in pea.Evidence that *rms1* and *rms5* regulate the same novel signal. Plant Physiol. 126: 1205-1213.

Motyka, V., Faiss, M., Strnad, M., Kamínek, M. and Schmülling, T. 1996.Changes in cytokinin content and cytokinin oxidase activity in response to derepression of *ipt* gene transcription in transgenic tobacco calli and plants. Plant Physiol. 112: 1035-1043.

Motyka, V. and Kaminek, M. 1994. Cytokinin oxidase from auxin- and cytokinin-dependent callus cultures of tobacco (*Nicotiana tabacum* L.). J. Plant Growth Regul. 13: 1-9.

Motyka, V., Vaňková, R., Čapková, V., Petrášek, J., Kamínek, M. and Schmülling, T. 2003. Cytokinin-induced upregulation of cytokinin oxidase activity in tobacco includes changes in enzyme glycosylation and secretion. Physiol. Plant. 117: 11-21.

Mouchel, C.F. and Leyser, O. 2007. Novel phytohormones involved in long-range signalling, Curr. Opin. Plant Biol. 10(5): 473-476.

Mravec, J., Kubeš, M., Bielach, A., Gaykova, V., Petrášek, J., Skůpa, P., Chand, S., Benková, E., Zažímalová, E. and Friml, J. 2008. Interaction of PIN and PGP transport mechanisms in auxin distribution-dependent development. Development.135: 3345-3354.

Müller, D. and Leyser, O. 2011. Auxin, cytokinin and the control of shoot branching. Ann. Bot. 107: 1203-1212.

Murphy, A. S., Hoogner, K. R., Peer, W. A. and Taiz, L. 2002. Identification, purification, and molecular cloning of N-1-naphthylphthalamic acid-binding plasma membrane associated aminopeptidases from *Arabidopsis*. Plant Physiol. 128: 935-950.

Napoli, C. 1996. Highly branched phenotype of the petunia *dad1-1* mutant is reversed by grafting. Plant Physiol. 111: 27-37.

Nishimuraa, C., Ohashia, Y., Satob, S., Katob, T., Tabatab, S. and Ueguchia, C. 2004. Histidine kinase homologs that act as cytokinin receptors possess overlapping functions in the regulation of shoot and root growth in *Arabidopsis*. Plant Cell. 16(6): 1365-1377.

Noh, B., Murphy, A.S.and Spalding, E.P. 2001. Multidrug resistance-like genes of*Arabidopsis* required for auxin transport and auxin-mediated development. Plant Cell. 13:2441-2454.

Nördstrom, A., Tarkowski, P., Tarkowska D, Norbaek, R., Åstot, C., Dolezal, K. and Sandberg, G. 2004. Auxin regulation of cytokinin biosynthesis in Arabidopsis thaliana: a factor of potential importance for auxin–cytokinin-regulated development. Proc. Natl. Acad. Sci. USA. 101: 8039-8044.

Okada, K., Ueda, J., Komaki, M. K., Bell, C. J.and Shimura, Y. 1991. Requirement of the auxin polar transport system in early stages of Arabidopsis floral bud formation. Plant Cell. 3: 677-684.

Ongaro, V. and Leyser, O. 2008. Hormonal control of shoot branching. J. Exp. Bot. 59(1):67-74.

Pačes, V., Werstiuk, E. and Hall, R.H. 1971.Conversion of N6-(Δ2-isopentenyl) adenosine to adenosine by enzyme activity in tobacco tissue. Plant Physiol. 48: 775-778.

Palni, L.M.S. and Horgan, R. 1983. Cytokinin biosynthesis in crowngall tissue of *Vinca rosea*: metabolism of isopentenyladenine. Phytochemistry. 22: 1597-1601.

Paponov, I. A., Teale, W. D., Trebar, M., Blilou, I. and Palme, K. 2005. The PIN auxin efflux facilitators: evolutionary and functional perspectives. Trends Plant Sci. 10:170-177.

Parry, G., Marchant, A., May, S., Swarup, R., Swarup, K., James, N., Graham, N. Allen, T., Martucci, T. Yemm, A. Napier, R., Manning, K., King, G. and Bennett, M. 2001. Quick on the uptake: characterization of a family of plant auxin influx carriers. J. Plant Growth Regul. 20: 217-225.

Peng, J., Richards, D. E., Hartley, N. M. Murphy, G. P., Devos, K. M., Flintham, J. E., Beales, J., Fish, L. J., Worland, A. J., Pelica, F., Sudhakar, D., Christou, P., Snape, J. W., Gale, M. D. and Harberd, N. P. 1999. Green revolution genes encode mutant gibberellin response modulators. Nature. 400: 256-261.

Petrásek, J. and Friml, J. 2009. Auxin transport routes in plant development. Development. 136: 2675-2688.

Petrášek, J., Mravec, J., Bouchard, R., Blakeslee, J., Abas, M., Seifertová, D., Wísniewska, J., Tadele, Z., Kubeš, M., Č ovanová, M. Dhonukshe, P., Skupa, P., Benková, E., Perry, L., Krecek, P., Lee, O. R., Fink, G. R., Geisler, M., Murphy, A. S., Luschnig, C., Zazímalová, E. and Friml, J. 2006. PIN proteins perform a rate-limiting function in cellular auxin efflux. Science. 312:914-918.

Pigliucci, M. 2005. Evolution of phenotypic plasticity: where are we going now? Trends Ecol. Evol. 20: 481-486.

Pischke, M.S., Jones L.G., Otsuga D., Fernandez D.E., Drews G.N. and Sussman M.R. 2002. An *Arabidopsis* histidine kinase is essential for megagametogenesis. Proc. Natl. Acad. Sci. USA. 99: 15800-15805.

Powell, G.K. and Morris, R.O. 1986. Nucleotide sequence and expression of *Pseudomonas savastanoi*cytokinin biosynthetic gene: homology with *Agrobacterium tumefacienstmr*and *tzs*loci. Nucleic Acids Res. 14: 2555-2565.

Prusinkiewicz, P., Crawford, S., Smith, R.S., Ljung, K., Bennett, T., Ongaro, V. and Leyser, O. 2009. Control of bud activation by an auxin transport switch.Proceedings of the Nat. Acad. Sci. USA. 106: 17431-17436.

Rashotte, A. M. and Goertzen, L. R. 2010. The CRF domain defines cytokinin response factor proteins in plants. BMC Plant Biol.10: 74.

Rashotte, A., Mason, M., Hutchison, C., Ferreira, F., Schaller, G.E. and Kieber, J.J. 2006. A subset of *Arabidopsis* AP2 transcription factors mediate cytokinin responses in concert with a two-component pathway. Proc. Natl. Acad. Sci. USA 103: 11081-11085.

Raven, J. 1975. Transport of indolacetic acid in plant cells in relation to pH and electrical potential gradients, and its significance for polar IAA transport.New Phytol. 74: 163-172.

Redig, P., Schmülling, T. and Van Onckelen, H. 1996.Analysis of cytokinin metabolism in *ipt* transgenic tobacco by liquid chromatography-tandem mass spectrometry. Plant Physiol. 122: 141-148.

Ringnér, M. 2008. What is principal component analysis? Nature Biotech. 26: 303-304.

Riou-Khamlichi, C., Huntley, R., Jacqmard, A.and Murray, J.A. 1999. Cytokinin activation of *Arabidopsis* cell division through a D-type cyclin. Science. 283: 1541-1544.

Robert, H.S. and Friml, J. 2009. Auxin and other signals on the move in plants. Nature Chem. Biol. 5(5): 325-332.

Rosegrant, M.W. and Cline S.A. 2003. Global Food Security: Challenges and Policies. Science.302: 1917-1919.

Rubery, P.H. and Sheldrake, A.R. 1974.Carrier-mediated auxin transport.Planta. 118:101-121.

Ruyter-Spira, C., Kohlen, W., Charnikhova, T., van Zeijl, A., van Bezouwen, L., de Ruijter, N., Cardoso, C., Lopez-Raez, J. A., Matusova, R., Bours, R., Verstappen, F. and Bouwmeester, H. 2011. Physiological effects of the synthetic strigolactone analog GR24 on root system architecture in *Arabidopsis*: Another belowground role for strigolactones? Plant Physiol. 155(2): 721-734.

Ruyter-Spira, C., Al-Babili, S., van der Krol, S. and Bouwmeester, H. 2013.The biology of strigolactones. Trends Plant Sci. 18(2): 72-83

Sachs T. 1981. The control of the patterned differentiation of vascular tissues. Adv. Bot. Res. 9: 151-262.

Sachs, T. and Thimann, K. 1967.The role of auxins and cytokinins in the release of buds from dominance. Am. J. Bot. 54: 136-144.

Sakakibara, H. 2006. Cytokinins: Activity, biosynthesis, and translocation. Annu. Rev. Plant Biol. 57: 431-449.

Sakakibara, H. 2005. Cytokinin biosynthesis and metabolism. In Davies PJ, ed, Plant Hormones: Biosynthesis, Signal Transduction, Action. Kluwer Academic Publishers, Boston. pp. 95-114.

Sakamoto, T. and Matsuoka, M. 2004.Generating high-yielding varieties by genetic manipulation of plant architecture.Curr.Opin.Biotech. 15: 144-147.

Samuelson, M.E., Eliasson, L. and Larsson, C.M. 1992.Nitrate-regulated growth and cytokinin responses in seminal roots of barley.Plant Physiol. 98: 309-315.

Santelia, D., Vincenzetti, V., Azzarello, E., Bovet, L., Fukao, Y., Düchtig, P., Mancuso S., Martinoia, E. and Geisler, M. 2005. MDR-like ABC transporter AtPGP4 is involved in auxin-mediated lateral root and root hair development. FEBS Lett. 579: 5399-5406.

Santner, A.Calderon-Villalobos, L.I.A. and Estelle, M. 2009. Plant hormones are versatile chemical regulators of plant growth. Nat. Chem. Biol. 5: 301-307.

Schmitz, G. and Theres, K. 2005. Shoot and inflorescence branching. Curr.Opin. Plant Biol. 8(5): 506-511.

Schmülling, T. 2004. Cytokinin.In Encyclopedia of Biological Chemistry (Eds. Lennarz, W., Lane, M.D.)Academic Press/Elsevier Science.

Schmülling, T., Werner, T., Riefler, M., Kruplová, E. and Bartina y Manns, I. 2003.Structure and function of cytokinin oxidase/dehydrogenase genes of maize, rice, *Arabidopsis* and other species. J. Plant Res. 116: 241-252.

Schnorr, K. M., Gaillard, C., Biget, E., Nygaad, P. and Laloue, M. 1996. A second form of adenine phosphoribosyltransferase in *Arabidopsis thaliana* with relative specificity towards cytokinins. Plant J. 9: 891-898.

Schoor, S., Farrow, S., Blaschke, H., Lee, S., Perry, G., Von-Schwartzenberg, K., Emery, N. and Moffatt, B. 2011. Adenosine kinase contributes to cytokinin interconversion in *Arabidopsis*. Plant Physiol. 157: 659-672.

Schwartz, S.H., Qin, X. and Loewen, M.C. 2004. The biochemical characterization of two carotenoid cleavage enzymes from *Arabidopsis* indicates that a carotenoid-derived compound inhibits lateral branching. J. Biol. Chem. 279: 46940-46945.

Sergeant, M.J., Li, J.J., Fox, C., Brookbank, N., Rea, D., Bugg, T.D. and Thompson, A.J. 2009. Selective inhibition of carotenoid cleavage dioxygenases: phenotypic effects on shoot branching. J. Biol. Chem. 284: 5257-5264.

Seto, Y., Kameoka, H., Yamaguchi, S. and Kyozuka, J. 2012. Recent Advances in Strigolactone Research: Chemical and Biological Aspects. Plant Cell Physiol. 53 (11): 1843-1853.

Shen, H., Luong, P. and Huq, E. 2007. The F-box protein MAX2 functions as a positive regulator of photomorphogenesis in *Arabidopsis*. Plant Physiol. 145:1471-1483.

Shimizu, S. and Mori, H. 1998. Analysis of Cycles of Dormancy and Growth in Pea Axillary Buds Based on mRNA Accumulation Patterns of Cell Cycle-Related Genes. Plant Cell Physiol 39: 255-262.

Shimizu-Sato, S., Tanaka, M. and Mori, H. 2009.Auxin–cytokinin interactions in the control of shoot branching. Plant Mol. Biol. 69:429-435.

Shimizu-Sato, S. and Mori, H. 2001.Control of outgrowth and dormancy in axillary buds. Plant Physiol. 127: 1405-1413.

Shinohara, N., Taylor, C. and Leyser, O. 2013. Strigolactone Can Promote or Inhibit Shoot Branching by Triggering Rapid Depletion of the Auxin Efflux Protein PIN1 from the Plasma Membrane. PLOS Biol. 11(1): 1-14.

Siedow J. N. 2001. Feeding Ten Billion People, Three Views. Plant Physiol. 126: 20-22.

Simons, J.L., Napoli, C.A., Janssen, B.J., Plummer, K.M. and Snowden, K.C. 2007.Analysis of the Decreased Apical Dominance genes of Petunia in the control of axillary branching. Plant Physiol. 143: 697-706.

Skoog, F. and Armstrong, D. J. 1970.Cytokinins.Annu. Rev. Plant. Physiol. 21: 359-384.

Skoog, F., Armstrong, D. J., Cherayil, J. D., Hampel, A. E. and Bock, R. M. 1966. Cytokinin activity: localization in transfer RNA preparations. Science. 154: 1354-1356.

Šmehilová, M., Galuszka, P., Bilyeu, K.D., Jaworek, P., Kowalska, M., Šebela, M., Sedlářová,.M., English, J.T. and Frébort, I. 2009.Subcellular localization and biochemical comparison of cytosolic and secreted cytokinin dehydrogenase enzymes from maize. J. Exp. Bot. 60:2701-2712.

Snow, R. 1929. The young leaf as the inhibiting organ. New Phytol.28**:** 345-358.

Snow, R. 1931. Experiments on Growth and Inhibition. Part II.New Phenomena of Inhibition.Proc. Roy. Soc. B. 108**:** 305-316.

Snow, R. 1932. Experiments on growth and inhibition.Part III- Inhibition and Growth Promotion. Proc. Roy. Soc. B. 111(769): 86-105.

Snow, R. 1937.On the nature of correlative inhibition.New Phytol.36(4): 283-300.

Snowden, K.C., Simkin, A.J., Janssen, B.J., Templeton, K.R., Loucas, H.M., Simons, J.L., Karunairetnam, S., Gleave, A.P., Clark, D.G. and Klee, H.J. 2005. The *decreased apical dominance1*/Petunia hybrida *Carotenoid Cleavage Dioxygenase8* gene affects branch production and plays a role in leaf senescence, root growth and flower development. Plant Cell. 17:746-759.

Snyder, W.E. 1949. Some responses pf plants to 2, 3, 5-triiodo-benzoic acid. Plant Physiol. 23: 195-206.

Sorefan, K., Booker, J., Haurogné, K., Goussot, M., Bainbridge, K., Foo, E., Chatfield, S., Ward, S., Beveridge, C., Rameau, C. and Leyser, O. 2003. *MAX4* and *RMS1* are orthologous dioxygenase-like genes that regulate shoot branching in *Arabidopsis* and pea. Genes and Development. 17:1469-1474.

Sossountzoy, L., Maldiney, R., Sotta, B., Sabbagh, I., Habricot, Y., Bonnet, M. and Miginiac, E.1988.Immunocytochemical localization of cytokinins in Craigella tomato and a sideshootless mutant.Planta. 175: 291-304.

Stirnberg, P., Chatfield, S.P. and Leyser, H.M.O. 1999.AXR1 acts after lateral bud formation to inhibit lateral bud growth in *Arabidopsis*. Plant Physiol. 121: 839-847.

Stirnberg, P., Furner, I.J. and Leyser, H.M.O. 2007. MAX2 participates in an SCF complex which acts locally at the node to suppress shoot branching. Plant J. 50: 80-94.

Stirnberg, P., van de Sande, K. and Leyser, H.M.O. 2002.*MAX1* and *MAX2* control shoot lateral branching in *Arabidopsis*. Development. 129: 1131-1141.

Suzuki, S., Miwa, K., Ishikawa, K., Yamada, H., Aiba, H. and Mizuno, T. 2001. The *Arabidopsis* sensor His-kinase, AHK4, can respond to cytokinins. Plant Cell Physiol. 42: 107-113.

Swarup, K., Benková, E., Swarup, R., Casimiro, I., Péret, B., Yang, Y., Parry, G., Nielsen, E., De Smet, I., Vanneste, S. Levesque, M. P., Carrier, D., James, N., Calvo, V., Ljung, K., Kramer, E., Roberts, R., Graham, N., Marillonnet, S., Patel, K., Jones, J. D., Taylor, C.G., Schachtman, D.P., May, S., Sandberg, G., Benfey, P., Friml, J., Kerr, I., Beeckman, T., Laplaze, L., Bennett, M. J. 2008. The auxin influx carrier LAX3 promotes lateral root emergence. Nat. Cell Biol. 10: 946-954.

Swarup, R., Friml, J., Marchant, A., Ljung, K., Sandberg, G., Palme, K. and Bennett, M. 2001. Localization of the auxin permease AUX1 suggests two functionally distinct hormone transport pathways operate in the *Arabidopsis* root apex. Genes Dev. 15:2648-2653.

Swarup, R., Kargul, J., Marchant, A., Zadik, D., Rahman, A., Mills, R., Yemm, A., May, S., Williams, L., Millner, P., Tsurumi, S., Moore, I., Napier, R., Kerr, I.D., Bennett, M.J. 2004.Structure-function analysis of the presumptive *Arabidopsis* auxin permease AUX1.Plant Cell. 16:3069-3083.

Takei, K., Dekishima Y, Eguchi T, Yamaya T, Sakakibara H. 2003. A new method for enzymatic preparation of isopentenyladenine-type and *trans*-zeatin-type cytokinins with radioisotope-labeling. J. Plant Res. 116(3):259-263.

Takei, K., Sakakibara, H. and Sugiyama, T. 2001a. Identification of genes encoding adenylate isopentenyltransferase, a cytokinin biosynthesis enzyme, in *Arabidopsis thaliana*. J. Biol. Chem. 276: 26405-26410.

Takei, K., Sakakibara, H., Taniguchi, M. and Sugiyama T. 2001b. Nitrogen dependent accumulation of cytokinins in root and the translocation to leaf: Implication of cytokinin species that induces gene expression of maize response regulator. Plant Cell Physiol. 42: 85-93.

Takei, K., Takahashi, T., Sugiyama, T., Yamaya, T. and Sakakibara, H.2002. Multiple routes communicating nitrogen availability from roots to shoots: A signal transduction pathway mediated by cytokinin. J. Exp. Bot. 53: 971-977.

Takei, K., Ueda, N., Aoki, K., Kuromori, T., Hirayama, T., Shinozaki, K., Yamaya, T. and Sakakibara, H. 2004a. AtIPT3 is a key determinant of nitrate-dependent cytokinin biosynthesis in *Arabidopsis*. Plant Cell Physiol. 45(8): 1053-1062.

Takei, K., Yamaya, T. and Sakakibara, H. 2004b. Arabidopsis CYP735A1 and CYP735A2 encode cytokinin hydroxylases that catalyze the biosynthesis of *trans*-zeatin. J. Biol.Chem. 279: 41866-41872.

Tamas, I.A., Schlossberg-Jacobs, J.L., Lim, R., Friedman, L.B. and Barone, C.C. 1989.Effect of plant growth substances on the growth of axillary buds in cultured stem segments of *Phaseolus vulgaris* L. Plant Growth Regul. 8: 165-183.

Tanaka, M., Takei, K., Kojima, M., Sakakibara, H. and Mori, H. 2006. Auxin controls local cytokinin biosynthesis in the nodal stem in apical dominance. Plant J. 45:1028-1036.

Terasaka, K., Blakeslee, J. J., Titapiwatanakun, B., Peer, W. A., Bandyopadhyay, A., Makam, S. N., Lee, O. R., Richards, E. L., Murphy, A. S., Sato, F. and Yazaki, K. 2005. PGP4, an ATP binding cassette P-glycoprotein, catalyzes auxin transport in *Arabidopsisthaliana* roots. Plant Cell. 17:2922-2939.

Thimann, K.V. and Skoog, F. 1933. Studies on the growth hormones of plants. III. The inhibition action of growth substance on bud development. Proc. Natl. Acad. Sci.U.S.A.19: 714-716.

Thimann, K.V. and Skoog, F. 1934. On the inhibition of bud development and other functions of growth substance in *Vicia faba*. Proc. R. Soc. Lond. B Biol. Sci. 114: 317-339.

To, J.P., Haberer, G., Ferreira, F.J., Deruere, J., Mason, M.G., Schaller, G.E., Alonso, J.M., Ecker, J.R. and Kieber, J.J. 2004. Type-A *Arabidopsis*response regulators are partially redundant negative regulators of cytokinin signalling. Plant Cell.16: 658-671.

To, J. P. and Kieber, J. J. 2008. Cytokinin signalling: two-components and more. Trends Plant Sci. 13: 85-92.

Tsuchiya, Y. and McCourt, P. 2009. Strigolactones: a new hormone with a past. Curr.Opin. Plant Biol. 12(5):556-61.

Turnbull, C.G., Booker, J.P. and Leyser, O. 2002.Micrografting techniques for testing long-distance signalling in *Arabidopsis*. Plant J 32: 255-262.

Turnbull, C.G.N., Raymond, M.A.A., Dodd, I.C. and Morris, S.E. 1997. Rapid increases in cytokinin concentration in lateral buds of chickpea (*Cicer arietinum* L.) during release of apical dominance. Planta.202: 271-276.

Ueguchi, C., Sato, S., Kato, T. and Tabata, S. 2001. The *AHK4* gene involved in the cytokinin-signalling pathway as a direct receptor molecule in *Arabidopsis thaliana*. Plant Cell Physiol. 42: 751-755.

Umehara, M., Hanada, A., Yoshida, S., Akiyama, K., Arite, T., Takeda-Kamiya, N., Magome, H., Kamiya, Y., Shirasu, K., Yoneyama, K., Kyozuka, J. and Yamaguchi, S. 2008. Inhibition of shoot branching by new terpenoid plant hormones.Nature. 455:196-200.

Van Staden, J. and Smith, A.R. 1978. The synthesis of cytokinins in excised roots of maize and tomato under aseptic conditions. Ann. Bot. 42: 751-753.

Veit, B. (2009). Hormone mediated regulation of the shoot apicalmeristem. Plant Mol. Biol. 69: 397-408.

Verrier, P., Bird, D., Buria, B., Dassa, E., Forestier, C., Geisler, M., Klein, M., Kolukisaoglu, U., Lee, Y., Martinoia, E. Murphy, A., Rea, P.A., Samuels, L., Schulz, B., Spalding, E.J., Yazaki, K.and Theodoulou, F.L. 2008. Plant ABC proteins - a unified nomenclature and updated inventory. Trends Plant Sci. 13: 151-159.

Vieten, A., Sauer, M., Brewer, P. B. and Friml, J. 2007. Molecular and cellular aspects of auxin-transport-mediated development. Trends Plant Sci. 12: 160-168.

Vogel, J.T., Walter, M.H., Giavalisco, P., Lytovchenko, A., Kohlen, W., Charnikhova, T., Simkin, A.J., Goulet, C., Strack, D., Bouwmeester, H.J., Fernie, A.R. and Klee, H.J. 2010.SlCCD7 controls strigolactone biosynthesis, shoot branching and mycorrhiza-induced apocarotenoid formation in tomato. Plant J. 61: 300-311.

Vogler, H. and Kuhlemeier, C. 2003. Simple hormones but complex signalling.Curr. Opin Plant Biol. 6(1): 51-56.

Vreman, H.J. and Skoog, F. 1972. Cytokinins in *Pisum*transfer ribonucleic acid. Plant Physiol. 49:848-851.

Vreman, H. J., Thomas, R. and Corse,J. 1978. Cytokinins in tRNA obtained from *Spinacia olearacea* L. leaves and isolated chloroplasts. Plant Physiol. 61: 296-306.

Vysotskaya, L.B., Veselov, S.Y.and Kudoyarova, G.R. 2010. Effect on shoot water relations, and cytokinin and abscisic acid levels of inducing expression of a gene coding for isopentenyltransferase in roots of transgenic tobacco plants. J. Exp. Bot. 61(13): 3709-3717.

Wang, Y. and Li, J. 2008. Molecular Basis of Plant Architecture.Annu. Rev. Plant Biol. 59: 253-279.

Wang, Y. and Li, J. 2006. Genes controlling plant architecture.Curr.Opin.Biotechnol.17: 123-129.

Ward, S.P. and Leyser, O. 2004. Shoot branching. Curr.Opin. Plant Biol. 7: 73-78.

Waters, M.T., Brewer, P.B., Bussell, J.D., Smith, S.M. and Beveridge, C.A. 2012.The *Arabidopsis*ortholog of rice *DWARF27* acts upstream of *MAX1* in the control of plant development by strigolactones. Plant Physiol. 159: 1073-1085.

Weigel, D. and Glazebrook, J. 2002. Arabidopsis: A Laboratory Manual. Cold Spring Harbor Laboratory Press, Cold Spring Harbor, New York. pp:168-169.

Werner, T., Motyka, V., Laucou, V., Smets, R., Van Onckelen, H. and Schmulling, T. 2003.Cytokinin-deficient transgenic *Arabidopsis* plants show multiple developmental alterations indicating opposite functions of cytokinins in the regulation of shoot and root meristem activity. Plant Cell.15: 2532-2550.

Werner, T., Motyka, V., Strnad, M. and Schmulling, T. 2001.Regulation of plant growth by cytokinin. Proc. Natl. Acad. Sci. USA. 98: 10487-10492.

Werner, T., Nehnevajova, E., Köllmer, I., Novák, O., Strnad, M., Krämer, U. and Schmülling, T. 2010. Root-specific reduction of cytokinincauses enhanced root growth, drought tolerance and leaf mineral enrichment in Arabidopsis and Tobacco. Plant Cell.22(12): 3905-3920.

Whitty, C.D. and Hall, R.H. 1974.A cytokinin oxidase in Zea mays. Can. J. Biochem.;52:787-799.

Wilson, Z.A. and Yang, C. 2004. Plant gametogenesis: conservation and contrasts in development. Reproduction. 128:483-492.

Wisniewska, J., Xu, J., Seifertová, D., Brewer, P.B. Ruzicka, K., Blilou, I., Rouquié, D., Benková, e., Scheres, B. and Friml, J. 2006. Polar PIN Localization Directs Auxin Flow in Plants. Science. 312 (5775): 883.

Wormit, A., Traub, M., Flörchinger, M., Neuhaus, H. E. and Möhlmann, T. 2004.Characterization of three novel members of the *Arabidopsis thaliana* equilibrative nucleoside transporter (ENT) family. Biochem J. 383: 19-26.

Xie, X., Yoneyama K. and Yoneyama K. 2010.The strigolactone story.Annu. Rev. Phytopathol. 48:93-117.

Yamada, H., Suzuki, T., Terada, K., Takei, K., Ishikawa, K., Miwa, K., Yamashino, T. and Mizuno, T. 2001. The *Arabidopsis* AHK4 histidine kinase is a cytokinin-binding receptor that transduces cytokinin signals across the membrane. Plant Cell Physiol. 42: 1017-1023.

Yang, X.C. and Hwa, C.M. 2008.Genetic modification of plant architecture and variety improvement in rice. Heredity.101:396-404.

Yang, Y., Hammes, U. Z., Taylor, C. G., Schachtman, D. P. and Nielsen, E. 2006.High-affinity auxin transport by the AUX1 influx carrier protein. Curr. Biol. 16:1123-1127.

Yokota, T., Sakai, H., Okuno, K., Yoneyama, K. and Takeuchi, Y. 1998. Alectrol and orobanchol, germination stimulants for *Orobanche minor* from its host red clover. Phytochemistry. 49: 1967-1973.

Yoneyama, K., Xie, X., Kusumoto, D., Sekimoto, H., Sugimoto, Y., Takeuchi, Y. and Yoneyama, K. 2007. Nitrogen deficiency as well as phosphorusdeficiency in sorghum promotes the production and exudation of 5-deoxystrigol, the host recognition signal for arbuscular mycorrhizalfungi and root parasites. Planta.227: 125-132

Yoneyama, K., Xie, X., Sekimoto, H., Takeuchi, Y., Ogasawara, S. and Akiyama, K. 2008. Strigolactones, host recognition signals for root parasitic plants and arbuscular mycorrhizal fungi, from Fabaceae plants. NewPhytol.179:484–492.

Yoneyama, K., Xie, X., Yoneyama, K. and Takeuchi, Y. 2009. Strigolactones: structures and biological activities. Pest Manag. Sci. 65(5):467-470

Zažímalová, E., Křeček, P., Skůpa, P., Hoyerová, K. and Petrášek, J. 2007. Polar transport of the plant hormone auxin – the role of PIN-FORMED (PIN) proteins. Cell. Mol. Life Sci. 64: 1621-1637.

Zhao Y. 2010. Auxin biosynthesis and its role in plant development.Annu. Rev. Plant Biol. 61:49-64.

Zimmermann, P., Hirsch-Hoffmann, M., Hennig, L. and Gruissem, W. 2004.GENEVESTIGATOR.Arabidopsis microarray database and analysis toolbox. Plant Physiol.136: 2621-2632.

Zou, J., Zhang, S., Zhang, W., Li, G., Chen Z., Zhai W., Zhao, X., Pan, X., Xie, Q. and Zhu, L. 2006. The rice HIGH-TILLERING *DWARF1* encoding an ortholog of *ArabidopsisMAX3* is required for negative regulation of the outgrowth of axillary buds. Plant J. 48: 687-698.

Zubko, E., Adams, C.J., Machaekova, I., Malbeck, J., Scollan, C. and Meyer, P. 2002. Activation tagging identifies a gene from Petunia hybrida responsible for the production of active cytokinins in plants. Plant J. 29:797–808.

APPENDICES

Appendix I

A- Cytokinin Biosynthetic Pathway (Taken from Kamada-Nobusada and Sakakibara, 2009)

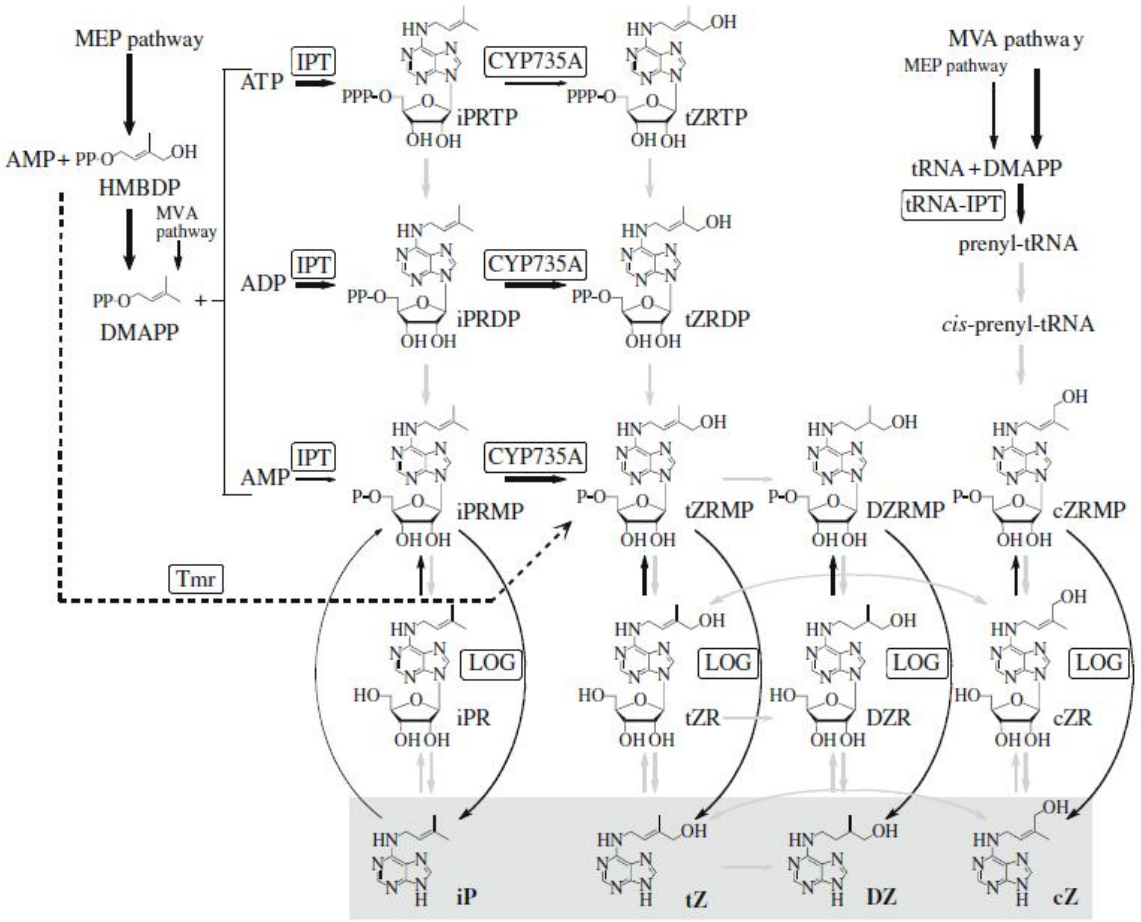

B- *N*-Glycosylation of Cytokinins (Taken from Bajguz and Piotrowska, 2009)

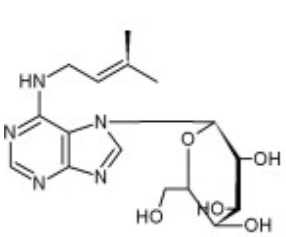

7-β-Glucosyl-*N*^{6}-(Δ^2-isopentenyl)adenine

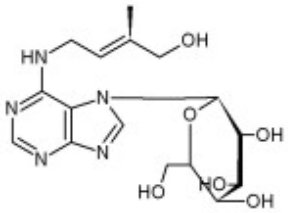

7-β-Glucosylzeatin

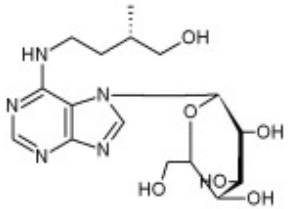

7-β-Glucosyldihydro-zeatin

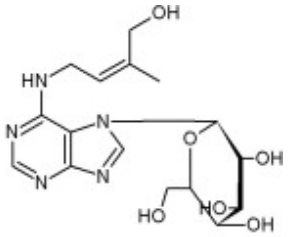

7-β-Glucosyl-*cis*-zeatin

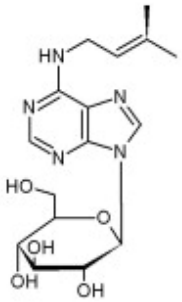

9-β-Glucosyl-*N*^{6}-(Δ^2-isopentenyl)adenine

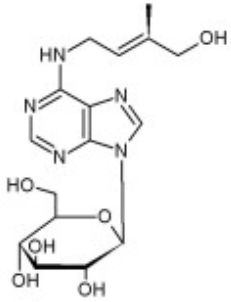

9-β-Glucosylzeatin

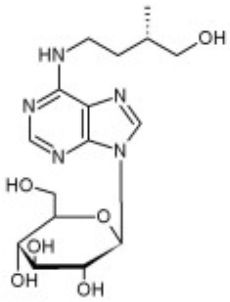

9-β-Glucosyldihydro-zeatin

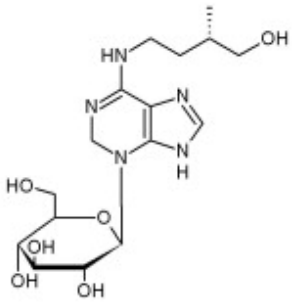

3-β-Glucosyldihydro-zeatin

C- *O*-Glycosylation of Cytokinins (Taken from Bajguz and Piotrowska, 2009)

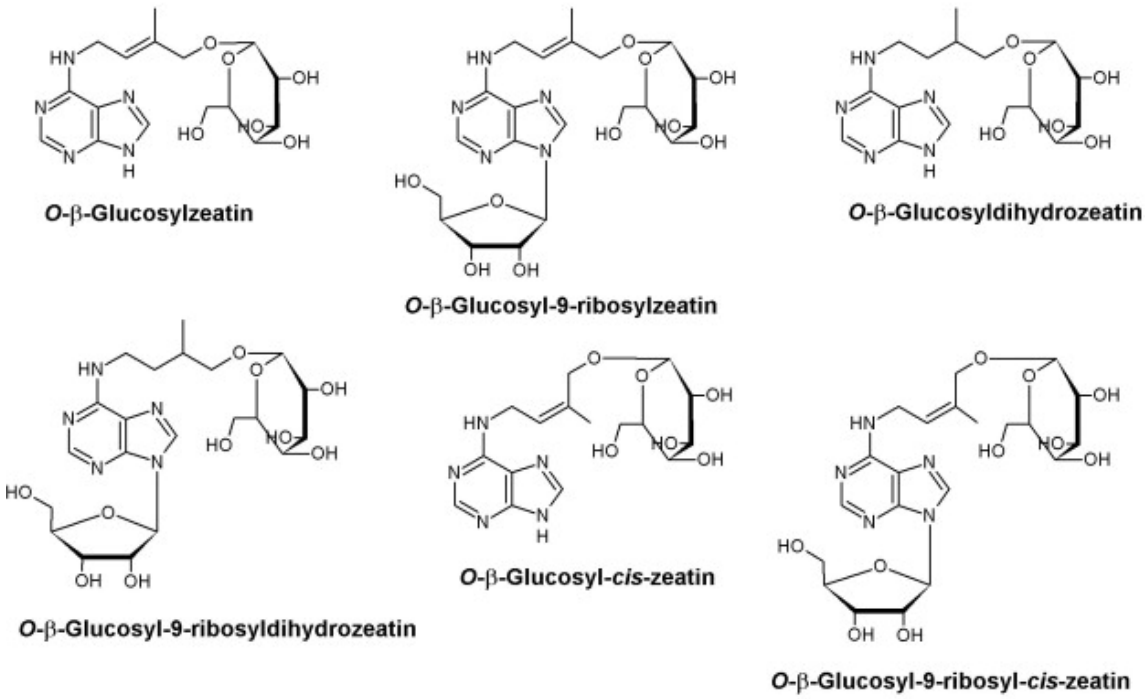

Appendix II

A- Information for genotyping of *max2-1* mutant allele

MAX2 wild-type Nucleotide Sequence

atggcttccactactctctccgacctccctgacgtcatcttatccaccatttcctctctc
gtatccgattcccgagctcgcaactctctctccctcgtctctcacaaattcctcgctctc
gaacgatccactcgctctcacctcactatccgtggcaacgctcgtgatctctccctcgtc
cccgactgtttccgatcaatctcacatctcgatctctctttcctctccccatggggtcac
actcttctcgcttctctcccaatcgatcaccagaaccttctcgctctccgtctcaaattc
tgtttccctttcgtcgagtctctaaacgtctacacacgatctccgagctctctcgagctt
ctacttcctcaatggccgagaattcgccacatcaagctcctccgatggcatcaacgagct
tctcagatccctaccggtggcgattttgttcctatttttgaacactgtggtggtttcctt
gagtctttagatctctccaacttctatcactggactgaagacttacctcctgtgcttctc
cgctatgctgacgtggcggcgaggcttacacggttagatctcttgacggcgtcgttcacc
gagggatacaaatcaagcgaaatcgttagtatcaccaaatcttgccctaatttgaagact
tttcgtgtagcttgtacgtttgatccgagatactttgaattcgtcggagacgagactctc
tccgccgtagctaccagttcccctaagttaacgcttctacacatggtggacacagcttcg
ttggcgaatcctagagctattccaggtacggaagctggagattcagctgtcacggcgggg
acgctaattgaagttttctcaggtttaccgaatctagaggagctggttcttgacgtagga
aaggatgtgaagcatagtggtgtagctttagaggcattgaattctaaatgcaagaagtta
agagtattgaagctaggacagttccaaggtgtttgctctgctacagaatggaggaggctc
gacggtgtggctttatgtggaggattgcagtcgttgtcgattaagaattccggcgatttg
actgatatgggtttggtggctatagggagaggatgttgtaagttgactacgtttgagatt
caagggtgtgagaatgtaacagtggatggactaagaacaatggttagtcttcggagtaag
actttgactgatgtgagaatctcttgctgcaagaatcttgacacagctgcttctttaaag
gcaattgagccgatttgtgatcggatcaagagactgcatatagactgtgtgtggtctggt
tcagaggacgaggaggtagaaggaagagtggaaactagtgaggctgaccacgaagaggag
gatgatggttacgagaggagccagaagaggtgcaagtattcattcgaggaagaacactgc
tcaactagtgatgtgaatggattctgttctgaagatagagtatgggagaaactggagtat
ctatctttatggatcaatgttggagaatttttgacgccattacctatgacaggactagat
gactgtccgaatttggaagagattaggatcaagatagaaggagattgcagaggtaaacgc
aggccagccgagccagagtttgggttaagttgtctcgctctctacccaaagctctcaaag
atgcagttagattgcggggacacaatcggtttcgcactgaccgcaccgccaatgcagatg
1740
gattgagtttatgggaaagattcttcttgaccggaattggaagcttgagcttgagcgag
cttgattattggccaccacaggatagagatgttaaccagaggagtctctcgcttcctgga
gcaggtctgttacaagagtgcctgactttgaggaagctgttcatccatggaacagctcat
gagcatttcatgaacttttttgttgagaatcccaaacttaagggatgtacagcttagagca
gactattatccggcgccggagaacgatatgagcacagagatgagagttggttcgtgtagc
cgattcgaggaccaattgaacagccgcaacatcattgactga

max2-1 mutant Nucleotide Sequence

atggcttccactactctctccgacctccctgacgtcatcttatccaccatttcctctctc
gtatccgattcccgagctcgcaactctctctccctcgtctctcacaaattcctcgctctc
gaacgatccactcgctctcacctcactatccgtggcaacgctcgtgatctctccctcgtc
cccgactgtttccgatcaatctcacatctcgatctctctttcctctccccatggggtcac
actcttctcgcttctctcccaatcgatcaccagaaccttctcgctctccgtctcaaattc
tgtttccctttcgtcgagtctctaaacgtctacacacgatctccgagctctctcgagctt
ctacttcctcaatggccgagaattcgccacatcaagctcctccgatggcatcaacgagct
tctcagatccctaccggtggcgattttgttcctatttttgaacactgtggtggtttcctt
gagtctttagatctctccaacttctatcactggactgaagacttacctcctgtgcttctc
cgctatgctgacgtggcggcgaggcttacacggttagatctcttgacggcgtcgttcacc
gagggatacaaatcaagcgaaatcgttagtatcaccaaatcttgccctaatttgaagact
tttcgtgtagcttgtacgtttgatccgagatactttgaattcgtcggagacgagactctc
tccgccgtagctaccagttcccctaagttaacgcttctacacatggtggacacagcttcg
ttggcgaatcctagagctattccaggtacggaagctggagattcagctgtcacggcgggg
acgctaattgaagttttctcaggtttaccgaatctagaggagctggttcttgacgtagga
aaggatgtgaagcatagtggtgtagctttagaggcattgaattctaaatgcaagaagtta
agagtattgaagctaggacagttccaaggtgtttgctctgctacagaatggaggaggctc
gacggtgtggctttatgtggaggattgcagtcgttgtcgattaagaattccggcgatttg
actgatatgggtttggtggctatagggagaggatgttgtaagttgactacgtttgagatt
caagggtgtgagaatgtaacagtggatggactaagaacaatggttagtcttcggagtaag
actttgactgatgtgagaatctcttgctgcaagaatcttgacacagctgcttctttaaag
gcaattgagccgatttgtgatcggatcaagagactgcatatagactgtgtgtggtctggt
tcagaggacgaggaggtagaaggaagagtggaaactagtgaggctgaccacgaagaggag
gatgatggttacgagaggagccagaagaggtgcaagtattcattcgaggaagaacactgc
tcaactagtgatgtgaatggattctgttctgaagatagagtatgggagaaactggagtat
ctatctttatggatcaatgttggagaatttttgacgccattacctatgacaggactagat
gactgtccgaatttggaagagattaggatcaagatagaaggagattgcagaggtaaacgc
aggccagccgagccagagtttgggttaagttgtctcgctctctacccaaagctctcaaag
atgcagttagattgcggggacacaatcggtttcgcactgaccgcaccgccaatgcagatg
1740
aatttgagtttatgggaaagattcttcttgaccggaattggaagcttgagcttgagcgag
cttgattattggccaccacaggatagagatgttaaccagaggagtctctcgcttcctgga
gcaggtctgttacaagagtgcctgactttgaggaagctgttcatccatggaacagctcat
gagcatttcatgaacttttttgttgagaatcccaaacttaagggatgtacagcttagagca
gactattatccggcgccggagaacgatatgagcacagagatgagagttggttcgtgtagc
cgattcgaggaccaattgaacagccgcaacatcattgactga

Restriction enzymes site cut Map

2082 base pairs of MAX2 Wild-type

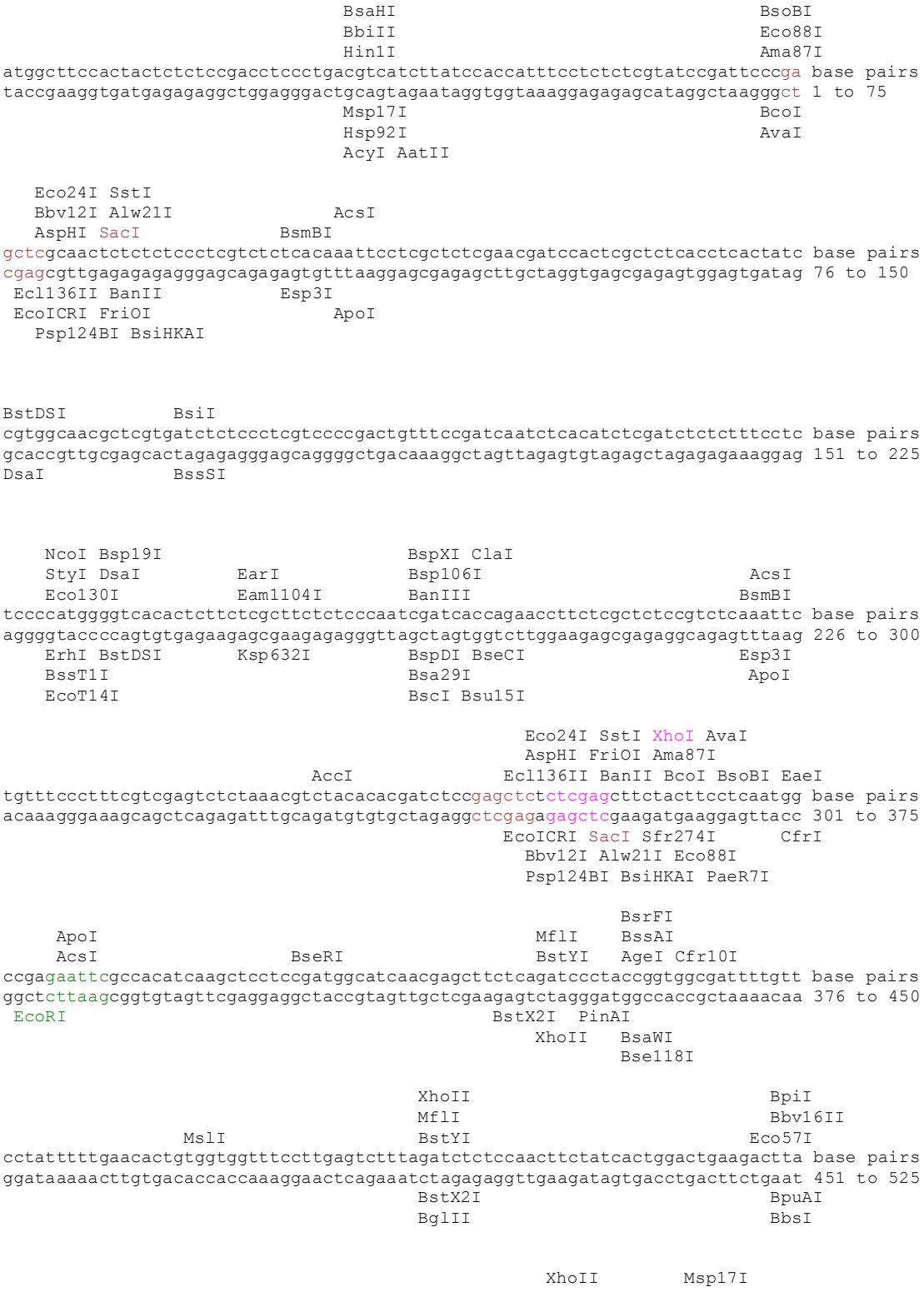

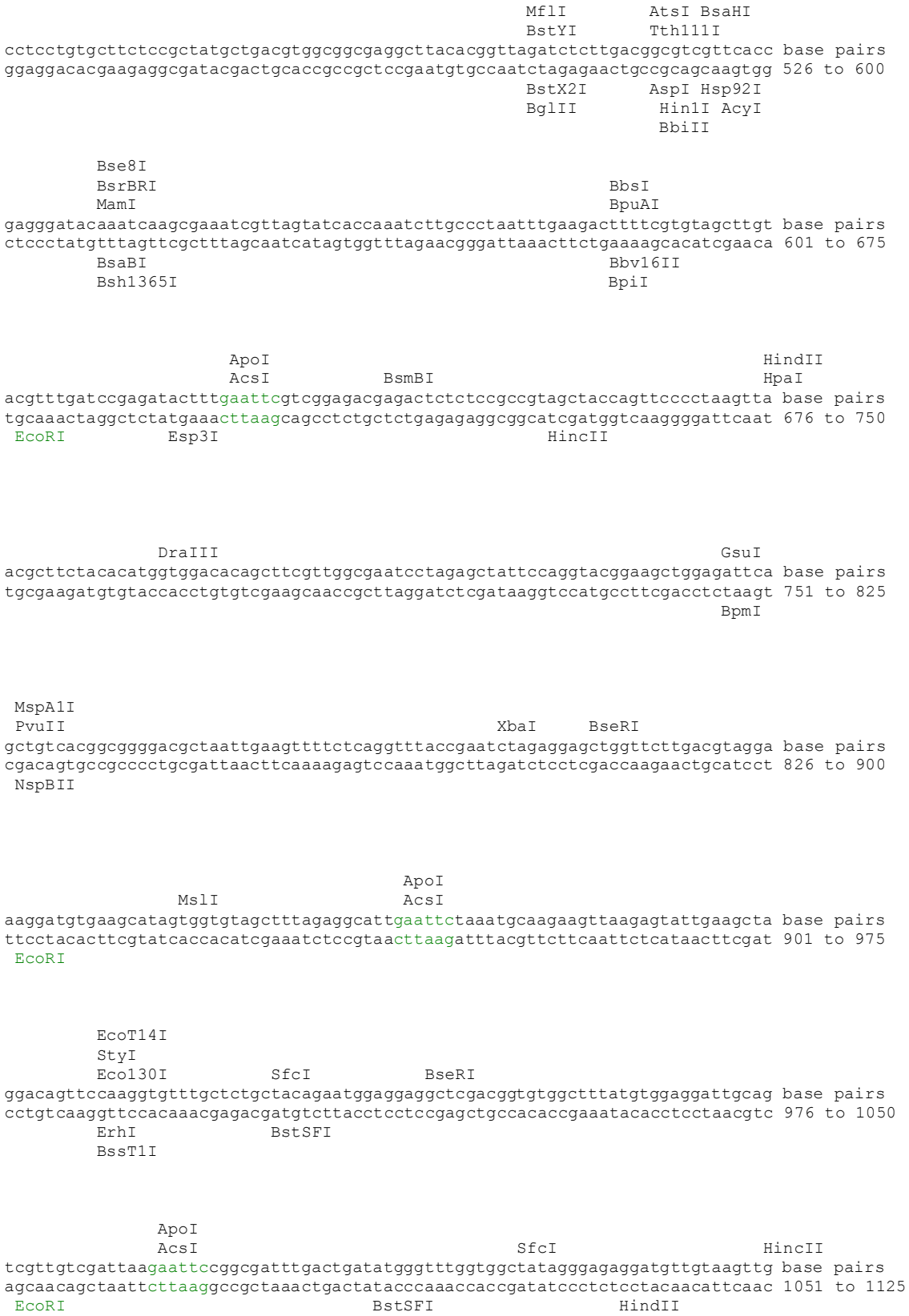
MflI AtsI BsaHI
BstYI Tth111I
cctcctgtgcttctccgctatgctgacgtggcggcgaggcttacacggttagatctcttgacggcgtcgttcacc base pairs
ggaggacacgaagaggcgatacgactgcaccgccgctccgaatgtgccaatctagagaactgccgcagcaagtgg 526 to 600
BstX2I AspI Hsp92I
BglII Hin1I AcyI
BbiII
Bse8I
BsrBRI BbsI
MamI BpuAI
gagggatacaaatcaagcgaaatcgttagtatcaccaaatcttgccctaatttgaagacttttcgtgtagcttgt base pairs
ctccctatgtttagttcgctttagcaatcatagtggtttagaacgggattaaacttctgaaaagcacatcgaaca 601 to 675
BsaBI Bbv16II
Bsh1365I BpiI
ApoI HindII
AcsI BsmBI HpaI
acgtttgatccgagatactttgaattcgtcggagacgagactctctccgccgtagctaccagttcccctaagtta base pairs
tgcaaactaggctctatgaaacttaagcagcctctgctctgagagaggcggcatcgatggtcaaggggattcaat 676 to 750
EcoRI Esp3I HincII
DraIII GsuI
acgcttctacacatggtggacacagcttcgttggcgaatcctagagctattccaggtacggaagctggagattca base pairs
tgcgaagatgtgtaccacctgtgtcgaagcaaccgcttaggatctcgataaggtccatgccttcgacctctaagt 751 to 825
BpmI
MspA1I
PvuII XbaI BseRI
gctgtcacggcggggacgctaattgaagttttctcaggtttaccgaatctagaggagctggttcttgacgtagga base pairs
cgacagtgccgcccctgcgattaacttcaaaagagtccaaatggcttagatctcctcgaccaagaactgcatcct 826 to 900
NspBII
ApoI
MslI AcsI
aaggatgtgaagcatagtggtgtagctttagaggcattgaattctaaatgcaagaagttaagagtattgaagcta base pairs
ttcctacacttcgtatcaccacatcgaaatctccgtaacttaagatttacgttcttcaattctcataacttcgat 901 to 975
EcoRI
EcoT14I
StyI
Eco130I SfcI BseRI
ggacagttccaaggtgtttgctctgctacagaatggaggaggctcgacggtgtggctttatgtggaggattgcag base pairs
cctgtcaaggttccacaaacgagacgatgtcttacctcctccgagctgccacaccgaaatacacctcctaacgtc 976 to 1050
ErhI BstSFI
BssT1I
ApoI
AcsI SfcI HincII
tcgttgtcgattaagaattccggcgatttgactgatatgggtttggtggctatagggagaggatgttgtaagttg base pairs
agcaacagctaattcttaaggccgctaaactgactatacccaaaccaccgatatccctctcctacaacattcaac 1051 to 1125
EcoRI BstSFI HindII

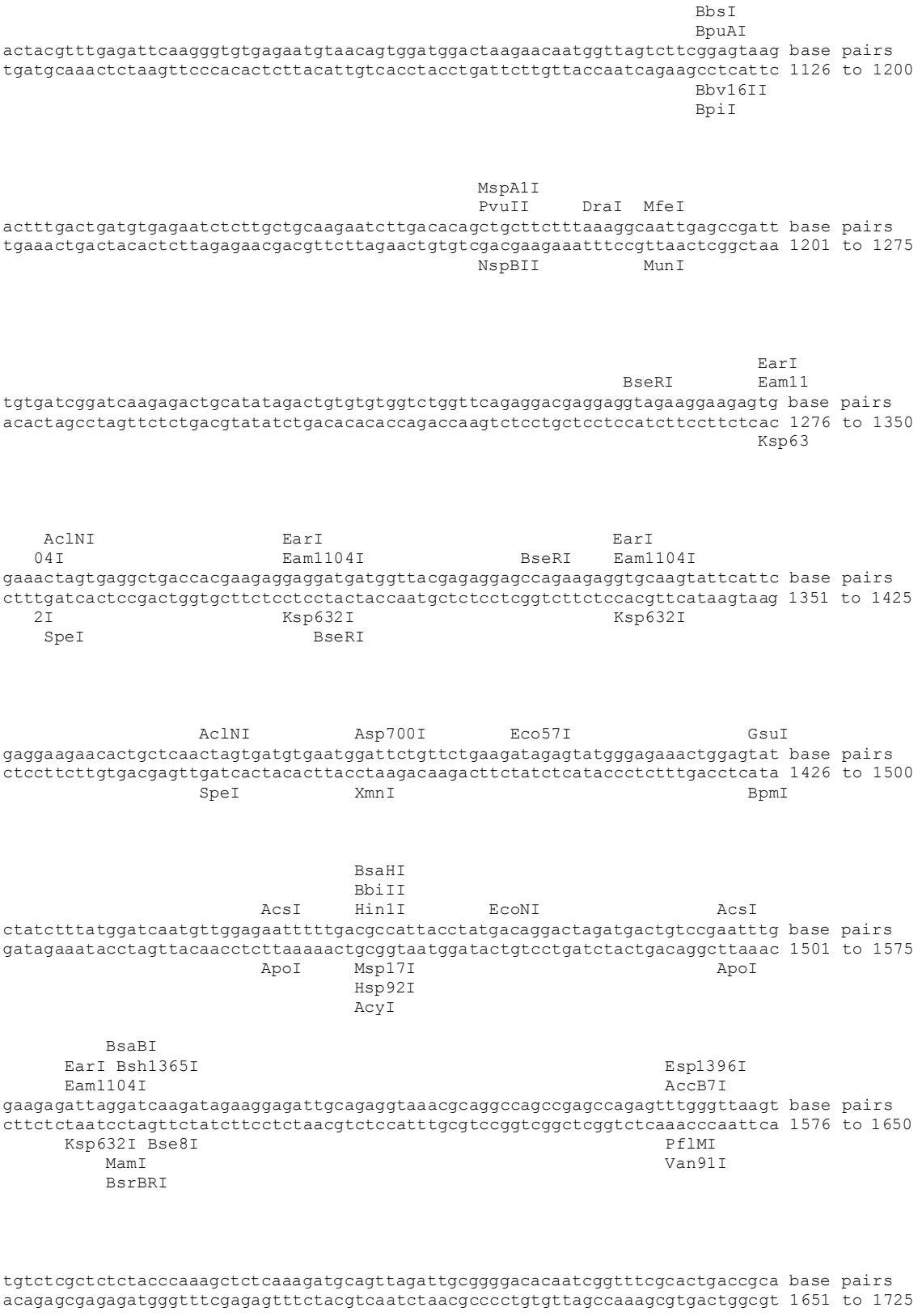
BbsI
BpuAI
actacgtttgagattcaagggtgtgagaatgtaacagtggatggactaagaacaatggttagtcttcggagtaag base pairs
tgatgcaaactctaagttcccacactcttacattgtcacctacctgattcttgttaccaatcagaagcctcattc 1126 to 1200
Bbv16II
BpiI
MspA1I
PvuII DraI MfeI
actttgactgatgtgagaatctcttgctgcaagaatcttgacacagctgcttctttaaaggcaattgagccgatt base pairs
tgaaactgactacactcttagagaacgacgttcttagaactgtgtcgacgaagaaatttccgttaactcggctaa 1201 to 1275
NspBII MunI
EarI
BseRI Eam11
tgtgatcggatcaagagactgcatatagactgtgtgtggtctggttcagaggacgaggaggtagaaggaagagtg base pairs
acactagcctagttctctgacgtatatctgacacacaccagaccaagtctcctgctcctccatcttccttctcac 1276 to 1350
Ksp63
AclNI
04I
EarI
Eam1104I
BseRI
EarI
Eam1104I
gaaactagtgaggctgaccacgaagaggaggatgatggttacgagaggagccagaagaggtgcaagtattcattc base pairs
ctttgatcactccgactggtgcttctcctcctactaccaatgctctcctcggtcttctccacgttcataagtaag 1351 to 1425
2I
SpeI
Ksp632I
BseRI
Ksp632I
AclNI
Asp700I
Eco57I
GsuI
gaggaagaacactgctcaactagtgatgtgaatggattctgttctgaagatagagtatgggagaaactggagtat base pairs
ctccttcttgtgacgagttgatcactacacttacctaagacaagacttctatctcataccctctttgacctcata 1426 to 1500
SpeI
XmnI
BpmI
BsaHI
BbiII
AcsI
Hin1I
EcoNI
AcsI
ctatctttatggatcaatgttggagaatttttgacgccattacctatgacaggactagatgactgtccgaatttg base pairs
gatagaaatacctagttacaacctcttaaaaactgcggtaatggatactgtcctgatctactgacaggcttaaac 1501 to 1575
ApoI
Msp17I
Hsp92I
AcyI
ApoI
BsaBI
EarI Bsh1365I
Eam1104I
Esp1396I
AccB7I
gaagagattaggatcaagatagaaggagattgcagaggtaaacgcaggccagccgagccagagtttgggttaagt base pairs
cttctctaatcctagttctatcttcctctaacgtctccatttgcgtccggtcggctcggtctcaaacccaattca 1576 to 1650
Ksp632I Bse8I
MamI
BsrBRI
PflMI
Van91I
tgtctcgctctctacccaaagctctcaaagatgcagttagattgcggggacacaatcggtttcgcactgaccgca base pairs
acagagcgagagatgggtttcgagagtttctacgtcaatctaacgcccctgtgttagccaaagcgtgactggcgt 1651 to 1725

```
1740                              BsaWI      HindIII
ccgccaatgcagatggattgagtttatgggaaagattcttcttgaccggaattggaagcttgagcttgagcgag base pairs
ggcggttacgtctacctaaactcaaataccctttctaagaagaactggccttaaccttcgaactcgaactcgctc 1726 to 1800


           BalI
           MscI                HindII                      BpmI
         EaeI                  HpaI       BseRI          EcoNI  BspMI
cttgattattggccaccacaggatagagatgttaaccagaggagtctctcgcttcctggagcaggtctgttacaa base pairs
gaactaataaccggtggtgtcctatctctacaattggtctcctcagagagcgaaggacctcgtccagacaatgtt 1801 to 1875
         CfrI                  HincII                      GsuI
           MluNI


                            NcoI Bsp19I
                            StyI DsaI
                     Asp700I Eco130I     BspHI      BspHI
gagtgcctgactttgaggaagctgttcatccatggaacagctcatgagcatttcatgaacttttttgttgagaatc base pairs
ctcacggactgaaactccttcgacaagtaggtaccttgtcgagtactcgtaaagtacttgaaaaacaactcttag 1876 to 1950
                     XmnI    ErhI BstDSI RcaI       RcaI
                             BssT1I
                             EcoT14I

      MspCI                              AccB1I NarI HaeII        MslI
      Bst98I   BsrGI                      KasI BbiII EheI       Alw21I
      BspTI    SspBI                     Eco64I BsaHI BbeI     AspHI
ccaaacttaagggatgtacagcttagagcagactattatccggcgccggagaacgatatgagcacagagatgaga base pairs
ggtttgaattccctacatgtcgaatctcgtctgataataggccgcggcctcttgctatactcgtgtctctactct 1951 to 2025
      AflII    Bsp1407I                  BanI Msp17I Bsp143II  Bbv12I
      Vha464I                            BshNI Hsp92I          BsiHKAI
      BfrI                                Hin1I AcyI BstH2I


                           MfeI
gttggtcgtgtagccgattcgaggaccaattgaacagccgcaacatcattgactga  base pairs
caaccagcacatcggctaagctcctggttaacttgtcggcgttgtagtaactgact  2026 to 2081
                           MunI
```

Restriction enzymes cut Map

2082 base pairs of *max2-1*mutant

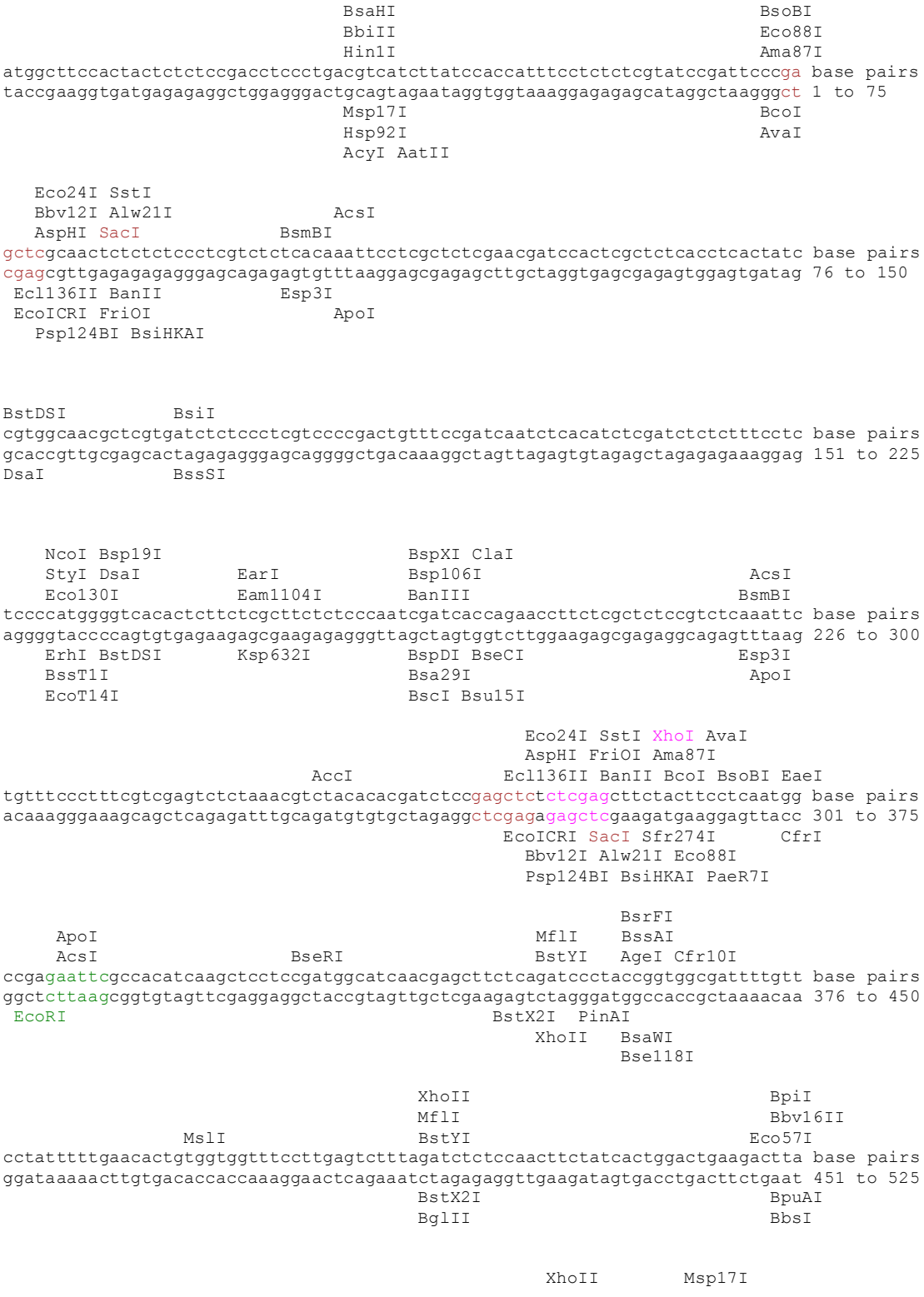

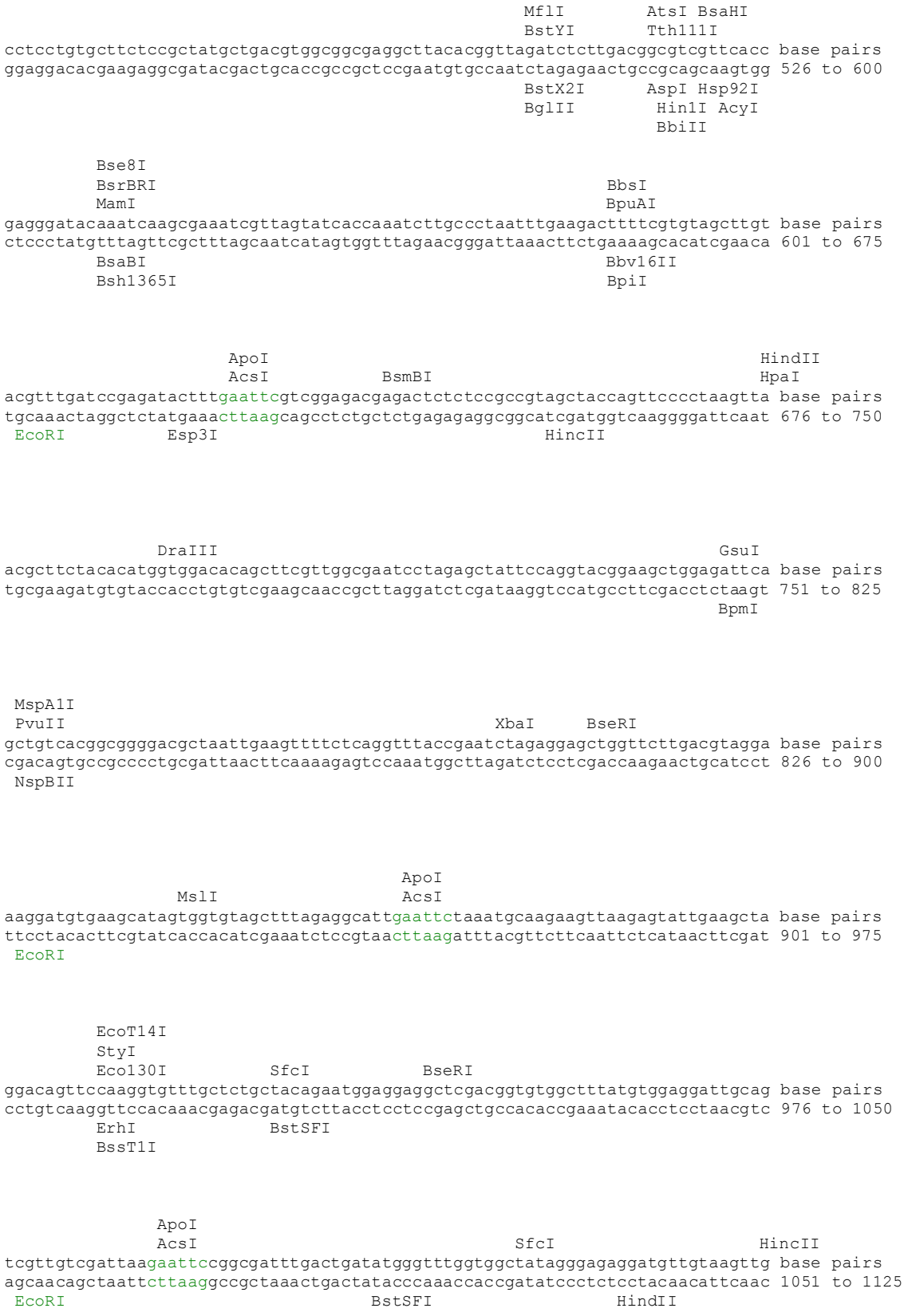
MflI AtsI BsaHI
BstYI Tth111I
cctcctgtgcttctccgctatgctgacgtggcggcgaggcttacacggttagatctcttgacggcgtcgttcacc base pairs
ggaggacacgaagaggcgatacgactgcaccgccgctccgaatgtgccaatctagagaactgccgcagcaagtgg 526 to 600
BstX2I AspI Hsp92I
BglII Hin1I AcyI
BbiII
Bse8I
BsrBRI BbsI
MamI BpuAI
gagggatacaaatcaagcgaaatcgttagtatcaccaaatcttgccctaatttgaagacttttcgtgtagcttgt base pairs
ctccctatgtttagttcgctttagcaatcatagtggtttagaacgggattaaacttctgaaaagcacatcgaaca 601 to 675
BsaBI Bbv16II
Bsh1365I BpiI
ApoI HindII
AcsI BsmBI HpaI
acgtttgatccgagatactttgaattcgtcggagacgagactctctccgccgtagctaccagttcccctaagtta base pairs
tgcaaactaggctctatgaaacttaagcagcctctgctctgagagaggcggcatcgatggtcaaggggattcaat 676 to 750
EcoRI Esp3I HincII
DraIII GsuI
acgcttctacacatggtggacacagcttcgttggcgaatcctagagctattccaggtacggaagctggagattca base pairs
tgcgaagatgtgtaccacctgtgtcgaagcaaccgcttaggatctcgataaggtccatgccttcgacctctaagt 751 to 825
BpmI
MspA1I
PvuII XbaI BseRI
gctgtcacggcggggacgctaattgaagttttctcaggtttaccgaatctagaggagctggttcttgacgtagga base pairs
cgacagtgccgcccctgcgattaacttcaaaagagtccaaatggcttagatctcctcgaccaagaactgcatcct 826 to 900
NspBII
ApoI
MslI AcsI
aaggatgtgaagcatagtggtgtagctttagaggcattgaattctaaatgcaagaagttaagagtattgaagcta base pairs
ttcctacacttcgtatcaccacatcgaaatctccgtaacttaagatttacgttcttcaattctcataacttcgat 901 to 975
EcoRI
EcoT14I
StyI
Eco130I SfcI BseRI
ggacagttccaaggtgtttgctctgctacagaatggaggaggctcgacggtgtggctttatgtggaggattgcag base pairs
cctgtcaaggttccacaaacgagacgatgtcttacctcctccgagctgccacaccgaaatacacctcctaacgtc 976 to 1050
ErhI BstSFI
BssT1I
ApoI
AcsI SfcI HincII
tcgttgtcgattaagaattccggcgatttgactgatatgggtttggtggctatagggagaggatgttgtaagttg base pairs
agcaacagctaattcttaaggccgctaaactgactatacccaaaccaccgatatccctctcctacaacattcaac 1051 to 1125
EcoRI BstSFI HindII

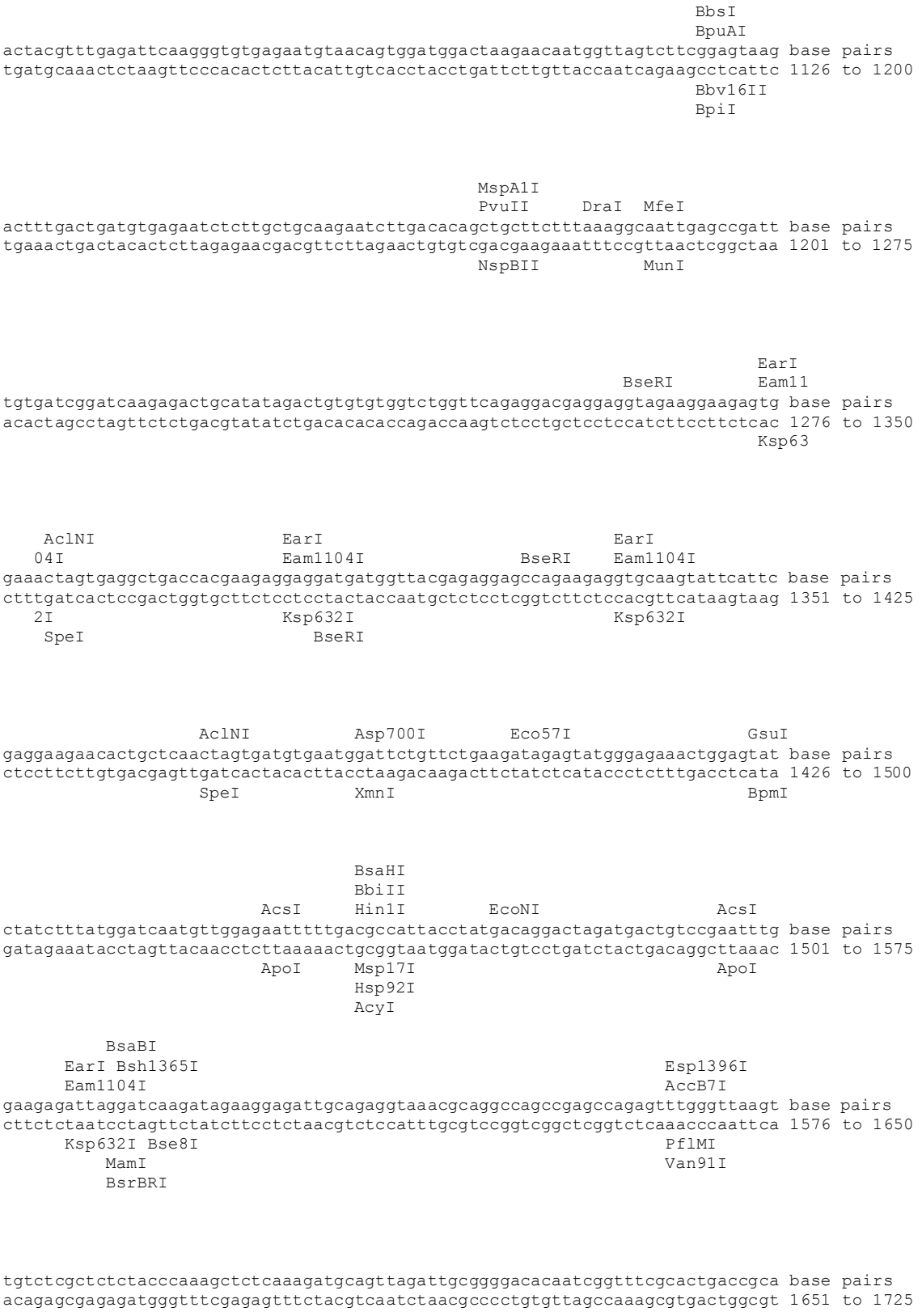
BbsI
BpuAI
actacgtttgagattcaagggtgtgagaatgtaacagtggatggactaagaacaatggttagtcttcggagtaag base pairs
tgatgcaaactctaagttcccacactcttacattgtcacctacctgattcttgttaccaatcagaagcctcattc 1126 to 1200
Bbv16II
BpiI
MspA1I
PvuII DraI MfeI
actttgactgatgtgagaatctcttgctgcaagaatcttgacacagctgcttctttaaaggcaattgagccgatt base pairs
tgaaactgactacactcttagagaacgacgttcttagaactgtgtcgacgaagaaatttccgttaactcggctaa 1201 to 1275
NspBII MunI
EarI
BseRI Eam11
tgtgatcggatcaagagactgcatatagactgtgtgtggtctggttcagaggacgaggaggtagaaggaagagtg base pairs
acactagcctagttctctgacgtatatctgacacacaccagaccaagtctcctgctcctccatcttccttctcac 1276 to 1350
Ksp63
AclNI
04I
EarI
Eam1104I
BseRI
EarI
Eam1104I
gaaactagtgaggctgaccacgaagaggaggatgatggttacgagaggagccagaagaggtgcaagtattcattc base pairs
ctttgatcactccgactggtgcttctcctcctactaccaatgctctcctcggtcttctccacgttcataagtaag 1351 to 1425
2I
SpeI
Ksp632I
BseRI
Ksp632I
AclNI
Asp700I
Eco57I
GsuI
gaggaagaacactgctcaactagtgatgtgaatggattctgttctgaagatagagtatgggagaaactggagtat base pairs
ctccttcttgtgacgagttgatcactacacttacctaagacaagacttctatctcataccctctttgacctcata 1426 to 1500
SpeI
XmnI
BpmI
BsaHI
BbiII
AcsI
Hin1I
EcoNI
AcsI
ctatctttatggatcaatgttggagaatttttgacgccattacctatgacaggactagatgactgtccgaatttg base pairs
gatagaaatacctagttacaacctcttaaaaactgcggtaatggatactgtcctgatctactgacaggcttaaac 1501 to 1575
ApoI
Msp17I
Hsp92I
AcyI
ApoI
BsaBI
EarI Bsh1365I
Eam1104I
Esp1396I
AccB7I
gaagagattaggatcaagatagaaggagattgcagaggtaaacgcaggccagccgagccagagtttgggttaagt base pairs
cttctctaatcctagttctatcttcctctaacgtctccatttgcgtccggtcggctcggtctcaaacccaattca 1576 to 1650
Ksp632I Bse8I
MamI
BsrBRI
PflMI
Van91I
tgtctcgctctctacccaaagctctcaaagatgcagttagattgcggggacacaatcggtttcgcactgaccgca base pairs
acagagcgagagatgggtttcgagagtttctacgtcaatctaacgcccctgtgttagccaaagcgtgactggcgt 1651 to 1725

```
AcsI                            BsaWI      HindIII
ccgccaatgcagatgaatttgagtttatgggaaagattcttcttgaccggaattggaagcttgagcttgagcgag base pairs
ggcggttacgtctacttaaactcaaataccctttctaagaagaactggccttaaccttcgaactcgaactcgctc 1726 to 1800
ApoI
1740


            BalI
            MscI                HindII                      BpmI
          EaeI                  HpaI       BseRI          EcoNI  BspMI
cttgattattggccaccacaggatagagatgttaaccagaggagtctctcgcttcctggagcaggtctgttacaa base pairs
gaactaataaccggtggtgtcctatctctacaattggtctcctcagagagcgaaggacctcgtccagacaatgtt 1801 to 1875
          CfrI                  HincII                      GsuI
            MluNI


                              NcoI Bsp19I
                              StyI DsaI
                       Asp700I Eco130I     BspHI      BspHI
gagtgcctgactttgaggaagctgttcatccatggaacagctcatgagcatttcatgaacttttttgttgagaatc base pairs
ctcacggactgaaactccttcgacaagtaggtaccttgtcgagtactcgtaaagtacttgaaaaacaactcttag 1876 to 1950
                       XmnI    ErhI BstDSI RcaI       RcaI
                               BssT1I
                               EcoT14I

      MspCI                                AccB1I NarI HaeII        MslI
      Bst98I   BsrGI                        KasI BbiII EheI       Alw21I
      BspTI    SspBI                        Eco64I BsaHI BbeI     AspHI
ccaaacttaagggatgtacagcttagagcagactattatccggcgccggagaacgatatgagcacagagatgaga base pairs
ggtttgaattccctacatgtcgaatctcgtctgataataggccgcggcctcttgctatactcgtgtctctactct 1951 to 2025
      AflII    Bsp1407I                    BanI Msp17I Bsp143II  Bbv12I
      Vha464I                              BshNI Hsp92I          BsiHKAI
      BfrI                                  Hin1I AcyI BstH2I


                             MfeI
gttggttcgtgtagccgattcgaggaccaattgaacagccgcaacatcattgactga  base pairs
caaccaagcacatcggctaagctcctggttaacttgtcggcgttgtagtaactgact  2026 to 2082
                             MunI
```

B- T-DNA Constructs Used to screen *max4-1* (Taken from Tissier *et al*., 1999)

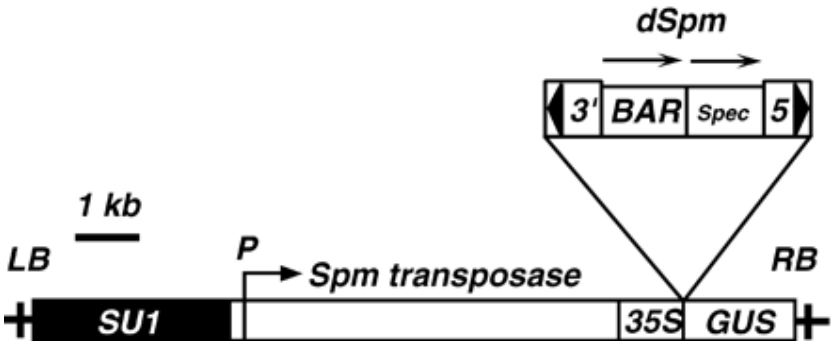

LB and RB, left and right borders, respectively; P, promoter driving the expression of the transposase (*Spm*, 35S, or *AtDMC1* promoters); Spec, spectinomycin resistance gene for selection in bacteria; *SU1*, counterselectable marker.

C- Whole Trays of Genotypes grown for Rosette Morphology

1- WT

2- max

3- atipt5,7

4-max4

5- atipt5,7,max2

6-atipt5,7,max4

Whole Trays of Genotypes grown for Rosette Morphology

7- atipt3,5

8-atipt3,5,max4

9- atipt3,7

10-atipt3,7,max4

9- atipt3,5,7

10-atipt3,5,7,max4

Whole Tray of Genotype grown for Rosette Morphology

11- atipt1,3,5,7

Appendix III

A- Analysis for expression of *AtIPT1 (red), AtIPT3 (blue), AtIPT5 (green)* and *AtIPT7 (yellow orange)*, using Sample Interface Tool of Genevestigator

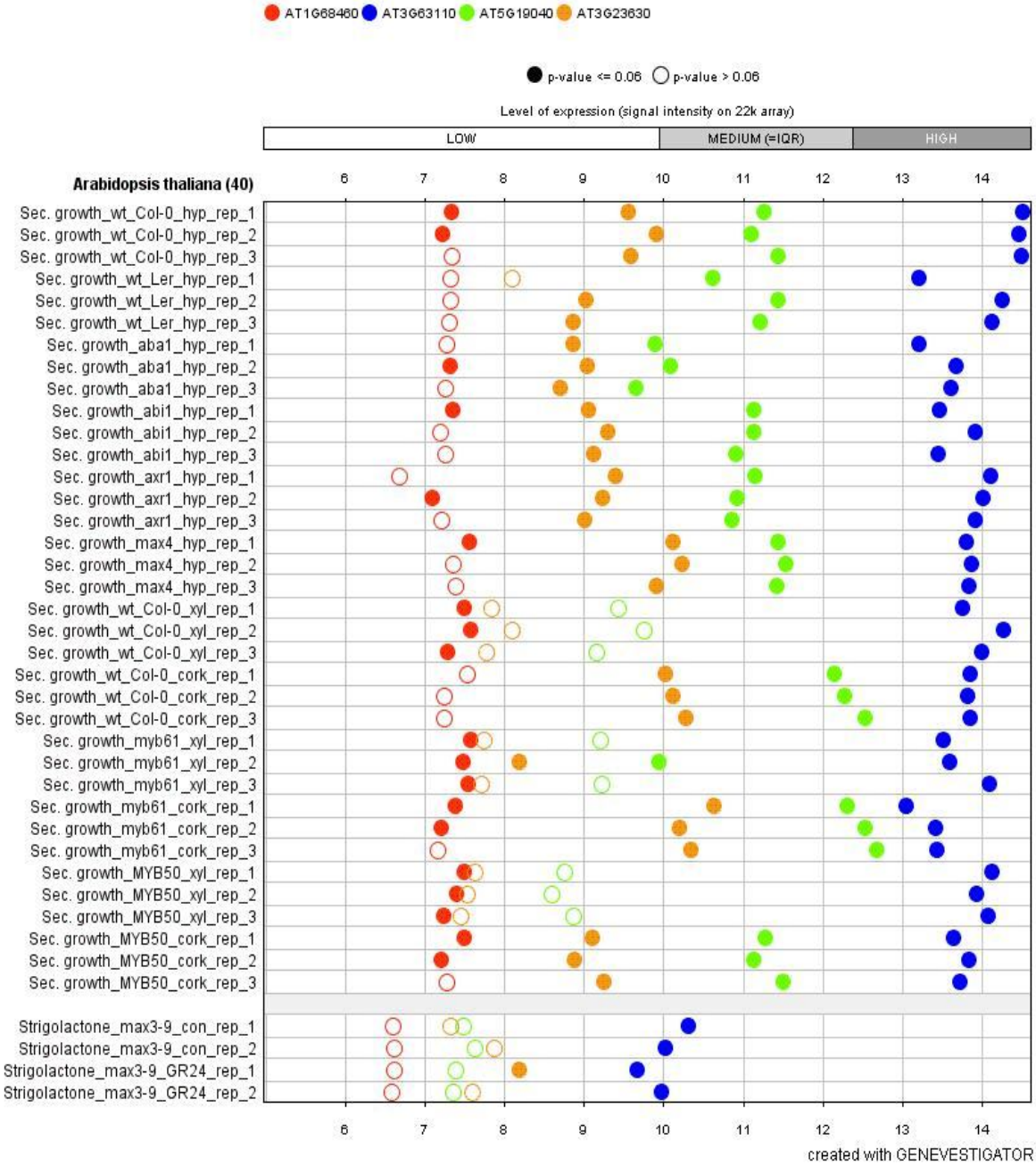

B- Analysis for expression of *AtIPT1 (red), AtIPT3 (blue), AtIPT5 (green)* and *AtIPT7(yellow orange)*, using Perturbation Interface Tool of Genevestigator

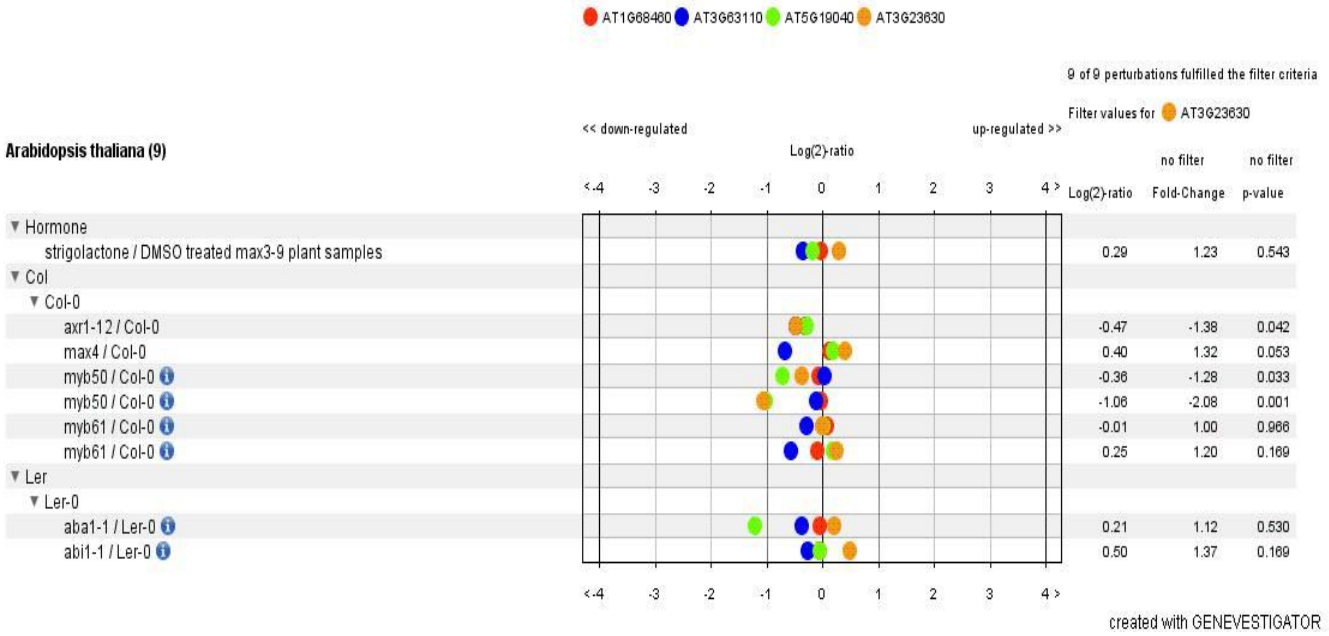

Appendix IV

A- Chromatogram of a mixture of D-labeled Cytokinin Standards

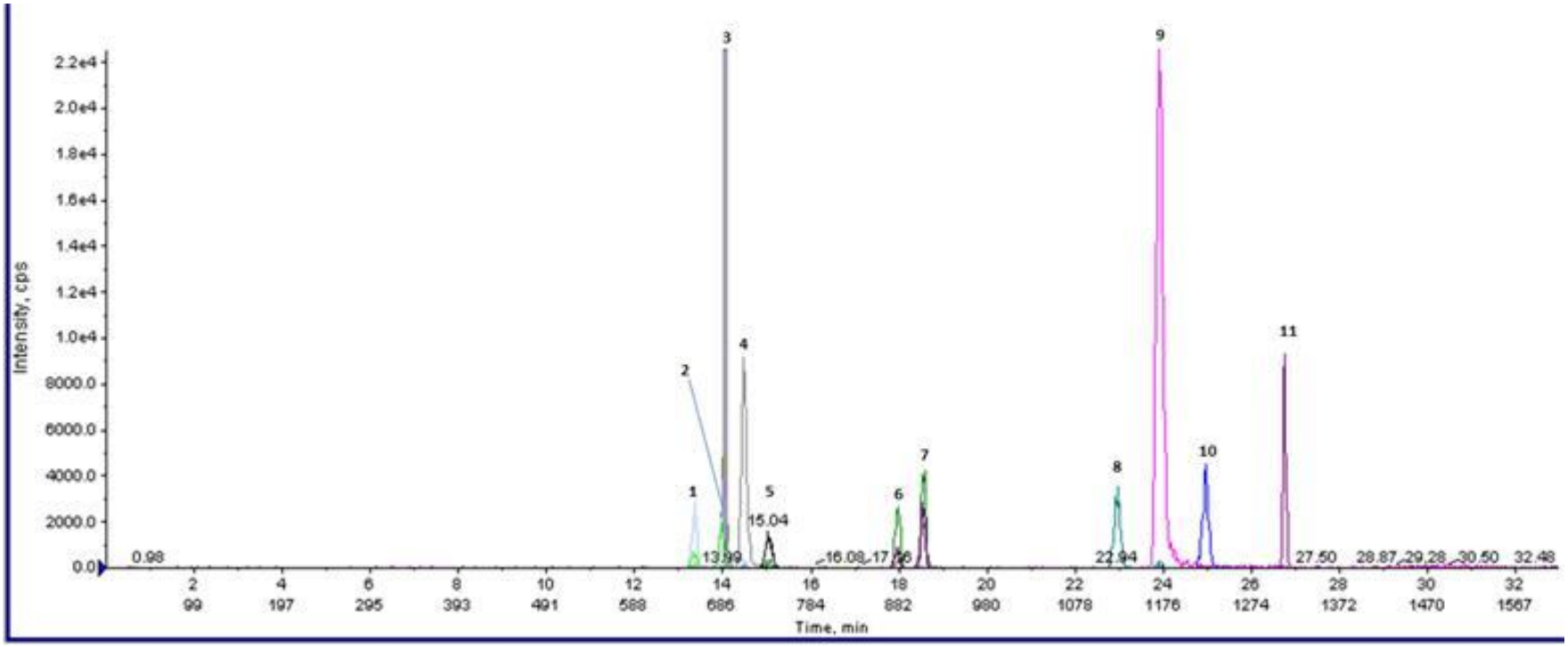

1 = zeatin 9-glucoside (D^5-Z9G); 2 = dihydrozeatin 9-glucoside (D^3-DZ9G); 3 = *trans*-zeatin (D^5-tZ); 4 = dihydrozeatin (D^3-DZ); 5 = zeatin riboside phosphate (D^5-tZRP); 6 = *trans*-zeatin roboside (D^5-tZR); 7 = dihydrozeatin riboside (D^3-DZR); 8 = isopentenyladenosine 9-glucoside (D^6 -iP9G); 9 = isopentenyl adenine (D^6 -iP); 10= iP riboside phosphate (D^6 -iPRP); 11= iP riboside (D^6 - iPR).

B- Quantification of CK levels in Shoot grown under long days

(n = 4 and Erorr bar = SE)

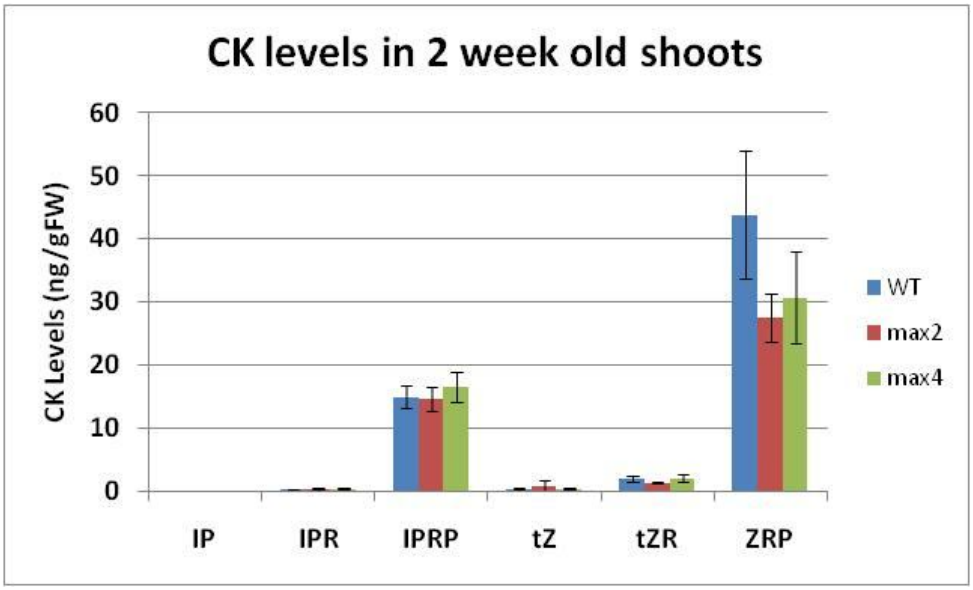

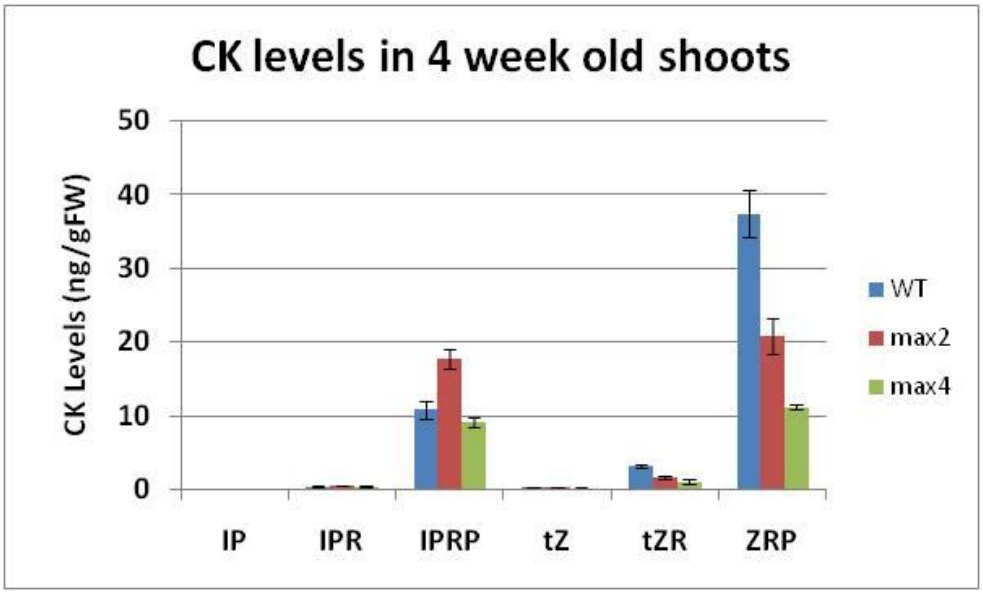

C- Quantification of CK levels in Shoot grown under short days
(n = 4 and Erorr bar = SE)

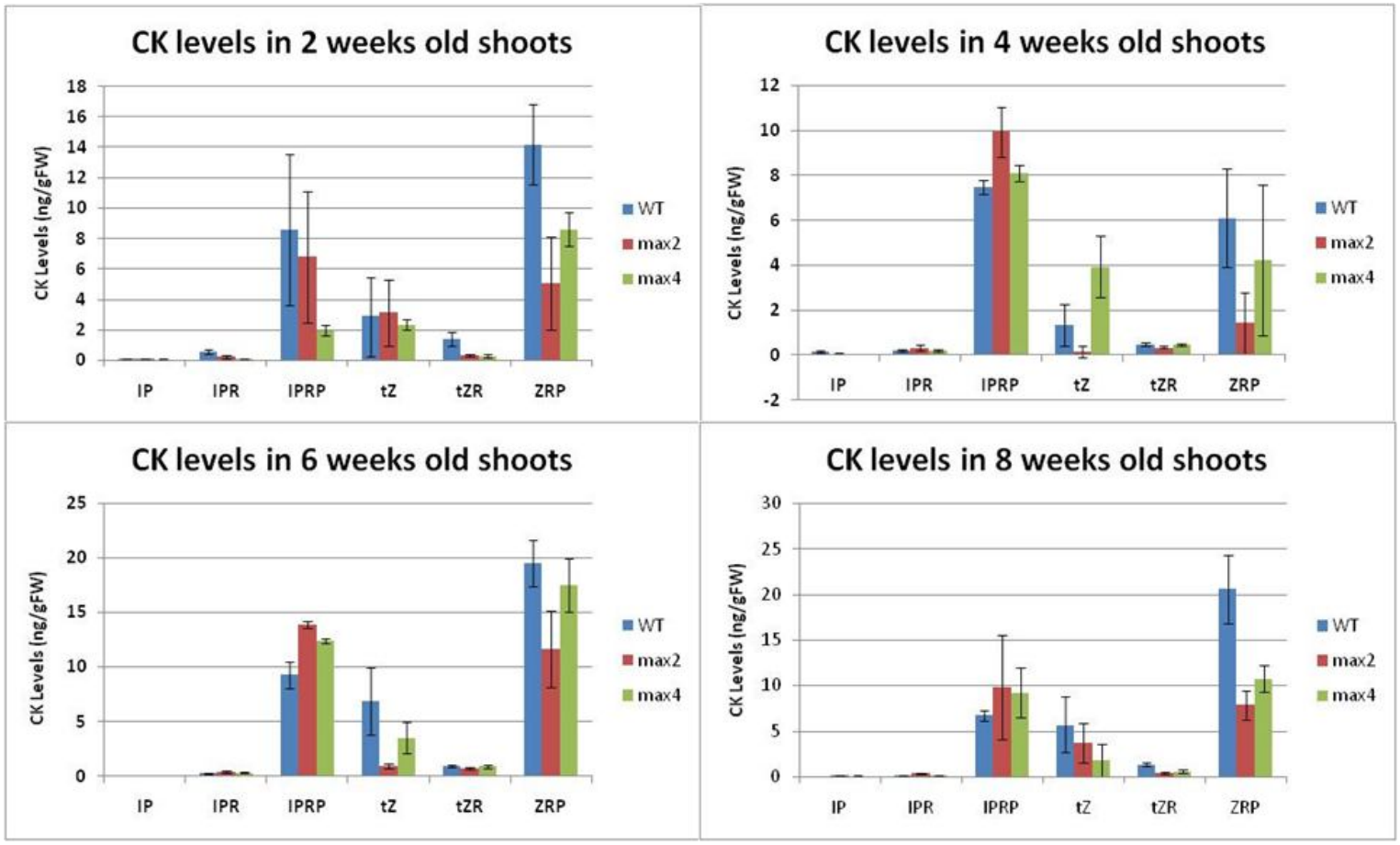

D- Scree Plots of PCA

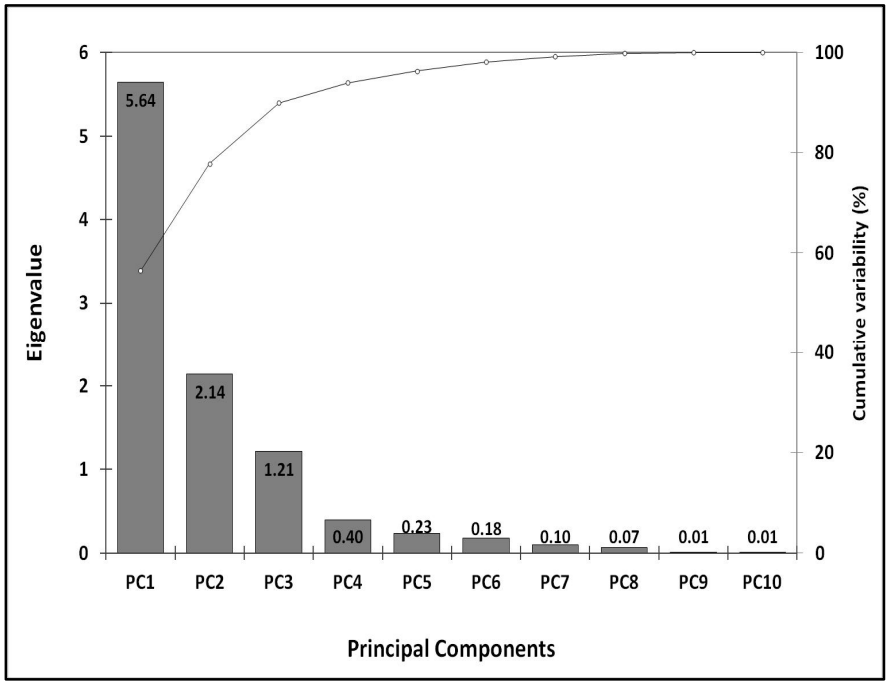

Scree plot of PCA for max genotypes.*The bar graph is between eigen values (y-axis) and number of principal components (x –axis) calculated for CK variables of max genotypes in shoot, phloem, roots and xylem.*

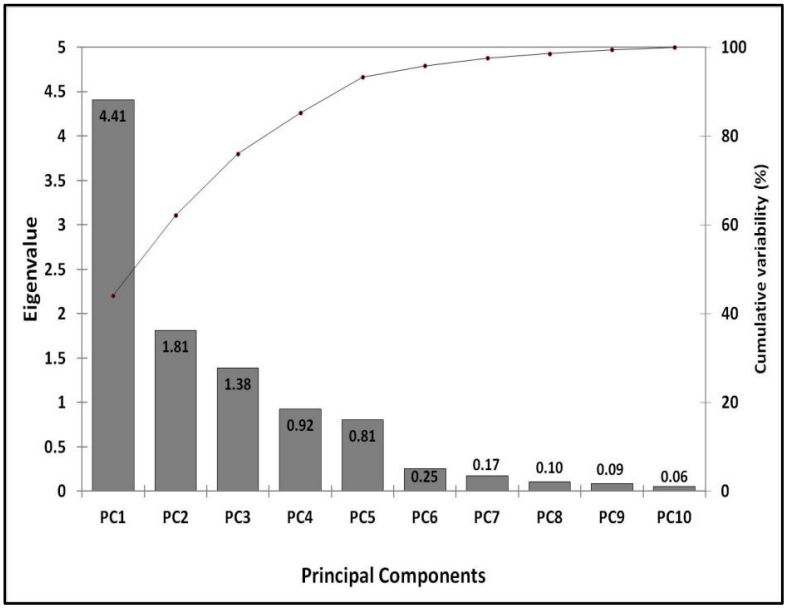

Scree plot of PCA for atipt double mutants in WT and max backgrounds.*The bar graph is between eigen values (y-axis) and number of principal components (x–axis) calculated for CK variables in shoot, phloem, roots and xylem of genotypes.*

Scree Plot of PCA

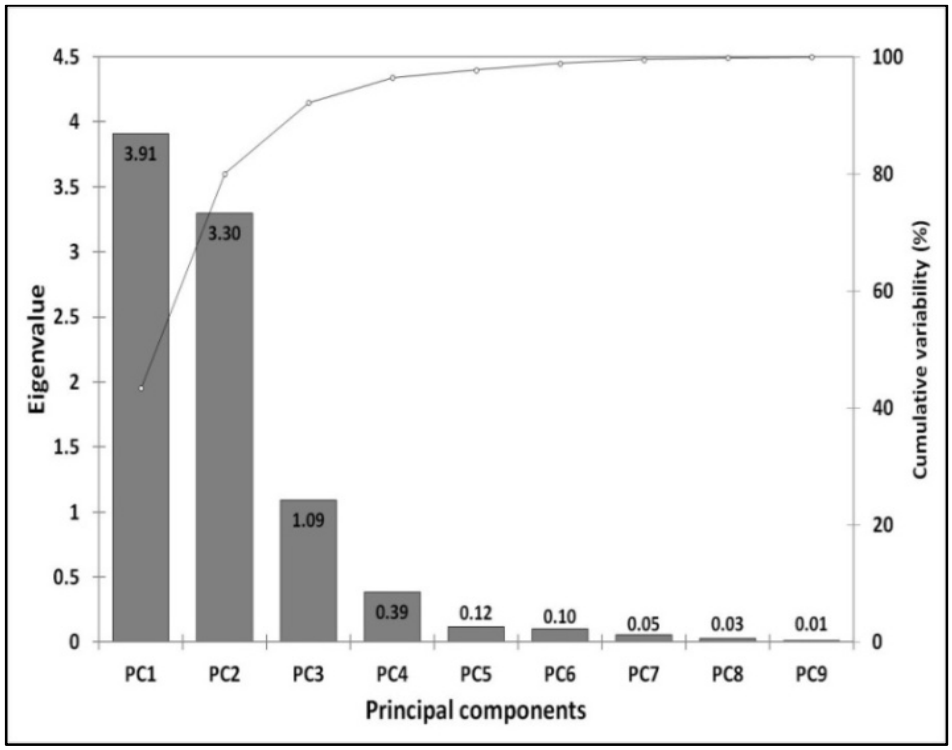

Scree plot of PCA for atipt triple mutant in WT and max backgrounds.*The bar graph is between eigen values (y-axis) and number of principal components (x–axis) calculated for CK variables in shoot and roots of genotypes.*

E-Loading Plots of PCA for CK levels in shoot, phloem, root and xylem of *atipt* double mutants in wild-type and *max* backgrounds

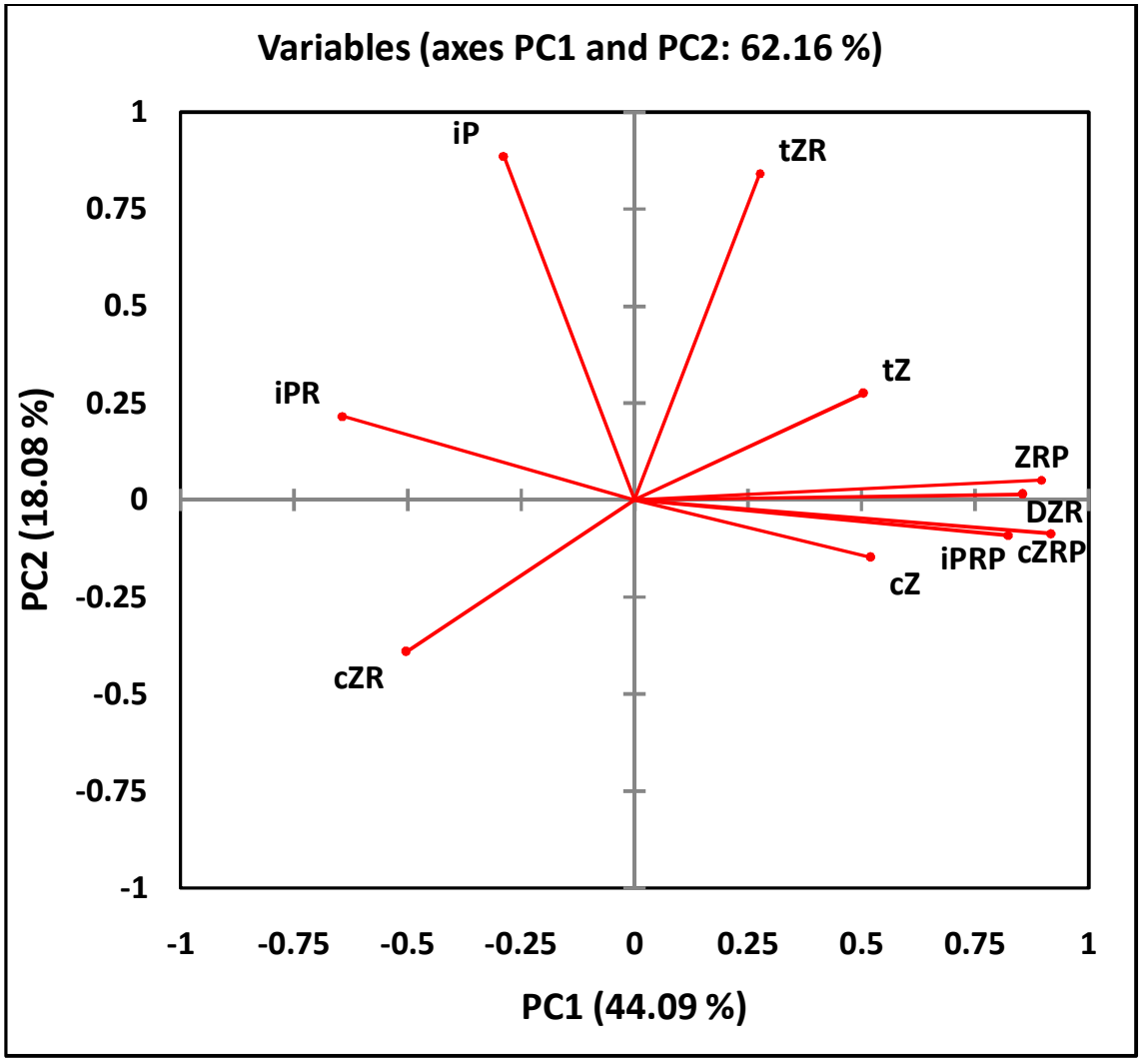

Loading Plots of PCA for CK levels in shoot, phloem, root and xylem of *atipt* double mutants in wild-type and *max* backgrounds